DOE/PC/91008-8
Distribution Category UC-122

Area Balance and Strain in an Extensional Fault System: Strategies for Improved Oil Recovery in Fractured Chalk, Gilbertown Field, Southwestern Alabama – Year 2

By
Jack C. Pashin
Dorothy E. Raymond
Andrew K. Rindsberg
Ganiu G. Alabi
Richard E. Carroll

September 1998

Work Performed Under Subcontract G4S51733 and Prime Contract DE-AC22-94PC91008

Prepared for
U.S. Department of Energy
Assistant Secretary for Fossil Energy

Rhonda Lindsey, Project Manager
National Petroleum Technology Office
P.O. Box 3628
Tulsa, OK 74101

Prepared by:
University of Alabama
Tuscaloosa, AL 35487

DISCLAIMER

DISCLAIMER

Portions of this document may be illegible in electronic image products. Images are produced from the best available original document.

CONTENTS

ILLUSTRATIONS

TABLES

ABSTRACT

Gilbertown Field is the oldest oil field in Alabama and has produced oil from fractured chalk of the Cretaceous Selma Group and glauconitic sandstone of the Eutaw Formation. Nearly all of Gilbertown Field is still in primary recovery, although waterflooding has been attempted locally. The objective of this project is to analyze the geologic structure and burial history of Mesozoic and Tertiary strata in Gilbertown Field and adjacent areas in order to suggest ways in which oil recovery can be improved. Indeed, the decline of oil production to marginally economic levels in recent years has made this type of analysis timely and practical. Key technical advancements being sought include understanding the relationship of requisite strain to production in Gilbertown reservoirs, incorporation of synsedimentary growth factors into models of area balance, quantification of the relationship between requisite strain and bed curvature, determination of the timing of hydrocarbon generation, and identification of the avenues and mechanisms of fluid transport.

The Gilbertown fault system is part of a horst-and-graben system that is interpreted to be detached at the base of the Louann Salt. Sequential restorations suggest that the fault system began forming as a half graben during the Jurassic, and the Early Cretaceous was the major episode of structural growth. By the end of the Early Cretaceous, however, the growth rate decreased and the asymmetric half graben evolved into a symmetric full graben. Faults offset strata as young as Miocene. A surface exposure shows that deformation is restricted mainly to the hanging wall and includes shear fractures and drag folds. Fracture studies reveal two distinct orthogonal joint systems in the study area.

The regional subsidence history is typical of extensional basins. More than half of the total effective subsidence can be accounted for by sediment loading and compaction. Thermal modeling demonstrates that Upper Cretaceous strata are undermature and that oil probably migrated from deep Jurassic source rocks.

The Eutaw Formation was divided into seven flooding-surface-bound parasequences. These parasequences are interpreted to have been deposited during regional transgression as part of a barrier shoreline system. Glauconite and carbonate cement are key sources of reservoir heterogeneity. High glauconite content makes the Eutaw a low-resistivity, low-contrast formation that is difficult to characterize quantitatively.

The Selma Group was deposited on a muddy carbonate shelf, and eight stratigraphic intervals were recognized. Mineralization of fractures occurred as warm fluid migrated from deep sources. Resistivity, dipmeter, and fracture identification logs indicate that reservoir-scale deformation is mainly in the hanging walls of the faults. This deformation includes minor faults and drag folds.

Structural modeling included area balancing, curvature analysis, and seal analysis. New area balancing techniques were developed to characterize growth strata. Curvature analysis indicates that the faults contain numerous fault bends that influence fracture distribution. Eutaw oil is produced strictly from footwall uplifts, whereas Selma oil is produced from fault-related fractures. Fault-seal analysis suggests that clay smear and mineralization may be significant trapping mechanisms in the Eutaw Formation. The critical seal for Selma reservoirs, by contrast, is where Tertiary clay in the hanging wall is juxtaposed with Selma chalk in the footwall.

The decline characteristics of Eutaw and Selma wells differ markedly, reflecting the respective conventional and fractured reservoirs. Decline curves of the most productive wells are affected significantly by the field's development history, which included an episode of near abandonment in the late 1960s followed by one of rejuvenation during the 1970s. Production and completion patterns identify opportunities for revitalization through infill drilling. In the Selma Group, for example, a tall oil column may remain untapped, and horizontal drilling may be the most viable technology to revive Selma production.

EXECUTIVE SUMMARY

Gilbertown Field, established in 1944, is the oldest oil field in Alabama and produces oil from fractured chalk of the Cretaceous Selma Group and glauconitic sandstone of the Eutaw Formation. Nearly all of Gilbertown field is still in primary recovery, although waterflooding has been attempted locally. The objective of this project is to analyze the geologic structure and burial history of Mesozoic and Tertiary strata in Gilbertown Field and adjacent areas in order to suggest ways in which oil recovery can be improved. Indeed, the decline of oil production to marginally economic levels in recent years has made this type of analysis timely and practical. Key technical advancements being sought include understanding the relationship of requisite strain to production in Gilbertown reservoirs, incorporation of synsedimentary growth factors into models of area balance, quantification of the relationship between requisite strain and bed curvature, determination of the timing of hydrocarbon generation, and identification of the avenues and mechanisms of fluid transport.

Structural maps and cross sections establish that the Gilbertown fault system is part of a horst-and-graben system that is interpreted to be detached at the base of the Louann Salt. Sequential restoration of cross sections suggests that the fault system began forming as an asymmetric half graben during the Jurassic. The Early Cretaceous was the major episode of structural growth and subsidence of the half graben. By the end of the Early Cretaceous, however, the growth rate of antithetic faults in the eastern part of the field became effectively equal to that of synthetic faults. Thus, the asymmetric half graben evolved into a symmetric full graben. Cross sections demonstrate significant growth of the graben in the Cretaceous section but show limited growth in the Tertiary section.

Geologic mapping of formations and fracture systems has added significantly to knowledge of the geology of the Gilbertown area. Faults offset strata as young as Miocene, whereas Quaternary alluvial deposits cut across structures in the area. An excellent exposure of one fault shows that deformation is restricted mainly to the hanging wall and that shear fractures and drag folds are significant structural components. Fracture studies reveal two distinct orthogonal joint systems in the study area. One joint system is interpreted to have formed as part of the tectonic stress field responsible for regional extension, whereas the other system apparently is forming today in response to regional uplift and unroofing.

Analysis of burial history indicates that the subsidence history of Jurassic and Tertiary strata in the Gilbertown area is typical of extensional basins. Factoring out the tectonic component of subsidence suggests that more than half of the total effective subsidence in the Gilbertown area can be accounted for by sediment loading and compaction. Thermal modeling demonstrates that source rocks in the Upper Cretaceous section are undermature. The most likely scenario is that oil was generated in the Smackover Formation and migrated along faults and fractures into what is now Gilbertown Field.

The Eutaw Formation was divided into seven flooding-surface-bound parasequences that could be mapped throughout the Gilbertown area. These parasequences are interpreted to have been deposited during regional transgression as part of a barrier shoreline system. Glauconite and carbonate cement are key sources of reservoir heterogeneity in the Eutaw Formation. High glauconite content makes the Eutaw a low-resistivity, low-contrast formation, and the limited log suite prevents characterization of the sandstone using shaly sand methodology. However, commercial core analyses enable quantification of basic reservoir properties.

The Selma Group was deposited on a muddy carbonate shelf, and eight stratigraphic intervals were traced throughout Gilbertown Field. Isotopic analysis indicates that mineralization of fractures occurred during burial and that slickensides continued forming near maximum burial. Evidence from resistivity, dipmeter, and fracture identification logs indicates that reservoir-scale deformation is mainly in the hanging walls of the faults. This deformation apparently includes minor faults, fractures, and drag folds.

Structural modeling included area balancing, curvature analysis, and seal analysis. New area balancing techniques were developed to characterize growth strata. Requisite strain calculations indicate that Jurassic strata deep in the Gilbertown graben contain a large component of small-scale deformation and that deformation in Upper Cretaceous strata is restricted to the fault zones, especially hanging-wall drag folds. Curvature analysis indicates that the faults where oil is produced from the Selma Group contain numerous fault bends. Transport of strata through these bends appears to have had a strong control on fracturing. Eutaw oil is produced strictly from footwall uplifts, whereas Selma oil is produced from fault-related fractures. Fault-seal analysis suggests that clay smear and mineralization may be significant trapping mechanisms in the Eutaw Formation. The critical seal for Selma reservoirs, by contrast, is where Porters Creek Clay in the hanging wall is juxtaposed with Selma chalk in the footwall, reflecting the predominance of hanging-wall deformation.

The decline characteristics of Eutaw and Selma wells differ markedly, reflecting development in conventional and fractured reservoirs, respectively. Decline curves of the most productive wells, moreover, are affected significantly by the field's development history, which included an episode of near abandonment in the late 1960s followed by one of rejuvenation during the 1970s. Plotting production and completion patterns on maps and cross sections identifies opportunities for revitalization through infill drilling. In the Selma Group, for example, a tall oil column may remain untapped, and horizontal drilling may be the most viable technology to revive Selma production.

Significant progress has been made toward understanding the structural geology of Gilbertown Field, and we have drawn some insight into the technologies that are best suited to revitalize the field. However, three major tasks remain to complete the project. These tasks include parts of Task 4 (Structural Modeling), Task 5 (Burial and Thermal Modeling), and Task 6 (Production Analysis). Personnel at the Geological Survey of Alabama are maintaining a vigorous technology transfer program as part of this project. Ongoing efforts include contacts with industry, technical reports and presentations, and workshops.

INTRODUCTION

The first commercial production of oil in Alabama was from naturally fractured chalk of the Upper Cretaceous Selma Group in Gilbertown Field (figs. 1, 2). Oil production has been reported from fractured chalk in the Gulf Coast basin since the 1920s, and Gilbertown Field was discovered in 1944. Many of the original fields are still producing oil, although production has declined greatly (Scholle, 1977; Lowe and Carington, 1990). Gilbertown Field is still largely in primary recovery, and production efforts focus on glauconitic sandstone of the Eutaw Formation rather than Selma chalk, which ceased producing in 1995. The applicability of improved recovery strategies to both these reservoirs has not been considered fully, and a large amount of oil may remain untapped.

Virtually all oil production from chalk in the United States is from extensional faults associated with salt domes and the peripheral faults defining the margin of the Mississippi interior salt basin. Similarly, the major oil production from chalk in the North Sea basin of Europe is from extensional fault and fracture systems related to salt movement (Brown, 1987; Meling, 1993). Many fields in the eastern part of the Gulf Coast basin produce from multiple pools in sandstone and carbonate of Jurassic to Tertiary age, and in most of those fields, fractured chalk is considered a reservoir of secondary importance. As a result, natural fracturing has received only passing consideration in field management plans, which have focused mainly on production from the conventional sandstone and carbonate reservoirs. This is unfortunate, because much additional oil may be produced from untapped fractured chalk in existing fields. Furthermore, fracturing may have a strong influence on the distribution and producibility of oil in traditional sandstone and carbonate reservoirs and should thus be considered when implementing plans for improved oil recovery. Indeed, as production from domestic oil fields continues to decline, it is imperative that recovery efficiency be optimized and that unconventional opportunities be pursued to avoid premature abandonment of existing fields.

For this reason, the Geological Survey of Alabama has undertaken an intensive multidisciplinary investigation of the impact of fracturing on the distribution and producibility of oil from extensional fault systems in Gilbertown Field and adjacent areas. This research project focuses on natural fracturing in the Selma Group as well as in conventional sandstone reservoirs of the underlying Eutaw Formation. This is the second annual report of a 3-year project that is designed to develop and apply advanced technical concepts in coordinated geoscience and engineering research.

Central to this research is the refinement and application of area balancing techniques to extensional structures in the Gilbertown area. These emerging, innovative techniques have the potential to constrain structural geometry and kinematics, quantify layer-parallel strain, and predict the distribution of fractures (Epard and Groshong, 1993; Groshong, 1994). As such, area balancing has immediate applications to developing strategies to improve oil recovery from fractured reservoirs. However, these techniques are still largely in the theoretical and experimental domains and therefore have yet to be applied rigorously to natural and practical settings. Our goal is to demonstrate comprehensively the utility of area balancing techniques in designing improved recovery programs for fractured oil reservoirs. In order to attain this goal, a coordinated multidisciplinary approach is required that synthesizes geologic, geophysical, and engineering data.

REGIONAL GEOLOGIC SETTING

This study focuses on southern Choctaw County, Alabama, and adjacent areas in the vicinity of the Gilbertown fault system (fig. 2). The Gilbertown fault system is one of many extensional structures in the eastern part of the Gulf Coast basin, a Mesozoic–Cenozoic rifted basin formed during the opening of the Gulf of Mexico (Salvador, 1987; Worrall and Snelson, 1989). Evaporite sedimentation associated with early rifting had a profound impact on the structural and sedimentologic evolution of the region and ultimately affected the generation and entrapment of hydrocarbons.

Stratigraphy and Sedimentation

Rifting commenced with extensional collapse of the Appalachian–Ouachita orogen near the start of the Mesozoic Era (Horton and others, 1984). Initially, coarse-grained, arkosic clastics of the Eagle Mills Formation were deposited in deep half grabens and grabens and are associated with basaltic dikes, sills, and flows (Guthrie and Raymond, 1992). As rifting continued, magmatism waned, and evaporite sedimentation prevailed until near the end of Jurassic time (fig. 3). Evaporite sedimentation marks initial opening of the Gulf of Mexico and began with deposition of the Werner Formation, which is a dominantly anhydritic unit with some coarse-grained clastics (Tolson and others, 1983). Above the Werner is the Louann Salt, which contains mainly massive halite intercalated with a lesser amount of anhydrite (Oxley and Minihan, 1969; Mink and others, 1985).

Above the Louann Salt are the Norphlet Sandstone and the limestone and dolomite of the Smackover Formation (fig. 3), which are of Late Jurassic age and are among the most important hydrocarbon reservoirs

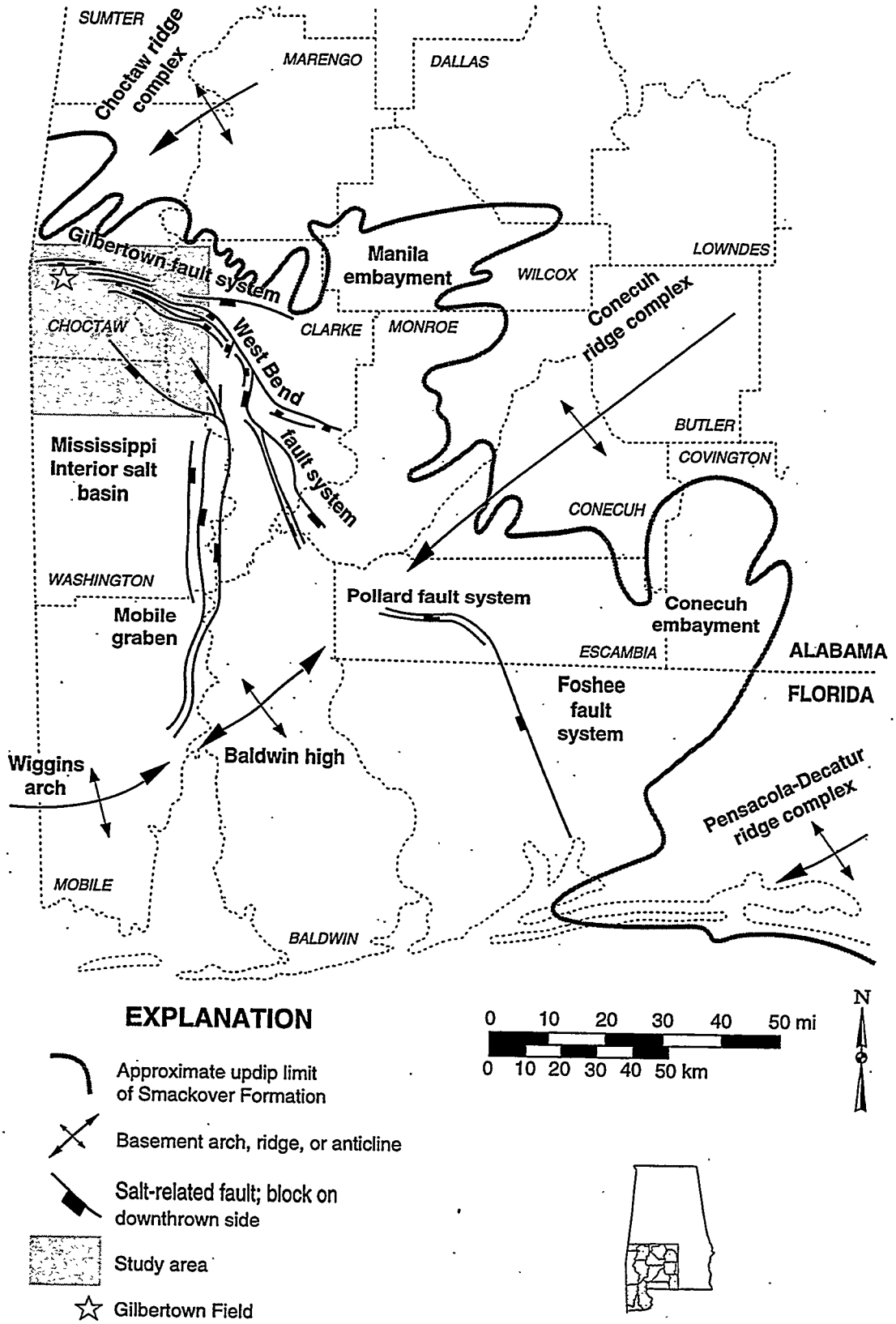

Figure 1.--Structural features in the Gulf Coast basin of southwest Alabama with location of study area and Gilbertown Field (modified from Mancini and others, 1991).

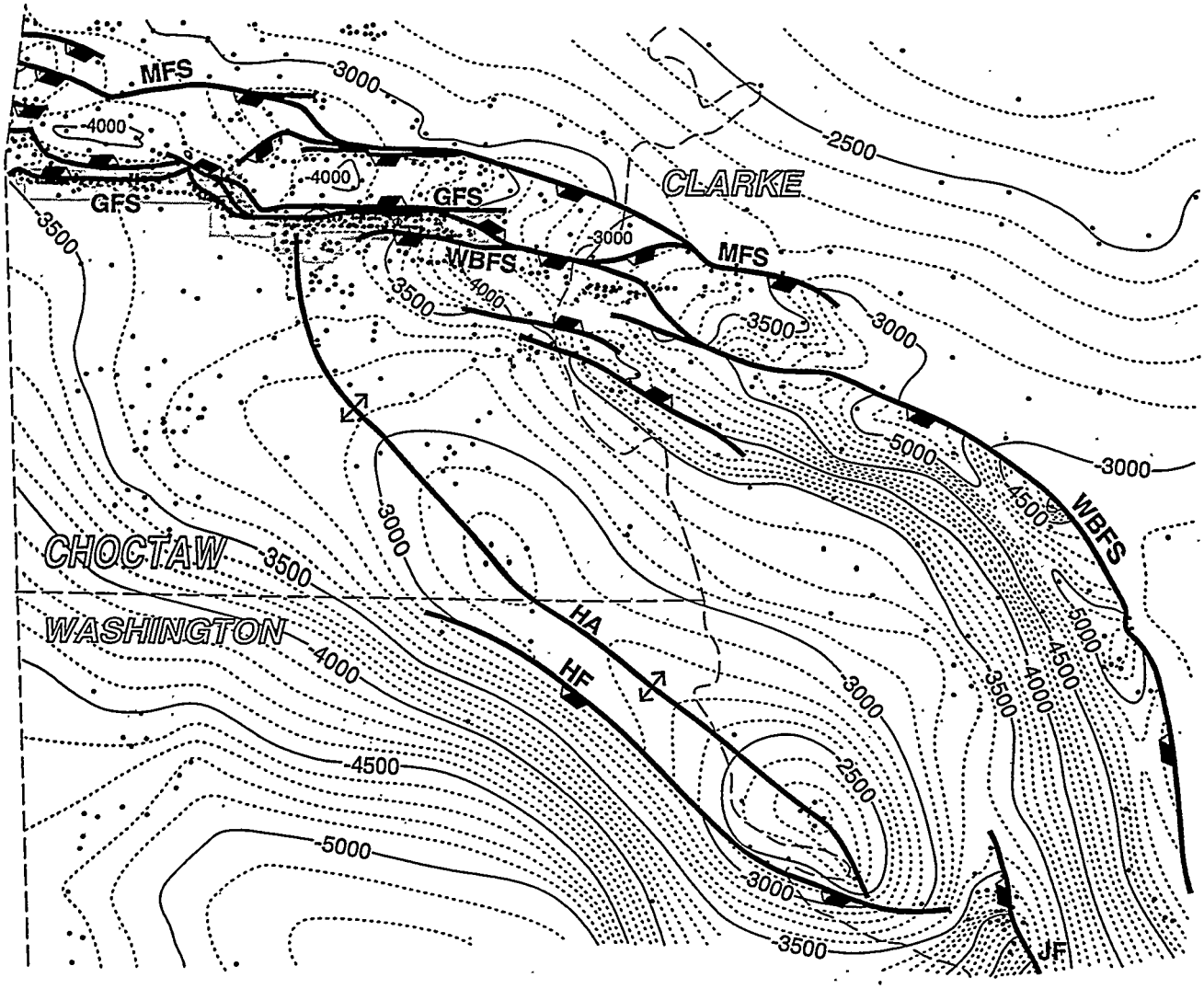

Figure 2.--Structural contour map of the top of the Eutaw Formation (Upper Cretaceous) showing the relationship of Gilbertown Field to the Gilbertown, Melvin, and West Bend fault systems and the Hatchetigbee anticline.

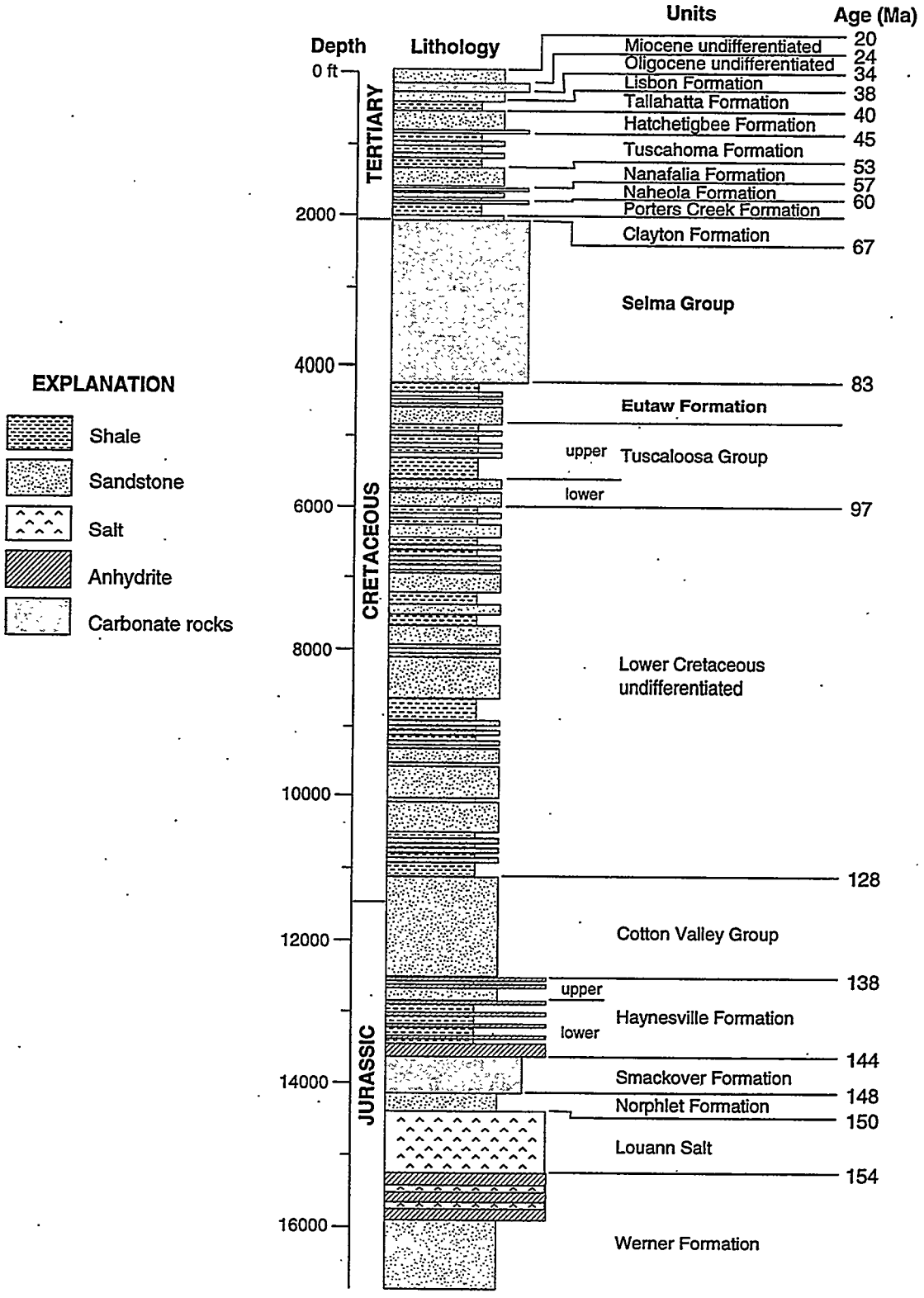

Figure 3.--Generalized stratigraphic section showing Jurassic through Tertiary stratigraphy and ages of marker beds in Gilbertown Field and adjacent areas.

in the eastern Gulf Coast basin. In the Gilbertown area, Upper Jurassic and Lower Cretaceous units have a cumulative thickness of approximately 9,000 feet. The Norphlet is dominantly an eolian unit and contains associated alluvial fan, wadi, and playa deposits (Mancini and others, 1985). The Smackover, by comparison, represents development of an extensive carbonate ramp above the Norphlet Formation (Ahr, 1973) and was deposited in a spectrum of intertidal, oolite-bank, and open-marine environments (Mancini and Benson, 1980; Benson, 1988). Following Smackover deposition, widespread intertidal to shallow marine evaporite deposition resumed, as represented by the Haynesville Formation (Harris and Dodman, 1982; Mann, 1988). The Haynesville Formation is transitional from the evaporite and carbonate sedimentation that dominated the Late Jurassic to the siliciclastic sedimentation that dominated much of Cretaceous time in southwest Alabama. The Cotton Valley Group spans the Jurassic–Cretaceous boundary and contains mainly coarse-grained arkosic clastics of alluvial origin in southwest Alabama (Tolson and others, 1983). Above the Cotton Valley, Lower Cretaceous strata are dominantly siliciclastic deposits with redbeds that accumulated in alluvial, coastal, and shallow shelf environments and contain numerous oil reservoirs south of the Gilbertown area (Eaves, 1976).

Upper Cretaceous strata are subdivided into the Tuscaloosa Group, the Eutaw Formation, and the Selma Group (fig. 3). The Tuscaloosa Group contains marginal to open-marine siliciclastics with minor redbeds and produces oil southeast of the Gilbertown area (Mancini and Payton, 1981; Mancini and others, 1987). In the Gilbertown area, the Tuscaloosa Group is approximately 600 feet thick. The Eutaw Formation is composed of sandstone and a lesser amount of mudstone and accumulated in beach-barrier and inner-shelf environments (Frazier and Taylor, 1980; Cook, 1993); the Eutaw is approximately 300 feet thick in the Gilbertown area. The Selma Group is composed of chalk and marl and is locally thicker than 1,300 feet near Gilbertown. The Selma signals regional inundation of the Eutaw barrier shoreline and establishment of an extremely widespread, muddy carbonate shelf that persisted for the remainder of Cretaceous time (Russell and others, 1983; Puckett, 1992).

Tertiary strata ranging from Paleocene to Miocene in age are the youngest deposits preserved in the Gilbertown area and locally have cumulative thickness in excess of 2,000 feet (fig. 3). Paleocene and Eocene strata include the Clayton through Lisbon Formations, which contain a cyclic succession of coastal-plain and shallow-marine siliciclastics, lignite, and marl (Gibson and others, 1982; Mancini and Tew, 1993). Oligocene strata are composed mainly of shallow-marine carbonate rocks (Tew, 1992), and Miocene strata contain mainly unconsolidated sand and gravel (Szabo and others, 1988) that appear to be of fluvial origin.

Structure and Tectonics

Southwest Alabama contains a diversity of basement and salt structures (fig. 1). Deep tests penetrate the Eagle Mills Formation and crystalline basement mainly northeast of the Mississippi interior salt basin and in the general area of the Wiggins arch (Horton and others, 1984; Mink and others, 1985; Guthrie and Raymond, 1992). Basement structures define a series of ridge complexes, such as the Choctaw and Conecuh ridge complexes. These ridge complexes separate embayments, such as the Manila and Conecuh embayments. In general, early rift clastics of the Eagle Mills Formation are present near the axes of the embayments and are absent on the basement ridges. Although the details of basement structure are obscured by sparse well control and the thick sedimentary cover, the ridges and embayments appear to define a series of horsts and grabens that began forming during extensional collapse of the Appalachian–Ouachita orogen and were subsequently modified by deep erosion.

Among the most conspicuous structural features in southwest Alabama are the peripheral normal faults (fig. 1). The peripheral fault trend in Alabama contains four major fault systems, which are the Gilbertown, West Bend, and Pollard fault systems and the Mobile graben. These fault systems define a series of arcuate half grabens with southwestward to westward polarity. The Gilbertown and West Bend fault systems are closely related and can be considered together as a single half graben system. Using the terminology of Rosendahl (1987) and Scott and Rosendahl (1989), the Gilbertown–West Bend system, the Mobile graben, and Pollard fault systems can be classified as overlapping half grabens with similar polarity.

The peripheral faults mark the northeast margin of the Mississippi interior salt basin and have therefore long been considered salt structures (Murray, 1961). Indeed, salt seeps have been observed along some of the faults (Copeland and others, 1976). The overall configuration of the faults, however, suggests some influence on fault geometry by basement. For example, the major fault bend where the Gilbertown fault system connects with the West Bend fault system corresponds with the boundary between the Choctaw ridge complex and the Manila embayment (fig. 1). Moreover, the discontinuity between the West Bend and Pollard fault systems corresponds with the crest of the Conecuh ridge complex, and the southern terminus of the Mobile graben is near the Wiggins arch. A common interpretation is that basement influenced the original distribution of Louann Salt and influenced where the salt could flow, but basinward withdrawal of the salt was the ultimate determinant of structural style in the

overlying part of the sedimentary cover (Rosenkrans and Marr, 1967; Martin, 1978).

Numerous salt-cored anticlines are associated with extensional faulting in southwest Alabama. Most of the anticlines contain concordant salt pillows in the cores, and only one salt dome within the Mobile graben can be classified as a true piercement structure (Joiner and Moore, 1966). One of the most prominent folds in southwest Alabama is the Hatchetigbee anticline (Hopkins, 1917; Moore, 1971). The axial trace of the anticline strikes northwest, crudely parallel to the West Bend fault system, and intersects the Gilbertown fault system at nearly a right angle (fig. 2). The petroleum potential of the Hatchetigbee anticline was recognized long ago (Hopkins, 1917), but to date, only dry wells have been drilled in the crestal region of the structure.

Part of the reason that the crest of the Hatchetigbee anticline is thus far non-productive is that shallow and deep structure differ markedly. Indeed, the Hatchetigbee anticline is not apparent in the Smackover structure map (fig. 4). Instead, isolated anticlinal structures, many of which produce oil from the Smackover Formation, are developed near and along the bounding faults. Development of the Hatchetigbee anticline only in Cretaceous and younger strata is characteristic of turtle structures in the Gulf Coast basin, which are a type of inversion structure formed by withdrawal of salt beyond the flanks of what were originally localized basins (Hughes, 1968). In the case of the Hatchetigbee anticline, salt apparently withdrew into isolated anticlinal structures and footwall uplifts that form some important Smackover traps.

Subsurface mapping reveals the extreme complexity of the Gilbertown fault system (fig. 2). The fault system contains numerous normal faults and is part of a full graben, herein termed the Gilbertown graben, that is in places wider than 5 miles. The Gilbertown fault system forms the south side of the graben, and the Melvin fault system forms the north side. The pattern of fault traces in the Gilbertown area is evidence for complex structural relay between the Gilbertown graben and the half graben bound by the West Bend fault system.

Vertical separation of the top of the Eutaw Formation across the Gilbertown fault system is approximately 400 feet (fig. 2). Displacement apparently increases with depth and, along parts of the fault system, vertical separation of the Smackover Formation exceeds 1,500 feet (fig. 4). Increasing displacement with depth has been noted by several workers, all of whom have suggested that the peripheral faults and associated salt-cored anticlines in Alabama are synsedimentary growth structures (Current, 1948; Copeland and others, 1976; Wilson and others, 1976) similar to the well-known examples in the western part of the Gulf Coast basin (Wilhelm and Ewing, 1972; Galloway, 1986).

GILBERTOWN FIELD

Gilbertown Field occupies approximately 18 square miles in southern Choctaw County and extends along the length of the Gilbertown fault system (fig. 2). In the early days of Gilbertown, Hunt Oil Company owned the western part of the field, and Carter Oil Company owned the eastern part. The discovery well, drilled by Hunt Oil Company in the western part of the field, is the A. R. Jackson no. 1 well. It was the first commercial oil well drilled in Alabama and initially produced approximately 30 barrels of 19.6° gravity oil per day at a depth of 2,575 to 2,585 feet from fractured chalk of the Selma Group. According to Toulmin and others (1951), the well was drilled on the basis of seismic surveying. The first well drilled in the eastern part of the field by Carter Oil Company was the Sam Alman no. 1, which was completed in sandstone of the Eutaw Formation at a depth of 3,336 to 3,348 feet in 1945. The Alman well was reportedly sited on the basis of surface investigations (Toulmin and others, 1951). Most recent development in Gilbertown Field was carried out by Belden and Blake Corporation, who operated the field from 1976 to 1991. Since 1991, wells in Gilbertown have changed hands several times, and Union Pacific Resources, Incorporated is now principal operator. Union Pacific is considering the possibility of waterflooding in the Eutaw Formation, and other operators are considering drilling new wells in the Eutaw Formation and in the Selma Group.

To date, 212 wells have been drilled in Gilbertown Field. Of these, 101 wells have been completed in the Eutaw Formation, and 40 have been completed in the Selma Group. Fifty dry wells have been drilled, and 21 wells are used for disposal of salt water, which is produced in volume. Most of the salt water disposal wells were originally completed as oil wells in the Eutaw Formation and have since been recompleted for deep injection of produced formation water into the Tuscaloosa Group. Only six Selma wells have been converted for disposal of produced water.

The dominant hydrocarbon trapping mechanism in Gilbertown Field is fault closure, and normal faults with variable displacement are distributed sporadically in Eutaw and Selma reservoirs throughout the field (Bolin and others, 1989). Selma chalk is productive only in the western part of the field, whereas the Eutaw Formation is productive throughout the field (fig. 5). Early investigators identified three pools in Gilbertown Field: the lower Eutaw, upper Eutaw, and the Selma (Braunstein, 1953). The lower Eutaw pool is in a series of quartzose sandstone units with low resistivity and strongly negative spontaneous potential. The upper Eutaw, by comparison, is developed in glauconitic sandstone with low resistivity and weakly negative spontaneous potential. During the 1970s, producers recognized that the Eutaw comprises a multitude of

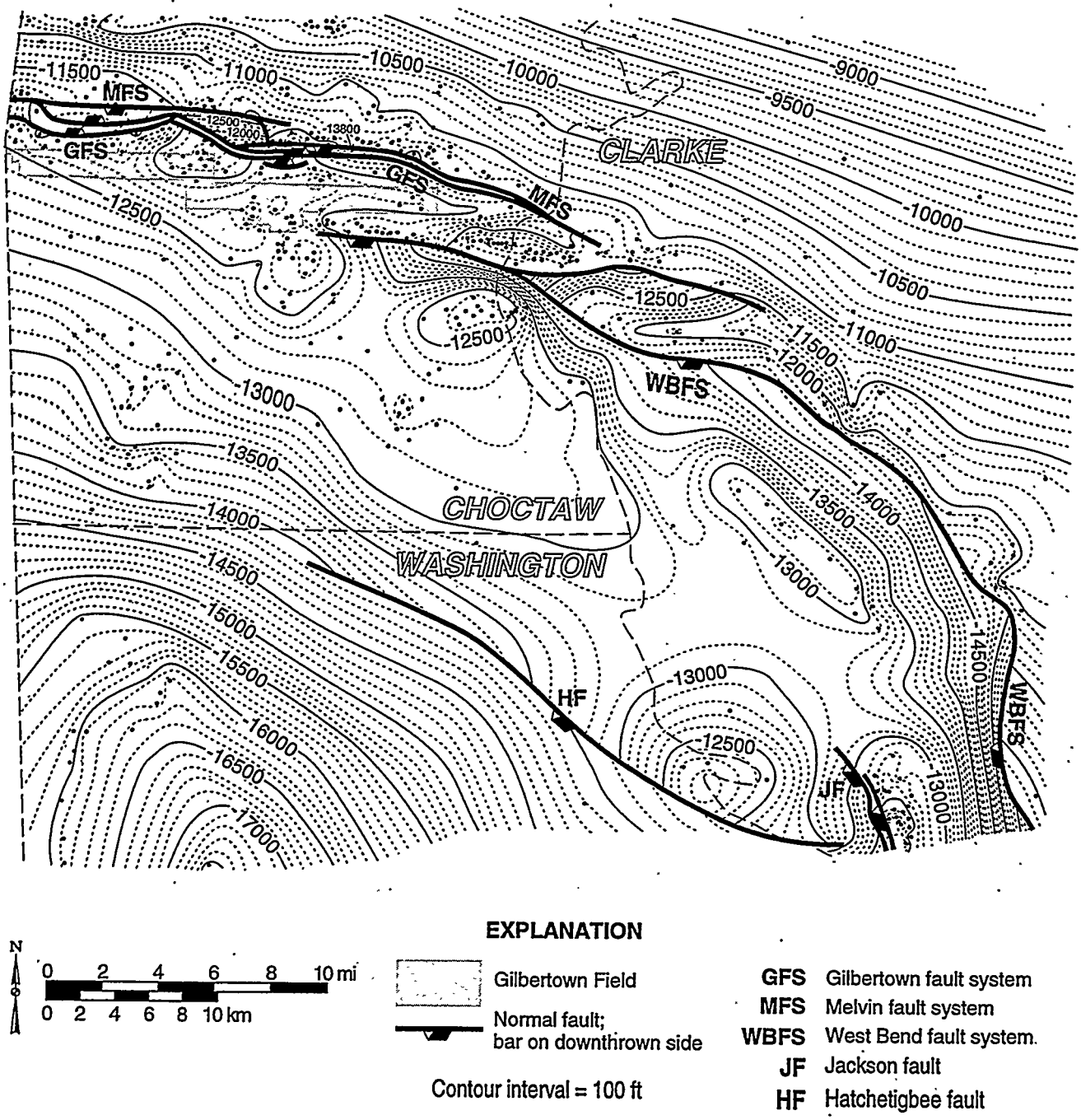

Figure 4.--Structural contour map of the top of the Smackover Formation (Jurassic) in the Gilbertown area.

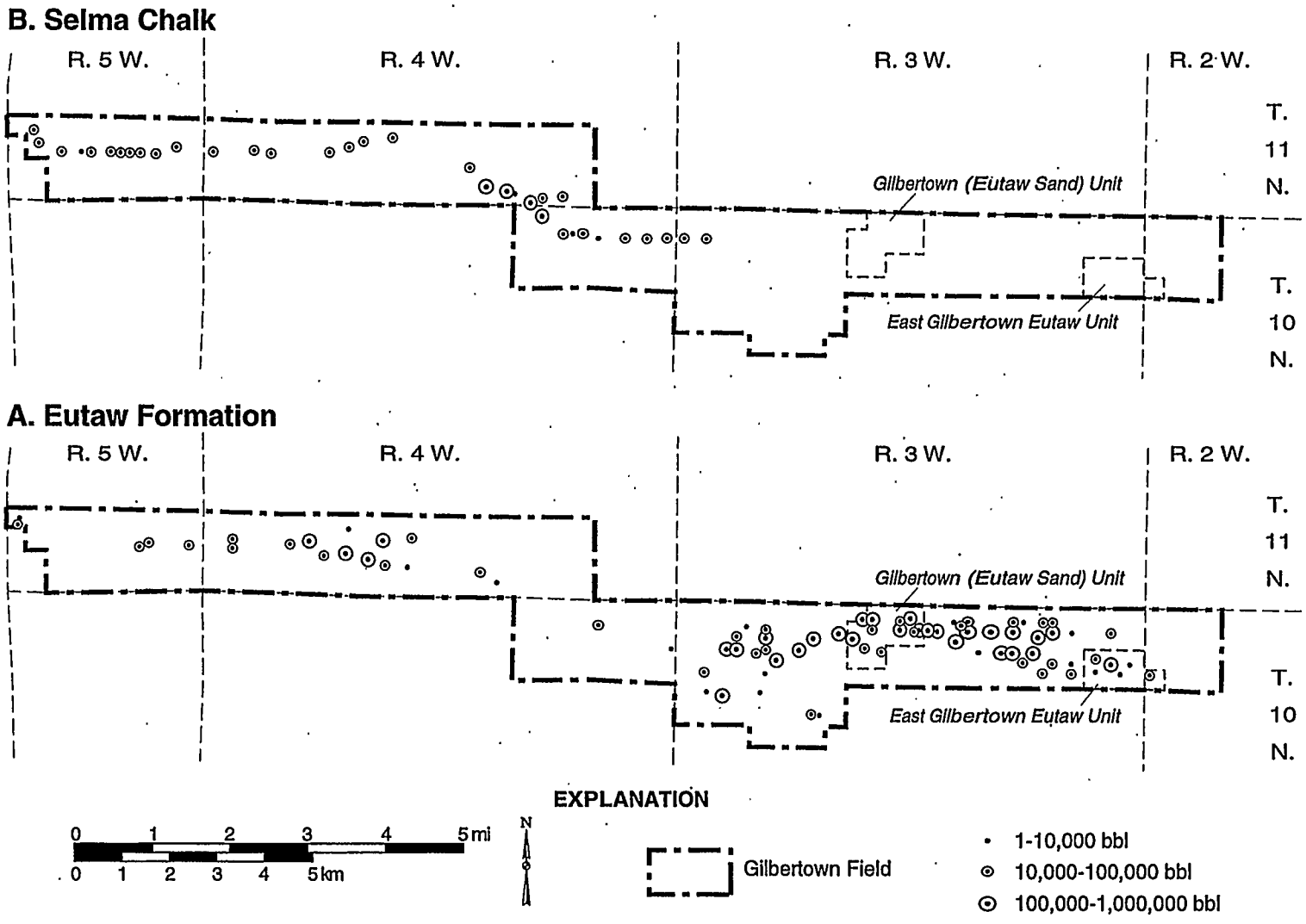

Figure 5.--Map of cumulative oil production of wells that have produced from the Selma Chalk and Eutaw Formation, Gilbertown Field.

sandstone lenses and may produce from as many as seven pools (Pashin and others, 1997). Porosity in Eutaw sandstone is typically 15 to 33 percent, and permeability ranges from 1 to 500 millidarcies; the pay column is generally less than 25 feet thick, and oil saturation is commonly 10 to 30 percent.

Selma production is strictly from faulted and fractured chalk, and productive intervals can be distinguished in many well logs by high resistivity and negative spontaneous potential (fig. 6). Productive zones in the Selma are as much as 150 feet thick and have exceptional effective fracture porosity, which is locally as high as 30 percent (Braunstein, 1953); estimates of permeability, oil saturation, and water saturation are not available. In most wells productive zones in the Selma are 400 to 700 feet above the Eutaw Formation. Even so, Selma and Eutaw production are mutually exclusive. Only one well has ever produced successfully from both formations.

Production in Gilbertown Field is by primary water drive, and waterflooding has been attempted only in the East Gilbertown Eutaw Unit and in the Gilbertown (Eutaw Sand) Unit (fig. 6). Oil and water are the principal fluids produced from the three pools in Gilbertown Field, and gas production is minimal. Cumulative oil production is now approaching 14 million barrels; 11.7 million have been produced from the Eutaw, and 2.1 million have been produced from the Selma. Oil production in Gilbertown reached a peak of 864,000 barrels in 1951 and has since declined markedly (fig. 7). In 1994, total oil production was 64,000 barrels and, of that, less than 1,000 barrels were from the Selma. In 1995 and 1996, total oil production was 36,000 and 29,000 barrels, respectively, and no oil was produced from the Selma. Gas production from Gilbertown Field has never exceeded 700 thousand cubic feet in a single year. By contrast, a large amount of water is produced from the field and, in 1985, water production reached a peak reported annual value of 10.3 million barrels.

The decline of oil production to marginally economic levels in Gilbertown Field makes assessment of improved recovery operations timely and practical. Detailed structural modeling is necessary to determine the nature and distribution of faults and fractures and, hence, what methods can be applied most effectively to Selma and Eutaw reservoirs. The following sections describe the concepts of area balance and strain in extensional structures and discuss how these concepts can be used to help design improved oil recovery strategies for Gilbertown and beyond.

AREA BALANCE AND STRAIN IN EXTENSIONAL STRUCTURES

The geometry of extensional and compressional detachment structures can be quantified using area balancing techniques (fig. 8). Area balancing provides a means of constraining structural cross sections, because layer-parallel transport and the position of the basal detachment can be calculated (Groshong, 1990, 1994; Epard and Groshong, 1993). Area balancing is, moreover, superior to commonly used length balancing techniques (Dahlstrom, 1969; Davison, 1986; Keller, 1990) because layer-parallel strain can be quantified (Groshong, 1994; Groshong and Epard, 1994, 1996). To employ these techniques, only basic stratigraphic data are required, preferably from several marker beds.

Area–depth relationships were first proposed for compressional structures by Chamberlin (1910) but were not applied to extensional structures until the study of Hansen (1965). Area–depth–strain relationships have been developed more recently and have been considered mainly in the context of sedimentary basin modeling (de Charpal and others, 1978; McKenzie, 1978). Until recently, however, area–depth–strain relationships were applied only to specific structural models that require basic assumptions about kinematics and rheological behavior that may be untestable or even erroneous when applied to a given set of structures (Groshong, 1994). Thus, the newly developed area balancing techniques developed by Groshong and Epard (1994) and Groshong (1994) offer a great advantage when analyzing area–depth–strain relationships, because they make no assumptions about rheology and kinematics and can be applied readily using basic measurements from geologic cross sections.

Two fundamental assumptions are used when area balancing cross sections. The first is that the cross-sectional area of a body of rock remains constant during deformation; this is the primary tenet of area balance originally put forth by Chamberlin (1910). The second assumption, which applies specifically to detached structures like those in the Gilbertown area, is that the structure must terminate downward at a basal detachment.

If the cross-sectional area of a structure is constant, then the area displaced above the basal detachment is equal to the area uplifted or downdropped relative to the original level, termed regional, so that:

$$S = DH, \qquad (1)$$

where S is displaced area, D is displacement distance of the block on the lower detachment, and H is depth to detachment. The area downdropped below regional in extensional structures is termed lost area. The sign convention is that displacement distance and the displaced area are negative in extensional structures and are positive in compressional structures. The cross section must obey the area–depth relationship at every structural level given by the depth, h, to a common reference level. Plotted on an area–depth graph (fig. 8), the relationship between structural levels is the straight line,

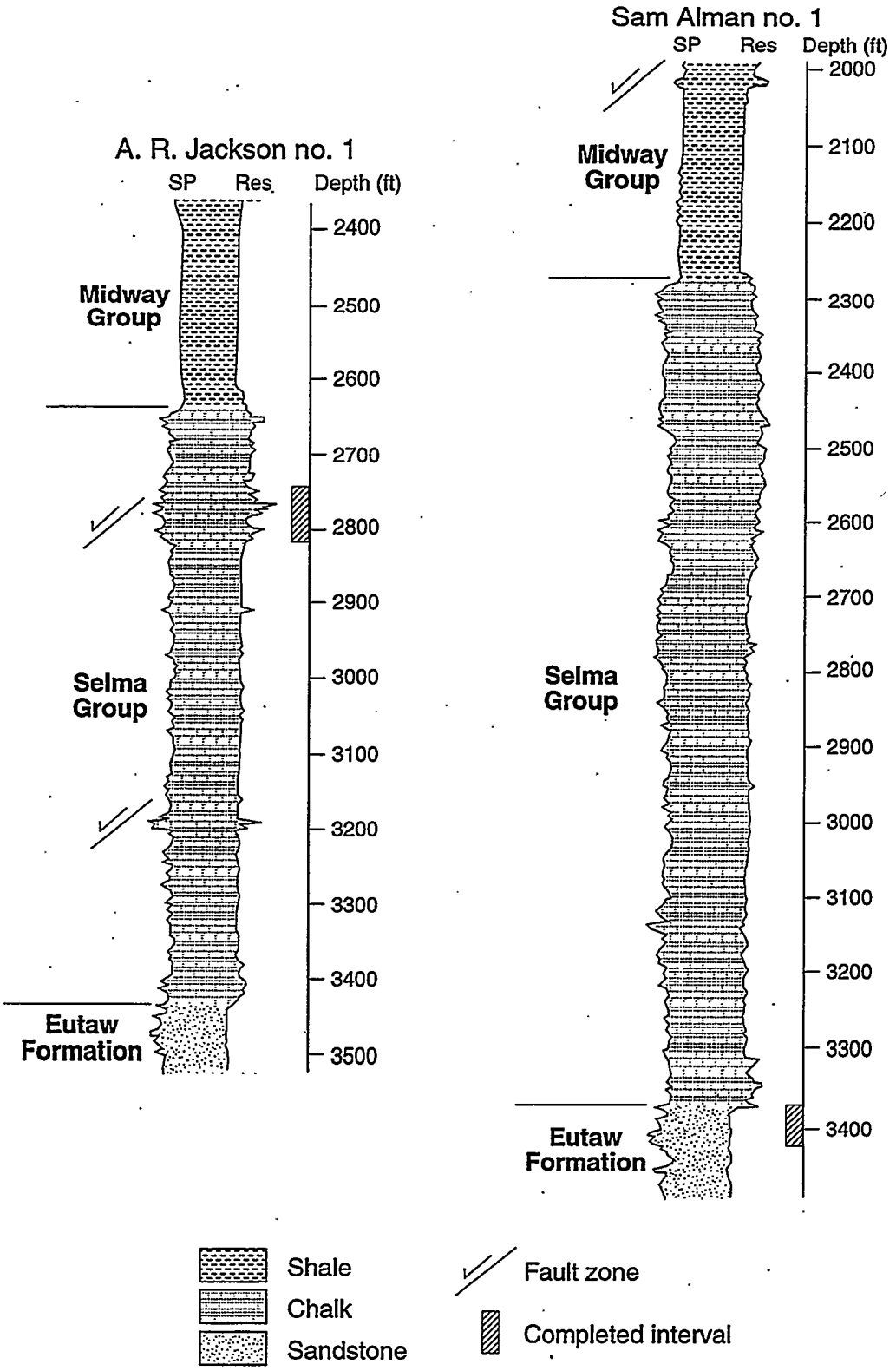

Figure 6.--Selected well logs showing characteristics of Selma and Eutaw reservoirs in Gilbertown field (modified from Braunstein, 1953).

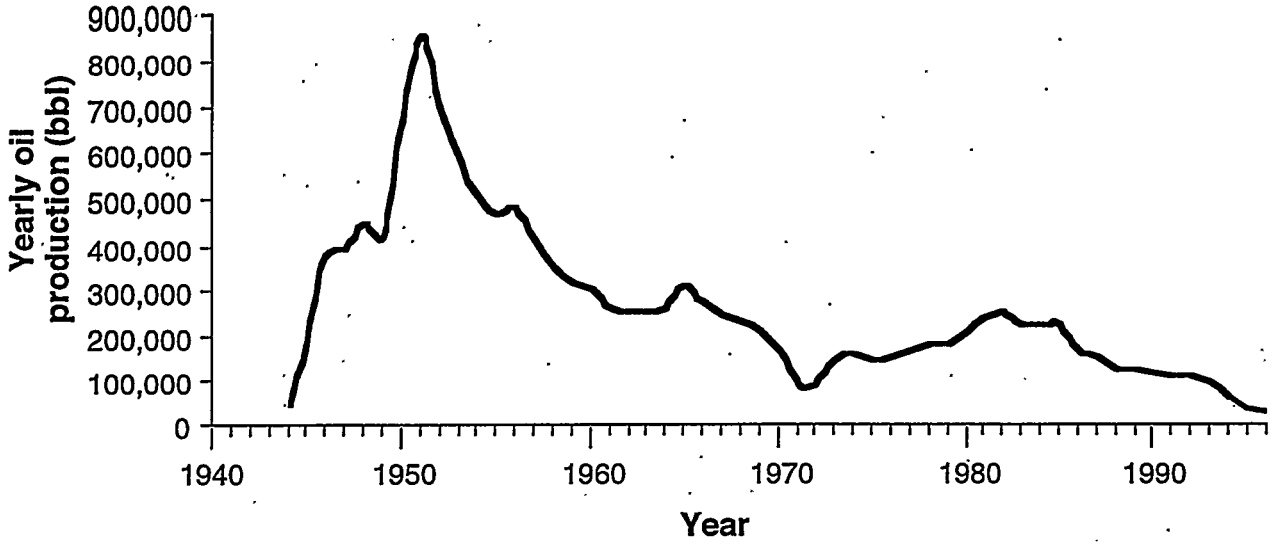

Figure 7.--Production history of Gilbertown Field showing major decline of oil production.

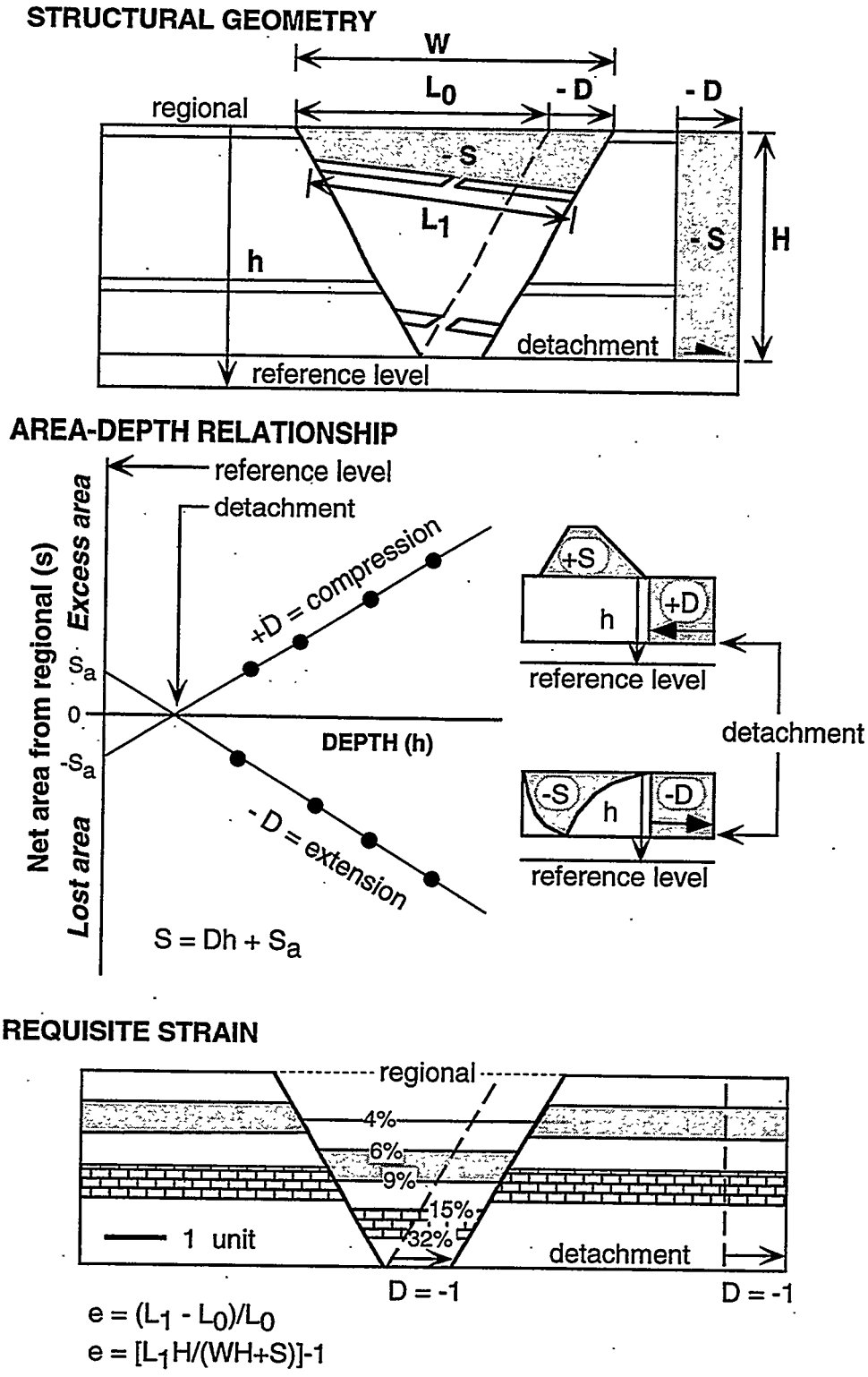

Figure 8.--Structural diagrams showing area-depth-strain relationships in extensional structures (modified from Groshong, 1994, Pashin and others, 1995).

$$S = Dh + S_a, \quad (2)$$

where S_a is the area intercept of the line. The slope of this line is the displacement distance on the lower detachment, and the detachment itself is located where lost or excess area projects to zero; the detachment may be above or below the arbitrary reference level. In a typical example, the displaced areas from multiple stratigraphic markers are plotted to define the area–depth line from which the displacement and depth to detachment are determined (fig. 8).

Beds within graben and half-graben systems typically undergo layer-parallel stretching strain, e, which can be quantified using area balancing techniques. Although some layer parallel strain can be ductile, the greatest proportion of the strain is by brittle faulting and associated fracturing. The layer-parallel strain is defined by the equation,

$$e = (L_1 - L_0)/L_0, \quad (3)$$

where the original bed length is L_0 and the observed bed length is L_1. The original bed length can be determined from area-depth relationships by

$$L_0 = W + D, \quad (4)$$

where W is the width of the graben at regional and D is extensional displacement which, according to the sign convention, is expressed as a negative value. A strain equation that can be used with measurements from geologic cross sections can be derived by solving (1) for D and substituting the result into (4) and then into (3). This transformation gives

$$e = [L_1H/(WH+S)]-1 \quad (5)$$

and is termed the requisite strain (Groshong and Epard, 1994). The term requisite strain is used because the derived value is the homogeneous strain required for the observed structural geometry to be area balanced.

Area balancing techniques have yet to be applied rigorously to hydrocarbon reservoirs. Thus far, these methods have been applied to well-constrained structures to validate the basic concepts (Groshong, 1994). Preliminary tests of the methodology in producing reservoirs have been made for coalbed methane fields in northern Alabama (Wang and others, 1993; Pashin and others, 1995). However, these tests have focused more on structural geometry than on the distribution of strain.

The fractured chalk of Gilbertown Field is an ideal place to test the importance of area–depth–strain relationships in the development and implementation of strategies for improved oil recovery from chalk and associated sandstone reservoirs. Abundant subsurface control provided by more than 50 years of drilling and seismic exploration enables tight constraint of reservoir geometry as well as reservoir properties. Additionally, the long production history of Gilbertown Field enables a thorough understanding of the relationship of oil and water production to structure and will aid greatly in predicting the effects of improved recovery strategies, such as infill drilling, horizontal drilling, waterflooding, and gas injection.

Determination and validation of extensional structural geometry through area balancing has broad application to fractured chalk and associated sandstone reservoirs. Indeed, all major chalk reservoirs in the United States and Europe are developed in extensional salt basins (Scholle, 1977). Furthermore, understanding detachment geometry is critical, because fracturing and second-order faulting in detached extensional structures is developed in large part by transport of the hanging-wall block through buried fault bends (McClay and Scott, 1991; Withjack and others, 1995). Structural analysis of Eutaw reservoirs will also be valuable because, although considerable research has been performed on reservoir heterogeneity in barrier-island deposits (Sharma and others, 1990a, b; Pashin and others, 1991; Kugler and others, 1994), investigators have not considered the effect of natural fractures on reservoir performance.

To balance structures in the Gulf Coast basin, however, the basic methodology requires further development. Area balancing techniques have yet to be applied to natural salt structures, which may present complications due to the typical regional elevation changes caused by salt movement. Furthermore, synsedimentary growth affects the slope of the line represented by equation (1), so a growth factor needs to be incorporated into the equation to derive accurate values of D.

Several investigators have considered the effect of stress in fractured chalk on fracturing and fluid flow (Teufel and Farrell, 1990; Teufel and Warpinski, 1990; Peterson and others, 1992), but the distribution of strain has yet to be examined. Examining strain will be a significant contribution, because natural fractures are a direct expression of strain and can indicate ancient and modern stress fields (Griggs and Handin, 1960; Stearns and Friedman, 1972; Watts, 1983). An important aspect of area balancing is that requisite strain can be calculated at multiple stratigraphic levels. Furthermore, if a closely spaced set of cross sections is constructed, the distribution of strain can be mapped at each level. As stated, the requisite strain calculation (equations 4 and 5) models only homogeneous strain between fault planes (fig. 8). However, curvature of beds between the fault planes can be calculated to determine how strain is distributed between faults (Narr, 1991; Lisle, 1994). If the relative distribution of strain is known, then requisite strain can be quantified precisely.

An enhanced knowledge of fracture architecture and strain distribution has immediate applications to the development and execution of improved oil recovery programs. For example, sites of exceptional strain can be identified that may contain untapped oil and can thus be prospective for infill drilling and horizontal drilling. Indeed, horizontal drilling has exceptional potential to increase oil recovery from fractured reservoirs (Selvig, 1991; McDonald, 1993). Additionally, understanding structural geometry and the distribution of strain can provide important information regarding the feasibility of infill, waterflood, and gas injection efforts. This is particularly critical in fractured chalk, where primary production and waterflooding can induce formation damage (Hermansson, 1990; Teufel, 1991, 1992). Recompleting wells in chalk may also present difficulties. For example, Simon and others (1982) indicated that oil-based drilling mud and fracture fluids help ensure integrity of fractured chalk reservoirs in the North Sea basin.

METHODS

This project employs an interdisciplinary approach that combines basic geologic methods, petrologic and geophysical methods, advanced structural modeling, subsidence and thermal modeling, and production analysis. This approach is establishing the importance of area balancing for understanding the distribution of strain, stress, and fractures in extensional fault systems and is further establishing how these factors determine the distribution and producibility of oil and associated fluids. With this increased understanding, the best decisions can be made regarding which technologies, such as waterflooding, gas injection, recompletion, infill drilling, and horizontal drilling, can be applied to improve oil recovery in fractured reservoirs in extensional terranes, thereby facilitating efficient management of oil fields in an economically sound and environmentally prudent manner.

Task 1: Subsurface Geology

More than 700 geophysical logs from the Gilbertown area were correlated to identify structurally significant stratigraphic markers and to identify faults. Markers in Jurassic through Tertiary strata were picked using resistivity and spontaneous potential logs. Faults were identified and vertical separations were quantified on the basis of missing section. Well locations, kelly bushings, depths of log picks, and vertical separations of faults were tabulated in a spreadsheet that was used to calculate the elevation of each marker and fault and the thickness of stratigraphic intervals between markers.

After logs were picked and elevations were calculated, a series of seven structural cross sections traversing the Gilbertown fault system and adjacent parts of the Hatchetigbee anticline was constructed. These cross sections are all perpendicular to the major fault traces and are designed to provide the best possible structural interpretation that can be used for area balancing. Well data were projected perpendicular to straight lines of cross section. After the cross sections were completed, area-balanced restorations were made of selected cross sections to characterize the structural evolution of the Gilbertown area. Detailed structural and stratigraphic cross sections were also made to determine the internal stratigraphy and depositional heterogeneity of the Selma Group and the Eutaw Formation.

Structural contour maps were made showing the elevation of all Jurassic through Tertiary stratigraphic markers in Gilbertown field and in adjacent areas; selected maps are included in this report. Using fault-cut information, faults were correlated among wells, and contour maps of fault surfaces were made. These maps aided greatly in constraining the structural contour maps because they show precisely the attitude, geometry, and horizontal separation of the faults in the reservoir intervals. In all, development of structural cross sections and maps was an iterative process in which each step of construction led to refinements.

To study stratigraphy and facies variations in the Eutaw Formation of Gilbertown Field, wells were correlated and six geologic cross sections were constructed using SP logs and a datum at the top of the Eutaw. Only the three strike cross sections are presented in this report; additional cross sections are in Pashin and others (1997). Perforated and producing zones were marked on a set of cross sections to indicate productive intervals in the Eutaw and thus to determine their distribution within the formation. Results of core analyses and core descriptions also were plotted on cross sections. Net sandstone isolith maps were then constructed for each stratigraphic interval of the Eutaw Formation using SP logs.

Cores from 22 wells in Gilbertown Field were suitable for study of the Eutaw Formation and the Selma Group. No continuous core is available. Only representative core samples from 1- or 10-foot intervals or sidewall cores could be used. Each core was described with the aid of a binocular microscope, and lithologic core logs were drawn for wells with samples representing a significant part of the Eutaw Formation. These core logs were then compared with a complete electric log of the Eutaw Formation to provide a composite core description.

Task 2: Surface Geology

The Gilbertown fault system has been mapped at the surface by several investigators (MacNeil, 1946; Toulmin and others, 1951; Szabo and others, 1988), but these maps are generalized and reveal little about

the distribution of fractures and other strain indicators. For this reason, an intensive investigation of the Gilbertown fault system and associated structures was conducted using standard field techniques.

Before field work began, the published literature and unpublished field notes were scanned for evidence of faulting at the surface in the Gilbertown area. A database of paleontologic field sites proved extremely useful, because the largest and freshest exposures in the field area are also classic fossil localities. Surface geologic methods in Gilbertown Field and vicinity include (1) observing the characteristics and measuring the orientation of faults and joints in outcrop, and (2) precise mapping of formations and members near faults.

For mapping and fracture analysis, every public road and quarry was examined, with a stop made at every fresh or large outcrop. Road-accessible river bluffs were examined in fall 1996, and suitable creek exposures were selected for study in winter 1997. River bluffs are the largest and freshest exposures and thus yield the most useful results. Creek beds and banks are less extensive but can be just as fresh as river bluffs; however, they are not readily accessible and can consume an inordinate amount of time. Roadcuts and small quarries are readily accessible, but most are deeply weathered. To help plot outcrop and fault patterns, all available remotely sensed imagery, including aerial photographs and satellite imagery, was examined.

Outcrops were examined closely to determine the presence of faults, joints, and contacts. The orientations of faults and fractures were measured with a Brunton compass, and the elevation of contacts was measured by altimeter or by reference to topographic maps. Outcrops were located on 7.5-minute topographic quadrangles, and data were recorded in level books. Photographs were taken to illustrate pertinent features. A detailed geologic map of the Gilbertown fault system and Hatchetigbee anticline was compiled that shows the distribution of all exposed formations and members. The orientations of more than 500 joints were measured and analyzed using basic statistical methods for directional data as discussed by Krause and Geijer (1987). Once the data were analyzed, joint modes were identified, and the vector-mean azimuth of each joint system at each field station was plotted on maps. Once plotted, the geologic significance of the joint systems was interpreted.

Task 3: Petrology and Log Analysis

Petrologic analysis of Eutaw reservoirs was performed to understand framework composition and the diagenetic factors affecting reservoir quality and geophysical log response. Thin sections were made and analyzed to determine primary rock composition and the composition and distribution of authigenic minerals. Six sandstone core samples representative of the various units were collected and used to prepare thin sections for petrographic study. Additional core samples then were collected from sandstone in the different units and additional thin sections were prepared. Each thin section was stained for calcite, sodium feldspar, and potassium feldspar. A blue tint in the glue was used to help identify porosity. Thin sections were point counted (approximately 300 points per slide) to determine framework grains, grain size, porosity, cement, and grain size.

To characterize formational fluids and thermal conditions in the Selma Group during diagenesis, samples of chalk, slickensides in the chalk, and sparry calcite in a vug were hand-picked under a binocular microscope. Each sample was packaged separately and sent for stable isotopic analysis for $\delta^{13}C$ and $\delta^{18}O$ at the University of Michigan Stable Isotope Laboratory. Carbonate samples weighing between 10 μg and 1 mg were placed in stainless steel boats. Calcite and dolomite samples were roasted at 380°C in vacuo for one hour to remove volatile contaminants. Aragonite was roasted at 200°C to prevent inversion to calcite. Samples were then placed in individual borosilicate reaction vessels and reacted at 72±2°C with 3 drops of anhydrous phosphoric acid for 8 minutes (12 minutes for dolomite) in a Finnigan "Kiel" extraction system coupled directly to the inlet of a Finnigan MAT 251 triple collector isotope ratio mass spectrometer. Isotopic enrichments were corrected for acid fractionation and ^{17}O contribution and are reported in ‰ notation relative to PDB. Samples have been calibrated to a best-fit regression line defined by NBS-18 and NBS-19 standards. Precision of data were monitored through daily analysis of a variety of powdered carbonate standards. At least six standards were reacted and analyzed daily, bracketing the sample suite at the beginning, middle, and end of the day's run. Measured precision was maintained at better than 0.1‰ for both carbon and oxygen isotope compositions.

The Eutaw Formation and Selma Group present disparate challenges for analyzing geophysical well logs. Low-resistivity glauconitic pay in the Eutaw Formation makes determination of porosity, oil saturation, and water saturation extremely difficult if not impossible because only spontaneous potential (SP) and resistivity logs are available for the reservoir intervals in nearly all wells. However, comparison of core logs, commercial core analyses, and completion data with the well logs indicates that some correlations between log signature, particularly spontaneous potential, and reservoir quality exist and can be quantified. Thus, all well logs of the Eutaw Formation in Gilbertown Field were digitized using Geographix Prizm software. Core-analysis data were depth-calibrated with the well logs, and least-squares regression analysis was performed to determine if correlations with data from well logs exist. Also,

statistical analysis of each reservoir interval proved useful for characterizing heterogeneity in the Eutaw Formation.

A more diverse log suite, including spontaneous potential, resistivity, dipmeter, and fracture identification logs (FILs), exists for wells that have produced from fractured chalk of the Selma Group. Many productive wells have high resistivity in fault zones, so spontaneous potential and resistivity curves were digitized using Geographix Prizm software. Dipmeter logs are available for some of the newer wells in Gilbertown Field and were compared with resistivity and completion data to help identify styles of deformation within productive zones. FILs were run on nearly all wells completed in the Selma Group since 1975 and provide additional information on the relationship between faulting and fracturing.

Task 4: Structural Modeling

The area balancing techniques described in detail in the introduction of this report were used to validate and restore the structural cross sections and to calculate requisite strain. To model growth strata, the basic area balancing techniques required modification. The lost-area method was used to calculate depth to detachment, displacement, and requisite strain in each cross section made under Task 1. Initial calculations of requisite strain were made to validate the structural cross sections. The cross sections were then revised, and new calculations were made to quantify reservoir-scale deformation that is below the level of detection. Next, data from other parts of the project were used to suggest how the remaining strain is distributed in Eutaw and Selma reservoirs.

Curvature analysis of bed and fault surfaces was performed using the Isomap module of the Geographix Exploration System to identify possible zones of enhanced fracturing in the Selma Group. First, structural contour maps were generated in Isomap using a minimum-curvature gridding algorithm. Next, second derivative surfaces were generated to model curvature. The derivative surfaces included total (mixed) curvature, as well as curvature in the strike (x) and dip (y) directions. Finally, three-dimensional models of the bed and fault surfaces were constructed using the 3D submodule of Isomap, and shaded representations of the second derivative surfaces were superimposed on the models to highlight zones of enhanced curvature.

Juxtaposition and seal diagrams (Allan, 1989; Knipe, 1992) were constructed to establish critical sealing relationships along strike of the faults. Juxtaposition diagrams, which show what formations are in contact along fault planes, were used by projecting hanging-wall and footwall elevations of contacts from the Eutaw Formation through the Naheola Formation to a vertical plane that parallels regional strike (east). Once the juxtaposition diagrams were complete, the sealing properties of each juxtaposed lithologic pair were evaluated on the basis of lithologic properties and patterns of hydrocarbon occurrence. Using this knowledge, the juxtaposition diagrams were then converted to seal diagrams.

Task 5: Burial and Thermal Modeling

To evaluate the thermal and maturation history of possible source rock units in the Gilbertown area, a burial history curve was constructed using data from the M. W. Smith Lumber, Incorporated 15–11 well (permit 3589). This burial history curve was made using BasinMod, which uses the decompaction curve of Falvey and Middleton (1981). Well 3589 was drilled down into the Werner Formation and thus provides the most complete stratigraphic record of any well in the Gilbertown area. Stratigraphic relationships indicate that no major disconformities exist in this well from the Jurassic through the Miocene. To analyze the complete subsidence history of the region, the Oligocene–Miocene section, which is preserved in parts of the study area but is not logged in wells, was added to the section.

Production data for 32 oil and condensate fields in the Gilbertown area were analyzed, and oil–gas production ratios were calculated to determine if the hydrocarbons in the Smackover of the Gilbertown area may have been locally derived. Samples were collected from well 3589 to process and make a vitrinite reflectance profile. To date, only samples from the Eutaw and Tuscahoma Formations have been analyzed successfully. Below these units, vitrinite reflectance data are extremely difficult to gather due to the extremely small size of vitrinite particles as well as thick successions of organic-poor redbeds.

Task 6: Production Analysis

In order to analyze production from Gilbertown Field, all production and completion data were compiled from the electronic database of the State Oil and Gas Board of Alabama. Water and gas production data are not available from most wells drilled before 1970, and oil production data for most early wells was reported annually. Therefore, only annual and cumulative oil production values were analyzed. Where possible, data were augmented using open-file information at the State Oil and Gas Board and with the files of Belden and Blake, Incorporated, which were donated to the Geological Survey of Alabama through the kindness of Charles D. Haynes of the University of Alabama. Production data were then analyzed to compare the decline characteristics of Selma and Eutaw wells. Cumulative production values of each well were then plotted on maps to identify the structural and depositional controls on well

performance. Completion data were analyzed to determine productive zones for each well, and the results were plotted on maps and cross sections.

ACCOMPLISHMENTS

During the past year, great progress has been made toward understanding the structure, stratigraphy, and controls on hydrocarbon recovery in Gilbertown Field. This chapter begins with a review of the structural geology of Gilbertown Field and adjacent areas. The discussion continues with the results of geologic mapping and an analysis of regional fracture systems. The subsequent discussion of burial and thermal history details the characteristics, distribution, and origin of hydrocarbon accumulations in the Gilbertown area. Next is a detailed treatment of reservoir geology in the Eutaw Formation and the Selma Group that includes stratigraphy, depositional environments, petrology, and the results of log analysis. The following section on structural modeling includes the results of area balancing, curvature analysis, and seal analysis. The final section of the chapter is on production analysis and synthesizes production and completion data with geologic data to suggest ways that hydrocarbon recovery in Gilbertown Field may be improved.

STRUCTURE OF GILBERTOWN FIELD

Numerous faults compose the Melvin, Gilbertown, and West Bend fault systems, and individual faults were labeled so they could be identified consistently (fig. 9). The Melvin fault system contains three major faults labeled A, B, and C. The Gilbertown fault system was subdivided into West Gilbertown faults A and B and East Gilbertown faults A and B. By comparison, the West Bend fault was mapped as a single fault.

Maps and cross sections establish that the Gilbertown and Melvin fault systems form a full graben extending the length of the map area, whereas the Gilbertown and West Bend fault systems form a horst that is restricted to the eastern end of the map area (fig. 9). The Gilbertown graben contains most of the faults in the map area and consists of two major segments containing faults that generally strike east. The western segment comprises Melvin fault A and the West Gilbertown faults, whereas the eastern segment contains Melvin faults B and C and the East Gilbertown faults. A structurally complex relay zone is present at the intersection of the two graben segments. The relay zone marks a lateral offset of the axis of the graben and is defined by faults striking southeast and northwest. The horst in the eastern part of the Gilbertown Field is formed principally by East Gilbertown fault A and the West Bend fault. The horst is an arcuate structure in which East Gilbertown fault A intersects the West Bend fault just beyond the eastern margin of Gilbertown Field.

Cross Sections

Cross sections establish that structural relationships change considerably with depth and along strike (figs. 10–18). For example, dip of the faults changes with depth. Interestingly, this change corresponds approximately with the base of the Selma Group. Below the Selma Group, faults generally dip 60°. In the Selma Group and younger units, by comparison, faults dip as gently as 45°. In some of the eastern cross sections, moreover, faults of opposite polarity nearly intersect at the level of the Smackover Formation. The cross sections also show evidence of considerable growth in the Cretaceous section and little or no growth in the Tertiary section. Because of insufficient data, however, evidence for growth in the Jurassic section is incomplete.

A key problem encountered when making cross sections is that direct control of the elevation of Jurassic stratigraphic units is limited along the axis of the graben. This is because Smackover reservoirs in the map area are primarily in footwall uplifts, so the major faults are typically penetrated no deeper than the Cotton Valley Group. To compensate for this problem, maps and cross sections were drawn by using vertical separations of fault cuts to estimate the elevation of the Jurassic units. Considering the probability of synsedimentary growth of the faults, however, Jurassic units may be slightly deeper than shown in cross section.

Each cross section reveals different nuances of structural style in the Gilbertown area. In cross section A–A', the westernmost cross section in the map area (fig. 11), Jurassic strata thicken southward and appear to roll over into West Gilbertown fault A. A significant footwall uplift in the Smackover and Haynesville Formations is apparent below the fault. Cretaceous strata roll over more strongly into West Gilbertown fault B than into fault A. These relationships suggest that, in this line of cross section, the West Gilbertown faults are the synthetic structures. Melvin fault A and West Gilbertown fault B apparently intersect in the Jurassic section, and the top of the Cotton Valley Group is anomalously deep.

Cross section B–B' traverses the center of the western graben segment but, unfortunately, is one of the least constrained cross sections (fig. 12). Vertical fault separations suggest that Jurassic strata are nearly

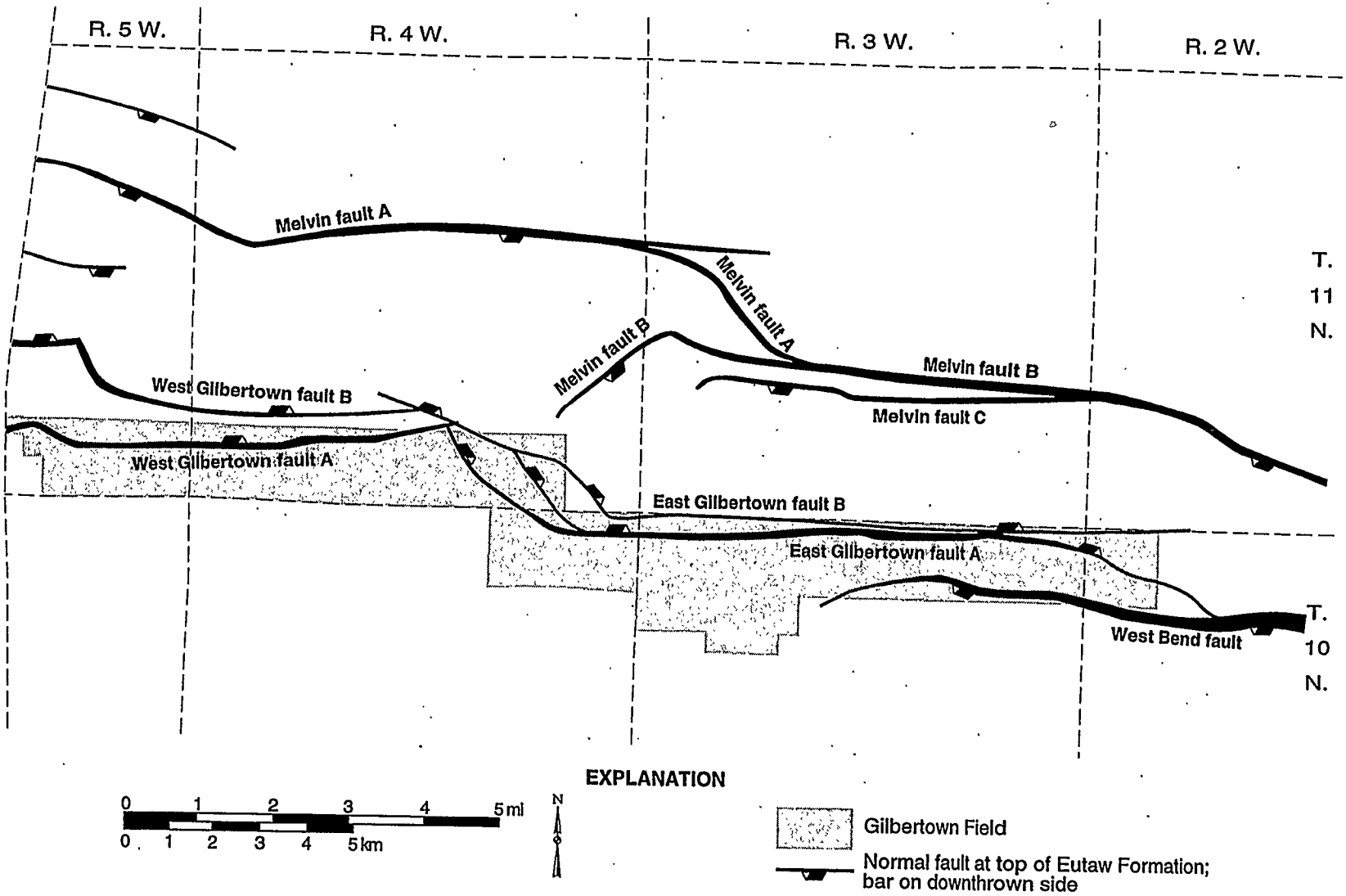

Figure 9.--Index map showing distribution and names of major faults, Gilbertown Field and adjacent areas.

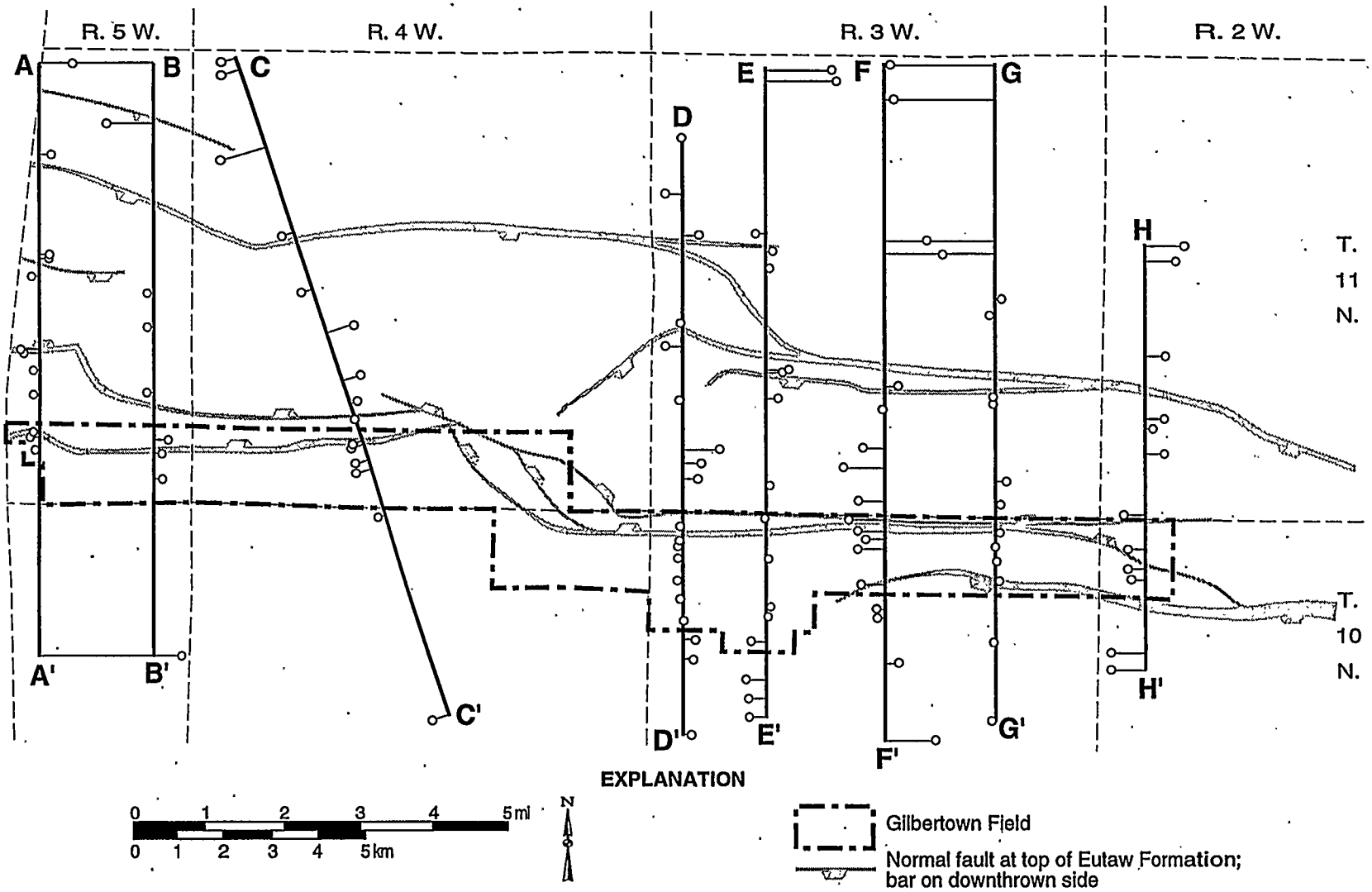

Figure 10.--Index map showing location of structural cross sections, Gilbertown Field and adjacent areas.

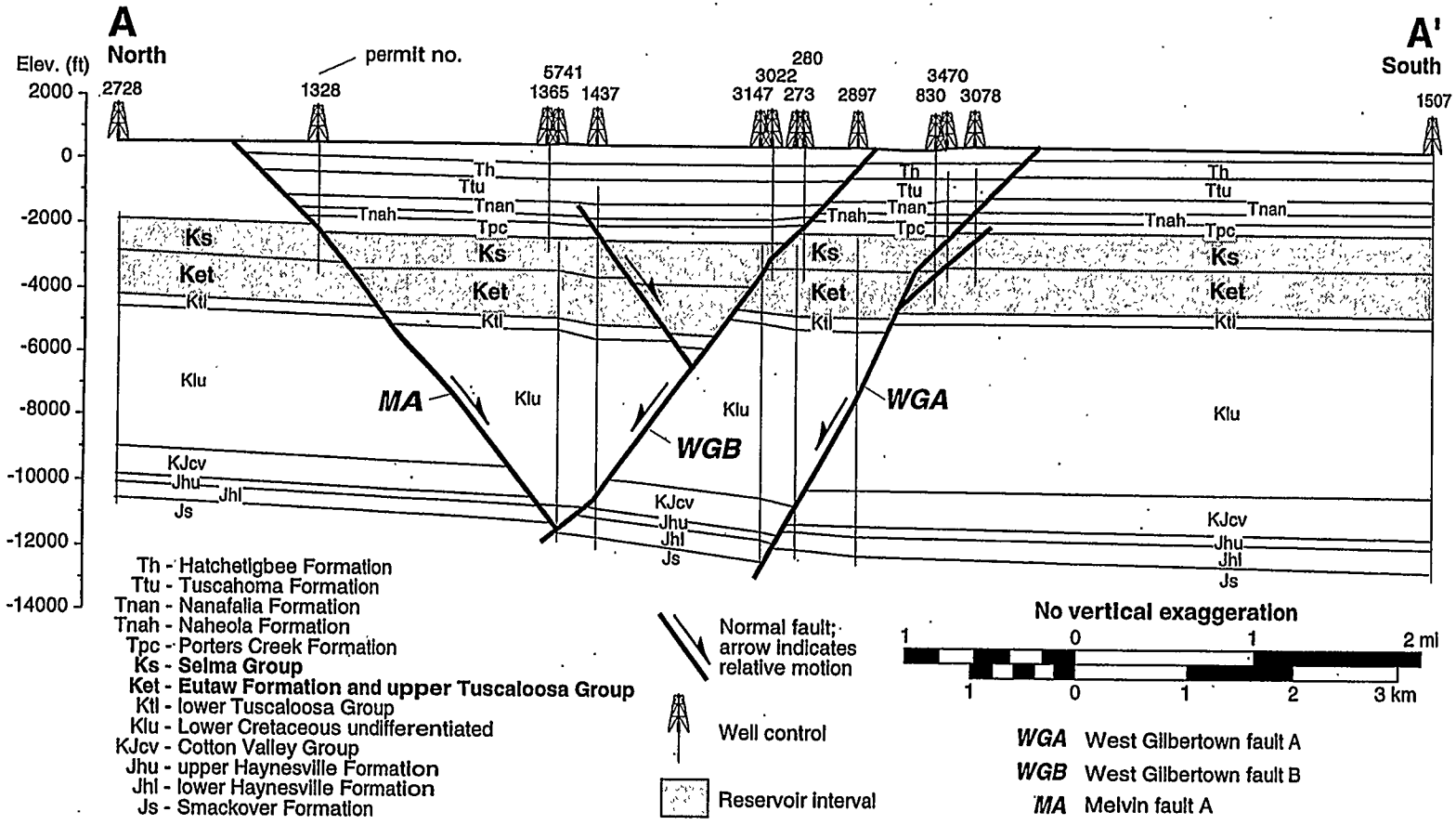

Figure 11.--Structural cross section A-A'. See figure 10 for location.

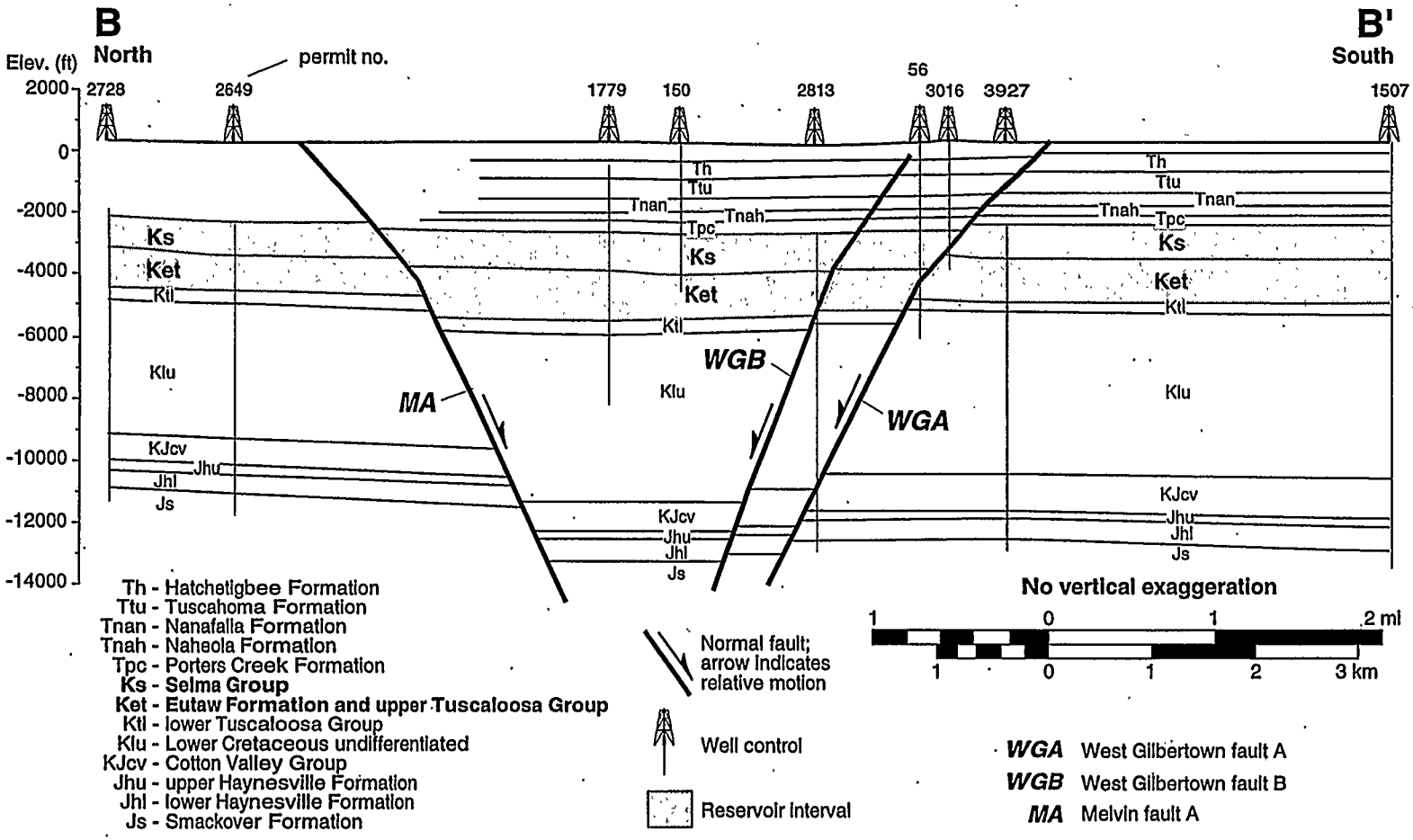

Figure 12.--Structural cross section B-B'. See figure 10 for location.

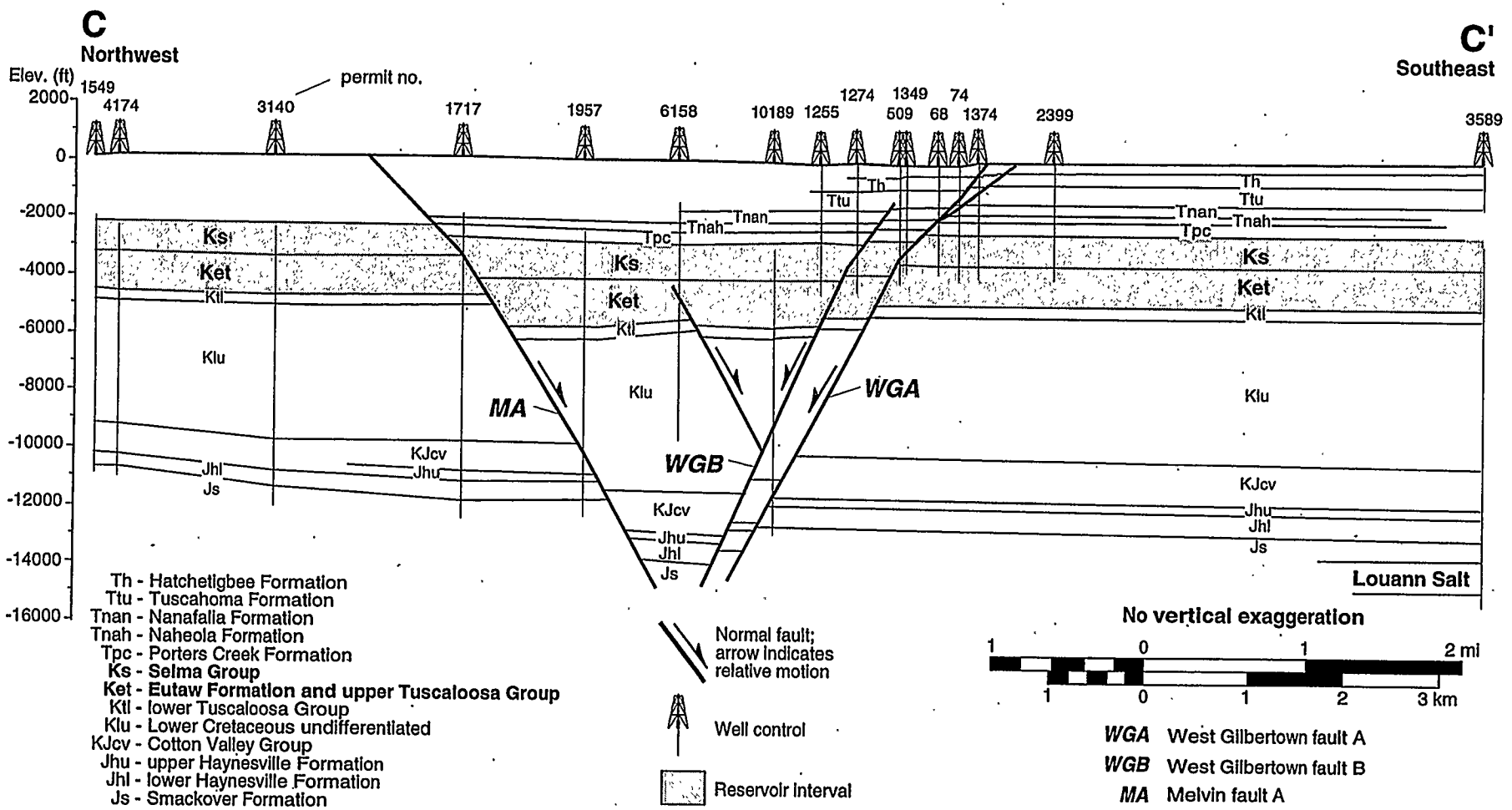

Figure 13.--Structural cross section C-C'. See figure 10 for location.

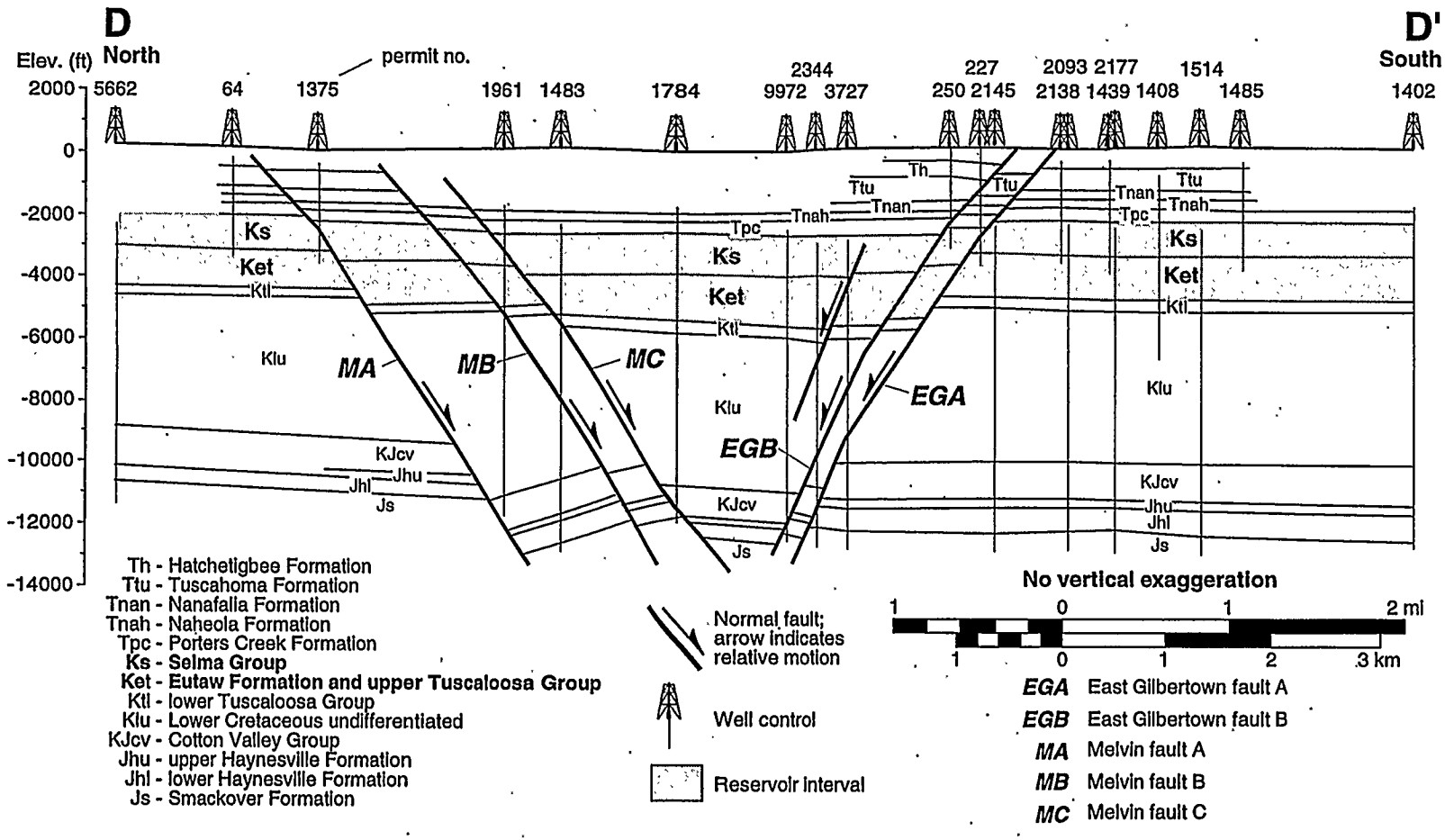

Figure 14.--Structural cross section D-D'. See figure 10 for location.

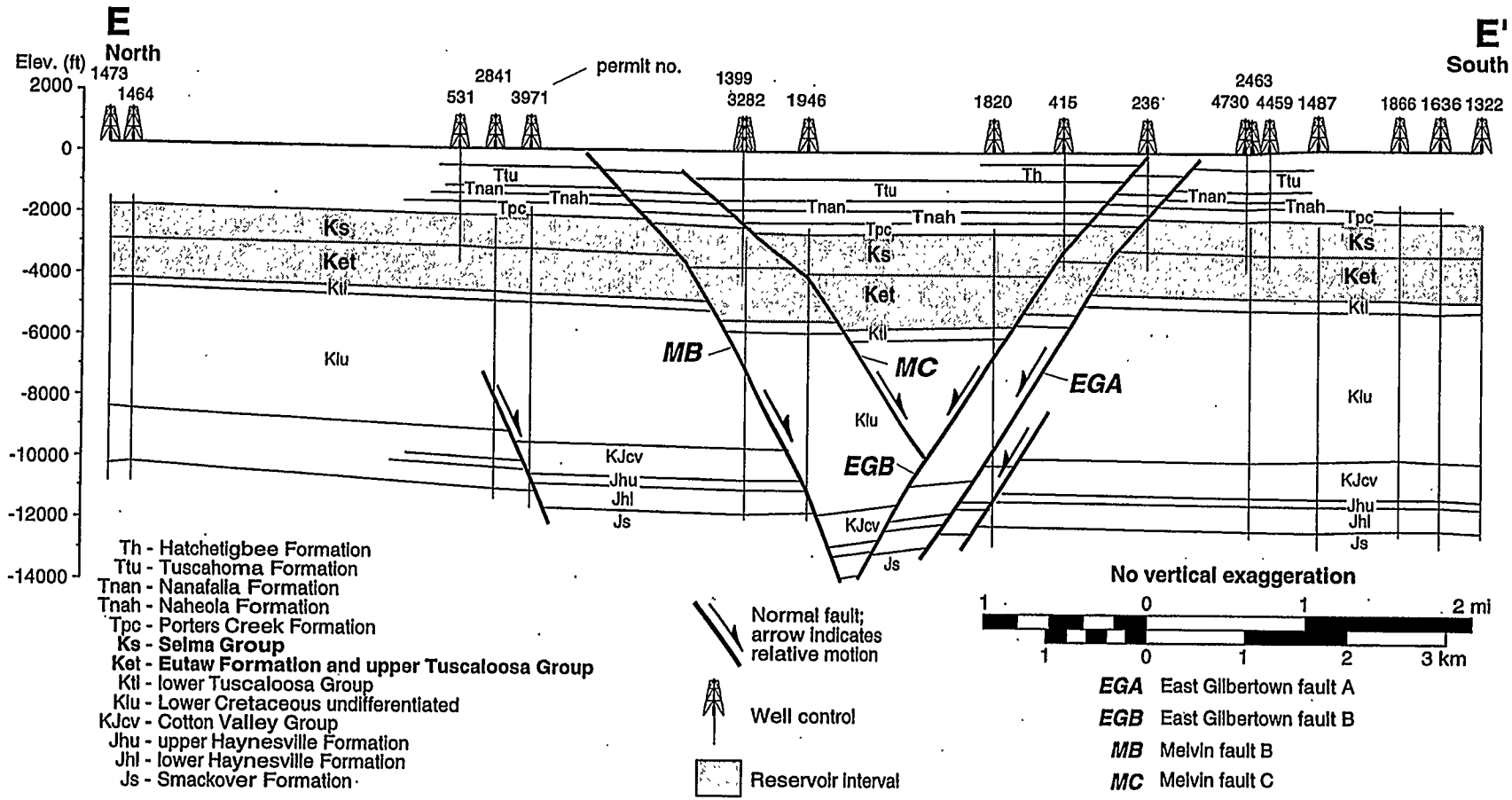

Figure 15.--Structural cross section E-E'. See figure 10 for location.

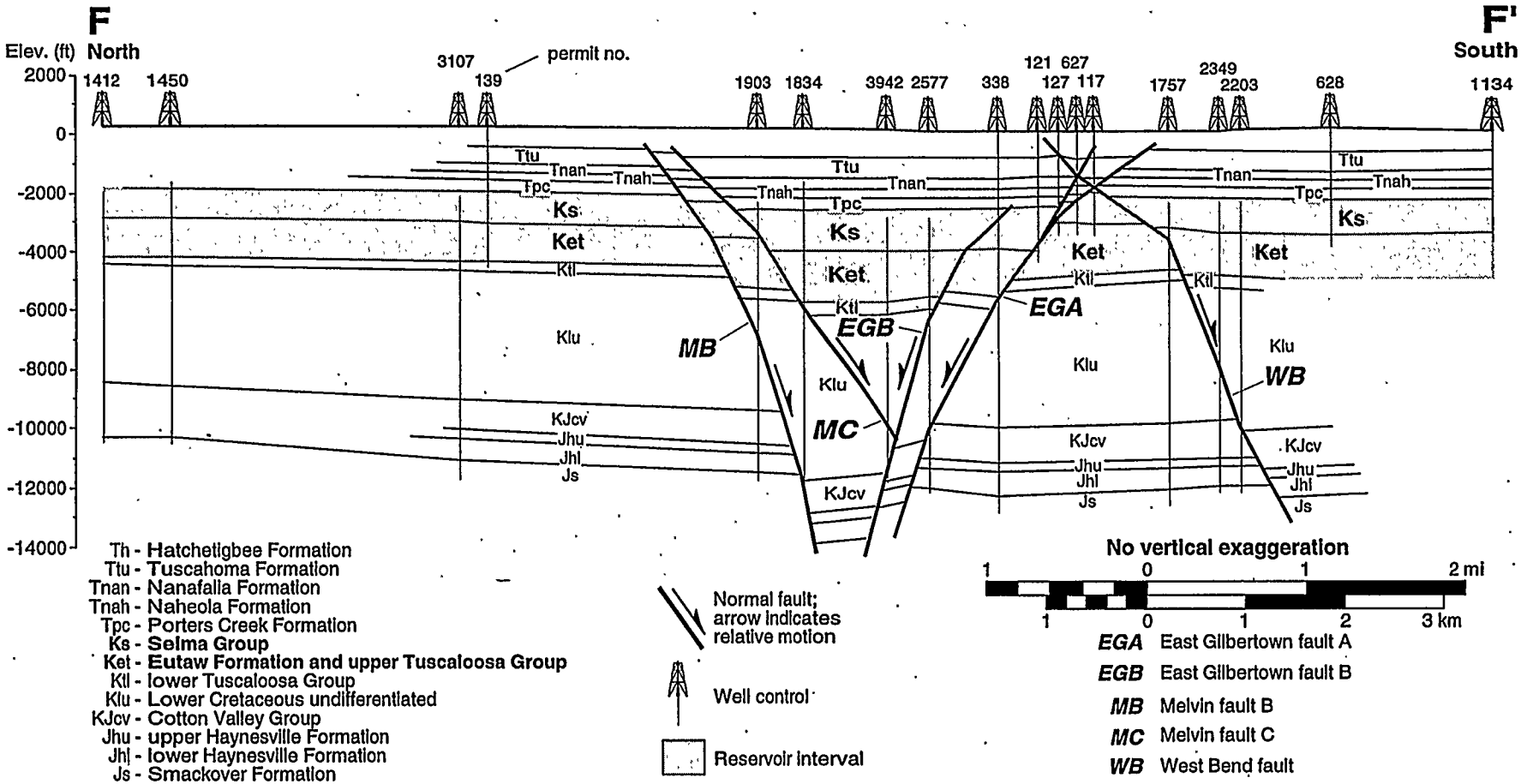

Figure 16.--Structural cross section F-F'. See figure 10 for location.

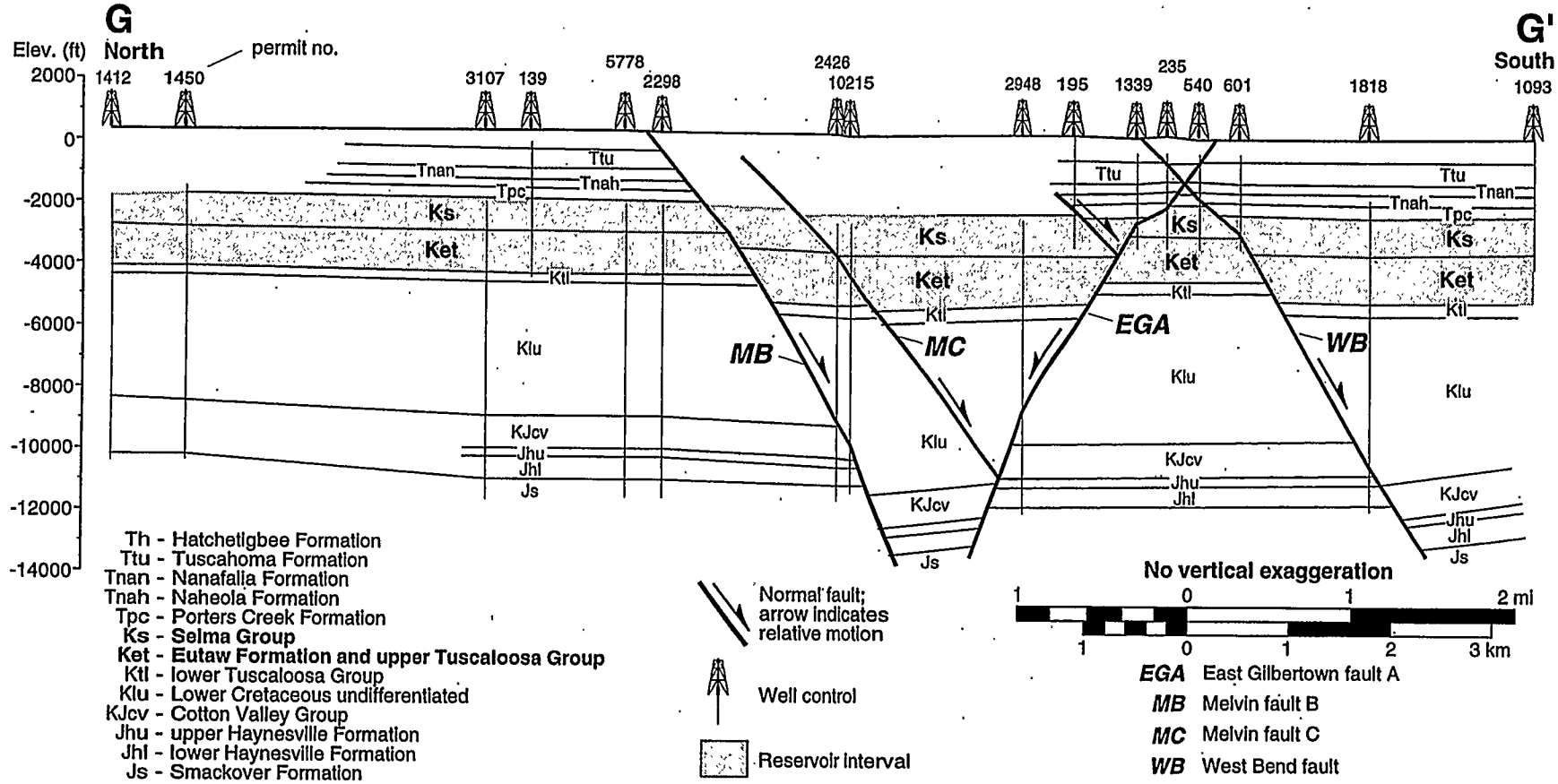

Figure 17.--Structural cross section G-G'. See figure 10 for location.

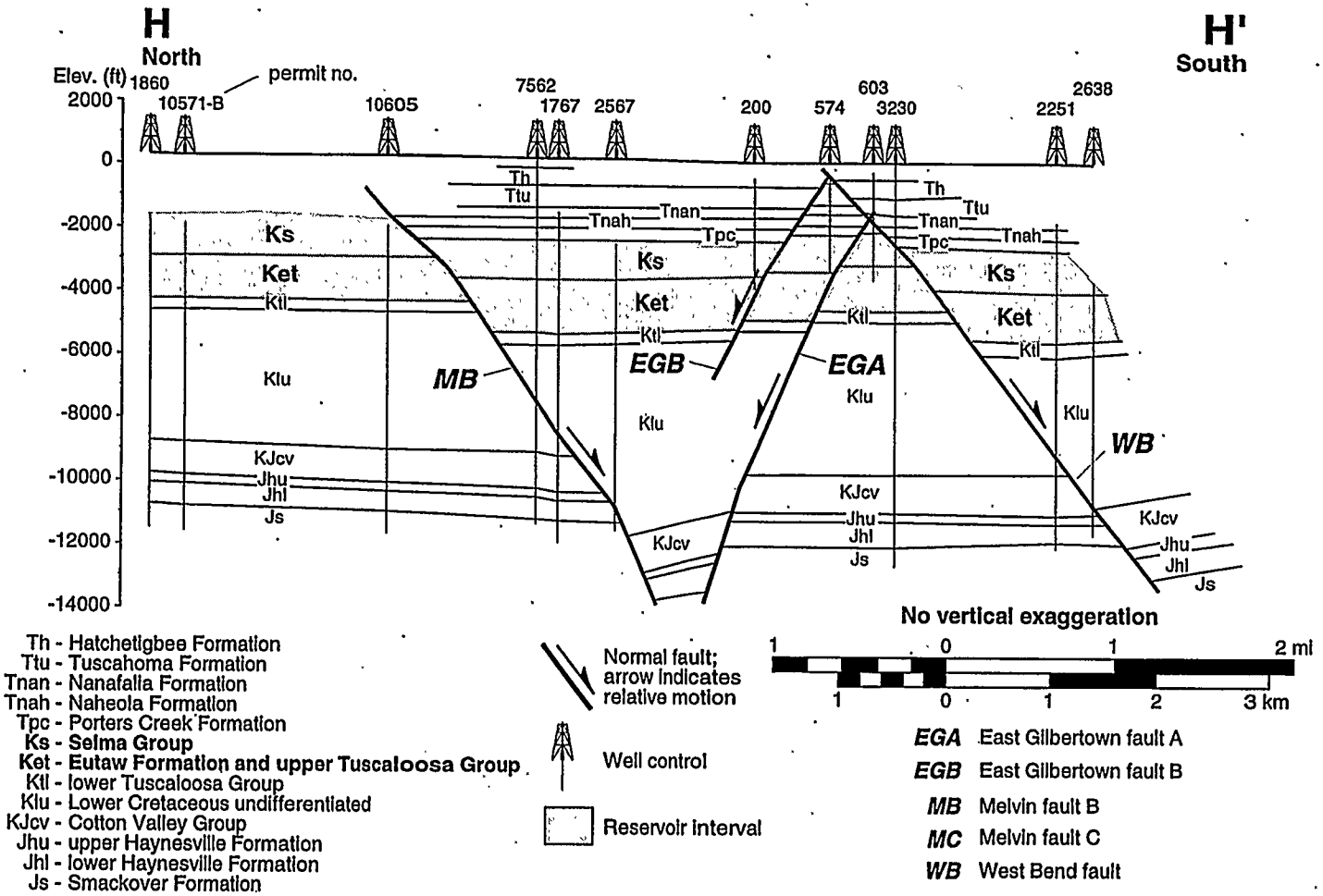

Figure 18.--Structural cross section H-H'. See figure 10 for location.

horizontal in the graben, and the overall geometry of the structure suggests that these strata roll over into the Melvin fault. Similar relationships are apparent in the Cretaceous section, and comparison of cross sections A–A' and B–B' indicate transfer of dominant fault slip from the West Gilbertown faults to Melvin fault A.

Cross section C–C' is better constrained than B–B' and is the only cross section that shows the position of the Louann Salt, which is only 868 feet thick at the south end of the cross section (fig. 13). Structural relationships in cross section C–C' are similar to those in B–B'. However, the graben is significantly narrower than in the cross sections to the west, and Cretaceous strata clearly roll over into Melvin fault A. One significant feature in cross section C–C' is a second-order fault in the central part of the graben that intersects West Gilbertown fault B. The fault has a vertical separation exceeding 300 feet in the Eutaw Formation, but no evidence for offset exists above the Eutaw, suggesting that the fault was a short-lived structure.

The only cross section traversing the relay zone connecting the two major segments of the Gilbertown graben is D–D', which contains all the major faults comprising the Melvin and East Gilbertown fault systems (fig. 14). South of the graben, a localized anticline and footwall uplift are developed in the Smackover and Haynesville formations but are not apparent in Cotton Valley and younger strata. Structure is very complex within the graben, and some strata dip as steeply as 17°. Jurassic strata roll over toward both sides of the graben but roll much more strongly into Melvin fault A than into East Gilbertown fault A. Conversely, Cretaceous strata roll more strongly into East Gilbertown fault A than into Melvin fault A, suggesting transfer of dominant slip from the north side of the graben toward the south during growth.

The western portion of the eastern graben segment is well shown in cross section E–E' (fig. 15). South of the graben, strata dip gently southward, and oil has been produced from a small anticline in the Jurassic section. In the graben, Melvin fault B nearly intersects East Gilbertown fault B at the level of the Smackover Formation, and Melvin fault C is interpreted to intersect East Gilbertown fault B in the Lower Cretaceous section. Jurassic strata clearly roll over into Melvin fault B, and the southernmost fault in the rollover system apparently penetrates strata no younger than Lower Cretaceous. Rollover folding is at best indistinct in the Cretaceous section. A fault with a vertical separation of 400 feet was identified in Lower Cretaceous and older strata north of the graben.

Cross section F–F' is the westernmost cross section showing the relationship between the horst and graben (fig. 16). Control on the orientation of Jurassic strata in the hanging wall of the West Bend fault does not exist. However, Cretaceous and Tertiary strata in the hanging wall dip southward, away from the fault, and no rollover fold is apparent. This configuration may reflect movement of strata above the shallow fault bend where dip of the fault increases from approximately 45° to more than 60°. Jurassic strata in the horst block are gently folded, and fault separations suggest that the lower Tuscaloosa Group dips significantly toward the north. Faults defining the horst block intersect just above the Selma Chalk. The faults apparently cross, forming a conjugate pair. Tertiary strata between the faults, moreover, are preserved in a complementary graben. The main graben is narrower than it is in cross section E–E', but otherwise, structural relationships are essentially the same.

Structural relationships in cross section G–G' resemble those in F–F', although some differences are worthy of mention (fig. 17). The shallow bend in the West Bend fault is less pronounced than in cross section F–F', and Cretaceous and Tertiary strata in the hanging wall dip away from the fault more gently. Control on the geometry of Jurassic strata in the horst block is minimal. As in cross section F–F', the West Bend fault and East Gilbertown fault A intersect to form a conjugate pair with a complementary graben, and the overall structural geometry is simpler in cross section G–G'. In the graben, East Gilbertown fault B is absent or has merged with East Gilbertown fault A. Another significant difference is that Jurassic and Cretaceous strata roll over, albeit weakly, into Melvin faults B and C.

H–H' is the easternmost cross section of the network (figs. 10, 18). The most notable difference between cross section H–H' and the previous two cross sections is the relationship between the West Bend fault and East Gilbertown fault A. In cross section H–H', the West Bend fault appears to be continuous, whereas the East Gilbertown fault is interpreted to terminate near or even abut the West Bend fault. No control exists on the position of the East Gilbertown faults in the deep subsurface. On the opposite side of the graben, Melvin fault C is absent or has merged with Melvin fault B. Additionally, Melvin fault B dips more gently in cross section H–H' than in other nearby cross sections.

Structural Contour Maps

A series of structure maps shows distinctive changes of the structural plan at different stratigraphic intervals. The deepest stratigraphic surface that could be mapped in the Gilbertown area is the top of the Cotton Valley Group (fig. 19). Most of the major faults composing the Gilbertown, Melvin, and West Bend fault systems are readily recognized (compare figs. 9 and 19). At the top of the Cotton Valley, however, the Gilbertown graben is wider than 2 miles only in a few places. Conversely, the horst is locally wider than 3 miles. Indeed, the only major fault that is absent is Melvin fault C, which is interpreted to intersect East Gilbertown fault B above the Cotton Valley Group.

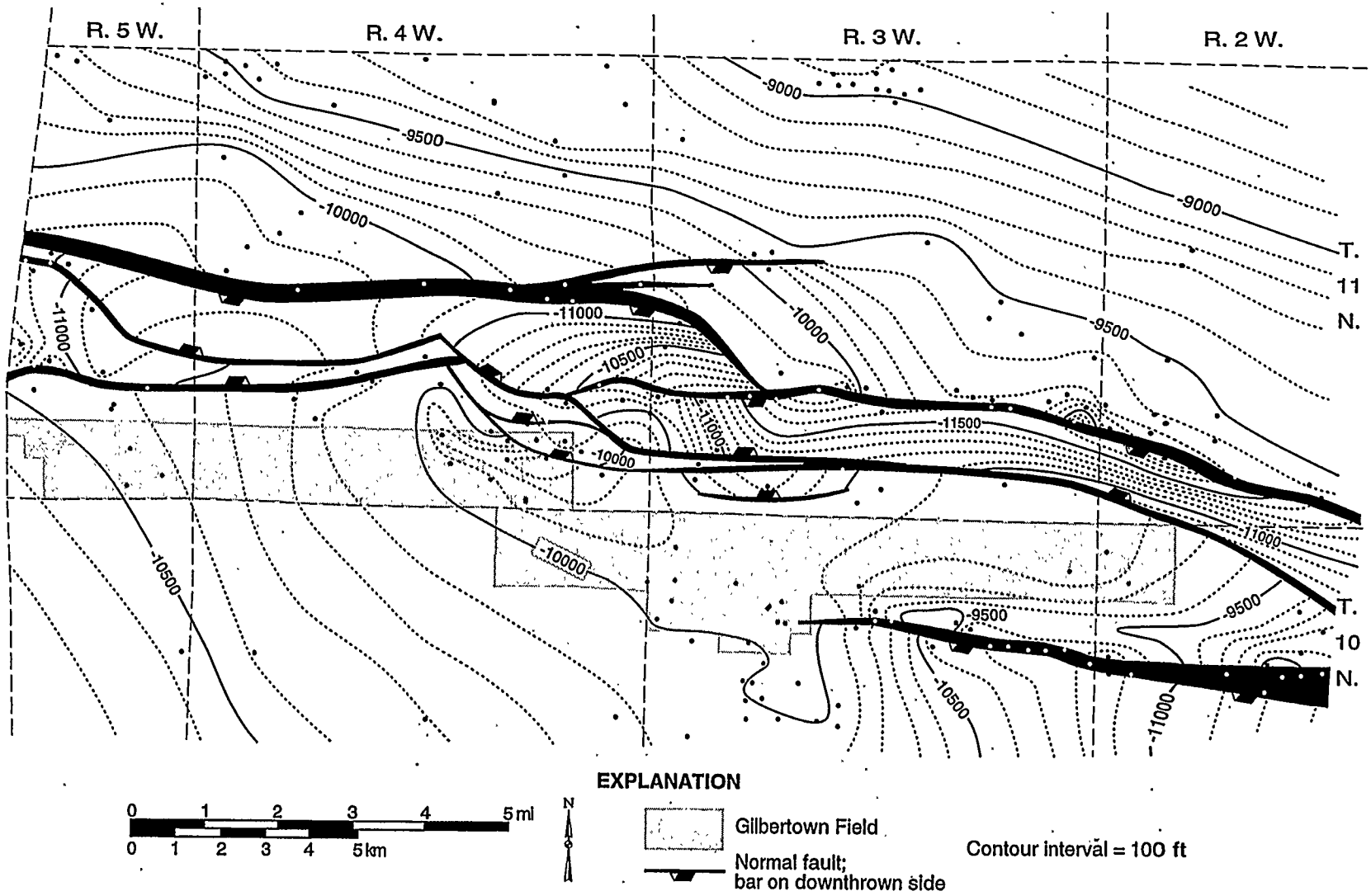

Figure 19.--Structural contour map of the top of the Cotton Valley Group, Gilbertown Field and adjacent areas.

Widely spaced contours in the western graben segment reflect the gentle dip of Jurassic strata in this area (fig. 19). In the relay zone and the eastern part of the graben, by contrast, the top of the Cotton Valley Group dips markedly toward the north as the Jurassic section rolls over into the Melvin fault system. The top of the Cotton Valley Group is essentially horizontal in the northwestern part of the horst and dips south–southeast in the eastern part. West of the horst, and immediately south of the relay zone, is a fault-bound anticline that has been drilled extensively in search of Smackover reservoirs.

A map of the top of the lower Tuscaloosa Group differs considerably from that of the top of the Cotton Valley Group (fig. 20). Throughout the map area, the graben is 2 to 3 miles wide, and the horst is only 1 mile wide. In contrast to the top of the Cotton Valley, the top of the lower Tuscaloosa appears to sag between the faults making up the western graben segment. The top of the lower Tuscaloosa sags less distinctly in the eastern segment, and rollover into the Melvin fault is not readily apparent. South of East Gilbertown fault A and in the horst, the top of the lower Tuscaloosa Group forms a simple fault-bound anticline. West of the horst, moreover, the fault-bound anticline that was drilled in search of Smackover reservoirs is absent.

The structural contour map of the top of the Eutaw Formation contains the tightest well control of any map presented in this study and provides a clear picture of the structural configuration of Eutaw sandstone reservoirs in Gilbertown Field (fig. 21). As with the top of the lower Tuscaloosa, the top of the Eutaw Formation sags between the faults defining the western graben segment. However, sagging at the top of the Eutaw is considerably less pronounced than at the top of the lower Tuscaloosa. The fault-bound anticline south of East Gilbertown fault A and in the horst has a configuration similar to that at the top of the lower Tuscaloosa Group. Immediately south of West Gilbertown fault A is a minor footwall uplift.

Structure at the top of the Selma Group differs from that at the top of the Eutaw Formation in some distinct ways (fig. 22). In the western part of the graben, widely spaced contours indicate that sagging is much less pronounced than in the Eutaw Formation and the Tuscaloosa Group. Structure is also subdued in the relay area and in the eastern graben segment. The most conspicuous difference is that the horst is extremely narrow, reflecting the near intersection of the West Bend fault and East Gilbertown fault A.

The top of the Nanafalia Formation was the youngest surface mapped (fig. 23). Structure in most of the map area resembles that at the top of the Selma Group, although Nanafalia structure is even more subdued. However, intersection of the West Bend fault and East Gilbertown fault A has resulted in markedly different structural patterns in the eastern part of Gilbertown Field. The West Bend fault appears to connect with East Gilbertown fault A, and the small graben formed by conjugate faults is mapped in the east-central part of the field.

Structural Evolution

The structural cross sections, structural contour maps, and area-balanced structural restorations provide evidence for a long and complex structural history in the Gilbertown area (fig. 24). Development of small anticlines and footwall uplifts in the Jurassic section indicate that some structures began developing early as sediment accumulated above the Louann Salt. Most of the anticlines finished forming prior to deposition of the Lower Cretaceous section. Although these structures were active only for a short time, they form significant traps for oil in the Smackover Formation. Footwall uplifts commonly form by accumulation of salt that has withdrawn from below the hanging wall (Hughes, 1968; Jenyon, 1986). Accordingly, the footwall uplifts provide the best evidence that the faults began forming during Jurassic time, because well control in the deepest parts of the Gilbertown graben is sparse. A lesser indication that faults began growing during the Jurassic is that the section is consistently thicker on the south side of the graben than on the north side (figs. 11–18).

Restoration of cross sections indicates that most of the deep structure that is present today had developed by the end of the Early Cretaceous (fig. 24). In the eastern graben segment and the relay zone, the deep structure is that of a half graben in which strata roll over into the Melvin fault system (figs. 14–18). In the western part, alternatively, Jurassic strata roll over into the Gilbertown fault system (fig. 11), indicating development of a half graben of opposite polarity, or are essentially flat-lying (figs. 12, 13), indicating early development of a full graben. The horst appears to have been an essentially passive structure during this time with only minor folding of the Jurassic section (figs. 16–18).

Half-graben development dominated the early structural history of the Gilbertown area, but restoration to the top of the Cretaceous reveals a change in overall structural style (fig. 24). In many parts of the graben where Jurassic strata roll over into the Melvin fault system, Upper Cretaceous strata do not exhibit rollover, suggesting that the half graben evolved into a nearly symmetrical full graben. This means that the half-graben rollover began collapsing as the rate of displacement on synthetic and antithetic faults became equal. Locally, however, half-graben formation continued through the Cretaceous. In cross section A–A', for example, Jurassic and Cretaceous strata roll over into the Gilbertown fault system (fig. 11). In the relay zone, by contrast, Jurassic strata roll over into the Melvin fault system, whereas Cretaceous strata roll over into the Gilbertown fault system, thus

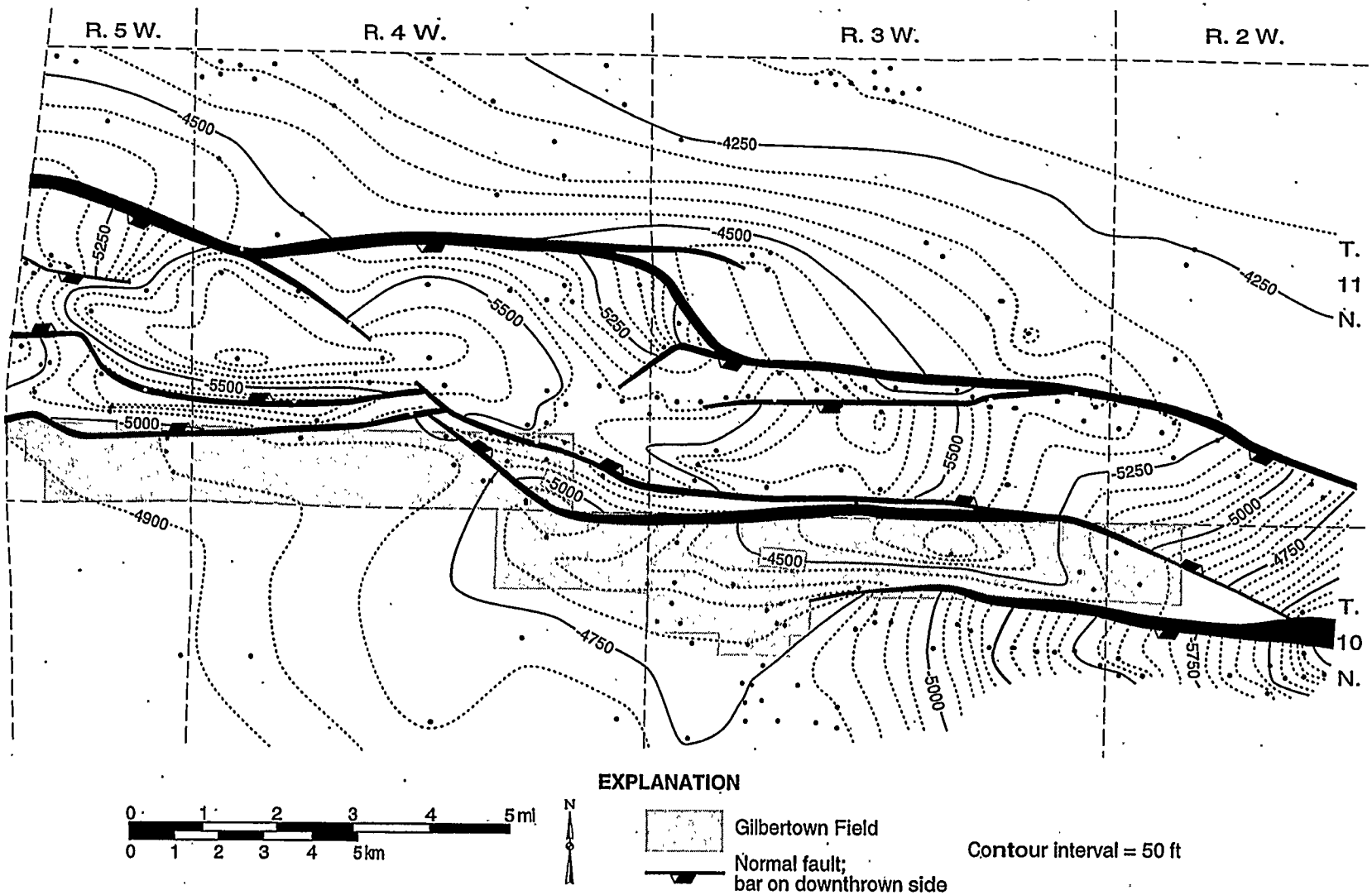

Figure 20.--Structural contour map of the top of the lower Tuscaloosa Group, Gilbertown Field and adjacent areas.

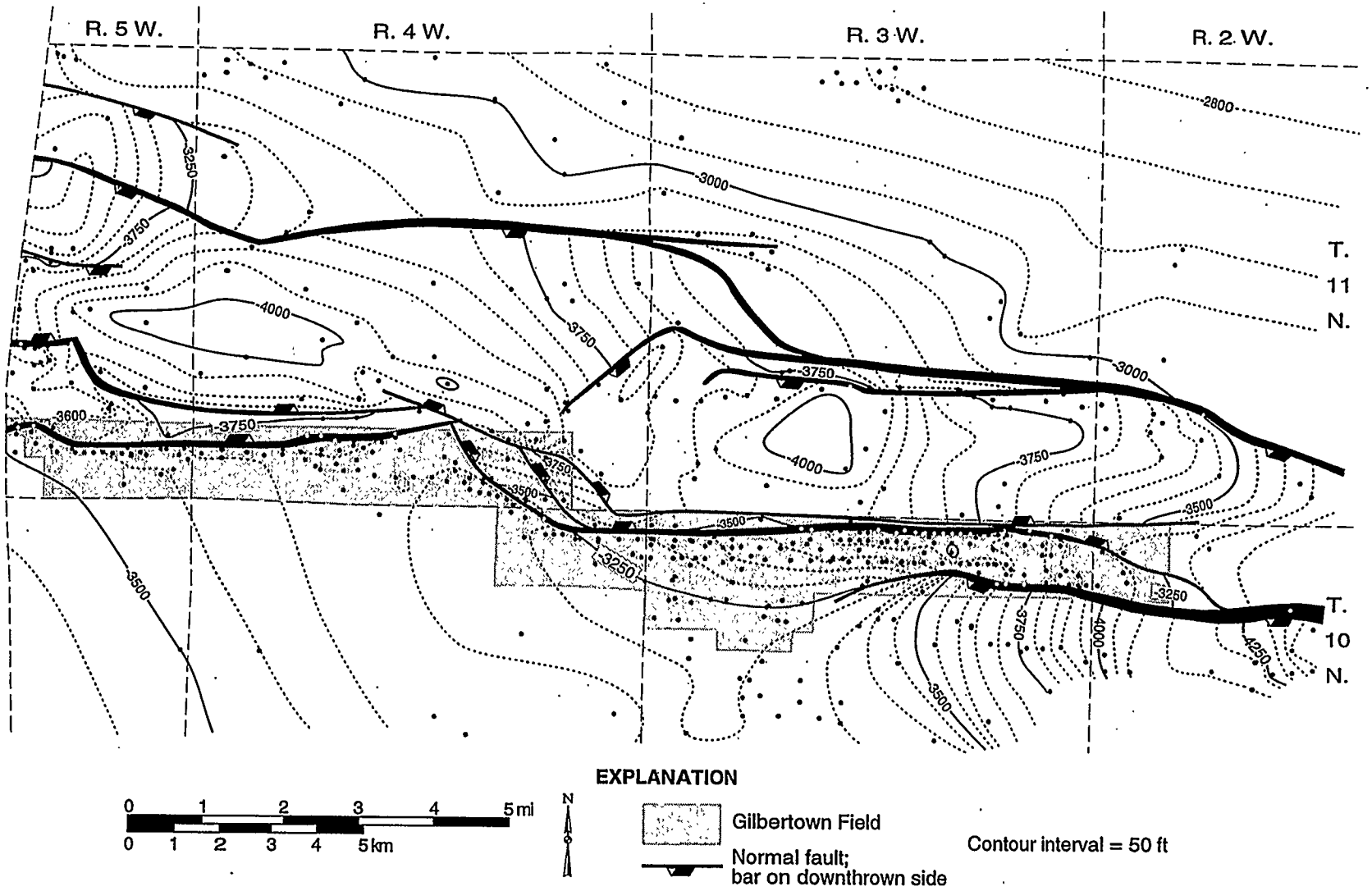

Figure 21.--Structural contour map of the top of the Eutaw Formation, Gilbertown Field and adjacent areas.

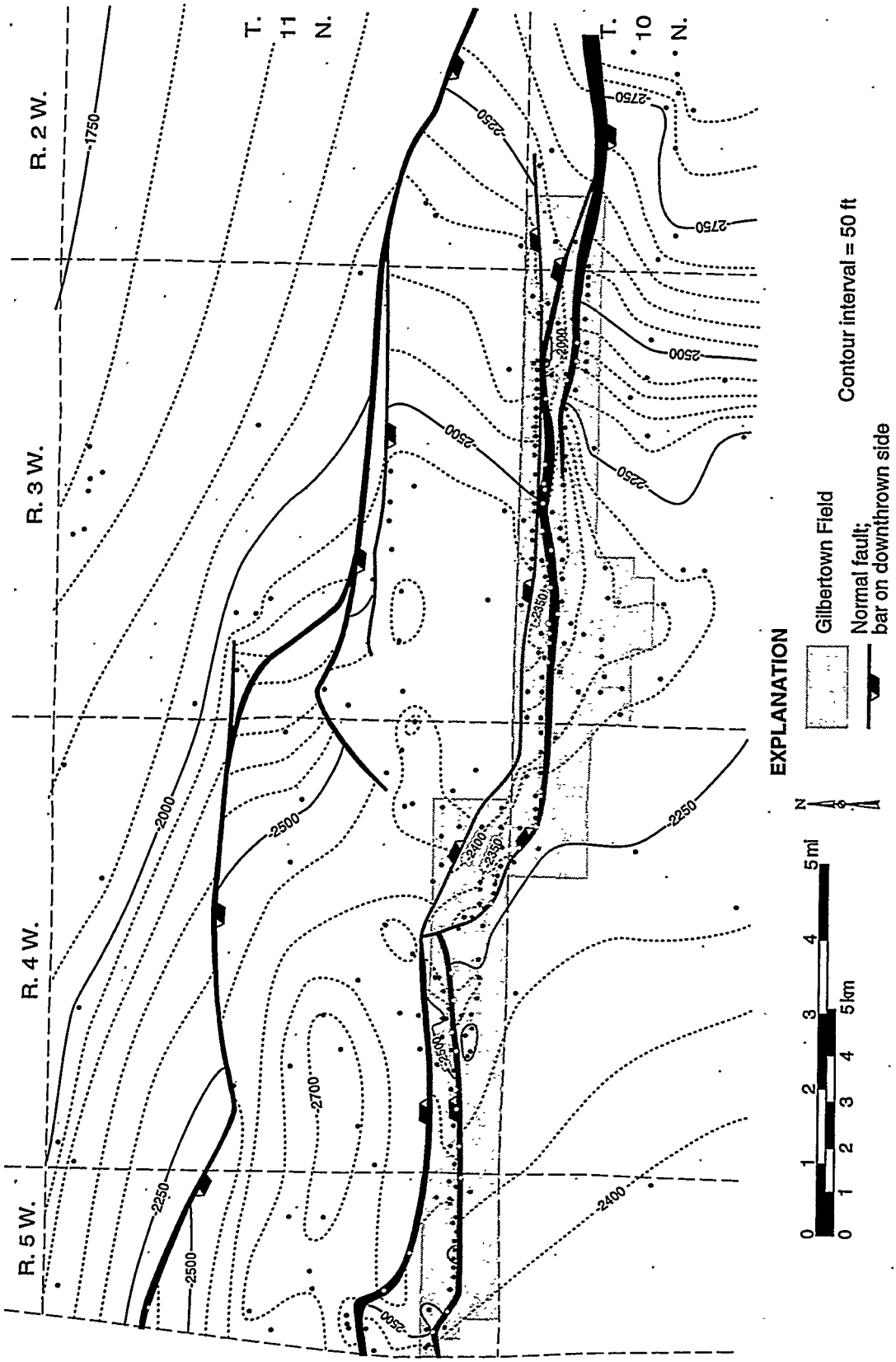

Figure 22.--Structural contour map of the top of the Selma Group, Gilbertown Field and adjacent areas.

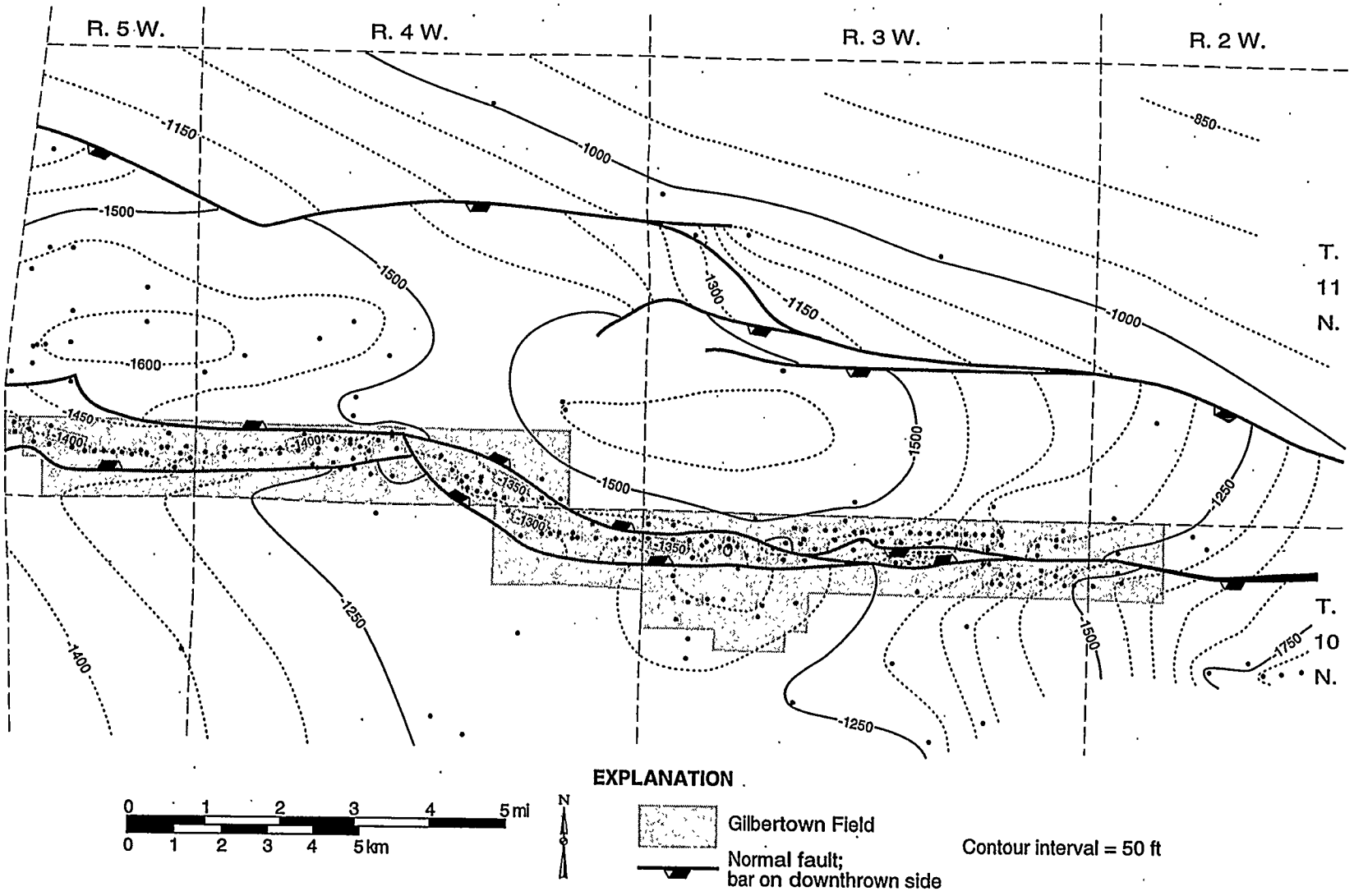

Figure 23.--Structural contour map of the top of the Nanafalia Formation, Gilbertown Field and adjacent areas.

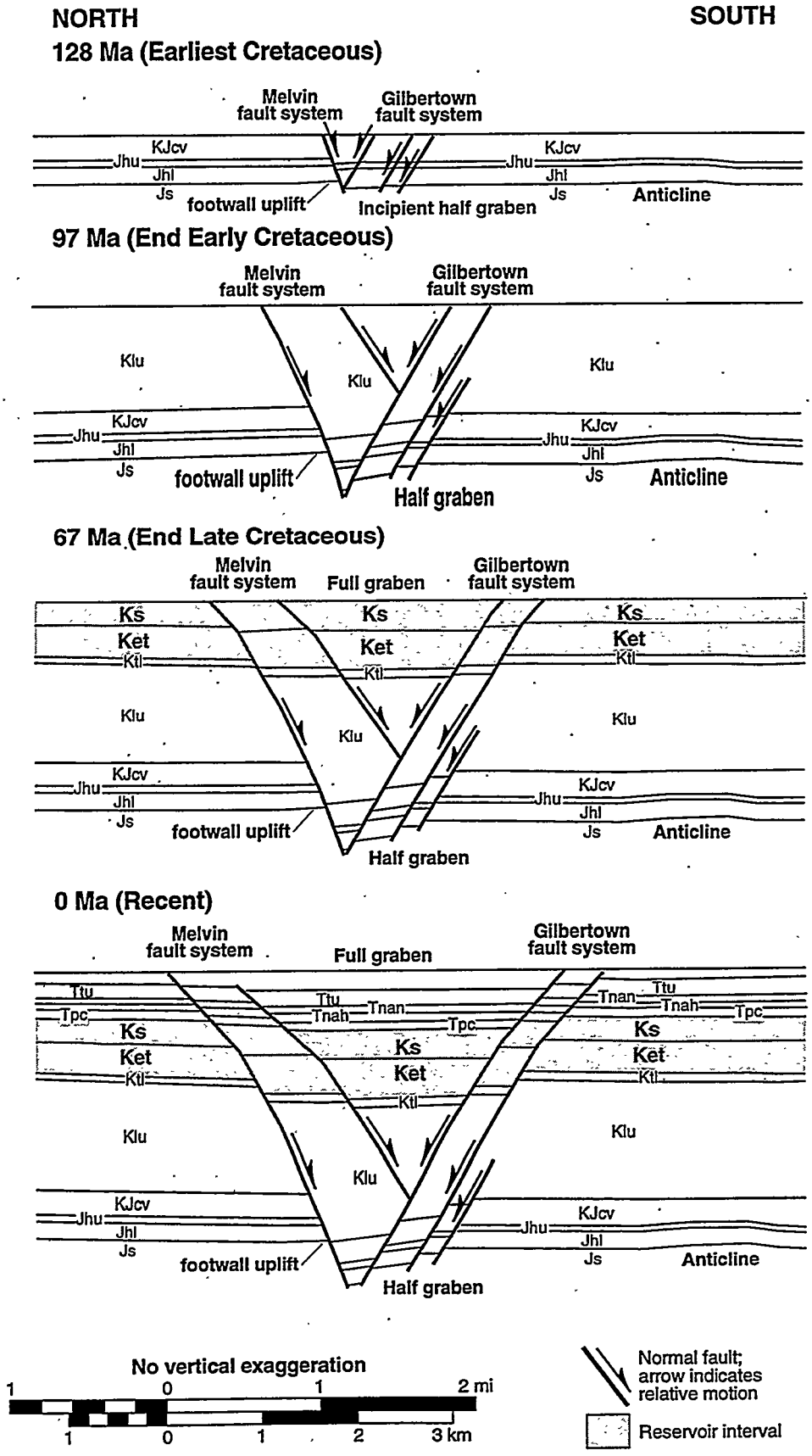

Figure 24.--Sequential restoration showing evolution of the graben formed by the Gilbertown and Melvin fault systems. Restoration based mainly on cross section E-E' (fig. 15).

providing evidence for local reversal of structural polarity during the Cretaceous (fig. 14).

Structural history during Tertiary time is less clear than that during the Cretaceous. Whereas structural growth is readily apparent in Cretaceous units (figs. 11–18), isopach maps in Pashin and others (1997) indicate that growth of Tertiary units across the faults is at best questionable with the exception of the small graben formed by conjugation of East Gilbertown fault A with the West Bend fault. Thus, two possibilities exist for interpreting Tertiary structural history. The first is that most faults ceased moving some time after Selma deposition and were reactivated after deposition of the Tuscahoma Formation. The second possibility is that, although faults may have moved some during the Tertiary, local depositional variability overwhelmed the effect of synsedimentary growth.

The decrease of fault dip near the start of Selma deposition is perhaps the most enigmatic structural event in the Gilbertown area (fig. 24). One interpretation is that dip decreased by refraction of the faults through the chalk, which is more brittle than the shale and sandstone that predominates in the Lower Cretaceous section through the Eutaw Formation. An alternative cause of low fault dip is compaction of the faults with the surrounding sediment (for example, Xiao and Suppe, 1980; Skuce, 1996). This may be the more appropriate interpretation, because chalk is highly compactible, and the faults have not been refracted back to a steep dip in the dominantly siliciclastic Tertiary section.

Conjugation of East Gilbertown fault A with the West Bend fault occurred shortly after Selma deposition (figs. 16, 17). Conjugate fault systems typically develop where the tip regions of opposed normal faults with subequal displacement overlap (Nicol and others, 1995). Growth strata provide evidence for simultaneous movement of opposed faults in conjugate systems (Horsfield, 1980), and simultaneous growth is apparent in cross sections of the Gilbertown area.

Most of the major faults appear to propagate to the surface, suggesting that final movement is Miocene or younger. The faults appear to be inactive today, because none of the structures are associated with topographic scarps, and streams cut freely across the Gilbertown and West Bend fault systems, as well as the Hatchetigbee anticline (Szabo and others, 1988). However, the distribution of faults at the surface is a matter of continuing debate and is discussed in the following section.

GEOLOGIC MAPPING

An intensive field investigation of the Gilbertown fault system and the Hatchetigbee anticline was performed to achieve two major goals. The first goal was to gain a comprehensive understanding of the surface geology in the Gilbertown area by determining the distribution of the exposed formations and delineating the surface traces of the major faults. The second goal was to characterize and analyze the fracture systems that are the source of effectively all permeability in chalk of the Selma Group.

Surface Geology

Investigation of the surface geology in the area of the Gilbertown fault system and Hatchetigbee anticline has provided new insight into the geology of the Gilbertown area (fig. 25). Field work proved quite challenging, considering that most strata cropping out in the field area are poorly consolidated. Major faults are frequently expressed at the surface by minor valleys and dips in the terrain, and are rarely or never exposed. Typically, roads dip and fault traces are covered with road fill. However, roadcuts near faults are common, and they can be used to bracket the fault trace and, occasionally, provide data for fracture analysis. Bracketing faults is especially difficult where the Lisbon Formation, which crops out in much of the field area, is faulted against itself. Where the terrain is deeply dissected, members of the Lisbon can be identified, and differences in elevation across the fault can be compared. Remotely sensed imagery, including aerial photographs and satellite imagery have provided additional constraint on the surface traces of faults.

Investigation of the surface geology in the Gilbertown area confirms the mapping efforts of Szabo and others (1988), although some minor improvements were made during this investigation (fig. 25). The oldest formation exposed in the map area is the Tuscahoma Formation, and the youngest Tertiary unit is unconsolidated sand and gravel of Miocene age. The quality of exposures varies significantly throughout the field area, but the Tallahatta Formation, which contains a significant quantity of siliceous mudstone, is resistant to weathering and thus shows fractures better than any other unit. Pleistocene terrace deposits are common along the east side of the Tombigbee River, which flows along the western boundaries of Marengo and Clarke Counties. Quaternary alluvium is preserved in a network of dendritic valleys that locally incise the Tertiary units by more than 300 feet.

Most major normal faults mapped in the subsurface were observed at the surface, but significant differences provide important information about the regional structural history. For example, only the western part of the Melvin fault system (Melvin fault A) was mapped at the surface (fig. 25). Limited exposure makes identification of the eastern part of the fault system (Melvin faults B and C) questionable. However, enough exposures of the Tallahatta Formation exist along the streams that the fault would probably be identified had it propagated to the surface.

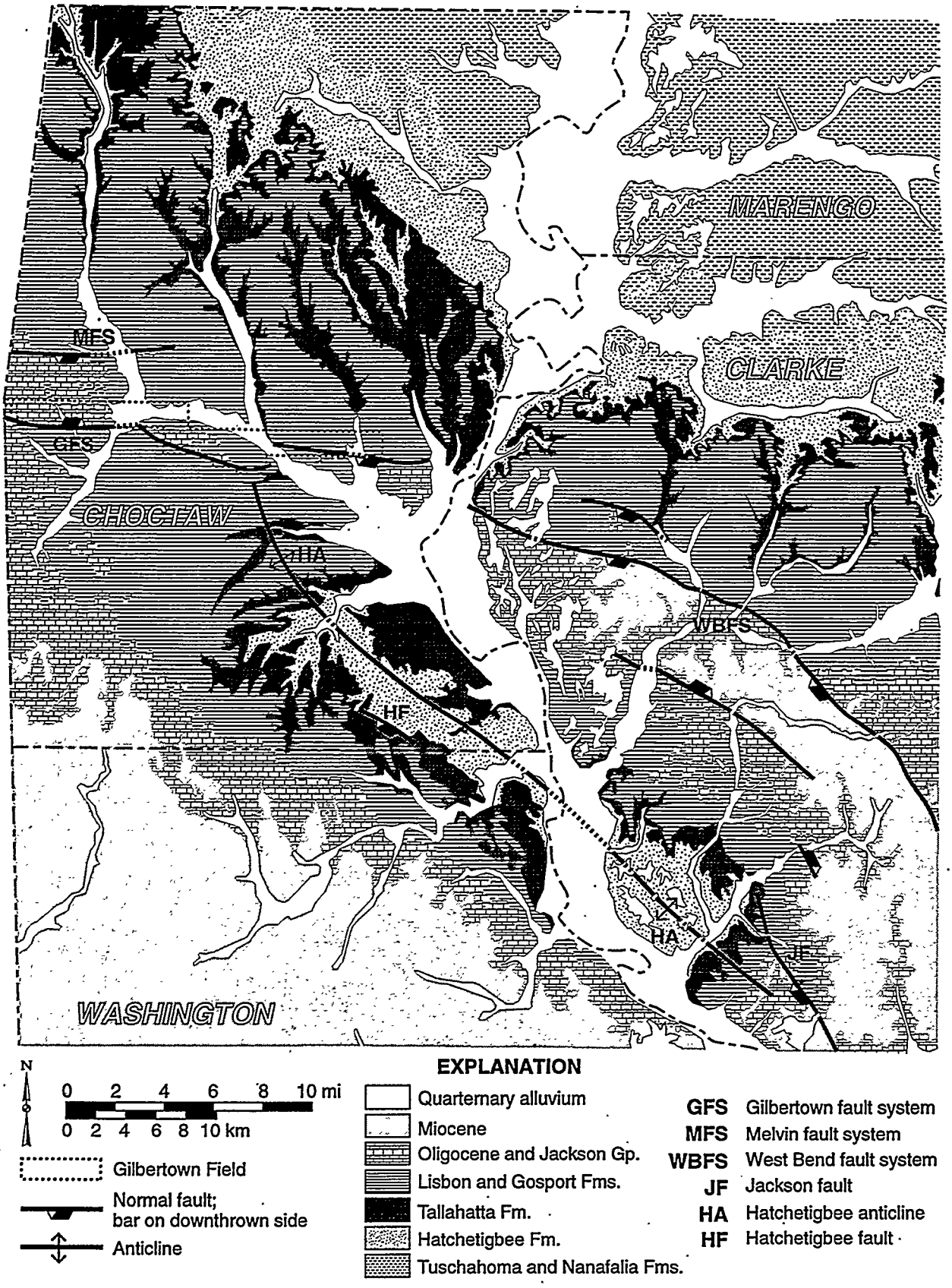

Figure 25.--Generalized geologic map of the Gilbertown fault system and Hatchetigbee anticline (modified from Szabo and others, 1988).

The Gilbertown fault system was mapped from the western edge of Choctaw County eastward into the relay zone (fig. 25). This fault appears to include parts of West Gilbertown fault A and East Gilbertown fault A, and faults corresponding to West Gilbertown fault B and East Gilbertown fault B were not identified. In Clarke County, the West Bend fault is readily identified at the surface where Oligocene limestone and Miocene siliciclastic deposits are preserved in the hanging wall, and approximately 4 miles to the south, an antithetic fault can be traced for a considerable distance. Recognition of the West Bend fault in Choctaw County is questionable, and the conjugation of the Gilbertown and West Bend fault systems could not be mapped. A fault that is downthrown toward the south was mapped in the eastern part of Gilbertown field, but the fault is south, or in the hanging wall, of the West Bend fault as mapped in the subsurface. One interpretation is that the West Bend fault is buried below the Eocene and younger sedimentary cover and that the fault that was mapped is a younger synthetic fault.

The oldest formation exposed in the crest of the Hatchetigbee anticline is the Hatchetigbee Sand, which is of Eocene age (fig. 25). Strata as young as Miocene are preserved along the flanks of the anticline, and Quaternary alluvium fills valleys that cut across the axial trace of the structure. Minor, northwest-striking normal faults have been observed approximately 3 miles south of the crest of the Hatchetigbee anticline by previous workers (MacNeil, 1946; Toulmin and others, 1951; Szabo and others, 1988), but none of these faults appears to have the continuity of a subsurface fault in a similar structural position that was first mapped by Moore (1971) (figs. 2, 25). The northwest tip of the Jackson fault offsets Eocene through Miocene strata near the eastern terminus of the Hatchetigbee anticline. The Jackson fault extends well south of the map area and is the major bounding fault of the Mobile graben.

Cross-cutting relationships suggest that the faults ceased movement at different times (fig. 25). Most faults moved at least until the Miocene, although parts of the Melvin and West Bend fault systems may have ceased movement during the Eocene or earlier. The Hatchetigbee anticline also incorporates strata as young as Miocene, suggesting that movement was effectively contemporaneous with regional faulting. Pleistocene terrace deposits and Quaternary alluvium are not tectonically deformed anywhere in the map area, and no fault scarps were observed in the field, indicating that faulting and folding ended by the close of Tertiary time. The gap between Miocene and Pleistocene deposition is the most significant hiatus in the Cenozoic section of southwest Alabama and appears to reflect a combination of falling base level, regional uplift, and valley incision that is antecedent to regional faulting and development of the Hatchetigbee anticline.

Fracture Analysis

Fractures in the Gilbertown area are of two major types: shear fractures and joints. Shear fractures are intimately associated with faults. Coffeeville Landing is the only outcrop in the field area where faults and shear fractures are exposed well enough to facilitate detailed analysis. Joints are exposed in numerous outcrops, yet no analysis of joint systems in the Gulf Coast basin of Alabama has been performed previously. To fill this need, and to determine the importance of jointing in Gilbertown reservoirs, quantitative assessment of the joint population in the field area is based on 575 measurements of joint orientation.

Faults and Shear Fractures at Coffeeville Landing

An exposure of the Lisbon Formation at Coffeeville Landing, which is on the east bank of the Tombigbee River in Clarke County (NE 1/4 NW 1/4 sec. 17, T. 9 N., R. 1 W.), provides a unique window into the relationship among faulting, folding, and fracturing in the Gilbertown area (fig. 26). The outcrop is under water much of the year, and the best time to visit is during the late summer when river level tends to be lowest. The Lisbon is composed mainly of poorly consolidated sand with abundant mollusc shells and includes prominent beds of dark-gray to brownish-gray clay that contains the distinctive trace fossil *Thallasinoides*. The clay beds are excellent markers that help define the major structures at Coffeeville Landing.

Two normal faults that strike approximately N. 85° E. and dip steeper than 70° N. are readily recognized in the outcrop (fig. 26). These faults are approximately 5 miles south of the West Bend fault and can be interpreted as antithetic structures that are part of the hanging-wall rollover of the West Bend fault system. Efforts to map the faults beyond the outcrop, however, were unsuccessful because of dense vegetation.

The faults separate three blocks of weakly deformed strata named from south to north the footwall block, the central fault block, and the hanging-wall block on the basis of structural position (fig. 26). Each fault block contains a unique internal stratigraphy. The footwall block contains lignitic sand near the base and is the only one without a clay bed, whereas the central fault block contains a single clay bed. Two clay beds are in the hanging-wall block, and near the top of the section is a well-indurated sandstone layer containing numerous echinoids. Because none of the blocks can be correlated, only gross estimates of fault displacement can be made. For the blocks not to correlate, each fault must have more than 25 feet of slip. The total thickness of the Lisbon Formation in the area of Coffeeville Landing is approximately 200 feet, and based on the

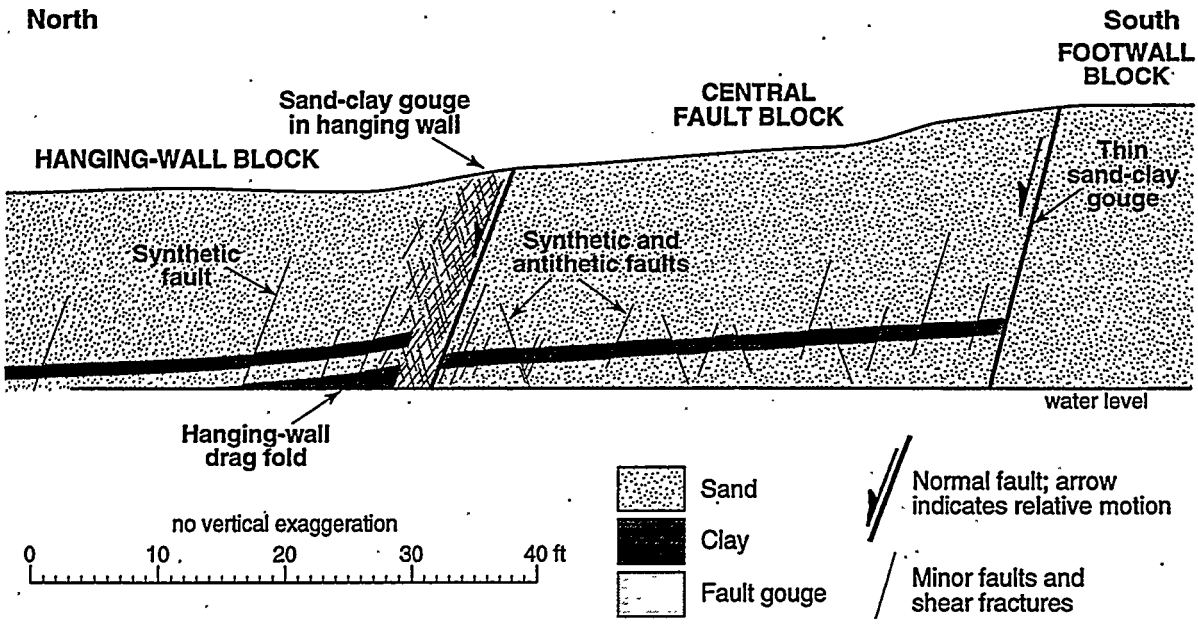

Figure 26.--Sketch of outcrop at Coffeeville Landing showing faults and fault-related fracturing in the Lisbon Formation.

thickness of the exposed section in the footwall and hanging-wall blocks, combined slip on the two faults cannot exceed 150 feet.

Few fractures and second-order faults were observed in the footwall block, although efforts were hampered by difficult access. The southern fault is planar and contains an argillaceous gouge that is only about 3 inches thick (fig. 26). Strata in the central fault block dip between 2 and 4° toward the north and contain numerous minor faults and shear fractures that are synthetic and antithetic to the main faults. The northern fault is planar and contains arenaceous and argillaceous gouge that is in places thicker than 5 feet. The southern edge of the gouge zone is sharply bounded by the main fault plane, whereas the northern edge is poorly defined, indicating that the gouge formed mainly by deformation of the proximal part of the hanging wall. Shear fractures, most of which are synthetic to and dip more gently than the fault plane, are abundant in the fault gouge. Clay beds in the hanging-wall block define a drag fold in which strata adjacent to the fault dip steeper than 5°. This drag fold is reminiscent of the sagging between faults that is apparent in structural contour maps of the Upper Cretaceous units in the Gilbertown graben (figs. 20–22). Whereas the central fault block contains numerous second-order synthetic and antithetic structures, synthetic faults predominate in the hanging-wall block.

Regional Joint Systems

Joints, which are extensional opening-mode fractures along which little or no movement has taken place, are found in all sedimentary basins and were referred to by Pollard and Aydin (1988) as "the most ubiquitous structure in the earth's crust." No information exists on jointing in the eastern part of the Gulf Coast basin, yet field investigation of the Gilbertown area revealed that joints are present in strata of Paleocene through Oligocene age. Nonsystematic joints lack preferred orientation, whereas systematic joints form subparallel sets. Joint surfaces form perpendicular to the least principal stress direction and parallel to the greatest principal stress direction. Joints typically comprise orthogonal systems composed of systematic joints and cross joints. Cross joints tend to be discontinuous and commonly curve, terminating at right angles to systematic joints, reflecting interaction of growing fractures with a preexisting free surface (Lachenbruch, 1962).

The spacing and surface morphology of joints appear to be a function of lithology, pore fluid, and stress history (La Pointe and Hudson, 1985). In most sedimentary rocks, joints are spaced on the order of 0.5 inch to more than 30 feet, and different beds in the same outcrop commonly display different spacing patterns and morphologies. For example, mechanically brittle rocks such as sandstone and limestone commonly contain planar joints with even spacing, whereas joints in the same area can be curved and irregularly spaced in more ductile rocks, such as shale. Spacing also is positively correlated with bed thickness (McQuillan, 1973).

Joints were observed in most outcrops of Cenozoic strata in the Gilbertown area, and the morphology and spacing of the joints vary with respect to lithology. Joints were only observed in fresh exposures of sand; the joint surfaces tend to be rough owing to poor consolidation and the abundant shell fragments in many beds. Joints in clay tend to be more planar and smoother than those in sand, and siliceous mudstone of the Tallahatta Formation is the most brittle and thus best jointed unit in the field area. Soft Oligocene limestone is the most poorly jointed rock type in the study area, and joint surfaces resemble those in sand. Joint spacing is extremely variable, and some fresh outcrops extending for more than 100 feet contain no joints. In other outcrops, however, joints are spaced between 1 and 10 feet. The best evidence for irregular joint spacing is in Oligocene limestone at the St. Stephens Quarry in Washington County (secs. 32, 33, and 34, T. 7 N., R. 1 W.), where quarry faces can be traced continuously for nearly a mile. Here, joints are developed in swarms up to 50 feet wide with individual joints spaced between 1 and 10 feet apart. The swarms are separated in places by more than 1,000 feet of limestone containing no natural fractures. Cross-cutting relationships between the joint sets were not identified, but system 2 joints at Coffeeville Landing clearly abut the synthetic faults in the hanging-wall block.

The limited extent of most outcrops makes determining relationships among joints difficult, and the only way to confidently define joint systems and to distinguish main joints from cross joints was through statistical analysis of joint orientation. In all, 575 measurements of joint orientation were made. A rose diagram showing all joint orientations in the field area reveals a polymodal distribution, signifying development of two joint systems (systems 1 and 2) with associated cross joints (fig. 27). A distinct boundary between system 1 and system 2 joints, and for that matter, system 1 and system 2 cross joints cannot be drawn with confidence, but there is little overlap between the main joint and cross joint modes. The main joints account for 77 percent of all directional readings. System 1 joints account for nearly 58 percent of all joint readings and have a vector-mean azimuth of 295°, or west–northwest. System 2 joints, by comparison, account for only 20 percent of all joint readings and have a vector-mean azimuth of 343°, or north–northwest.

Maps showing the vector mean azimuth of joints and cross joints at each field station were plotted with respect to regional structure and the outcrop pattern of the Tallahatta Formation where most data were obtained (figs. 28–31). One set of maps shows raw

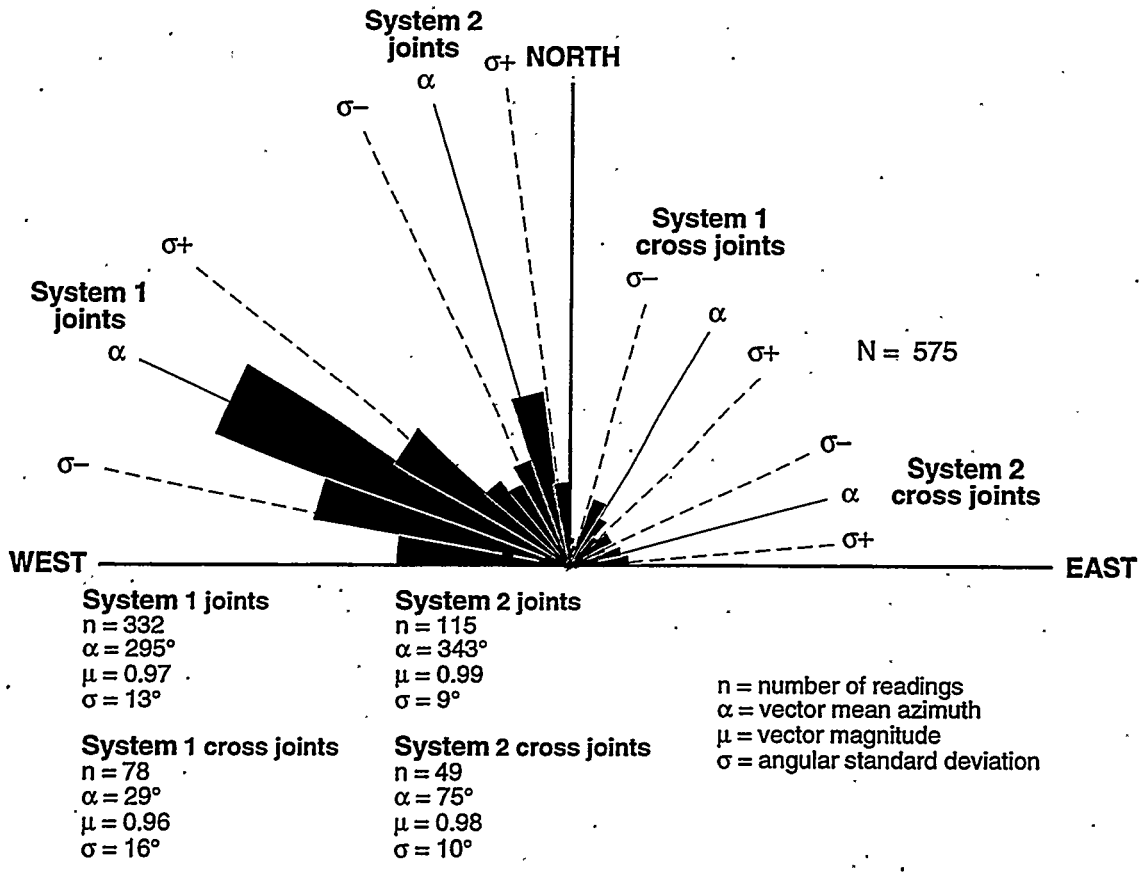

Figure 27.--Rose diagram with statistical summary of joint systems in the Gilbertown area.

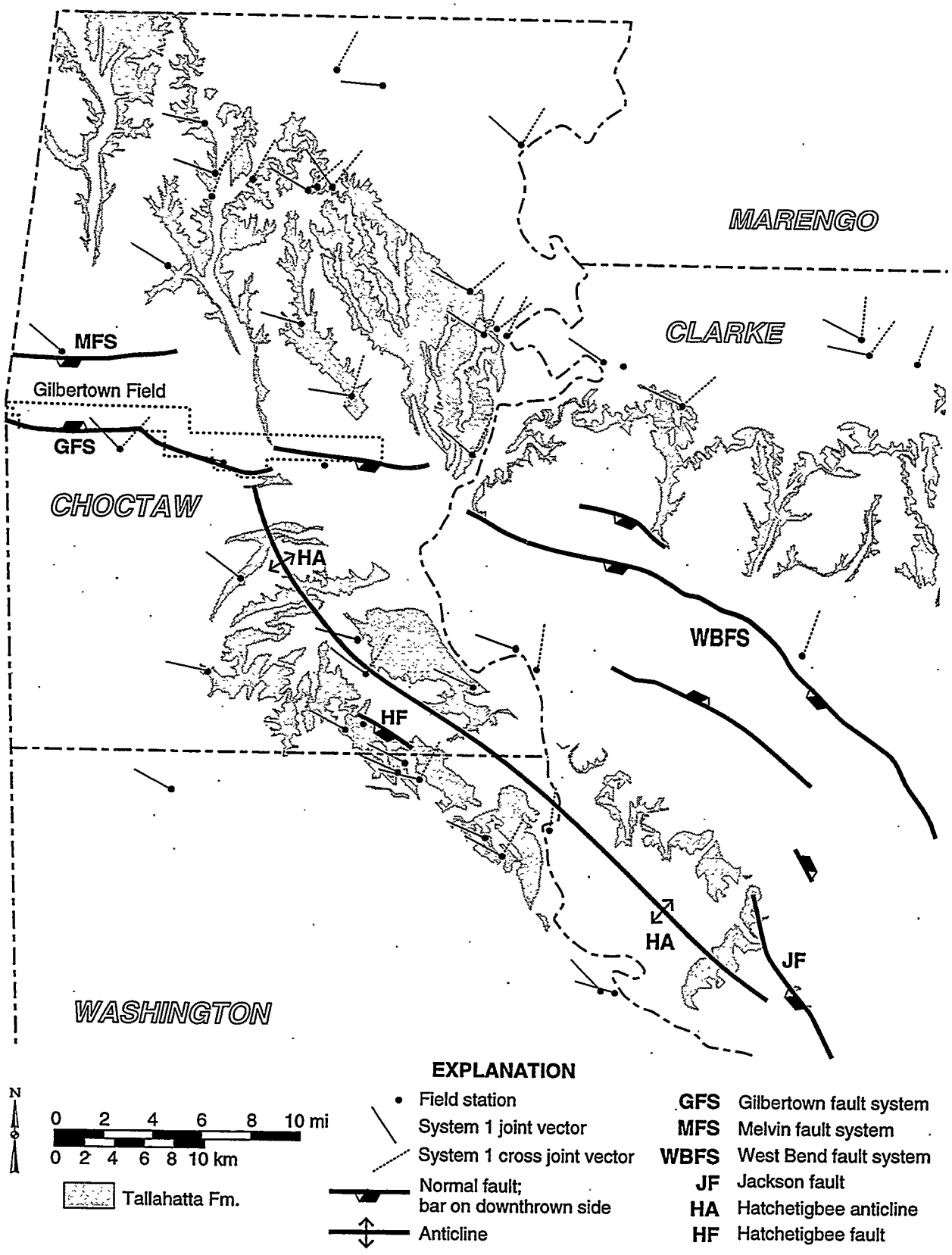

Figure 28.--Map of raw system 1 joint vectors in the Gilbertown area.

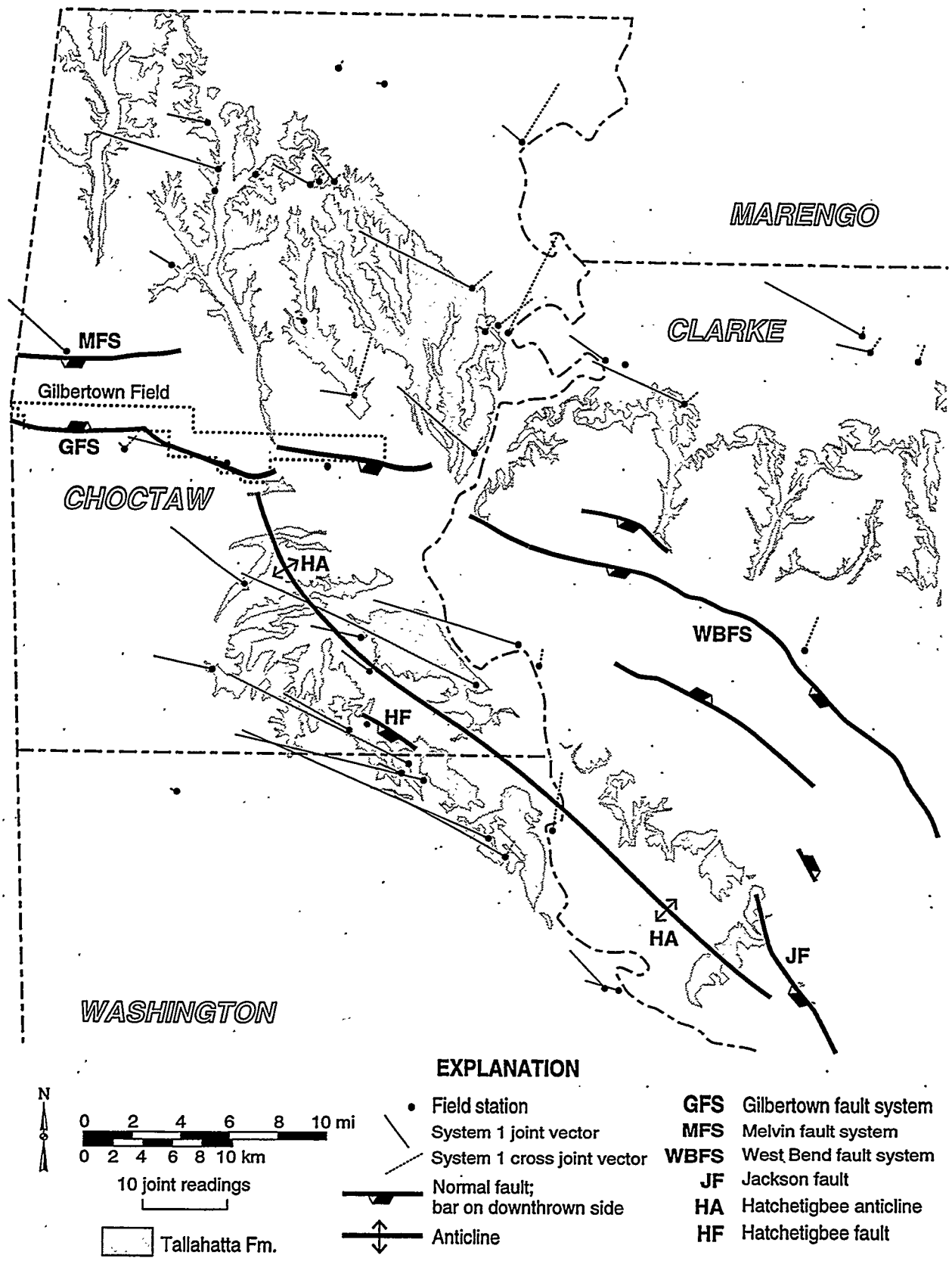

Figure 29.--Map of weighted system 1 joint vectors in the Gilbertown area.

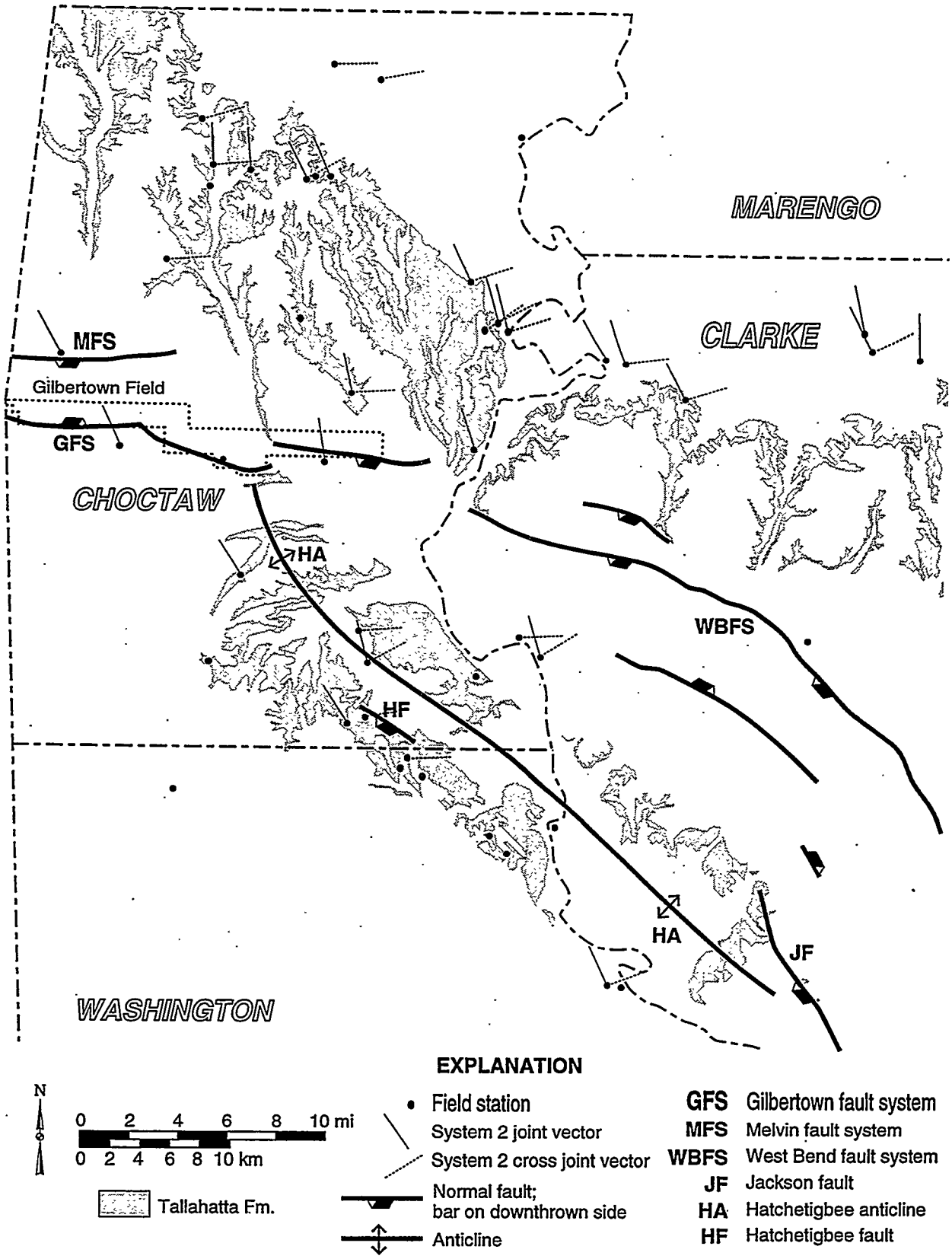

Figure 30.--Map of raw system 2 joint vectors in the Gilbertown area.

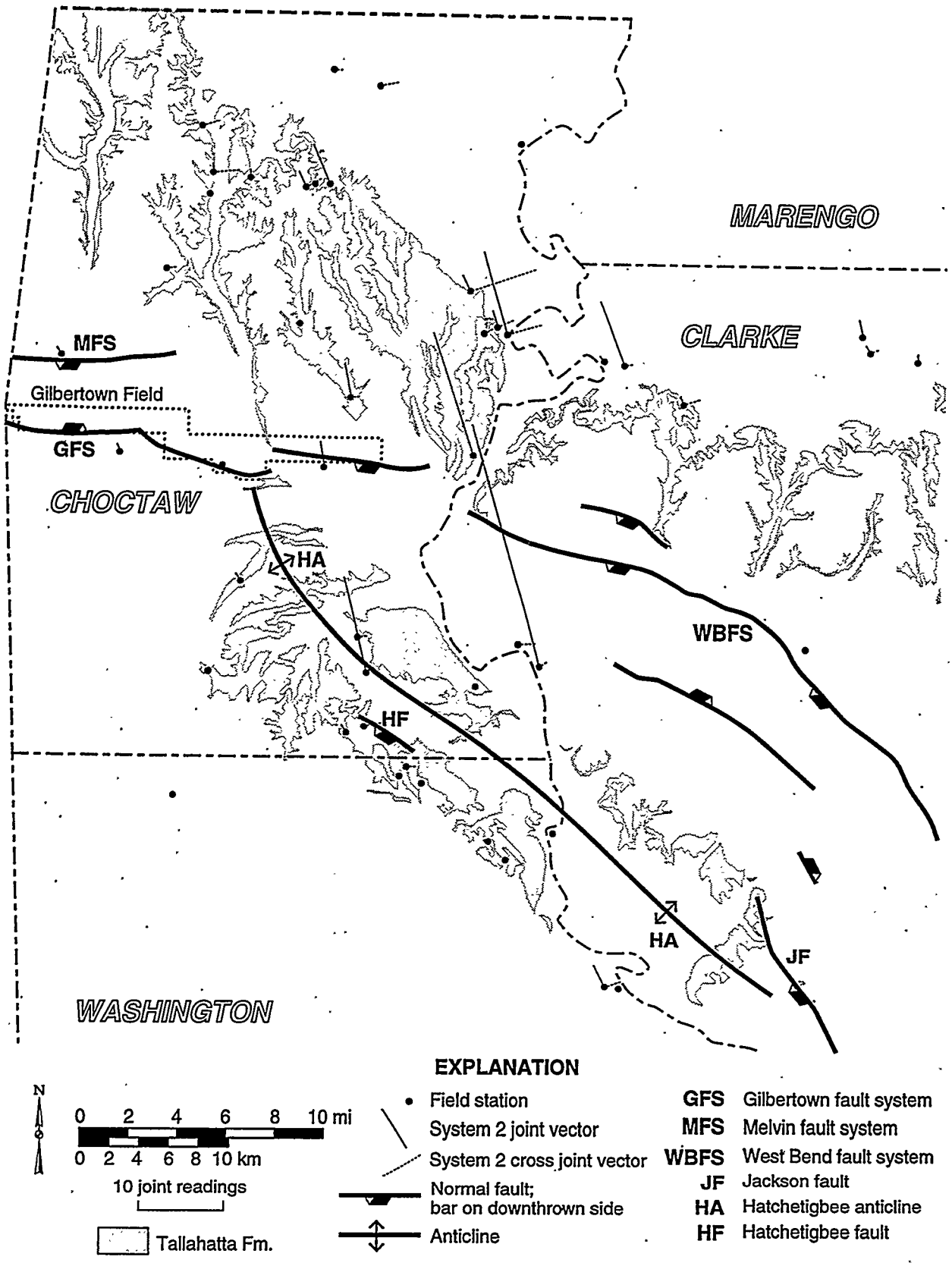

Figure 31.--Map of weighted system 2 joint vectors in the Gilbertown area.

vectors (figs. 28, 30), whereas another set shows vectors weighted according to the number of joint readings (figs. 29, 31). Both joint systems maintain uniform orientation throughout the map area, and system 2 vectors are more consistently aligned than system 1 vectors. System 1 joints are distributed throughout the field area; they are oblique to most of the normal faults and strike nearly parallel to the axial trace of the Hatchetigbee anticline. System 2 joints are also distributed throughout the field area, but most of these joints are exposed along the Tombigbee River near the Clarke–Choctaw County line. System 2 joints are strongly oblique to all structures other than the Jackson fault. However, these joints closely parallel some long hillsides defined by the outcrop pattern of the Tallahatta Formation in northern Choctaw County, as well as some straight segments of the Tombigbee River.

Consistent orientation of each joint system throughout the map area (figs. 28–31) indicates that the fractures formed in response to regional stresses, as is typical of many sedimentary basins (Nickelsen and Hough, 1967; Engelder, 1985), rather than to the local stresses associated with folding and faulting. Near parallelism of system 1 joints to the axial trace of the Hatchetigbee anticline (figs. 28, 29) suggests that these fractures formed as part of the regional extensional stress field responsible for the major folds and faults in the field area. Cross-cutting relationships suggest that system 2 joints are younger than the folds and faults and are thus the product of a neotectonic stress field in which the maximum compressive stress is oriented north–northwest. Parallelism of the joints to long hillsides and concentration of joints in the valley of the Tombigbee River (figs. 30, 31) suggests that these fractures are modern unloading joints related to regional uplift and valley incision.

Fractures with surfaces bearing features like plumose structure and hackle marks have been interpreted to form rapidly under conditions of high pore-fluid pressure caused by high tectonic stress (Engelder and Lacazette, 1990). Joints in the Gilbertown area lack such high-stress features and can thus be interpreted as having formed under relatively low pore pressure and perhaps over a longer period. Moreover, the poorly consolidated formations that dominate the surface geology of the Gilbertown area were almost certainly poor transmitters of tectonic stress.

If system 1 joints indeed formed under the same stress regime as the Hatchetigbee anticline and the Gilbertown, Melvin, and West Bend fault systems, then a high probability exists that these fractures extend well into the subsurface, perhaps beyond the depth of Selma and Eutaw reservoirs. Conversely, system 2 joints apparently reflect ongoing geomorphic processes and accordingly may not extend downward to reservoir depths. Therefore, system 1 joints may be a source of permeability in the Selma Group. Furthermore, these fractures strike approximately 25° northwest of the main faults, indicating that joints may be important connectors between strike-parallel shear fractures.

BURIAL AND THERMAL HISTORY

The distribution of hydrocarbons in the Gilbertown area raises questions about the burial and thermal history of the eastern Gulf Coast basin. The only field producing hydrocarbons from post-Jurassic strata in the area of the Gilbertown fault system and Hatchetigbee anticline is Gilbertown Field (fig. 2); all other fields in the area produce from the Norphlet and Smackover Formation. In the following sections, we present the burial and thermal history of Jurassic through Tertiary strata in the Gilbertown area and identify the probable source rocks and migration pathways.

Burial History

The burial history curve, which is based largely on the M. W. Smith Lumber Inc. 15–11 well (permit 3589), reflects a simple burial history characterized by decelerating subsidence and sedimentation rates from Jurassic through Miocene time (fig. 32). Maximum burial depth was apparently reached during the Miocene, and the Miocene–Quaternary unconformity suggests that the region has been undergoing uplift and erosion since that time. Erosional relief on this unconformity indicates that a minimum of 300 feet of section has been denuded.

Decelerating subsidence curves are typical of extensional basins and reflect lithospheric contraction as the crust cools during the late stages of rifting (Sclater and Christie, 1980). Factoring out the tectonic component of subsidence reveals some key characteristics of basin formation in southwestern Alabama (fig. 32). Tectonic subsidence was apparently a significant component of total subsidence during the Jurassic and Early Cretaceous. However, the curve flattens significantly during the Cretaceous, indicating that the crust was effectively cool and that no external tectonic forces were required to drive subsidence and fault growth by the time the Eutaw Formation and Selma Group were deposited. Comparison of the total tectonic subsidence curve with the total effective subsidence curve suggests that more than 50 percent of the basin fill is the product of sediment loading and compaction. The effect of compaction is especially apparent from 40 to 15 million years ago. During this time, Jurassic strata are interpreted to have ceased subsiding, but compaction of Lower Cretaceous and younger strata provided sufficient accommodation space for Eocene through Miocene sediment to accumulate.

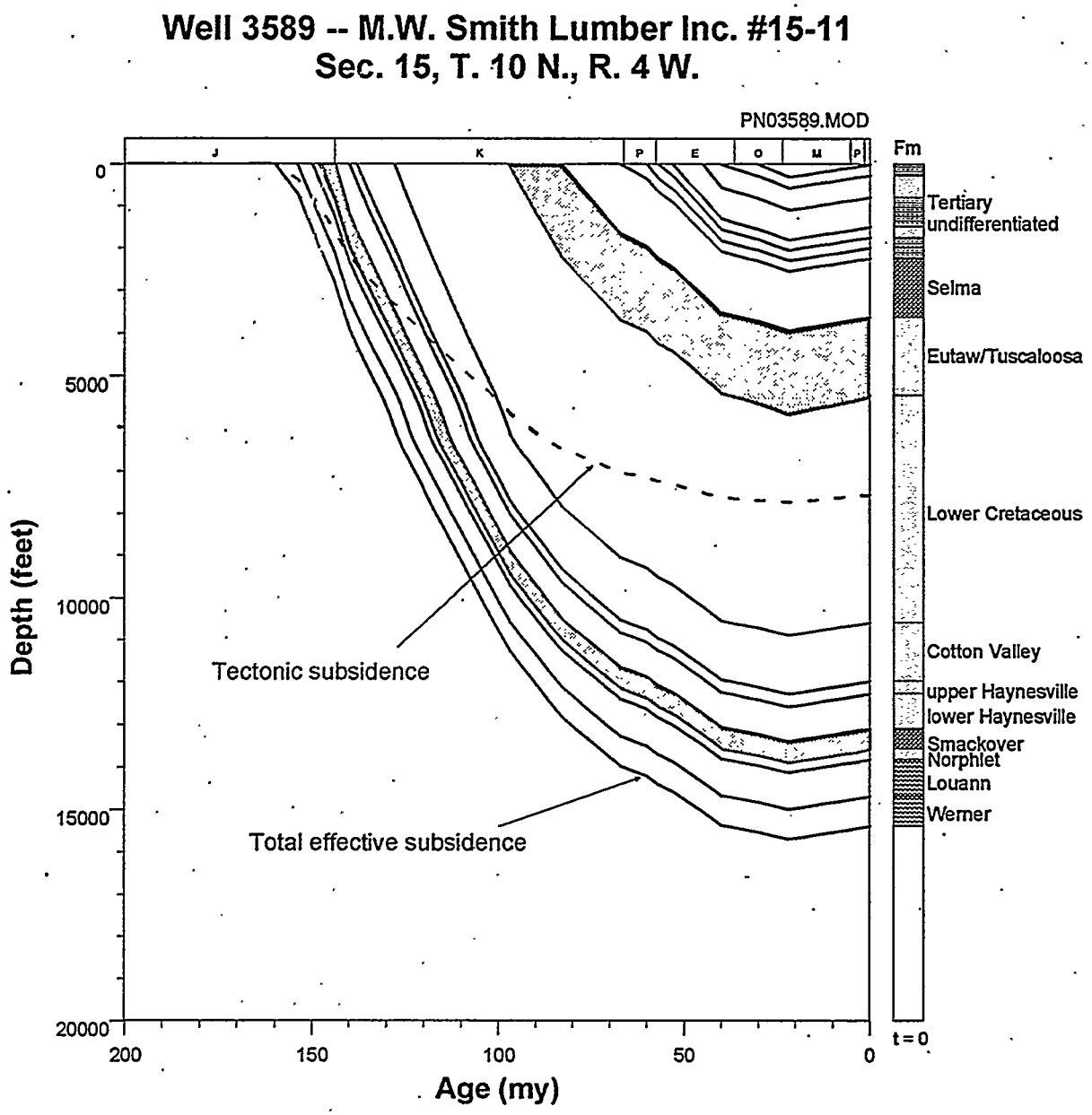

Figure 32.--Burial history for well 3589 generated in BasinMod. Dashed line indicates rate of basin subsidence.

Thermal History and Source Rock Maturation

Sassen and Moore (1988) suggested that laminated lime mudstone in the Jurassic Smackover Formation is the principal hydrocarbon source rock throughout the eastern Gulf Coast basin and that the current pattern of hydrocarbon production from the Smackover can be explained by thermal maturity trends. These trends have been characterized using Thermal Alteration Index (TAI) measurements from dinoflagellates and appear to be loosely correlated with burial depth (Kopaska-Merkel and Schmoker, 1994). TAI can be correlated to vitrinite reflectance (table 1), which is a more precise measurement of thermal maturity (fig. 33). Vitrinite, however, is rare below the Tuscaloosa Group, and especially so in Smackover carbonates.

Smackover micrite may also be the source of oil in the Cretaceous reservoirs of Gilbertown field (Claypool and Mancini, 1989). This is indicated by the geochemical similarity of Gilbertown oil to oil, condensate, and organic matter in the Smackover. Based on the work of Kopaska-Merkel and Schmoker (1994), the effective vitrinite reflectance of the Smackover Formation in the area of well 3589 is approximately 0.7 percent (fig. 33). This indicates that the Smackover is thermally at or near peak oil generation (table 1). Combining this knowledge with what is known of the burial history allows estimation of the timing of hydrocarbon generation.

A critical variable in this process is the duration and magnitude of heat to which the source rock has been subjected. By varying the geothermal gradient over time, a model of the timing of thermal maturation can be made. The current geothermal gradient of pre-Cretaceous rocks in the area of well 3589 is approximately 1.8°C/100m (1.0°F/100 ft) (Wilson and Tew, 1985), and current surface temperatures average 20°C (68°F). Based on these values, manipulation of past geothermal gradients can generate models resulting in the current thermal maturation values for the Smackover Formation.

Thermal windows generated by BasinMod and superimposed on burial history curves illustrate one possible geothermal maturation scenario (fig. 34). Assuming that the synrift geothermal gradient during the Jurassic was at least as high as the current value, a much lower gradient is needed during the syndrift Cretaceous and early Paleocene to arrive at known maturation values based on TAI (fig. 34; table 2). This result suggests that regional uplift of the study area since the Miocene may be thermally driven, although the mechanism of heating is unknown, and the accuracy of the TAI data is questionable. Heating of the rocks due to the higher paleogeothermal gradients of the Jurassic and Early Cretaceous probably had little effect on the total maturation of the rocks, because the Smackover did not attain the depth and temperatures needed to significantly heat the kerogen in the rocks. The Smackover Formation probably began generating oil as recently as 60 Ma in well 3589 and is apparently now near peak oil generation. In other words, hydrocarbon generation in the Gilbertown area appears to be an ongoing process at depth. Based on our thermal model, the Smackover attained a maximum temperature of 90° to 100°C (194° to 212°F) within the last 10 million years.

Table 1.--Relationship between temperature, TAI, vitrinite reflectance, maturity, and hydrocarbon generation (modified from Cardott and Lambert, 1985).

Temperature (°C)	TAI	Vitrinite Reflectance R_o (%)	Maturity	Hydrocarbon Generation
50–65	1+		Immature	Biogenic methane
	2-- to 2	0.35–0.6		First oil formation
		0.6–0.7		Peak oil generation
	3--	0.95		Main phase of oil expulsion
120–170		1.0	Mature	Peak condensate and wet-gas generation
		1.2		Peak dry-gas generation
	3 to 3--	1.3–1.4		Oil floor
	3+	2.0		Condensate and wet-gas floor
>200	4	3.0–5.0	Post Mature	Dry-gas preservation limit

Table 2.--Geothermal gradients and intervals used in modeling the thermal maturation history (fig. 4).

Age (Ma)	Gradient (°C/100m)	Tectonic regime
160–120	2.0	Late rifting
120–30	1.3	Drifting
30–0	1.8	Uplift

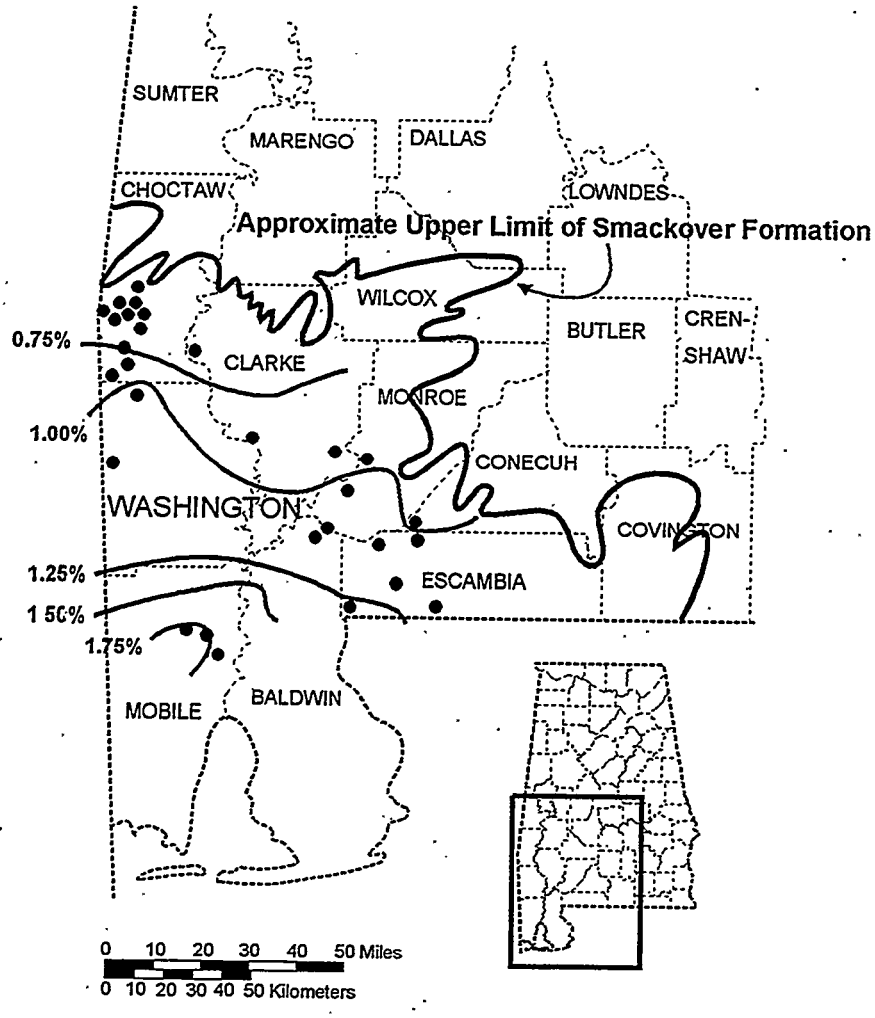

Figure 33.--TAI-based vitrinite reflectance map of southwest Alabama showing location of well 3589 (modified from Kopaska-Merkel and Schmoker, 1994).

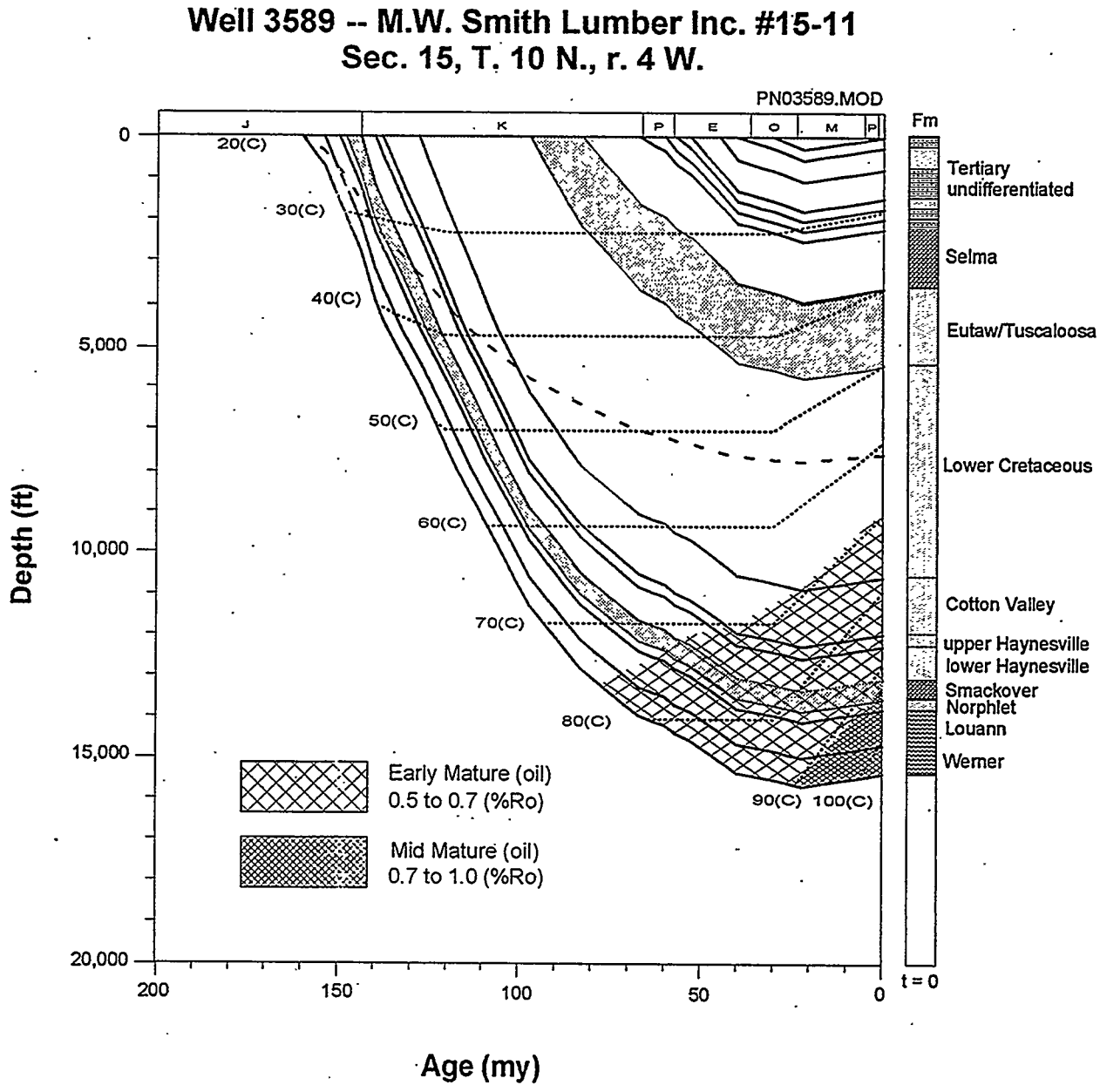

Figure 34.--Thermal maturation history for well 3589 generated in BasinMod. Dashed line indicates rate of tectonic subsidence.

Vitrinite reflectance values of 0.35 percent for the Tuscahoma Sand and 0.48 percent for the Eutaw Formation at 920 feet and 3,762 feet respectively, coupled with the results of the thermal history modeling, indicate that rocks as deep as 10,000 feet in well 3589 are undermature with respect to oil generation. For example, the Eutaw Formation and Selma Group have only attained maximum temperatures of 40° to 50°C (104° to 122°F), which is well below the minimum temperature needed to generate oil. This result confirms that Eutaw and Selma oil in Gilbertown Field was not generated in place, but has migrated from deeper, more thermally mature areas.

Distribution of Oil and Gas

Where hydrocarbon accumulations are generated locally, their composition reflects the maturation level of the source. As a source rock matures thermally and passes beyond peak oil generation, the amount of oil generated decreases, and the amount of gas generated increases until it becomes overmature and hydrocarbon generation ceases. The ratio of oil production to gas production for a gas or oil field should, therefore, reflect the maturation level of its hydrocarbon source rock if those hydrocarbons are generated locally.

Production data for 32 oil and condensate fields in the Gilbertown area were analyzed, and oil–gas production ratios were calculated to determine whether hydrocarbons produced from the Smackover Formation in the Gilbertown area were locally derived (table 3). If we assume that thermal maturation of the rocks is mainly the result of increasing temperature with depth, we would expect to see an inverse relationship between depth (i.e., increased temperature) and the oil–gas ratio (diminishing oil production). Figure 35 shows the results of plotting the oil–gas production ratio against depth. The r^2 of 0.75 of the regression line indicates that a significant correlation exists between the two variables. It suggests, therefore, that the hydrocarbons produced from each field are being generated locally under maturation conditions controlled by the depth of the source rock.

Gilbertown Field has an extremely high oil–gas ratio and plots as an extreme outlier relative to the Smackover data (fig. 35). Considering that Upper Cretaceous strata are undermature and that the oil has geochemical affinity with that in the Smackover Formation, a logical conclusion is that the oil indeed migrated into the field from deep Smackover sources. The extremely high oil–gas ratio, moreover, may indicate that the oil trapped in Gilbertown Field may have been generated when the Smackover was just becoming mature. Gilbertown oil is quite heavy relative to that in Jurassic reservoirs (Claypool and Mancini, 1989), and this heaviness may reflect degradation of the oil as it migrated through Lower Cretaceous redbeds.

The Smackover and Eutaw structure maps (figs. 2, 4) can be used to identify potential pathways along which oil migrated into Gilbertown Field. One scenario is that oil generated throughout the study area simply percolated upward from the Smackover Formation and was trapped along the Gilbertown fault system. This scenario is extremely unlikely, however, because a large amount of oil would have also been trapped in the Eutaw Formation near the crest of the Hatchetigbee anticline. Alternatively, Smackover contours define a large footwall uplift on the south side of the Gilbertown fault system (fig. 4). This uplift may have fed oil to the fault system, associated fractures and adjacent strata, ultimately charging the Cretaceous reservoirs with oil. Oil may have also migrated into the faults from the Gilbertown graben. Here, Smackover sources are deeper and are thus probably more mature than in the adjacent footwall uplifts.

RESERVOIR GEOLOGY

The previous sections provide a regional geologic framework for characterizing Eutaw and Selma reservoirs, and this section focuses on heterogeneity within these reservoirs. The discussion of the Eutaw Formation focuses on stratigraphy, sandstone petrology, and depositional environments. By contrast, the discussion of the Selma Group emphasizes stratigraphy, calcite mineralization, and structural interpretations using geophysical well logs.

Eutaw Formation

Stratigraphy and Depositional Environments

In Gilbertown Field, the Eutaw Formation contains up to 290 feet of interbedded sandstone, mudstone, and shale (fig. 36). The Eutaw sharply overlies the Tuscaloosa Group and is sharply overlain by chalk of the Selma Group. The Eutaw forms a fining- and thinning-upward succession, and on the basis of SP logs, is subdivided into seven laterally correlative units designated as E1 through E7. Intervals E2 through E7 were cored in at least one well, and oil has been produced from the top of interval E1 through interval E7. Eutaw sandstone is light-olive-gray to yellowish-gray or dark-yellowish-brown, is in part silty and argillaceous, is generally friable, and is locally stained or even saturated with oil. Some oil-saturated sandstone is so poorly cemented that it crumbles when touched. Producers consider the Eutaw Formation as low-resistivity, low-contrast pay, and indeed, resistivity of the sandstone is approximately as low as that of the associated shale. Cross sections demonstrate that the thickness of intervals E1 through E7 is fairly consistent throughout Gilbertown Field (figs. 37–40). However, the cross sections and net sandstone isolith maps (figs.

Table 3.—Oil and gas production from 33 oil and condensate fields in the Gilbertown area through October 1997.
All fields produce from the Smackover Formation except Gilbertown.

Oil/Condensate Field	Production		Oil–Gas	Reservoir
	Oil (bbl)	Gas (Mcf)	Ratio	Depth
Gilbertown	14,081,685	5,311*	614.22**	3,300
Turkey Creek	3,013,749	150,639	20.01	12,385
Toxey	1,856,731	96,123	19.32	10,460
Pace Creek	186,821	13,419	13.92	11,195
Northeast Melvin	66,124	6,965	9.49	10,960
Melvin	235,128	39,032	6.02	11,180
Thornton Springs	69,146	16,323	4.24	11,250
West Bend	666,445	215,177	3.10	12,425
Wimberly	2,134,940	692,724	3.08	11,260
West Barrytown	642,509	228,328	2.81	12,060
Bucatunna Creek	1,221,109	450,928	2.71	12,080
Stave Creek	3,181,423	1,219,271	2.61	12,465
Chappell Hill	2,192,972	872,012	2.51	11,415
South Womack Hill	1,135,085	515,799	2.20	11,400
Sugar Ridge	4,192,147	1,986,398	2.11	11,590
Barrytown	3,516,485	1,687,351	2.08	11,850
Womack Hill	29,698,153	14,749,388	2.01	11,440
North Choctaw Ridge	8,078,085	4,228,089	1.91	11,965
Mill Creek	1,048,818	691,791	1.52	12,335
Puss Cuss Creek	69,683	57,258	1.22	13,535
Southwest Barrytown	10,417	10,515	0.99	12,425
Gin Creek	440,700	470,938	0.94	13,580
Little Mill Creek	977,186	1,094,991	0.89	12,360
Silas	387,115	670,480	0.58	13,570
Zion Chapel	382,503	752,808	0.51	14,065
Choctaw Ridge	189,166	511,251	0.37	11,945
Crosbys Creek (Condensate)	1,719,227	4,987,860	0.34	16,410
Southeast Chatom (Condensate)	958,695	5,575,798	0.17	16,580
Souwilpa Creek (Condensate)	36,710	223,773	0.16	13,720
Chatom (Condensate)	16,100,033	173,952,793	0.09	16,080
Healing Springs (Conensate)	557,893	7,483,516	0.07	16,015
Copeland (Condensate)	829,568	14,210,043	0.06	16,620
Red Creek (Condensate)	321,213	5,763,913	0.06	16,250

*Gas production data incomplete for early history of field.
**Oil–gas ratio computed using only 1987–1997 production data.

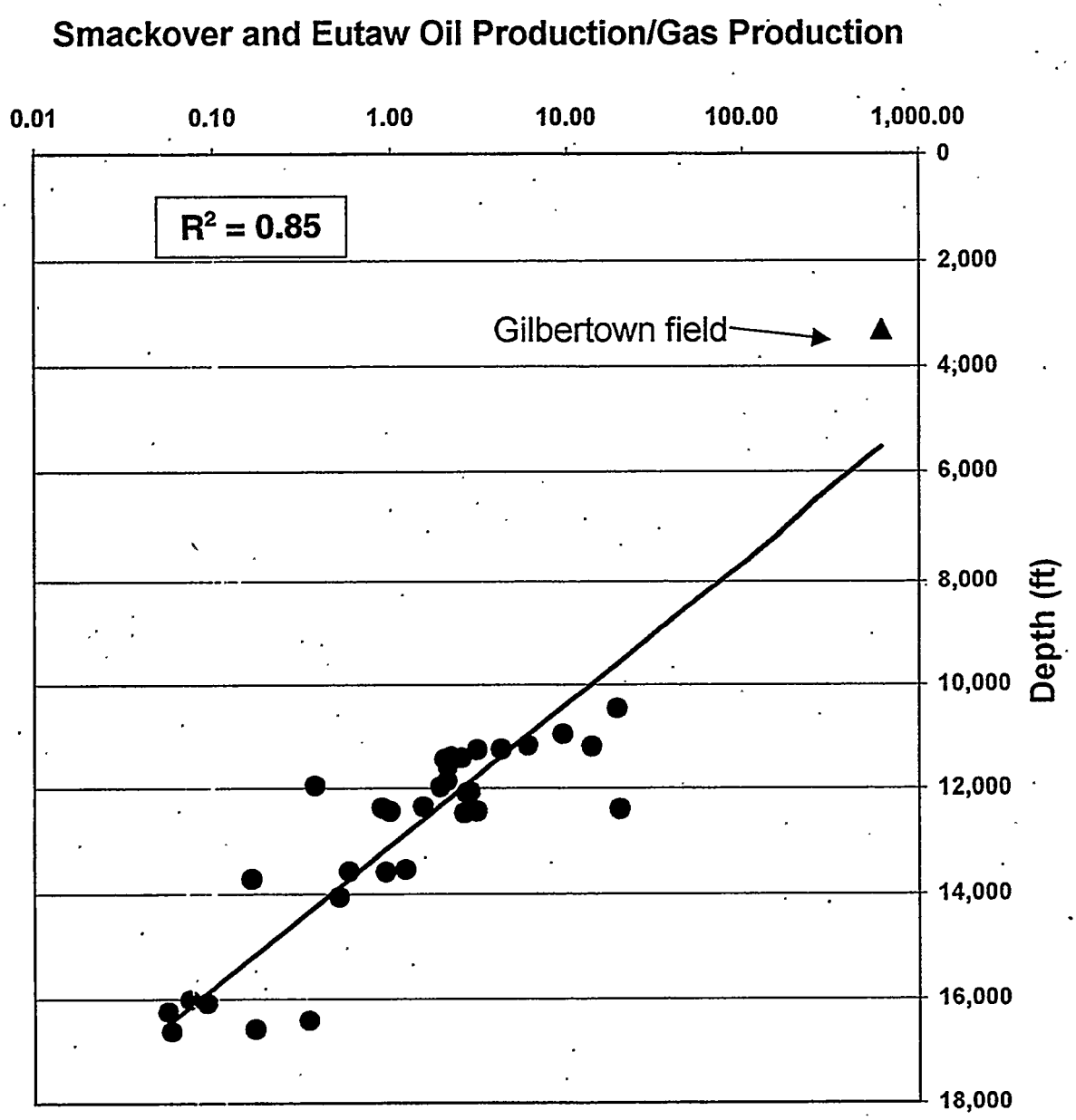

Figure 35.–Scattergram of oil-gas production ratio versus depth for 33 oil and condensate fields in the Gilbertown area.

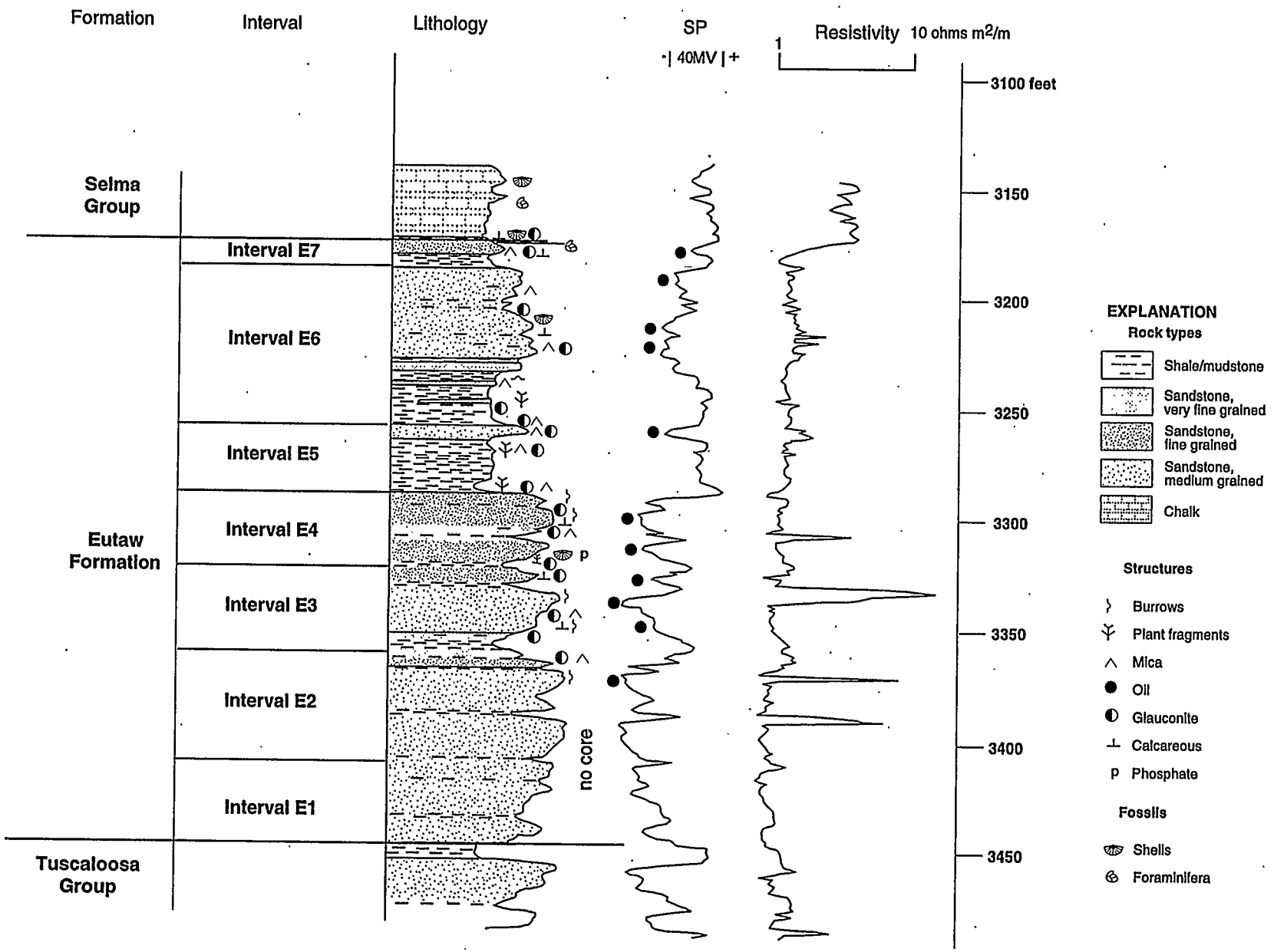

Figure 36.--Composite section and geophysical well log of the Eutaw Formation in Gilbertown Field.

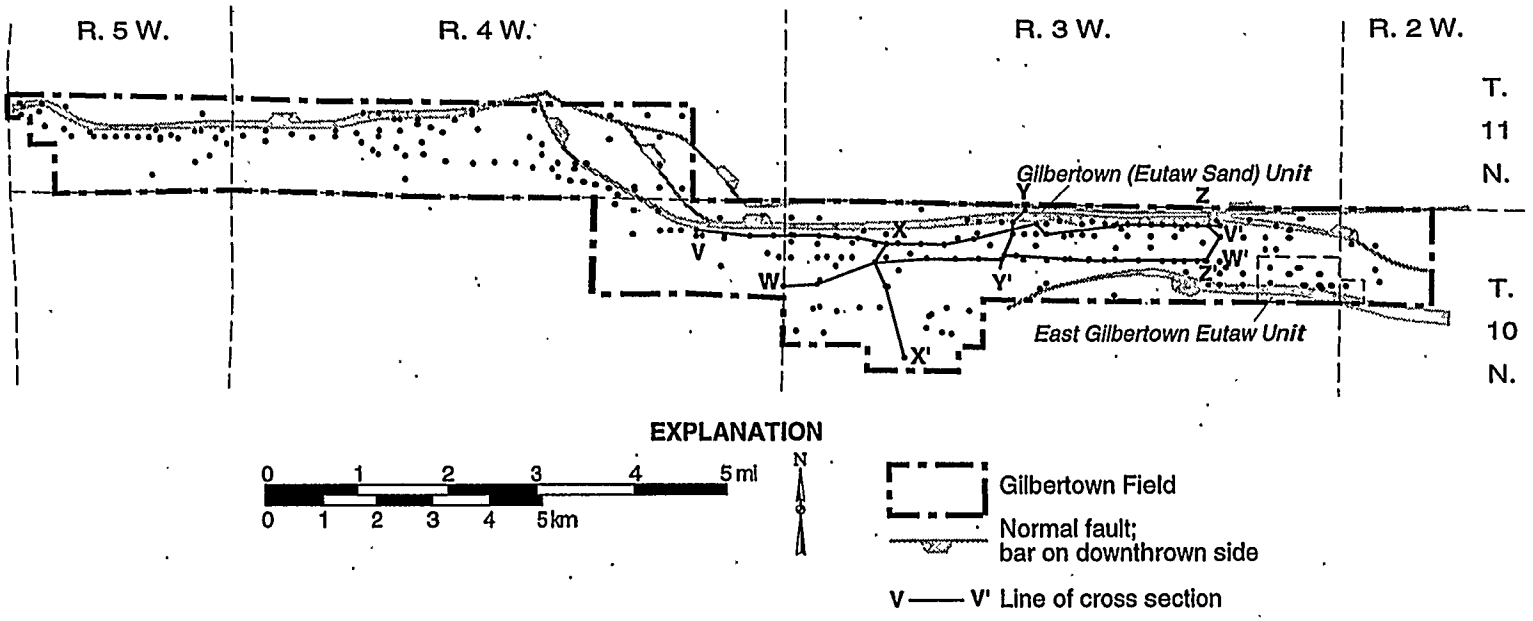

Figure 37.--Index map showing location of stratigraphic cross sections of the Eutaw Formation, eastern Gilbertown Field. Selected cross sections are published in this report, and additional cross sections are in Pashin and others (1997).

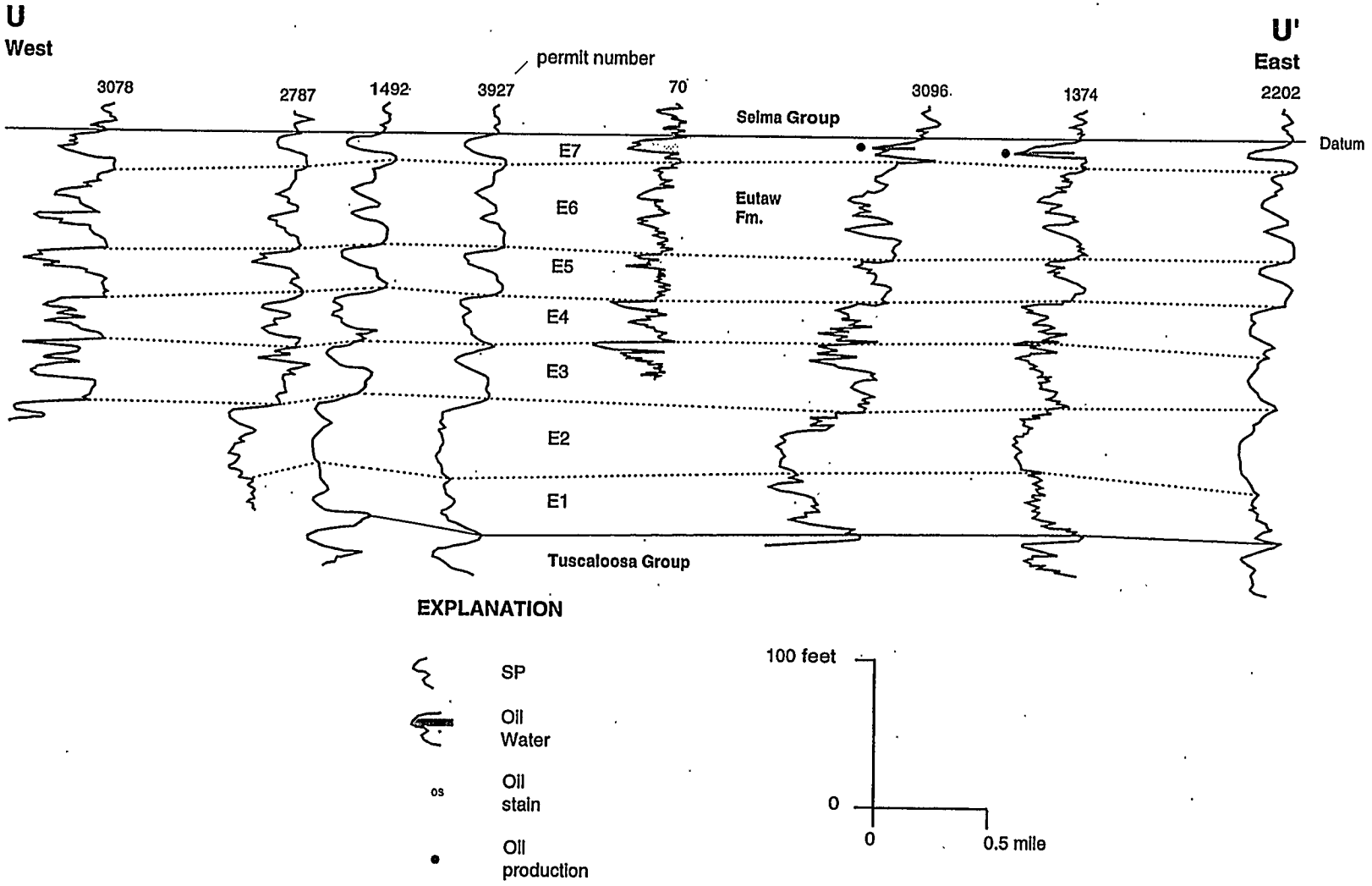

Figure 38.--Stratigraphic cross section U-U' of the Eutaw Formation, western Gilbertown Field. See figure 37 for location.

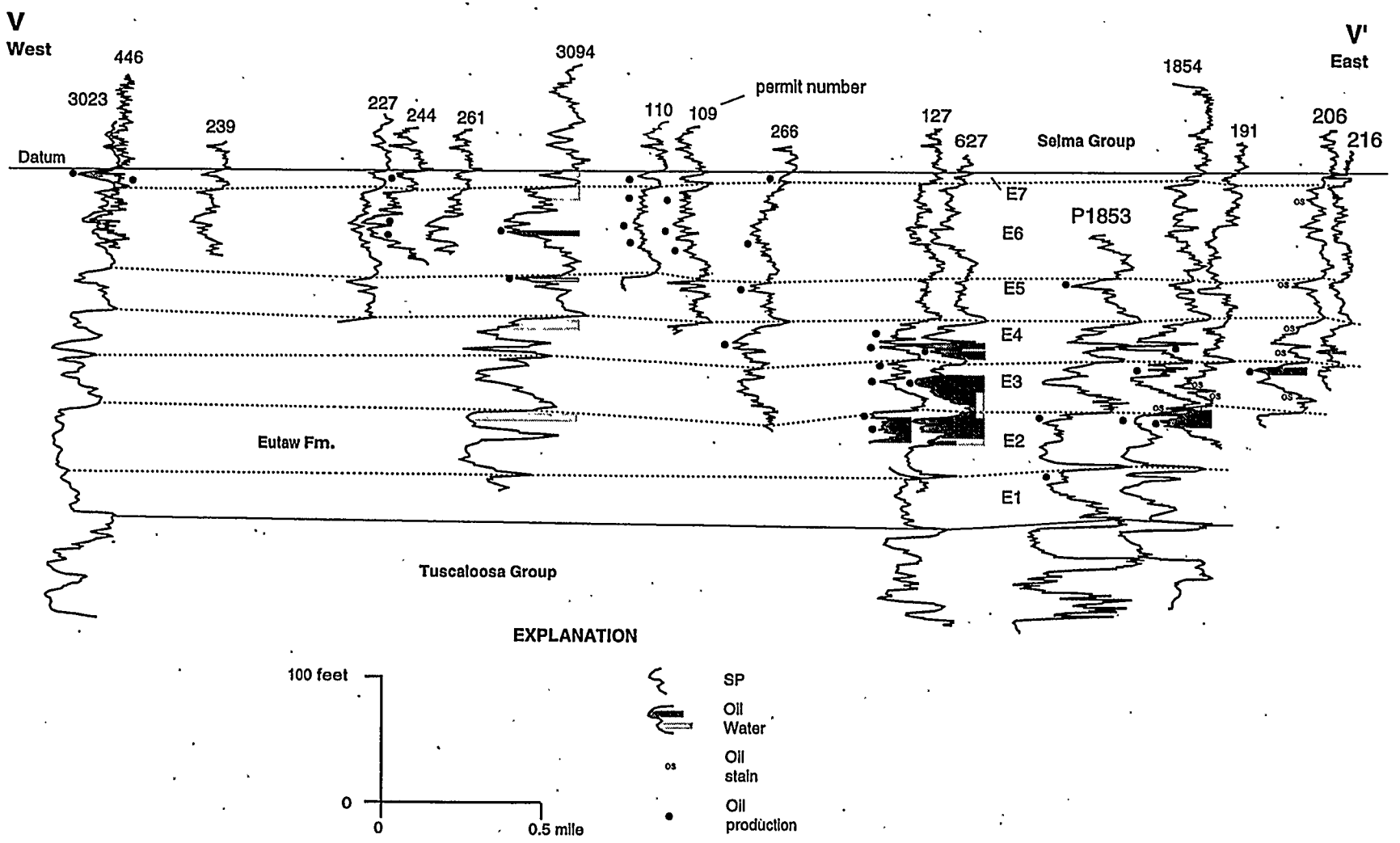

Figure 39.--Stratigraphic cross section V-V' of the Eutaw Formation, eastern Gilbertown Field. See figure 37 for location.

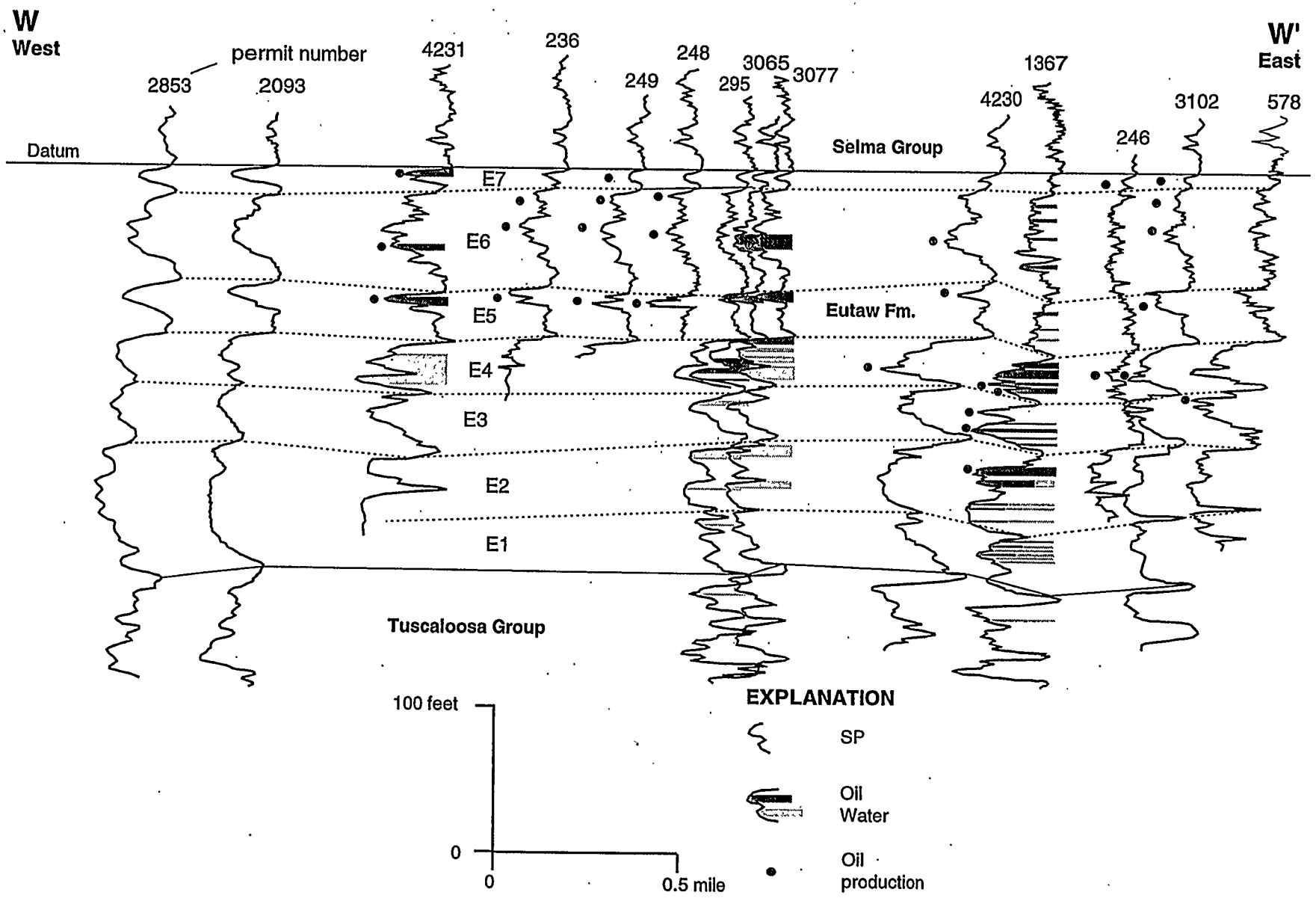

Figure 40.--Stratigraphic cross section W-W' of the Eutaw Formation, eastern Gilbertown Field. See figure 37 for location.

41–47) reveal significant facies variations within the intervals.

Well logs indicate that the Eutaw Formation sharply overlies the Tuscaloosa Group in Gilbertown Field (figs. 37–40). Interval E1 is approximately 40 feet thick; it is composed mainly of sandstone and contains some localized shale partings. However, a lack of core makes determination of grain size impossible. Updip of Gilbertown Field, Cook (1993) reported that the basal Eutaw sandstone is coarse grained and contains gravel with phosphate nodules at the base. The top of interval E1, like most intervals of the Eutaw, is ideally a sandstone–shale contact. However, the shale at the base of interval E2 is absent in some areas, thus making identification of the contact difficult. Net sandstone thickness in interval E1 varies considerably, ranging from less than 20 feet in the footwall of West Gilbertown fault A to more than 50 feet in the hanging wall of the West Bend fault (fig. 41). Oil is produced from interval E1 only in two wells which are in the horst immediately adjacent to East Gilbertown fault A.

Interval E2 is also approximately 40 feet thick and contains predominantly sandstone. Core is only available in the upper part of the interval and contains sandstone with burrows. In SP logs, the sandstone has a blocky to fining-upward signature and locally contains a significant amount of shale near the middle (figs. 36–40). Net sandstone thickness in interval E2 is the most variable in the Eutaw Formation, ranging from less than 20 feet to more than 80 feet (fig. 42). Oil is produced from the sandstone only in the structurally highest part of the horst formed by East Gilbertown fault A and the West Bend fault.

Intervals E3, E4, and E5 are each thinner than 40 feet and each tend to form coarsening-upward successions (figs. 36–40). Sandstone in these intervals is glauconitic and is generally very fine to medium grained; E5 is locally coarse grained. Phosphatic grains, shell fragments, and aragonite prisms were observed in the sandstone, and some of the associated shale contains carbonaceous plant fragments. Net sandstone thickness in intervals E3 and E4 ranges from less than 10 feet in the footwall of West Gilbertown A to more than 40 feet in the eastern part of the field (figs. 43–45). Sandstone in interval E5 is thinner than 15 feet throughout most of the field and reaches a thickness of more than 40 feet along the north side of the horst. As in interval E2, oil production in intervals E3 through E5 is restricted to the horst.

Interval E6 is about 70 feet thick and is composed of interbedded sandstone and shale (figs. 36–40). At the base is a widespread shale containing glauconite grains and carbonaceous plant fragments. Horizontal burrows were noted in the upper part of the basal shale. At the top of the interval is medium-grained sandstone containing thin interbeds of shale that give the interval a distinctive, serrate log signature. Phosphate and plant fragments are common in the middle of the interval, and broken mollusc shells and *Inoceramus* prisms were noted in the upper part. Some planktonic foraminifera were noted in thin section. The sandstone content of interval E6 generally increases toward the west. Net sandstone thickness increases from less than 20 feet in the western part of the field to more than 50 feet in the eastern part (fig. 46). Sandstone thickness also tends to decrease southward from the Gilbertown fault system. Note that oil is produced from interval E6 in two main areas that skirt the structurally highest part of the field.

Interval E7, which is the thinnest interval in the Eutaw Formation, is between 10 and 25 feet thick and consists of shale overlain by fine-grained sandstone, which is in turn overlain sharply by the Selma Group (figs. 36–40). This sandstone tends to be extremely glauconitic and is probably equivalent to the Tombigbee Sand Member of the Eutaw Formation. The sandstone is locally cemented with calcite and contains foraminifera, mica, and glauconite at the top. The sandstone extends throughout most of Gilbertown Field but passes into shale in the east central part. Sandstone is locally absent along East Gilbertown fault A and thickens southward from the Gilbertown fault system to more than 20 feet (fig. 47). Oil production comes from several areas along the southern margin of the Gilbertown fault system.

Little can be said with confidence about the depositional environments of the Eutaw Formation in Gilbertown Field, because a lack of continuous core prevents identification of bedding sequences and sedimentary structures. Investigators in other parts of Alabama have interpreted the Eutaw Formation as transgressive beach and shelf deposits (Frazier and Taylor, 1980; Cook, 1993), and the Eutaw of Gilbertown Field is perhaps considered in terms of this general framework.

The Tuscaloosa Group forms a thick, coarsening-upward interval and thus is interpreted to mark a major progradation of sediment into the Gulf Coast basin during a relative highstand of sea level. The sharp base of the Eutaw is probably a lowstand surface of erosion, or sequence boundary, and the thinning- and fining-upward succession of the Eutaw is compatible with a transgressive origin. Indeed, presence of shells and foraminiferan tests in the core samples confirms deposition in marine environments (fig. 36). However, abundant plant fragments in some sandstone and in shale indicate input of sediment from terrestrial environments. The sharp base of the Selma Group is interpreted as a transgressive ravinement that formed as Eutaw beaches were inundated and a muddy carbonate shelf was established across southwest Alabama (Russell and others, 1983; Puckett, 1992; Mancini and Tew, 1997).

The seven intervals of the Eutaw Formation (figs. 36–40) are interpreted as a set of vertically stacked parasequences. Parasequence boundaries within the Eutaw are defined at shale–sandstone contacts. General

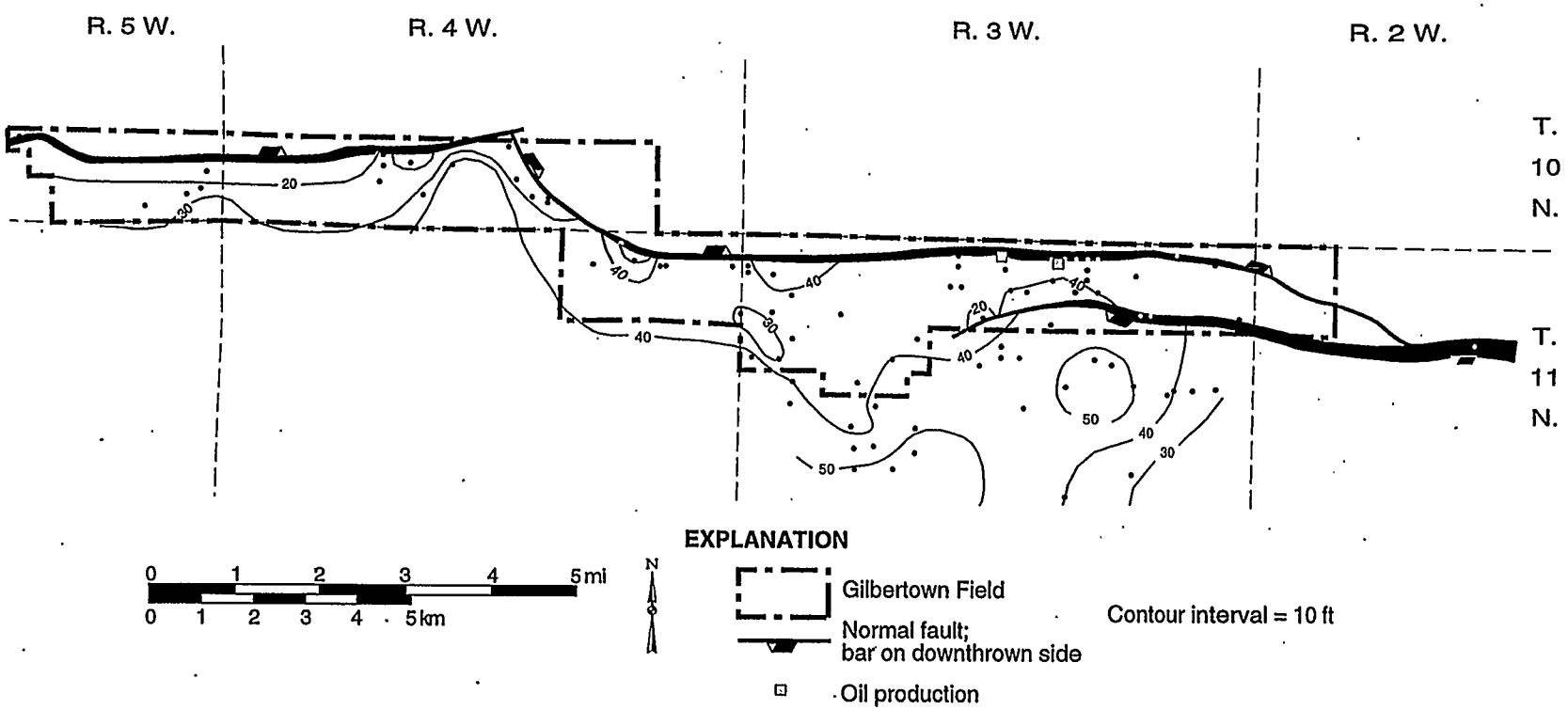

Figure 41.--Net sandstone isolith map of interval E1, Gilbertown field and adjacent areas.

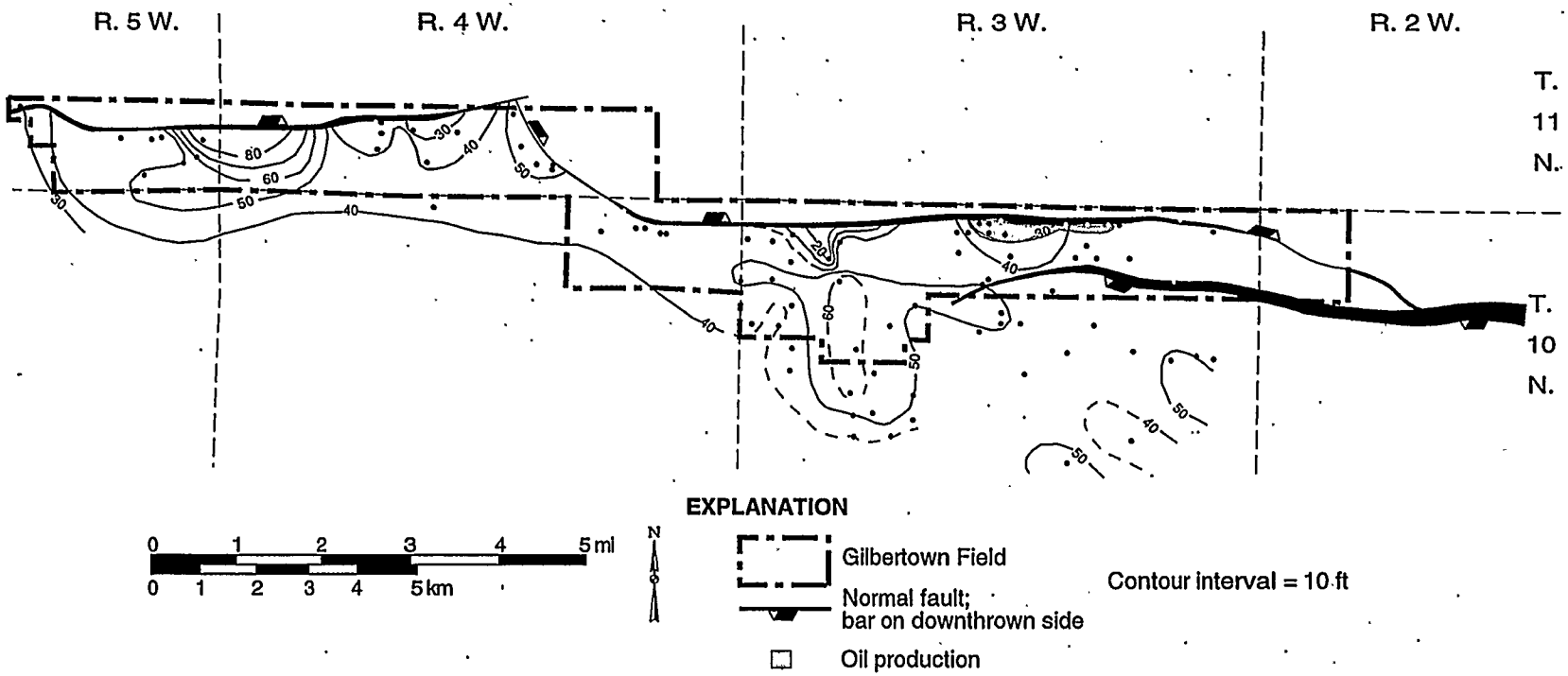

Figure 42.--Net sandstone isolith map of interval E2, Gilbertown field and adjacent areas.

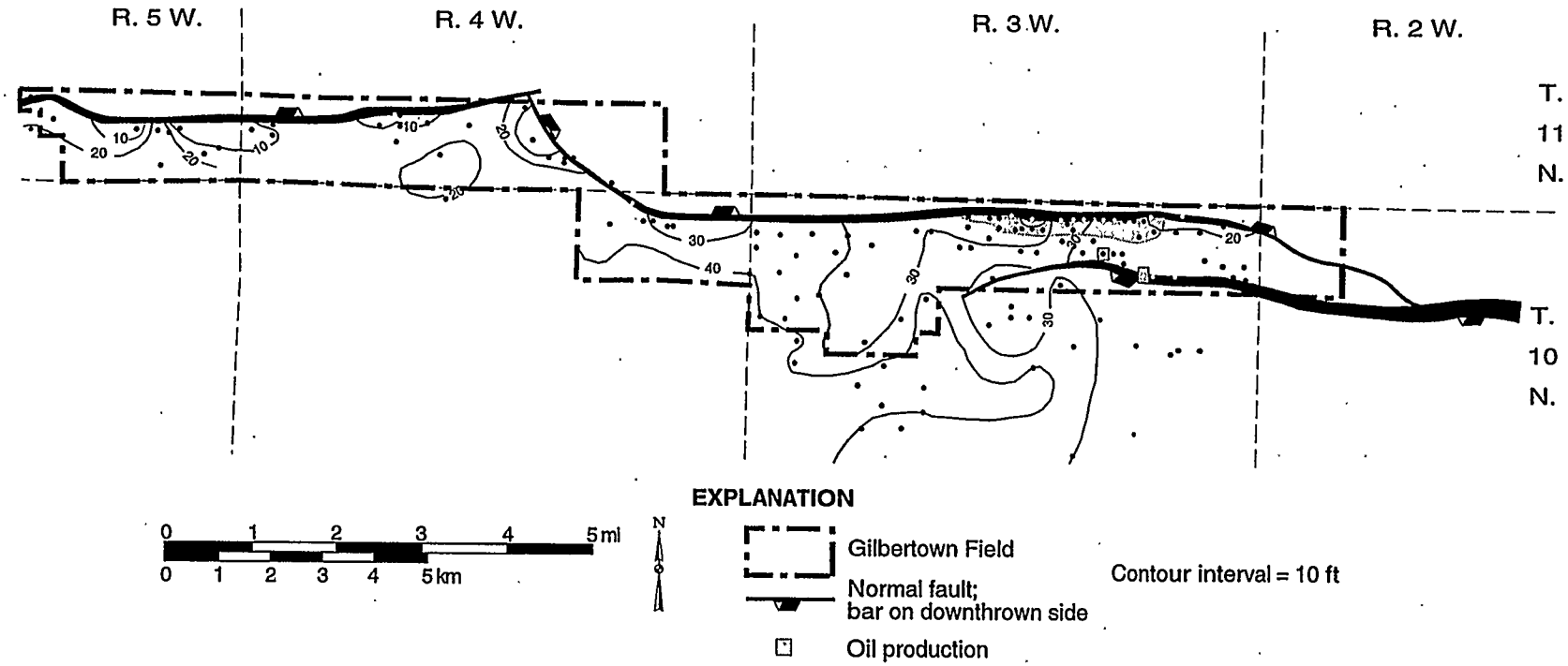

Figure 43.--Net sandstone isolith map of interval E3, Gilbertown field and adjacent areas.

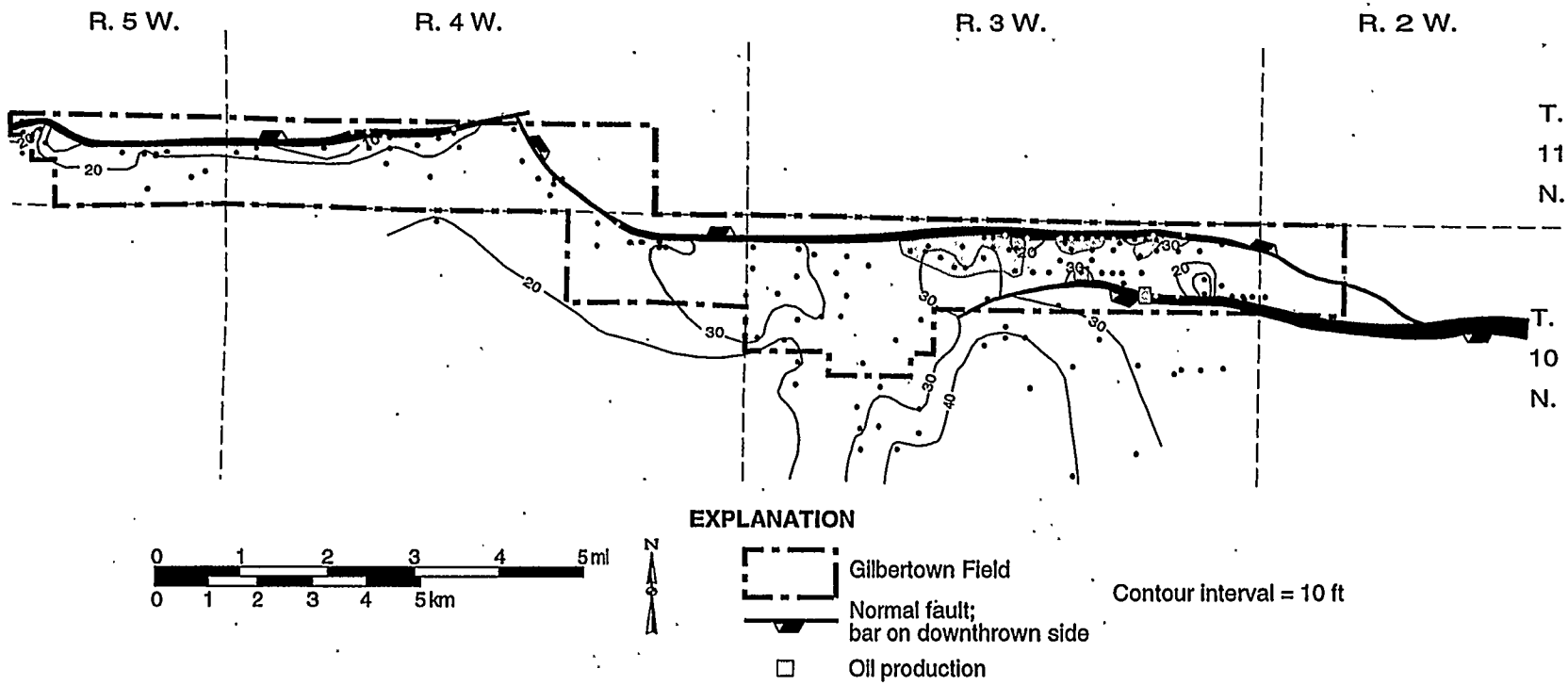

Figure 44.--Net sandstone isolith map of interval E4, Gilbertown field and adjacent areas.

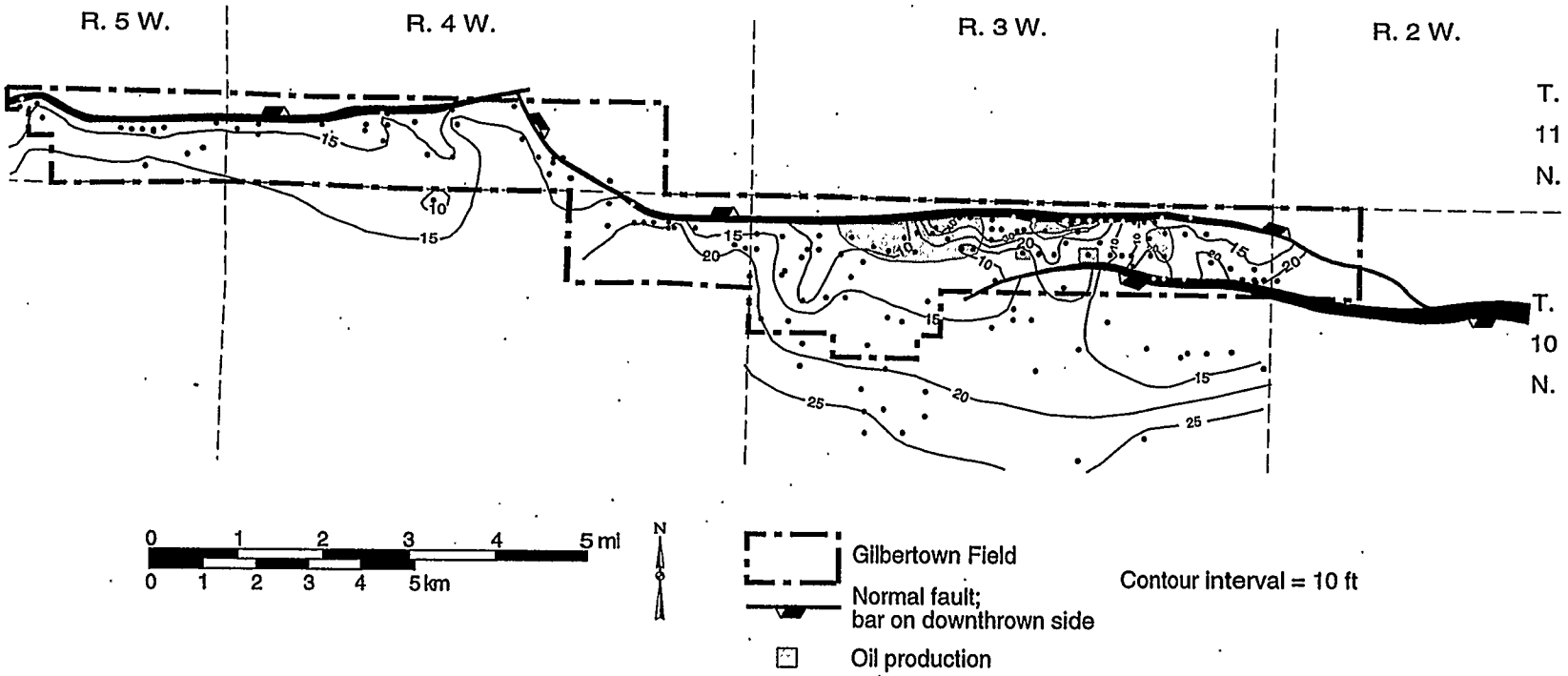

Figure 45.--Net sandstone isolith map of interval E5, Gilbertown field and adjacent areas.

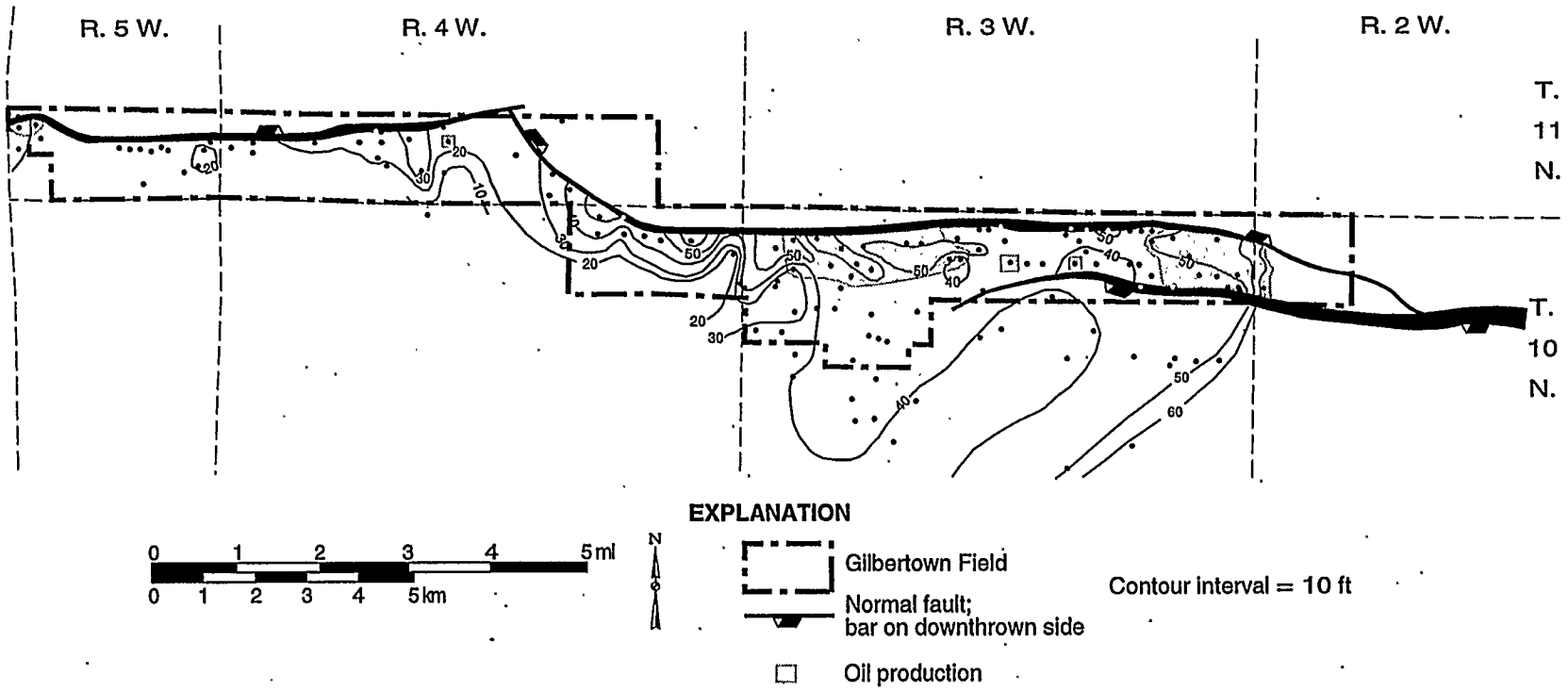

Figure 46.--Net sandstone isolith map of interval E6, Gilbertown field and adjacent areas.

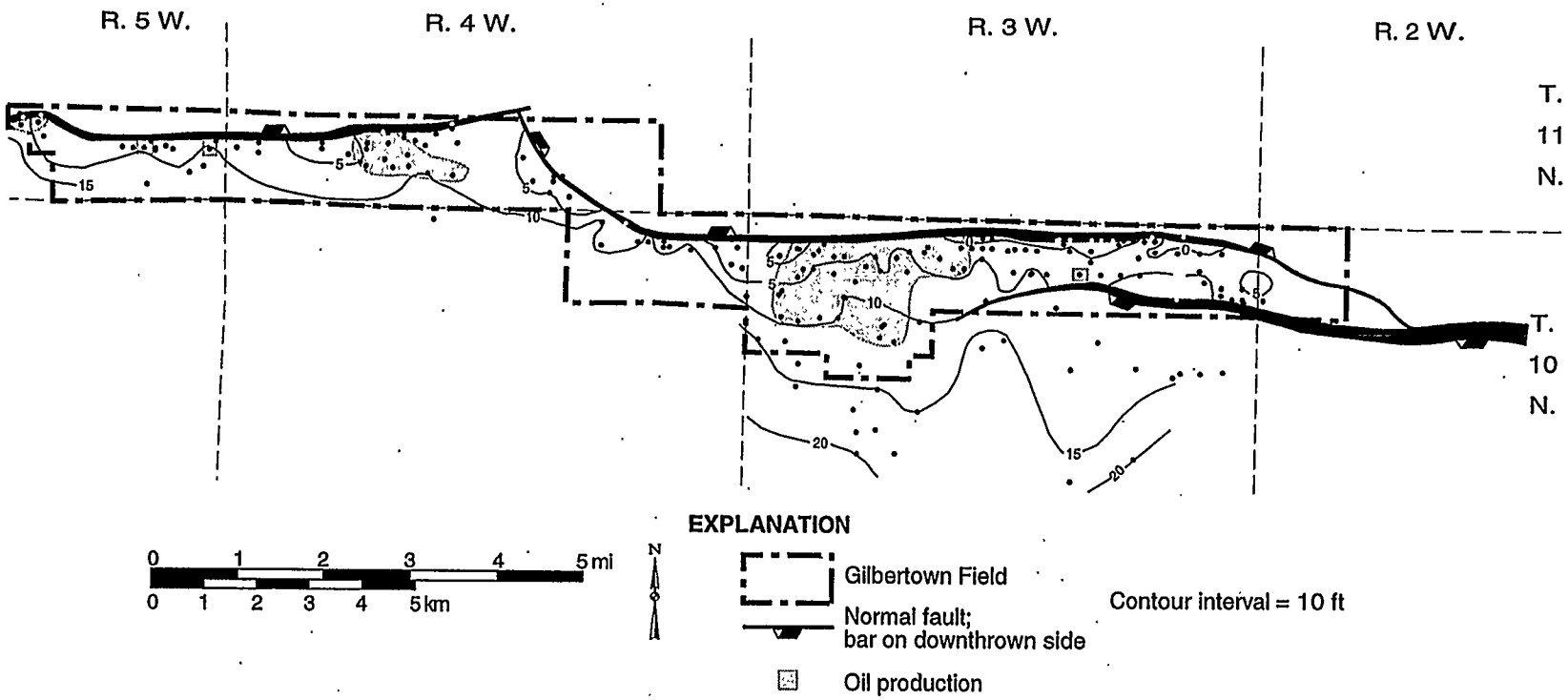

Figure 47.--Net sandstone isolith map of interval E7, Gilbertown field and adjacent areas.

fining upward of intervals E1 and E2 is suggestive of aggradation, which is characteristic of migrating inlets and tidal channels. By contrast, general coarsening upward of intervals 3 through 7 suggests that they are progradational and are bound by flooding surfaces. However, it is unclear from stratigraphic evidence alone whether progradation took place on the shelf or in a back-barrier setting, although petrologic evidence cited in the next section provides evidence for freshwater influence of diagenesis.

Petrology

Petrology is a major consideration when characterizing Eutaw reservoirs, because glauconite has a strong influence on reservoir quality and geophysical log characteristics. Framework composition and cementation also are important controls on reservoir quality. Therefore, the following sections characterize Eutaw sandstone in terms of framework composition and the authigenesis of glauconite and intergranular cement.

Framework Composition.—Quartz is the primary framework grain in Eutaw sandstone, and monocrystalline quartz constitutes 73 to 92 percent of the framework grains (figs. 48, 49). In most thin sections quartz is angular to subangular and tends to be strongly undulose. In sandstone from interval E3, quartz forms 73 to 88 percent of the framework grains; in E4, quartz is 73 to 87 percent; in E5, 84 percent; and in E6, 92 percent. Polycrystalline quartz, excluding chert, composes 9 percent or less of the quartz population. The proportion of chert increases upward in the Eutaw Formation.

Feldspar grains (fig. 50) comprise 4 to 20 percent of the framework grains, and potassium feldspar is slightly more abundant than plagioclase. The feldspar is generally angular and is partly sericitized or vacuolized. Partial replacement of feldspar by illite and calcite was noted in some samples. Some of the glauconite in the Eutaw Formation appears to be pseudomorphous after feldspar, as is discussed in the following section.

Rock fragments make up about 2 to 13 percent of the framework grains and include chert, schist, phyllite, and shale/mudstone. Other allogenic detrital grains include muscovite, zircon, epidote, opaque minerals, and fossil fragments. Muscovite composes 18 to 100 percent of the allogenic grains and locally constitutes 10 percent of the total detrital grains in the sandstone. Plotting framework composition on the QFL diagram of McBride (1963), Eutaw sandstone can be classified mainly as subarkose (fig. 48).

Glauconite.—Glauconite constitutes a large and variable component of the Eutaw Formation, composing up to 44 percent of the sandstone. The glauconite is primarily green, but brown limonitic glauconite is locally common. In oil-saturated sandstone, glauconite absorbed oil to the point that it appears black and opaque in thin section (fig. 51). Two types of glauconite are common in the Eutaw: glauconitic mica (true glauconite) and ferric illite. True glauconite is the most common form in the Eutaw Formation and is generally well rounded, having a peloidal habit, and has a dark central core. By comparison, ferric illite grains are rectangular and contain internal layering that is commonly detached (fig. 49). These grains appear pseudomorphous after feldspar and can form up to 38 percent of the total glauconite in some sandstone units. Ferric illite can be distinguished readily by its micaceous lamellar structure, length-parallel extinction, rectilinear grain shape, and selective replacement of twinned feldspar that results in a characteristic "accordion" or "book" glauconite.

True glauconite is thought to be of fecal origin (Odom, 1984; Chaudhuri and others, 1994) and can form by marine diagenesis (Cloud, 1955; Odin and Matter, 1981; Velde, 1985). Ferric illite, alternatively, is thought to form by diagenesis of feldspar, mica, pyroxene, and other chemically complex silicate minerals (e.g., Takahashi, 1939; Galliher, 1935; Light, 1952; Bailey and Atherton, 1969). Dasgupta and others (1990) and Chaudhuri and others (1994) described both types of glauconite in sandstone from India. They concluded that the glauconite may result from the direct pseudomorphism of K-feldspar by glauconite and ferric illite in the early burial stage. They further concluded that true glauconite formed in marine water, whereas ferric illite formed in fresh water. Glauconization apparently occurred at the sediment–water interface in the intertidal zone. They interpreted the coexistence of glauconite and ferric illite in some sandstone to result from mechanical mixing and influxes of fresh water into a marine environment.

Abundant glauconite and alteration of feldspar into ferric illite present difficulties for classifying Eutaw sandstone. If the glauconite is considered to be entirely authigenic and the sandstone is plotted on a standard QFL diagram that excludes glauconite (McBride, 1963), then the sandstone is primarily subarkose (fig. 48). If the ferric illite part of the glauconite were counted as feldspar, much of the Eutaw sandstone would be considered arkose. Regardless of origin, glauconite is an extremely important grain type in the Eutaw Formation. Thus, point-count data were plotted on a ternary diagram having quartz, feldspar plus lithic fragments, and glauconite as the end members (fig. 52). This diagram shows that the percentage of glauconite grains is about the same as that of feldspar plus rock fragments.

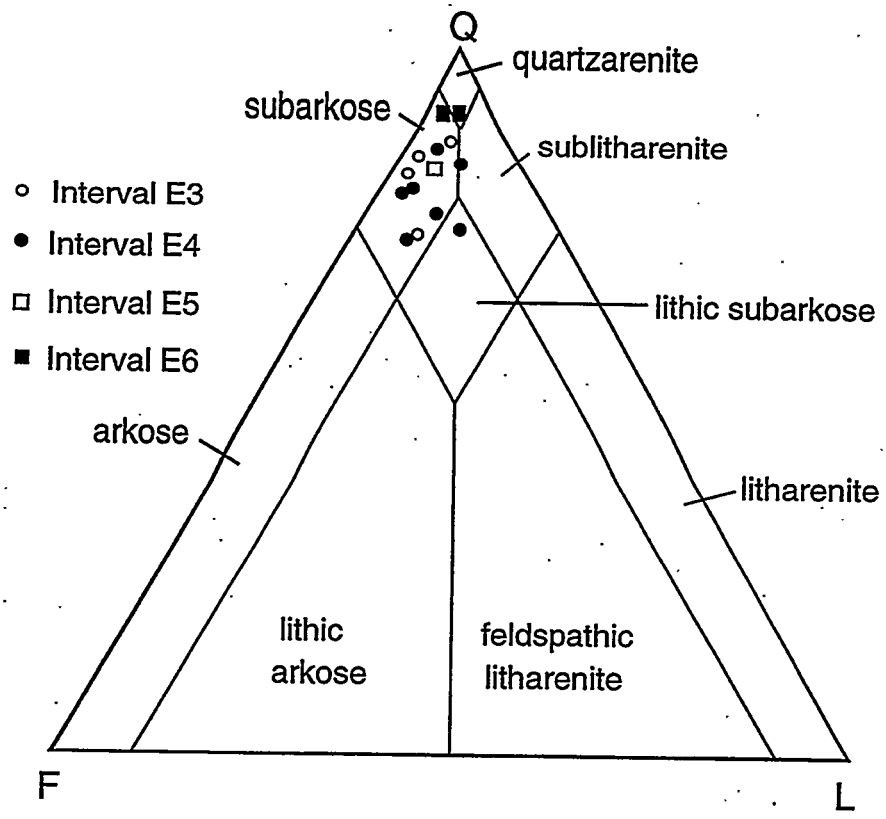

Figure 48.--QFL plot showing framework composition of Eutaw sandstone in Gilbertown Field. Sandstone classification from McBride (1963).

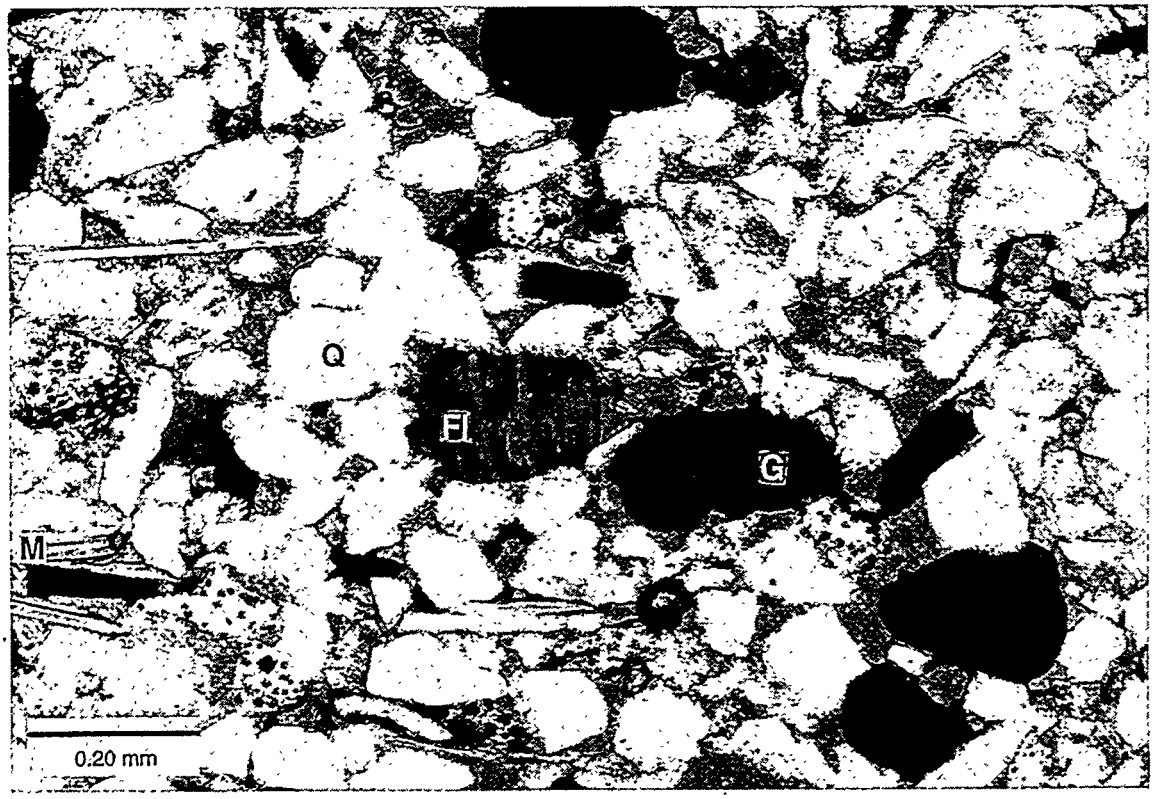

Figure 49.--Photomicrograph of subarkose from interval E4 in Gilbertown Field (permit 236, depth between 3,399 and 3,401 feet). Note open pore system (blue) and lack of compaction of mica (M). Q = quartz, G = true glauconite, FI = ferric illite pseudomorphous after feldspar.

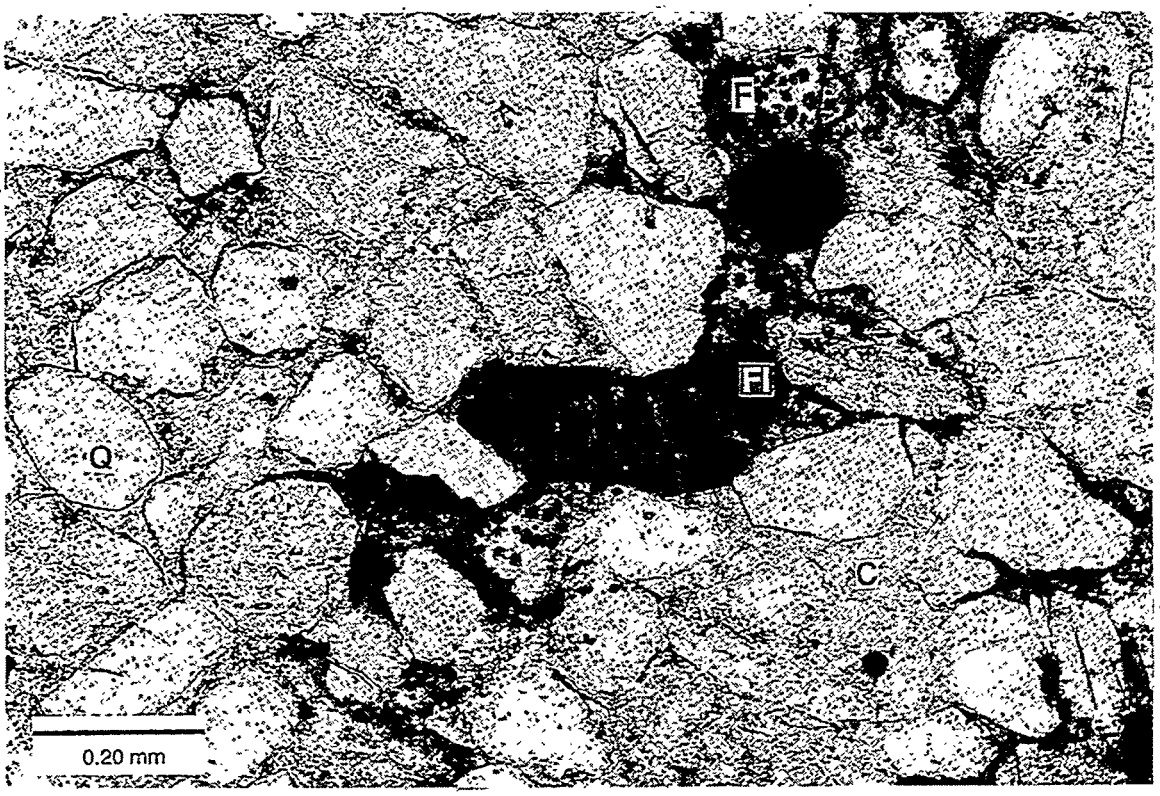

Figure 50.--Photomicrograph of sandstone in Eutaw Formation of Gilbertown Field with poikilotopic calcite cement (permit 131, depth between 3,203 and 3,213 feet). C = calcite, Q = quartz, F = feldspar, and G = glauconite (ferric illite).

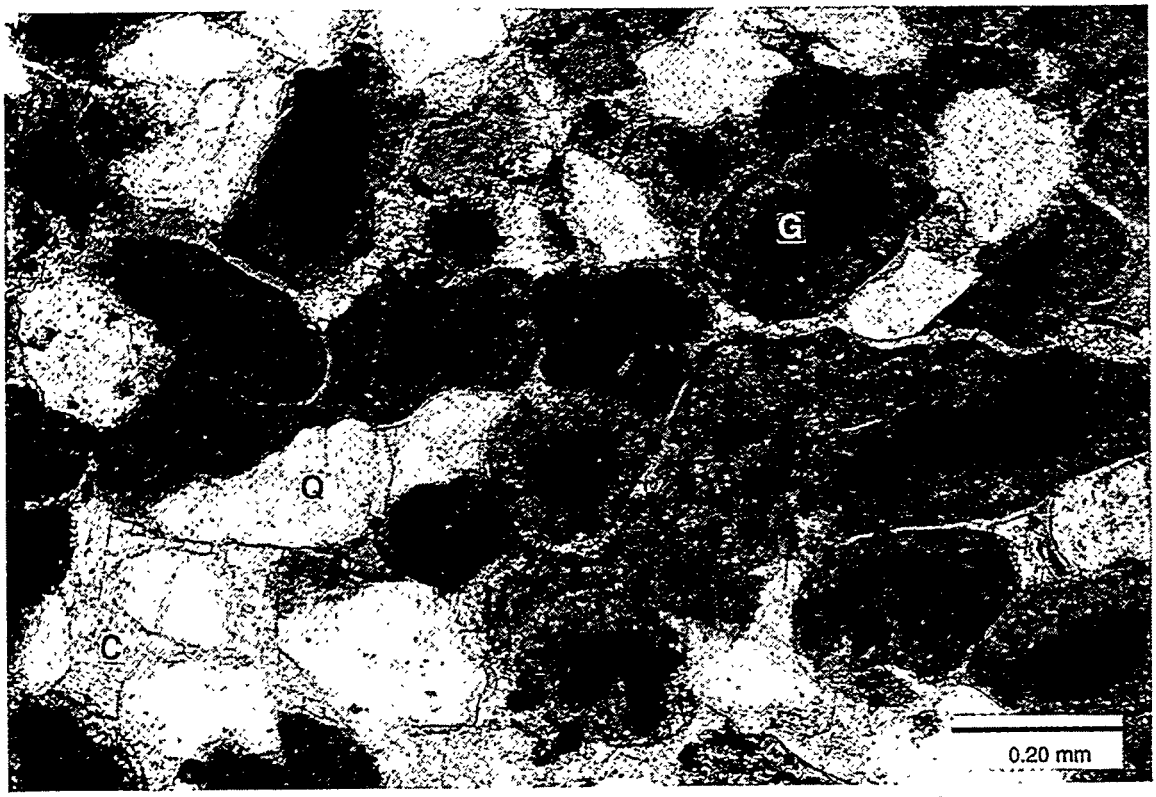

Figure 51.--Photomicrograph of glauconitic sandstone from interval E3 of the Eutaw Formation in Gilbertown Field (permit 131, depth between 3,203 and 3,213 feet). C = calcite, Q = quartz, G = peloidal glauconite (true glauconite). Note porosity rims around glauconite grains.

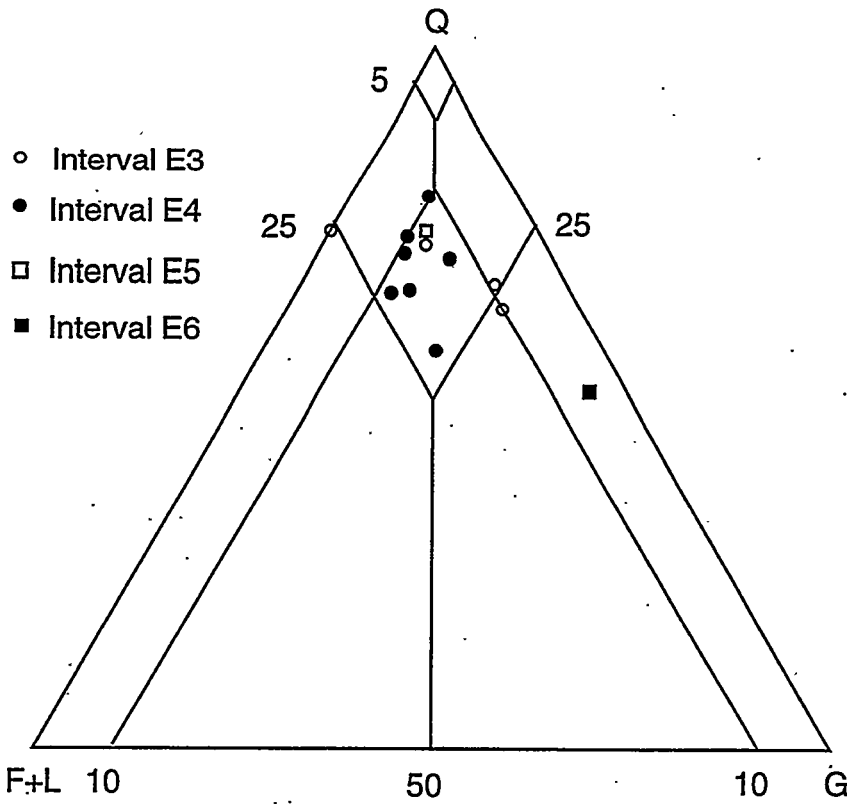

Figure 52.--QF+LG plot of Eutaw sandstone showing abundance of glauconite (G).

Cement and Porosity.—Much of the sandstone in the Eutaw Formation has an open pore system and lacks authigenic minerals other than glauconite (fig. 49). However, carbonate cement is common in many parts of the Eutaw Formation and includes siderite, calcite, and aragonite (figs. 50, 53). Siderite has a patchy distribution and ranges from isolated rhombs to dense patches of intergranular cement that occlude porosity (fig. 53). Although the distribution of siderite is irregular, the rhombs are generally smaller than 7 micrometers.

Poikilotopic calcite cement is present in some Eutaw thin sections (fig. 50), and occurrences of calcite and siderite are mutually exclusive. Calcite has a patchy distribution and occludes all porosity in parts of the reservoir. The mineral commonly is clear, but in some thin sections it has a murky appearance owing to clay inclusions. In some calcite-cemented sandstone, a thin zone of porosity rims peloidal glauconite grains (fig. 51). In interval E6, calcite cement locally fills fractures in the glauconite indicating compaction prior to cementation by calcite. Aragonite was only identified in interval E6, where it forms isopachous rims coating glauconite grains.

Cementation is clearly a major source of heterogeneity within each Eutaw sandstone interval, but the limited amount of core makes spatial trends difficult to discern. In interval E6, however, lateral variation of cementation is readily apparent. E6 sandstone generally has higher shale content than that in other parts of the Eutaw Formation, and the amount of carbonate cement increases toward the structurally highest part of the reservoir.

All of the carbonate minerals apparently precipitated early because compaction of glauconite and mica are minimal. Aragonite precipitated first in the meteoric zone because it forms isopachous grain coatings, and poikilotopic calcite apparently formed slightly later during burial when the Eutaw had entered the phreatic zone. The place of siderite in the paragenetic sequence is unclear; however, siderite typically forms near the sediment–water interface in a range of marine and terrestrial environments characterized by reducing conditions (Berner, 1981; Mozley and Wersin, 1992; Coleman, 1985; Curtis and Coleman, 1986). In nearshore and intertidal environments, siderite can form in the presence of alternating anoxic and oxic pore waters (Mozley and Wersin, 1992).

Porosity in the Eutaw Formation approaches 40 percent where authigenic cement is lacking, and in places, dissolution of minerals appears to have enhanced the pore system. Vacuolization provides some evidence for feldspar dissolution, and pores as large as sand grains may mark locations where grains have been dissolved completely (fig. 49). The thin rims of porosity around glauconite grains may reflect dissolution of isopachous aragonite (fig. 51). Minimal compaction of soft grains, like mica and glauconite, and the presence of oversize pores and floating grains in some sandstone (fig. 49) may also reflect dissolution of pore-filling cement (Schmidt and McDonald, 1979).

Log and Core Analysis

Assessing the quality of Eutaw reservoirs is extremely difficult in Gilbertown Field, because only SP and resisitivity logs were run in more than 90 percent of the wells. This limited log suite presents a particular problem for Eutaw sandstone, which is a low-resistivity, low-contrast reservoir (Cook and others, 1990). Low resistivity can be attributed to conductive iron-rich minerals, namely glauconite and siderite, which can form up to 30 percent of the sandstone. Clay minerals can cause erroneous calculation of porosity and water saturation from well logs (Hilchie, 1978), and the low resistivity of the glauconitic sandstone merely compounds this problem. Were density and neutron porosity logs available, shaly sand analysis (Asquith and Gibson, 1982) would have potential for characterizing Eutaw reservoirs. Since this is not possible, the only other approach is to determine if some way exists to correlate SP and resistivity curves with porosity and permeability data from commercial core analyses. However, no significant correlations between log data and core data were found.

This having failed, the only recourse was to perform a general statistical analysis of the core data to derive generalized values that could be applied to each stratigraphic interval in the Eutaw Formation (table 4). Although this approach is less desirable than determining porosity, the statistical analysis quantifies the variability of reservoir quality and reveals relationships among the seven Eutaw sandstone intervals.

The three variables analyzed are porosity, permeability, and oil saturation (table 4). All of these variables are log-normally distributed, and the statistics were calculated accordingly. Porosity of Eutaw sandstone is generally high, ranging from 12.7 to 39.7 percent, and has a log-normal mean of 25.5 percent. Porosity is highest in interval E2 and generally decreases upward, reaching a minimum in interval E6 (fig. 54), which is finest grained and contains the most shale, glauconite, and carbonate cement.

Permeability in the Eutaw Formation typically varies between 8 and 290 millidarcies (md) and has a log-normal mean of nearly 50 md. Mean permeability decreases upward in the formation and has a maximum value of 166 md in interval E2 and reaches a minimum value of 17 md in interval E6. Permeability is extremely heterogeneous in intervals E1 through E3, with values as high as 700 md being common (fig. 54). The upper limit of the standard deviation decreases markedly upward in section to less than 100 md in intervals E6 and E7. This extreme decrease of permeability is apparently related not only to

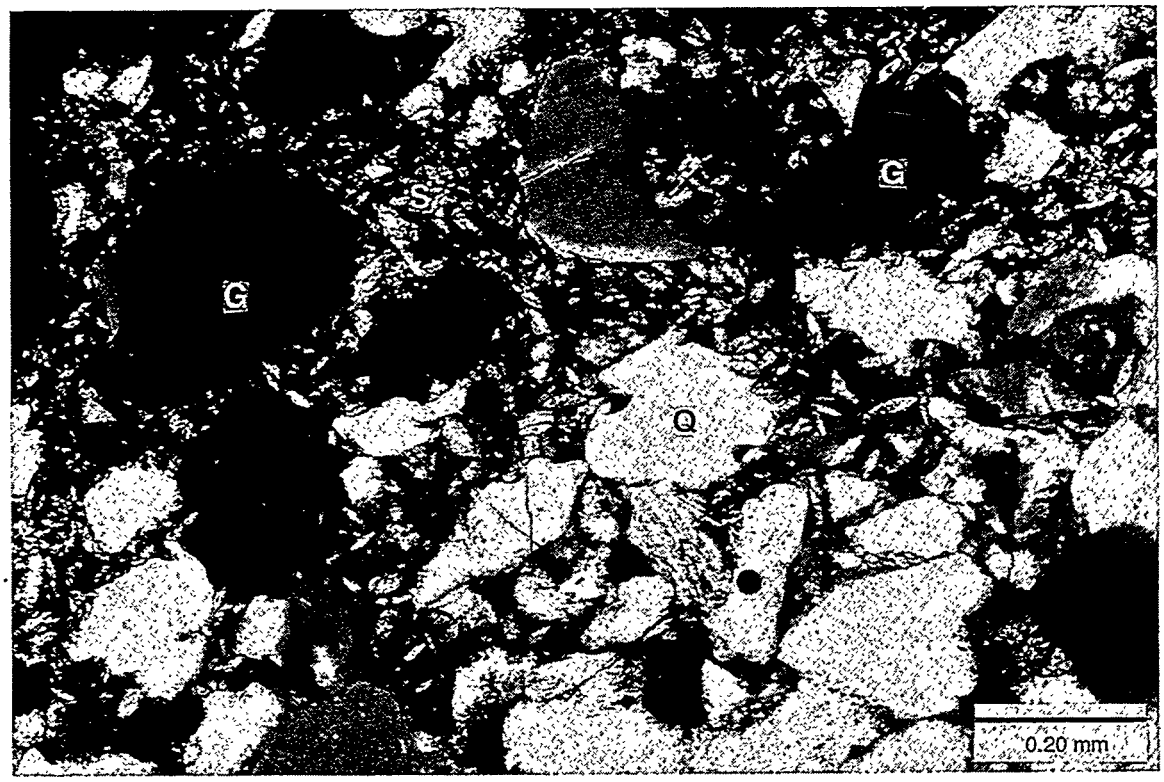

Figure 53.--Siderite-cemented sandstone in interval E4 of the Eutaw Formation in Gilbertown Field (permit 206, depth between 3,296 and 3,313 feet). S = siderite, Q = quartz, G = oil-stained peloidal glauconite (true glauconite).

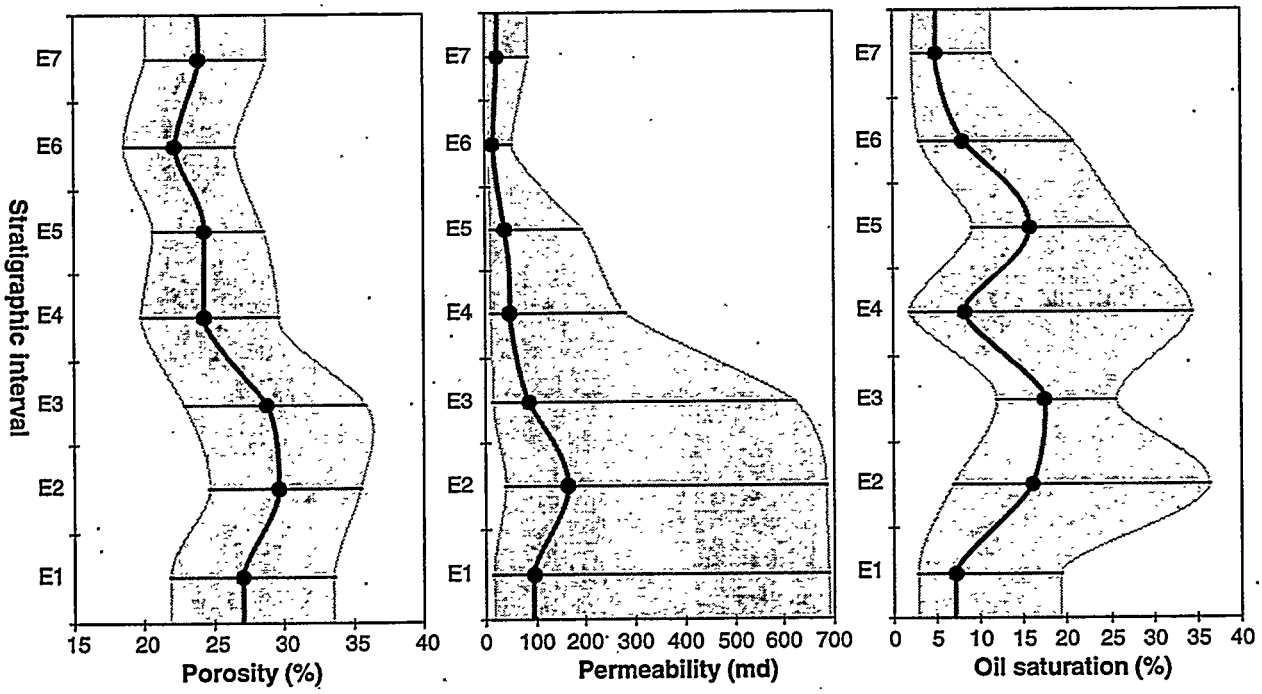

Figure 54.--Stratigraphic variation of reservoir quality in the Eutaw Formation, Gilbertown Field. Dark line is log-normal mean, shaded area is log-normal standard deviation.

Table 4.--Results of statistical analysis of commercial core-analysis data, Eutaw Formation.

	n	Log normal mean	Maximum	Minimum	$10^{\sigma-}$	$10^{\sigma+}$	Std. error of log x
All intervals							
Porosity (%)	319	25.5	39.7	12.7	20.6	31.7	0.01
Permeability (md)	308	49.7	5470.0	0.0	8.5	289.7	0.04
Oil Saturation (%)	185	9.6	38.5	0.0	3.5	26.7	0.03
Interval E7							
Porosity (%)	51	24.0	33.5	15.1	20.1	28.7	0.01
Permeability (md)	42	22.4	540.0	0.0	5.8	86.5	0.09
Oil Saturation (%)	34	5.1	23.2	0.0	2.3	11.4	0.06
Interval E6							
Porosity (%)	56	22.2	33.3	12.7	18.7	26.5	0.01
Permeability (md)	55	16.8	450.0	1.1	5.4	52.1	0.07
Oil Saturation (%)	44	8.0	35.0	0.0	3.1	20.7	0.06
Interval E5							
Porosity (%)	26	24.3	30.6	17.1	20.7	28.6	0.01
Permeability (md)	26	37.7	530.0	2.6	7.4	192.3	0.14
Oil Saturation (%)	17	15.8	30.7	0.0	9.2	27.4	0.06
Interval E4							
Porosity (%)	66	24.3	36.9	16.0	19.9	29.7	0.01
Permeability (md)	66	48.9	2220.0	2.8	8.5	281.8	0.09
Oil Saturation (%)	32	8.2	38.5	0.0	2.0	34.5	0.11
Interval E3							
Porosity (%)	58	28.7	39.7	15.2	23.0	35.8	0.01
Permeability (md)	57	87.3	5470.0	3.3	12.3	620.9	0.11
Oil Saturation (%)	25	17.5	31.6	0.0	11.9	25.6	0.03
Interval E2							
Porosity (%)	52	29.6	37.4	16.9	24.7	35.5	0.01
Permeability (md)	52	165.6	1580.0	5.2	39.9	687.1	0.09
Oil Saturation (%)	26	15.9	35.2	0.0	6.9	36.4	0.07
Interval E1							
Porosity (%)	10	27.1	37.0	19.4	21.9	33.6	0.03
Permeability (md)	10	97.7	1670.0	6.2	13.9	688.7	0.27
Oil Saturation (%)	10	7.2	37.0	0.0	2.7	19.2	0.16

decreasing grain size, but to clogging of pore throats by clay and cement. Because of this, porosity and permeability in the Eutaw Formation correlate with an r^2 of only 0.70 (fig. 55).

Much of the core-analysis data comes from water-bearing zones in the Eutaw Formation, so statistics for oil saturation were calculated only where oil saturation values are greater than zero (table 4). Mean oil saturation in the Eutaw is only 9.6 percent, although values between 3.5 and 26.7 percent are common. Oil saturation values vary considerably by stratigraphic interval, with values tending to be high in intervals E2, E4, and E5 (fig. 54). The reasons for this variation, however, are unclear.

Selma Group

Stratigraphy and Depositional Environments

Correlating well logs reveals a distinctive internal stratigraphy within the Selma Group that can be recognized throughout the Gilbertown area (fig. 56). Eight intervals, labeled S1 through S8, could be identified in the Selma Group. Interval S1 sharply overlies Eutaw sandstone and is distinguished by higher resistivity resulting from higher quartz content than other parts of the Selma Group in the area. The other intervals can be distinguished most easily by changes in spontaneous potential (SP). Intervals with negative deflection on the SP curve tend to have lower resistivity than those with a positive deflection. Examination of well samples indicates that, despite significant variation of geophysical log properties, lithologic variation within the chalk is minimal. In general, intervals with a negative SP deflection are slightly darker and more micaceous than other intervals.

A calcisphere packstone corresponding to the Arcola Member of the Mooreville Chalk was identified at the approximate depth of a thin, negative-SP marker near the middle of the Selma Group (fig. 56). The Arcola Member marks the top of the Mooreville Formation. In the upper part of the Selma Group, intervals with a

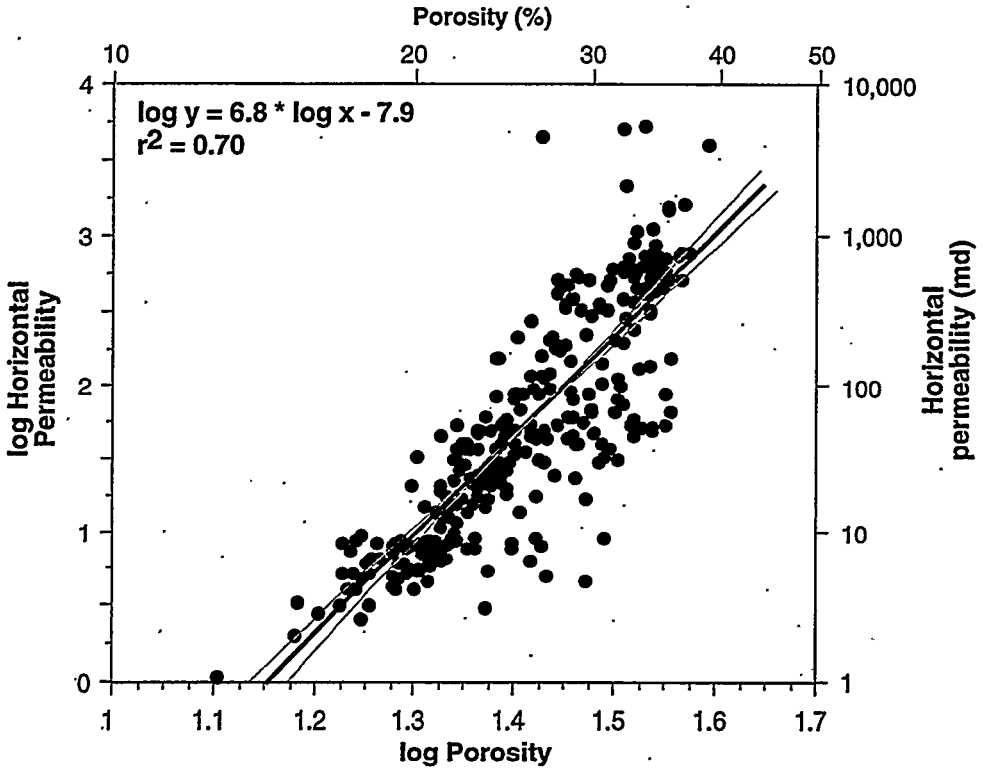

Figure 55.--Scattergram showing correlation between porosity and permeability in Eutaw sandstone. Moderate r^2 value related to heterogeneous cementation of Eutaw reservoirs.

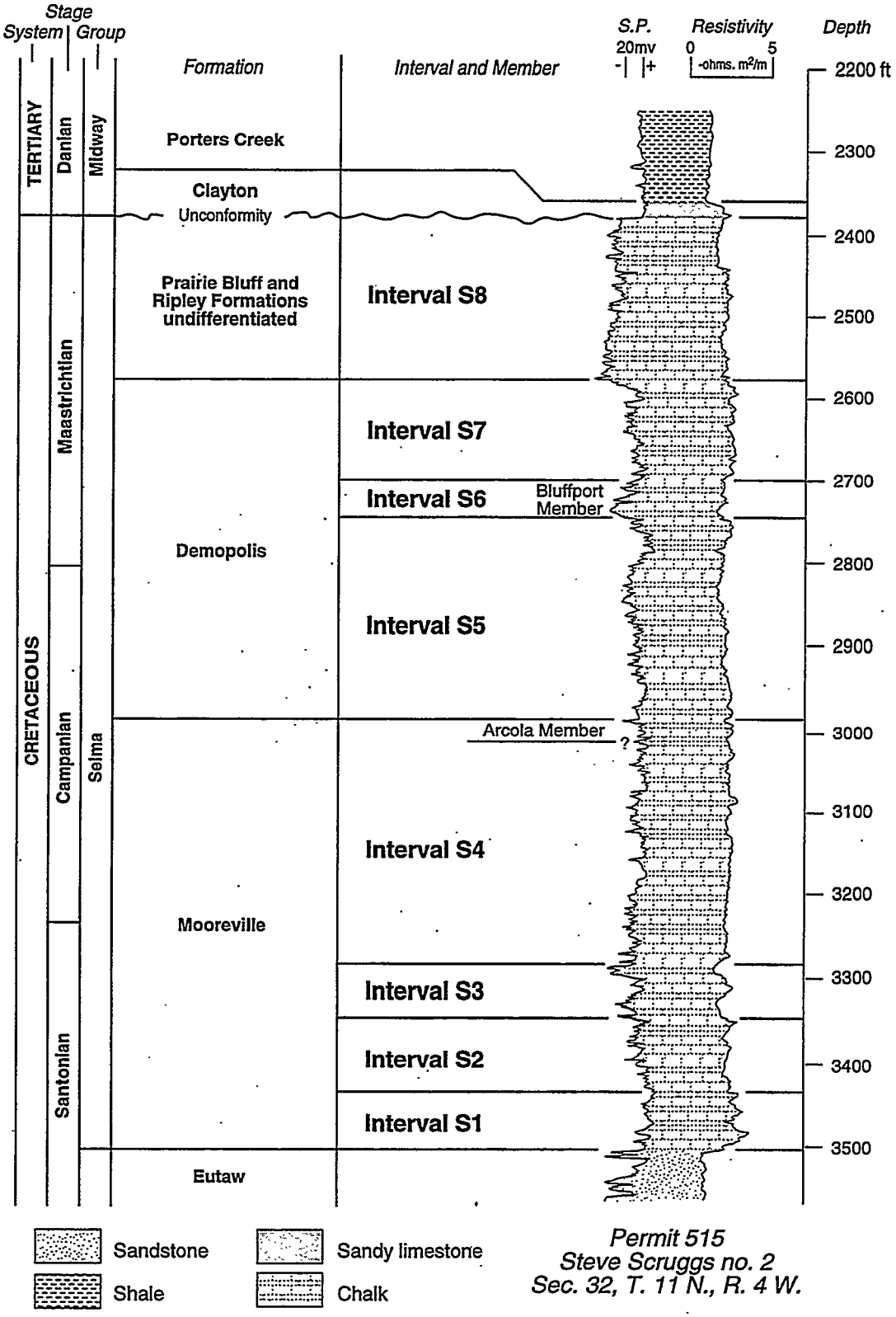

Figure 56.--Stratigraphy of the Selma Group, Gilbertown Field and adjacent areas.

negative SP deflection correlate provisionally with the Bluffport Member of the Demopolis Chalk (interval S6) and with the Prairie Bluff and Ripley Formations (interval S8). The Selma Group is overlain by the Clayton Formation, which is a sandy limestone thinner than 20 feet. The Clayton Formation has moderate resistivity similar to that of the Selma Group and positive SP similar to that of the shale of the overlying Porters Creek Formation.

The widespread distribution of each chalk interval is compatible with the interpretation of a muddy carbonate shelf (Russell and others, 1983; Puckett, 1992). Quartz in interval S1 probably reflects reworking of Eutaw sediment, which was still being deposited in updip parts of the Gulf Coast basin (Mancini and Tew, 1997). The relatively pure chalk of intervals S2 through S5 is interpreted to represent open-shelf deposition, and the calcisphere packstone of the Arcola Member is an enigmatic unit that to this date has defied interpretation. The slightly argillaceous chalk of the Bluffport Member (interval S6) signals renewed clastic influx into the study area, and interval S7 heralds a temporary return to open-shelf deposition. In outcrop the Ripley Formation contains shale and sandstone that were apparently deposited in marginal-marine and inner-shelf environments (Russell and others, 1983), and the argillaceous chalk of interval S8 is a distal expression of the encroachment of Ripley sediment onto the Selma shelf. The Prairie Bluff Formation in outcrop is dominantly chalk but is rich in clastic material. In the Gilbertown area, the Prairie Bluff is either indistinguishable from chalk equivalent to the Ripley Formation or was eroded prior to deposition of the Clayton Formation.

Minimal lithologic variation within the chalk suggests that each stratigraphic interval has similar mechanical properties. Therefore, internal stratigraphy is not predicted to be a major control on the distribution of fractures in the Selma Group. Even so, the SP and resistivity signatures of the chalk provide for fine stratigraphic subdivision that enables identification of faults with less than 25 feet of vertical separation on the basis of missing and shortened section (fig. 57). For this reason, careful correlation of well logs is critical for identifying potential productive zones in the Selma Group.

Petrology: Stable Isotope Analysis

The stable isotope ^{18}O has value for determining paleotemperatures during deposition of carbonate rocks and during precipitation of authigenic cement. Assuming isotopic equilibrium, the $\delta^{18}O$ value of calcite is controlled by the temperature of precipitation and the isotopic composition of the parent water (Dickson and others, 1990). One potential source of variation in $\delta^{18}O$ values of diagenetic calcite cements is progressive temperature change due to burial of the host sediment.

Values for chalk, slickensides, and sparry calcite obtained for the six samples from the Selma fall into three distinct fields (fig. 58, table 5). Values of $\delta^{18}O$ for chalk samples range from -3.31 to -3.58 ‰ (PDB) and are consistent with $\delta^{18}O$ values reported from Cretaceous limestone in the literature (Veizer and Hoefs, 1976; and Viezer, 1983). The $\delta^{18}O$ value for the sparry calcite from the vug in the core of permit 266 is -5.10 ‰ (PDB), a value lighter than that of the host chalk. The $\delta^{18}O$ values for the slickensides in the chalk range from -7.55 to -7.95 ‰ (PDB), lighter values than those for the sparry calcite or the chalk. The $\delta^{18}O$ values were plotted on a graph showing the variation of the $\delta^{18}O$ of calcite as a function of temperature (Veizer, 1983) (fig. 59). The graph indicates that chalk formed at about 32°C (89°F), vug calcite at about 39°C (102°F), and calcite slickensides at about 55° to 57°C (131 to 135°F).

Comparison of these paleotemperatures with the burial and thermal model (fig. 34) indicates that the calcite vug fill formed during the Eocene near maximum burial. The slickensides, however, record higher temperatures than can be accounted for by simple burial and thermal modeling. Explanations for the high temperatures recorded by the slickensides include migration of fluid along faults from deep sources and friction during fault movement.

The $\delta^{13}C$ of calcite is relatively insensitive to changes in temperature (Veizer, 1983) and is used rather to monitor the $\delta^{13}C$ of the total dissolved carbon (TDC) in the solutions from which they precipitate. Hudson (1977) summarized the range of $\delta^{13}C$ values for modern and ancient marine limestone, cement, and soil carbonate. Values of $\delta^{13}C$ for the five samples studied fall within a narrow range of 1.08 to 1.76 ‰ (PDB) (fig. 58, table 5). These values are consistent with chalk and marine carbon (Hudson, 1977), suggesting that diagenetic carbonate in the Selma Group was derived locally from chalk.

Table 5.--Results of stable isotope analysis of chalk and calcite fracture fills in the Selma Group.

Permit	Sample	$\delta^{13}C$	$\delta^{18}O$
446	slickensides	1.65	-7.95
266	slickensides	1.30	-7.55
266	vug-fill spar	1.08	-5.10
266	chalk	1.76	-3.58
446	chalk	1.69	-3.31

Log Analysis

Very little core of the Selma Group in Gilbertown Field survives today, so it is nearly impossible to observe faults and fractures directly. Therefore, geophysical well logs are the only tools that can be

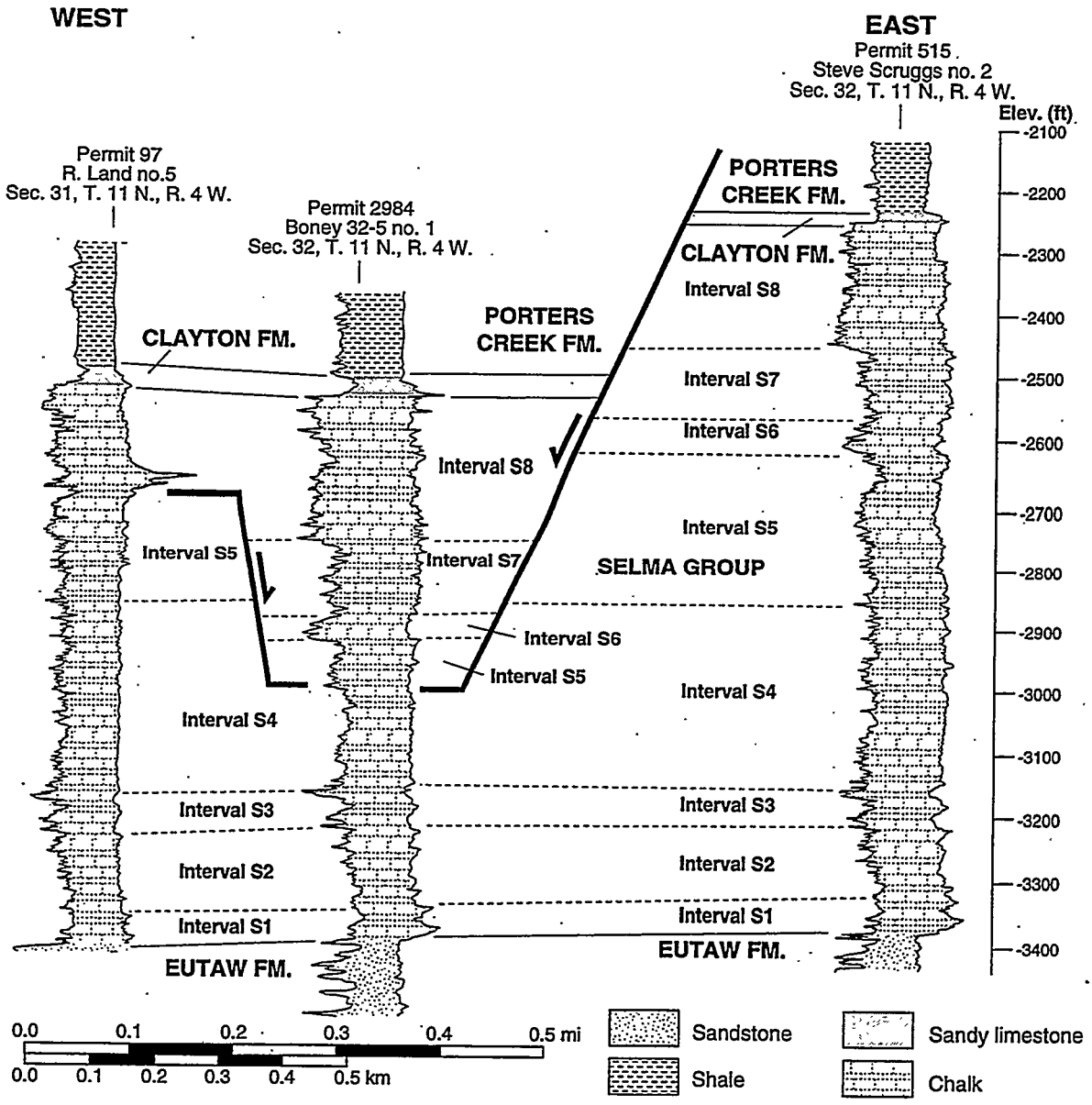

Figure 57.--Correlation of selected well logs penetrating West Gilbertown fault A, Gilbertown Field. Note diagnosis of faults based on missing stratigraphy and high resistivity of faulted interval in permit 97.

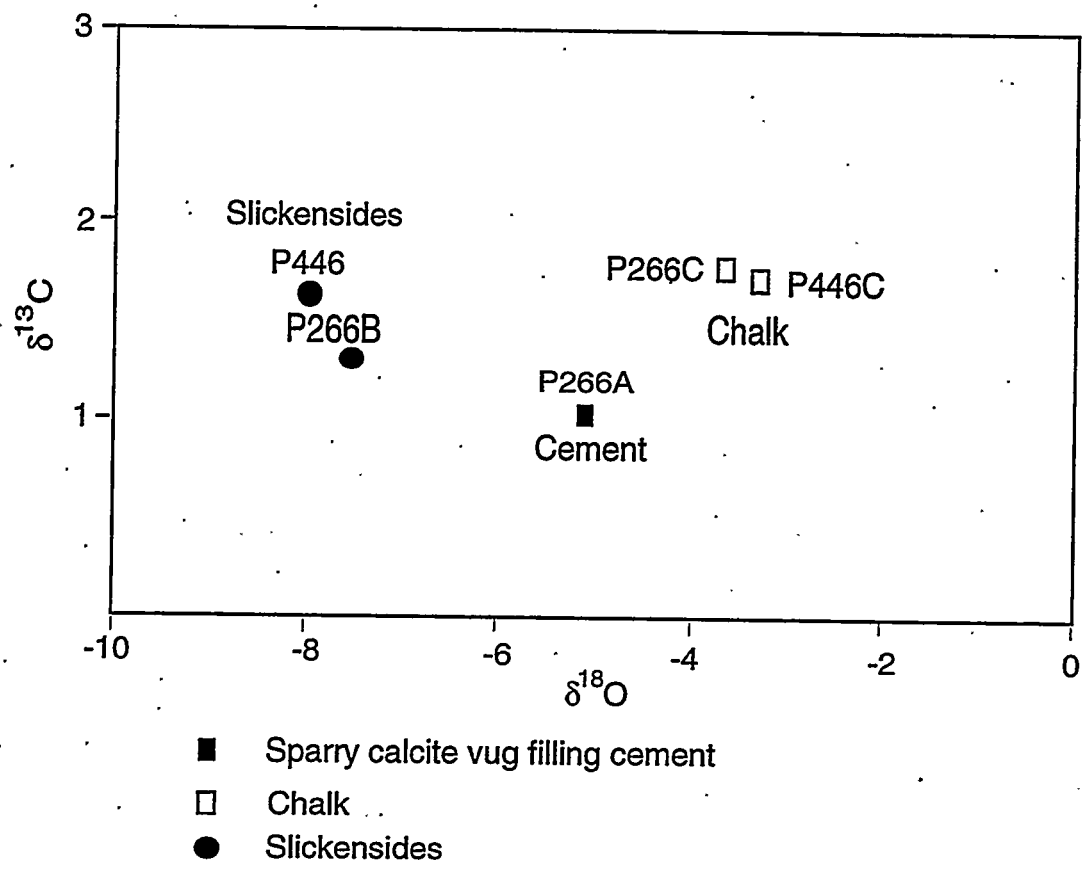

Figure 58.--Scatterplot showing $\delta^{13}C$ and $\delta^{18}O$ values in the Selma Group, Gilbertown Field.

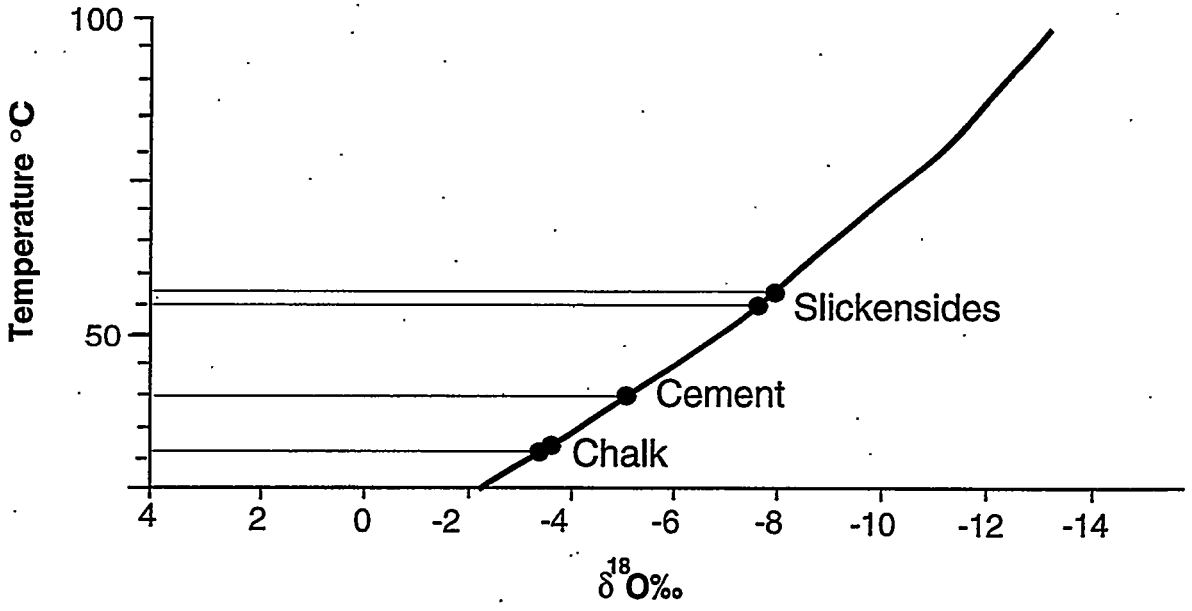

Figure 59.--Variation of $\delta^{18}O$ values of calcite in the Selma Group as a function of temperature in Gilbertown Field (diagram after Veizer, 1983).

used to predict fractures. Three sets of well logs appear useful for predicting fractures in the Selma Group, and these include SP–resistivity logs, dipmeter logs, and fracture identification logs.

SP and Resistivity Logs.—As already mentioned, SP logs are useful for identifying normal faults on the basis of missing section (fig. 57). Faults are associated with zones of exceptional resistivity, such as in well 97. High-resistivity zones are apparently caused by calcite fracture fillings. Plotting zones of anomalously high resistivity on strike cross sections of the faults reveals some basic relationships among the wells that have produced successfully from the Selma Group (fig. 60). Note that all of the wells have penetrated the hanging-wall blocks and that fault splays are common, especially along East Gilbertown fault A. The vast majority of fault cuts identified by missing stratigraphy are associated with a high-resistivity anomaly, and the anomalies typically range in thickness from 10 to 50 feet. Only one well contains anomalies in the footwall of the Gilbertown fault system. Moreover, the thickest anomalies extend from the fault cut upward into the hanging-wall block. This result suggests that fracturing is mainly in the hanging wall of the Gilbertown fault system, as was originally suggested by Braunstein (1953).

Dipmeter Logs.—Dipmeter logs were run on only two wells that produced from the Selma Group, but these logs contain a wealth of structural information supporting the hypothesis of dominant hanging-wall deformation. Well 4195 is located along East Gilbertown fault A in the eastern part of the relay zone and contains two faults (fig. 61). High-quality dipmeter interpretations are shown as arrows with black dots, whereas low-quality solutions based on only 3 of 4 resistivity pads have white dots. Fault cuts were identified by correlating the SP and resistivity curves with logs of nearby wells lacking faults in the Selma Group.

Dip in the footwall of the deepest fault is minimal in well 4195 (fig. 61). The fault cut is expressed in the dipmeter log as a single low-quality point dipping steeper than 35° NE. Dips return to near zero immediately above the fault cut and then gradually increase to nearly 35°. The dipmeter records nearly 200 feet of dipping strata in the hanging wall, and nearly all the dip arrows mark a north–northeast dip, which is perpendicular to strike of the fault. Dip magnitude is erratic between depths of 2,900 and 3,000 feet, and low-quality three-pad solutions abound. Above 2,900 feet, however, dip gradually decreases from more than 30° NE, returning to the gentle dips that predominate in the footwall. Increasing dip at the base of the deformed zone is common in footwall drag folds (Schlumberger, 1989; Berg and Avery, 1995), but deformation is clearly in the hanging wall of the fault, which is more suggestive of a folded block within the fault zone. Erratic dip magnitudes in the heart of the deformed zone may reflect small-scale faulting and folding, and the preponderance of three-pad solutions may signify steep dip and shielding of resistivity pads by fractures and faults. Decreasing dip magnitude at the top of the deformed zone is typical of hanging-wall drag folds. In all, the structural style may resemble that which was observed in outcrop at Coffeeville Landing, where a dipping block is preserved within the fault zone, and a large drag fold is developed in the hanging wall (fig. 26).

The shallower of the two faults in permit 4195 has a strong high-resistivity anomaly in the hanging wall immediately adjacent to the fault, but dipmeter results suggest that a much broader zone is involved in the deformation (fig. 61). Dip magnitudes in the hanging wall are as high as 45°, and the dip arrows form a "bag of nails" pattern in which dip direction and magnitude are erratic. As in the deformed zone associated with the deeper fault, moreover, three-pad solutions predominate. Bags of nails typify pervasively sheared zones in Tertiary growth faults of the Gulf Coast basin (Berg and Avery, 1995). However, the SP log indicates that intervals S7 and S8 have been shortened by only 50 feet (15 percent), and most four-pad solution points mark dips gentler than 10 degrees. Accordingly, the erratic dipmeter signature may be more closely related to shielding of resistivity pads by fractures and small-scale faults than to intense shearing.

Fracture Identification Logs.—Fracture identification logs (FILs) were run on most of the Selma wells drilled after 1975. Belden and Blake, Incorporated used these logs to select perforation zones in the Selma Group (fig. 62). During drilling, oil shows were not recorded in any of the Belden and Blake wells, yet nearly all of the wells completed in the Selma Group on the basis of FILs produced more than 10,000 barrels of oil.

FILs are presentations of the high-resolution conductivity data that can be used to calculate dipmeters (Schlumberger, 1989). However, dipmeters were not calculated when the logs were recorded, and we are trying to determine if the operator or Schlumberger still has the original data. The main tools used for fracture detection in FILs are four conductivity curves and the two curves generated by a four-arm caliper. If fractures are absent, the four conductivity curves are ideally identical, reflecting uniform conditions around the full circumference of the borehole. If one or more conductivity pads contacts a fracture, however, the curves should differ. Using the orientation and correlation curves, it is then possible to calculate the orientation of fractures contacting multiple pads or to identify which part of the borehole a fracture contacted a single pad. Fracturing can also be indicated by the caliper curves, which can record

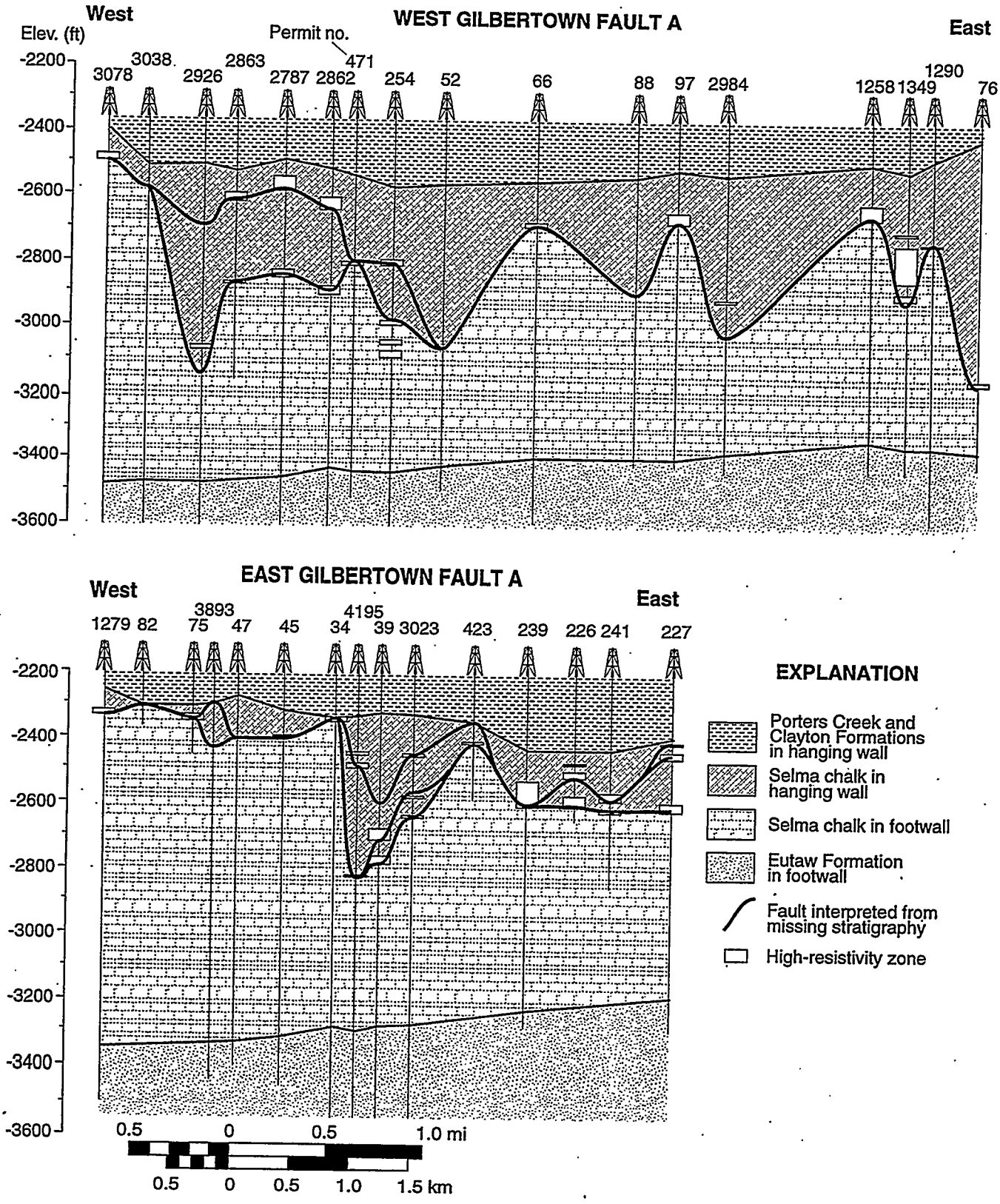

Figure 60.--Strike cross sections showing fault cuts and distribution of high-resistivity zones in wells that have produced oil from the Selma Group.

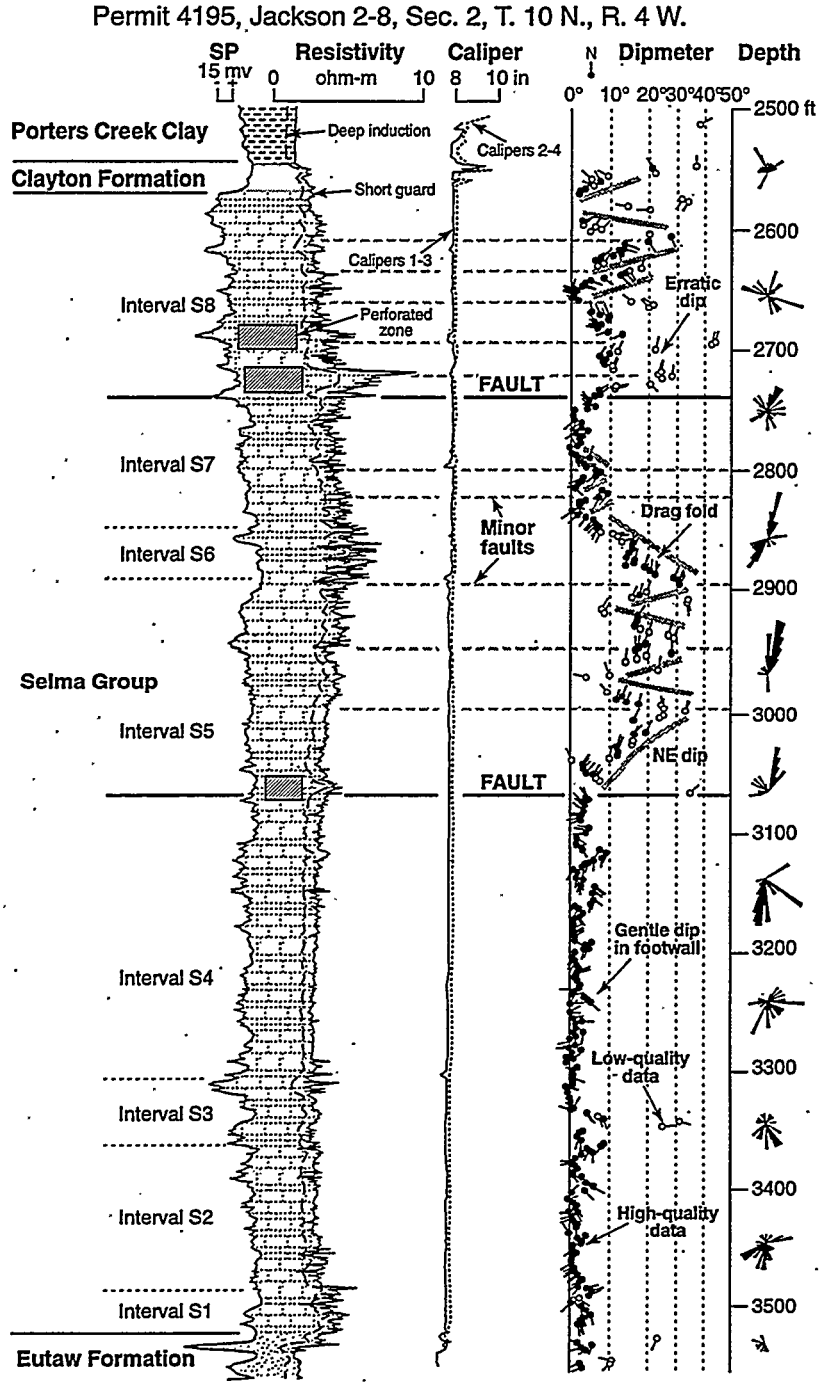

Figure 61.--Dipmeter log of the Selma Group in Gilbertown Field showing characteristics of hanging-wall deformation.

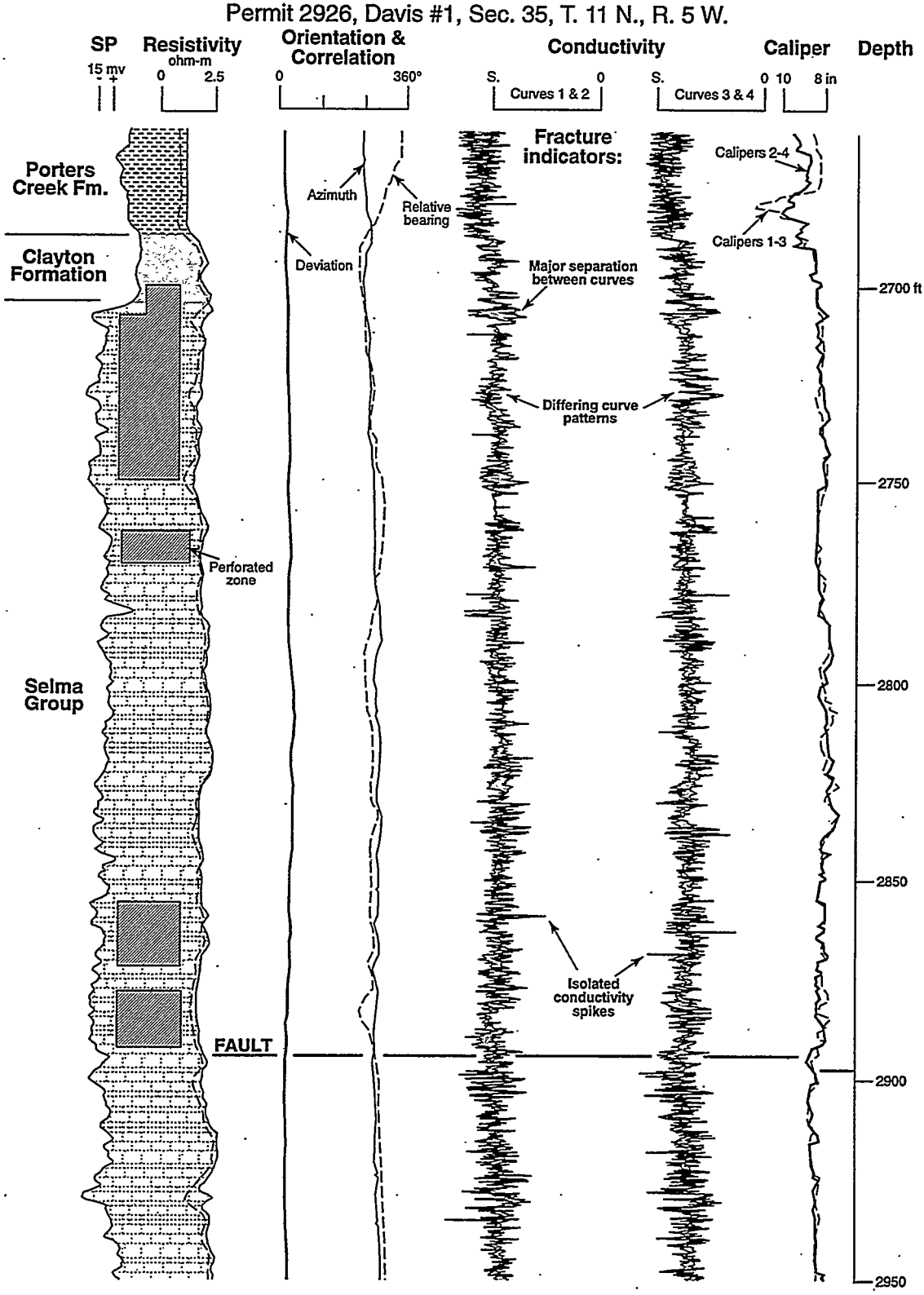

Figure 62.--Fracture identification log (FIL) of the upper part of the Selma Group in Gilbertown Field. Perforated zones were chosen on the basis of FIL characteristics.

widening of the borehole by caving along fractures or narrowing of the borehole by accumulation of mud cake at fracture apertures.

The application of FILs in developing the Selma Group in Gilbertown Field can be shown using well 2926, which produced oil successfully from the Selma Group, as an example (fig. 62). This well was drilled along the western part of West Gilbertown fault A and shows no resistivity anomaly associated with faulting. The caliper curves in all wells show expansion of the borehole by more than 2 inches at the base of the clay shale of the Porters Creek Formation, but the cause of this caving is not known. The calipers show minimal variation of borehole width within the Selma Group and are thus of limited use for fracture identification.

The conductivity curves show promise for detecting fractures within the Selma Group, but cores and borehole imagery are not available to verify the presence of fractures. The main criteria used to recognize fractures in the Selma Group were major separations between conductivity curves on the same curve track, different curve patterns on each track, or isolated conductivity spikes (fig. 62). Note that well 2926 was perforated where differences among conductivity curves are most pronounced, although a zone with significant differences among curves was left unperforated at depths between 2,800 to 2,850 feet.

STRUCTURAL MODELING

During the last year, structural modeling employed a three-pronged approach involving area balancing, curvature analysis, and seal analysis. Area balancing was used to validate the structural cross sections and to calculate requisite strain. Analysis of curvature in beds and faults was used to identify zones of potential fracturing. Finally, seal analysis was used to determine critical fault juxtapositions and to develop a model of hydrocarbon trapping in Gilbertown Field.

Area Balance and Strain
Theoretical Advances

In the previous year of this project it was recognized that Jurassic strata in the Gilbertown graben system are characterized by a straight area–depth line, indicating minimal structural growth, and that Cretaceous and Tertiary strata are characterized by a curved area–depth line that signifies major structural growth (Pashin and others, 1997). For the sake of simplicity, the Jurassic section (Smackover through Cotton Valley) is referred to as the pre-growth interval, and the Cretaceous–Tertiary section (post-Cotton Valley) is referred to as the growth interval. These relationships have been modeled successfully with a representative area-balanced growth structure (fig. 63).

The model shows that the boundary between the growth and pre-growth intervals (fig. 63A) is at a sharp inflection point in the area–depth graph (fig. 63B). The points representing the pre-growth interval fall on a straight line because they all share the same displacement. The slope of the best-fitting straight line for the model (-4.5 units) is the total displacement on the lower detachment (extension is negative), and the point at which the lost area goes to zero is the location of the lower detachment (-9.62 units below the reference level). The area-depth relationship of the pre-growth beds thus provides the location of the lower detachment if it is not visible on the cross section. The growth beds have lost areas that decrease upward both because of the growth and because the displacement decreases upward.

The procedure for accurately calculating the requisite strain in both the pre-growth and the growth sequence is as follows. For the pre-growth interval the requisite strain can be calculated from

$$e = [L_1 / (W+D)] - 1, \qquad (6)$$

which is a permutation of equation (4) from the introduction of this report. Equation (6) applies to the values on the best-fit straight line because it uses the same value of D for each horizon. For the growth interval, the requisite strain can only be calculated from equation (5), which is given in the introduction. To use equation (5), it is necessary to know the depth to detachment, either from the area–depth line of the pre-growth interval, or by direct observation. With this equation it is possible for each unit to have a different amount of displacement (D), as is characteristic of a growth sequence.

The requisite strain in the model (table 6) is layer-parallel extension that increases downward in the graben to a maximum at the lower detachment. The probability of small-scale deformation, including fracturing, thus increases downward in the model. The pre-growth sequence is significantly extended and thinned by the deformation, and the structural thinning is quite obvious on the cross section. The growth sequence includes depositional thickening that is greater than the structural thinning, giving a net thickness increase in each growth unit. The structural thinning can be recognized from the area balance in spite of the net thickness increase because the lost areas are a function only of the depth to detachment and are not affected by the growth.

Intrabed deformation indicated by the requisite strain is homogeneously distributed in the model (figs. 63, 64A). In natural examples it is anticipated that the requisite strain would be expressed as faults that are too small to be resolved at the scale of the cross section (fig. 64B). Most well-exposed grabens contain second-order faults. The second-order faults accommodate some or all of the necessary extension implied by the model and reduce the magnitude of the requisite strain that must be present in the blocks between the faults. If

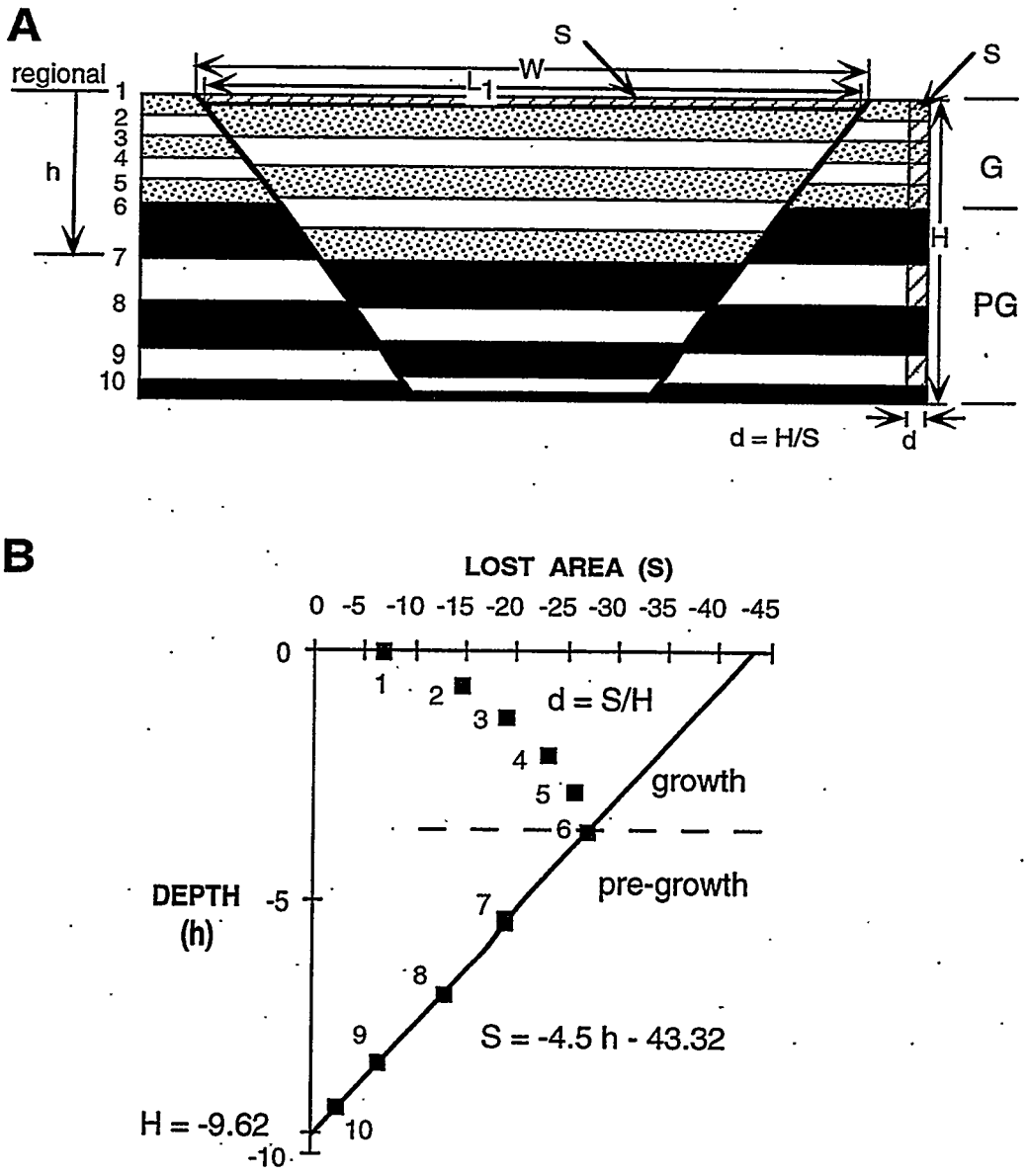

Figure 63.--Model of an area-balanced full graben. Reference level is at top of cross section (regional of bed 1). A. Cross section. The diagonal line pattern is the lost area caused by one increment of displacement on the lower detachment. The lower detachment is at the base of the cross section. G = growth sequence, PG = pre-growth sequence. B. Area-depth-strain relationship. Lost area is negative. Bed 6 is boundary between growth and pre-growth intervals.

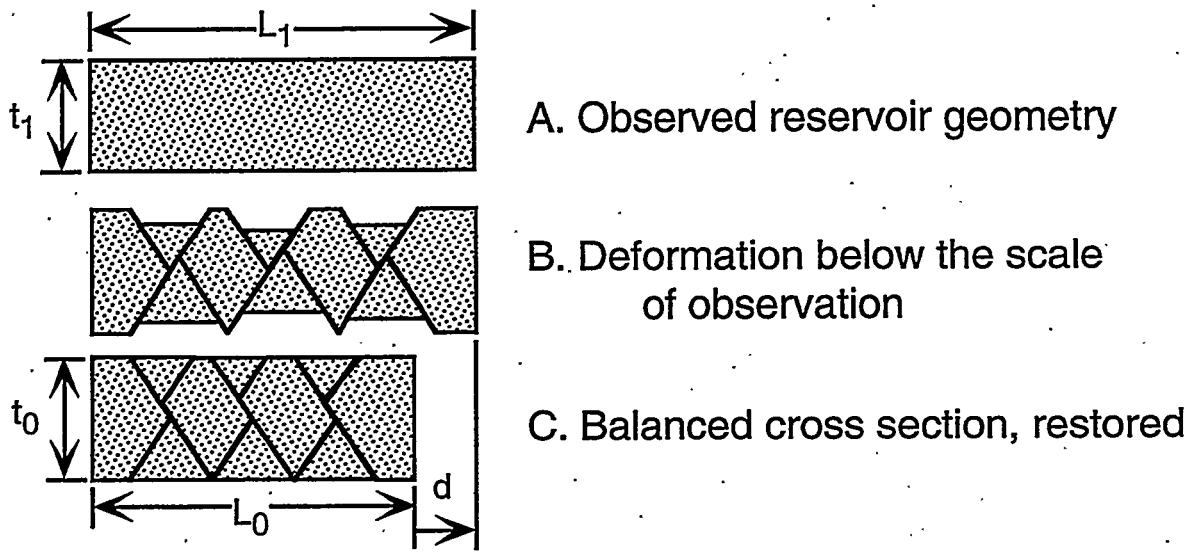

Figure 64.--Bulk shape change in a reservoir produced by displacement on faults too small to resolve at the scale of observation. A. Low-resolution profile showing apparently homogeneous extension and thinning. B. High-resolution profile of the same structure showing the same amount of bulk extension and thinning. C. Restored high-resolution profile showing the original bed length and thickness. The amount of extension is d.

the bed length is constant between the visible faults, the requisite strain will be zero, and no smaller-scale fractures are predicted. Restoration of the cross section provides a cross check on the geometric interpretation and restores the unit to its original length and thickness (fig. 64C).

Application to Gilbertown

Cross section C–C' provides the type example for the interpretation of the Gilbertown graben (fig. 65). This section was chosen because a deep well provides the location of the top and base of the Louann Salt. The initial area–depth curve for this cross section resembles that of the full graben model (figs. 63, 65). The Jurassic section falls on a straight line suggestive of an effective pre-growth origin with respect to the footwall regional, whereas the Cretaceous units show strong stratigraphic growth. Based on the resolution of the data, however, small amounts of stratigraphic growth in the lower four units cannot be ruled out, and structural restoration provides some evidence for incipient growth of the fault systems and salt-cored anticlines during the Jurassic (fig. 24). The best-fit line through the pre-growth interval implies a detachment below the Louann Salt. Thus, the detachment predicted by this method is probably too deep and may well reflect construction of the Jurassic beds within the graben using projected fault cut data rather than by direct observation. Forcing the area–depth line through the base of the salt, where the detachment is suspected to lie, is not much different than the best-fit line.

Requisite strains calculated for the cross section (table 7) are large in the effective pre-growth section (Smackover–Cotton Valley) and are very low and negative in the growth section (Lower Cretaceous–Selma). In the pre-growth section, the downward increase of extension fits the theoretical model of requisite strain in a full graben. It is inferred that there is significant amount of sub-section-scale deformation in the lower units.

Table 6.--Requisite strain calculated for full graben model of Figure 63.

Bed	Requisite Strain %
1	+ 0.9
2	+ 2.6
3	+ 4.6
4	+ 7.0
5	+ 10.3
6	+ 15.2
7	+ 24.0
8	+ 37.5
9	+ 66.2
10	+ 104.2

Table 7.--Requisite strain for cross-section C–C'. Computed with detachment at -14.27 kft below sea level. HW means measurements are made with respect to hanging-wall regional. Main growth units are Lower Cretaceous through Selma. Extension is positive.

Top of interval	Requisite Strain (%)
Selma	- 2.4
Eutaw	- 0.8
Lower Tuscaloosa	- 1.9
Lower Cretaceous	- 1.2
Cotton Valley	+ 7.7
upper Haynesville–HW	+ 19.0
lower Haynesville–HW	+ 24.3
Smackover–HW	+ 47.8

Requisite strain in the growth section is not only small but is negative (table 7). This is true of every cross section in the graben system. Negative strain indicates layer-parallel contraction, which is extremely unlikely in the extensional passive-margin setting of the northern Gulf Coast basin. Therefore, the requisite strains are either the result of measurement errors or require the geometry of the cross section to be changed. Both alternatives are considered below.

Lengths and areas were measured using the Canvas computer program. Errors in measurement can occur because of the finite width of the lines being measured. The measurement error is negligible for the length and elevation of the growth beds, which include the Gilbertown reservoirs, because it is a small portion of the total. In general, we have found that measurement errors lead to requisite strain variations of about 1 percent or less. Small changes in the position of the regional also affect the requisite strain by causing the depth to detachment and the displacement to change. Once again, the effects are very small for beds far from the lower detachment, namely the growth beds.

All cross sections, including C–C' (fig. 65), were constructed with the beds as straight line segments between the control points (figs. 11–18). This gives the shortest bed length consistent with the data. While this procedure gives good results overall, the beds probably depart from straight lines, especially in the proximal hanging walls. Indeed, sags between the faults are readily apparent in structure contour maps (figs. 20–22), and deformation of the proximal hanging wall, including drag folding, is apparent in outcrop (fig. 26) and in dipmeter logs (fig. 61). A likely possibility is that the beds are significantly curved near the faults because of fault drag. The magnitude of this effect is shown using the geometry of the top of the Eutaw Formation on a revised version of the Gilbertown graben in cross section C–C' (fig. 66). The straight-line bed has a length of 14.05 kilofeet (kft) and gives a requisite strain of -0.8 percent (table 7). The bed drawn

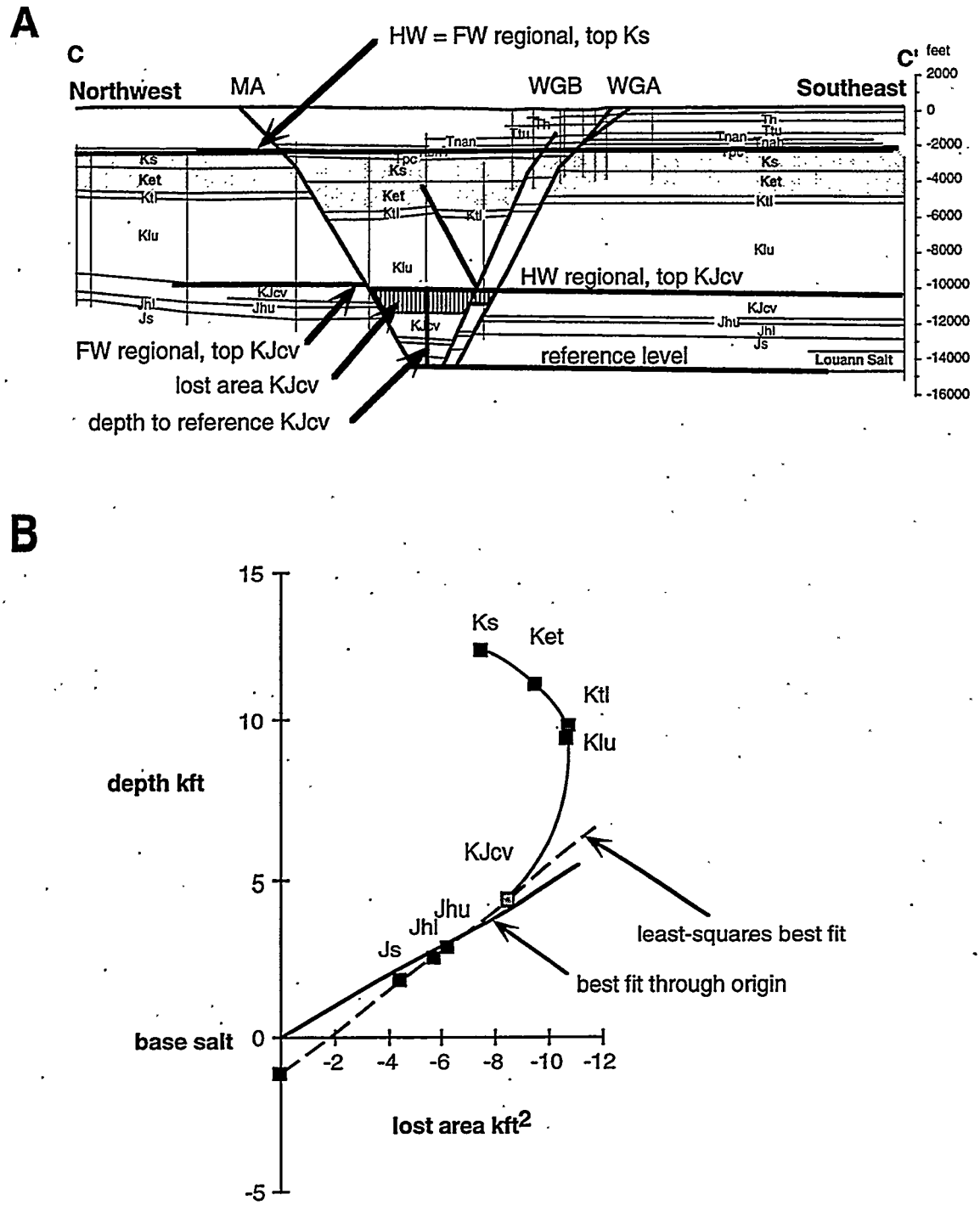

Figure 65.--Planar-bed interpretation of the Gilbertown graben. A. Cross section C-C' (see Figure 10 for location). WGA = West Gilbertown fault A, WGB = West Gilbertown fault B, MA = Melvin fault A. B. Area-depth relationship. Scales are in kilofeet and kilofeet^2. The regionals for the units Js through Jkcv are taken from the hanging wall. Hanging-wall and footwall regionals are the same for younger units.

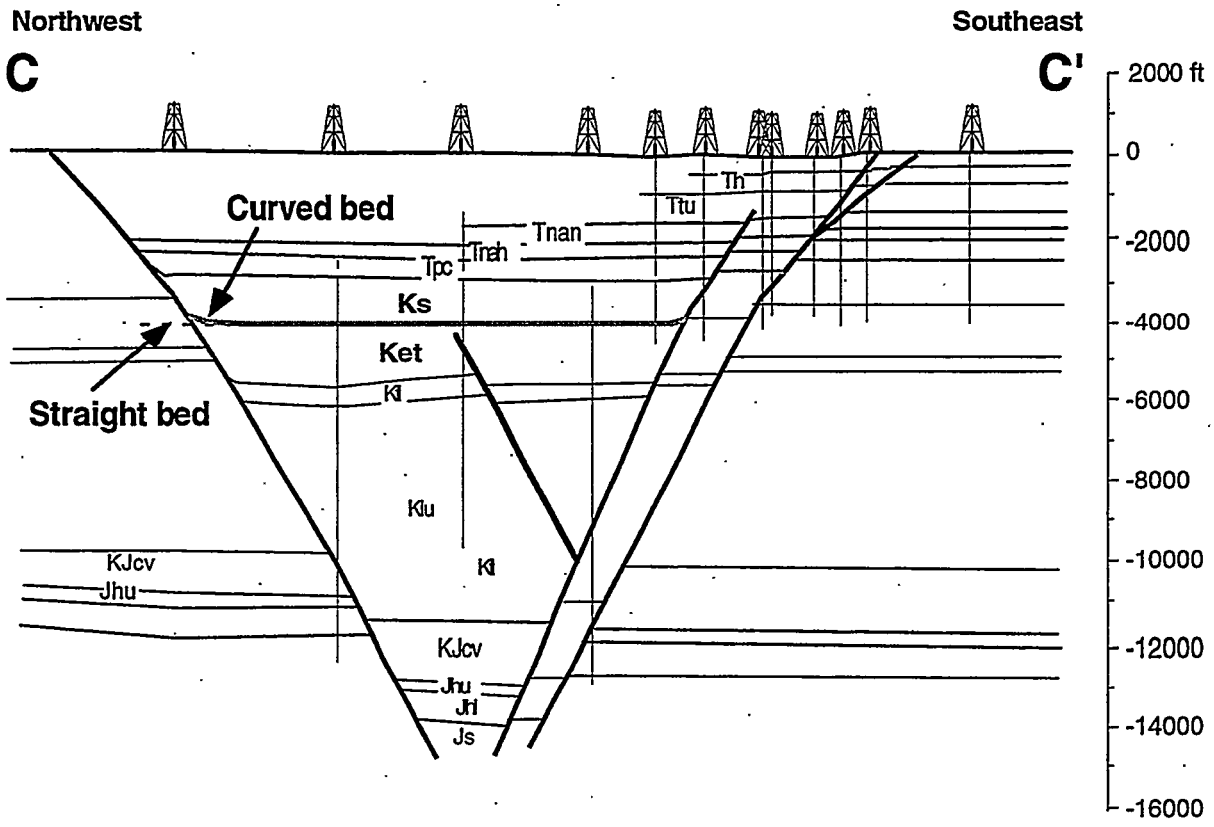

Figure 66.--Curved bed interpretation simulating drag folding in cross section C-C' in the Gilbertown graben. This small change of bed length is required for proper area balance of Upper Cretaceous units in the Gilbertown graben.

to show fault drag has a curved bed length of 14.42 kft and gives a requisite strain of +1.0 percent (table 8). Thus, the increase in bed length of 0.37 kft is enough to shift the requisite strain 2 percent, in this case from compression (negative) to extension (positive). The length of 0.37 kft is about twice the amount of the low-magnification measurement error.

All the cross sections have been redrawn to eliminate the negative requisite strains by introducing bed curvature (drag) near the faults. The results tabulated in table 7 show a close agreement in the calculated depth to the lower detachment, based on the best-fit line through the pre-growth area-depth points. The requisite strains in the growth sequence are all positive (extensional) and small, indicating that the revised cross sections are improved significantly from the straight-line versions. These results help confirm that virtually all of the curvature in the growth beds is located in the hanging-wall drag folds adjacent to the major faults. However, the precise mechanism of drag folding remains unclear.

Curvature Analysis

Curvature analysis has been used to predict strain and fracturing for more than 50 years (Woodring and others, 1940; Harris and others, 1960). Numerous investigators have analyzed bed curvature (Narr, 1991; Lisle, 1994), but the curvature of fault surfaces remains largely unaddressed. Indeed, fault curvature may be a critical control on fracture development, because folding is typically the direct product of transport of strata through fault bends regardless of tectonic setting (Groshong, 1990; Suppe, 1983; Christie–Blick and Biddle, 1985).

Bed curvature and fault curvature may both be related to fracture development in Gilbertown Field. Results of structural analysis indicate that the critical bed curvatures in the Selma Group are related to deformation, including drag folding, in the immediate hanging walls of the faults (figs. 26, 61, 66). Consequently, bed curvature is difficult to model in Gilbertown Field, because only a few wells penetrate major lithologic contacts within this deformation zone. Therefore, the second derivative maps of the bed surfaces show minimal curvature, and what curvature is shown is not relevant to oil production from the Selma Group.

Fortunately, nearly every well in Gilbertown Field penetrates a fault, so plenty of data exist to model curvature of the fault surfaces. A structural contour map of West Gilbertown fault A and East Gilbertown fault A that was generated in Geographix Isomap shows the available well control and the location of wells that produced more than 10,000 barrels of oil from the Selma Group (fig. 67). Some curvature is obvious, such as the major bend in East Gilbertown fault A at the edge of the relay zone, but most curvature is too subtle to identify in the map. Three-dimensional grid plots of the fault surfaces make irregularities of the fault surfaces easier to see, especially in the relay zone of East Gilbertown fault A (fig. 68).

Superimposing second derivative surfaces on the grid plots in the 3D submodule of Isomap accentuates subtle curvature that is otherwise difficult if not impossible to discern (figs. 69–71). Dark shading marks negative curvature, and light shading marks positive curvature. The plots of total curvature document numerous irregularities in the fault surfaces (fig. 69). Irregularities on the shallow part of West Gilbertown fault A are small and are most subtle along the central third of the fault trace. Well control along the deep part of the fault is sparse and irregularly distributed (fig. 68), and the areas of enhanced curvature reflect this distribution (fig. 69). Irregularities along East Gilbertown fault A are broader and more pronounced than those along the western fault, and the curvature signature of the relay zone and the straight fault segment differ markedly. Strong, broad curvature patterns in the relay zone accentuate a number of fault bends along which strike and dip of the fault surface vary by more than 15°. Curvature of the eastern fault segment is less pronounced than in the relay zone, and a series of elongate negative curvatures define a series of grooves in the upper part of the fault surface.

Isomap enables users to isolate X (east–west) and Y (north–south) components of curvature (figs. 70, 71). This functionality is especially useful in Gilbertown Field, where the major faults strike due east, and thus enables isolation of strike and dip components of curvature. The strike curvature plot of West Gilbertown fault A reveals a system of grooves and ridges; variation is most pronounced along the eastern and western thirds of the fault and is relatively subdued in the central third (fig. 70). By comparison, the amplitude and spacing of grooves and ridges is fairly constant along the length of East Gilbertown fault A. Interestingly, bends deeper on the fault surface are more pronounced within the relay zone than at the boundary between the relay zone and the eastern fault segment.

Superimposing curvature in the Y direction establishes that multiple fault bends are present along the shallow part of West Gilbertown fault A (fig. 71). The deepest set of positive curvatures (light) marks the upward decrease of fault dip at the base of the Selma Group, and negative curvatures higher on the fault suggest a tendency of the fault to steepen in the Tertiary section. At the western end of the diagram, however, evidence of dip variation is subdued by a strong groove that parallels dip of the fault. Positive curvature on the shallow part of East Gilbertown fault A reflects downward increasing dip in the Upper Cretaceous section. The eastern segment of the fault

Table 8. Area–depth–strain relationships for all cross sections with fault drag included. Requisite strains in percent, calculation based on regional detachment at -14.80 kft. * depth of detachment below sea level, kft. ** displacement on lower detachment, kft.

Cross section	H*	D**	Ks	Ket	Ktl	Klu	KJcv	Jhu	Jhl	Js
A–A'	-14.82	-1.25	1	1	2	2	7	10	11	14
B–B'	-14.81	-1.83	1	1	3	4	22	26	32	56
C–C'	-14.79	-1.92	0	1	1	4	8	21	23	26
D–D'	-14.79	-2.16	1	1	0	0	5	5	5	12
E–E'	-14.79	-1.68	1	1	1	0	5	15	11	16
F–F'	-14.82	-1.33	0	0	0	0	9	19	21	27
G–G'	-14.81	-1.34	1	0	1	2	8	8	12	30
H–H'	-14.76	-1.33	0	1	0	0	4	11	14	29

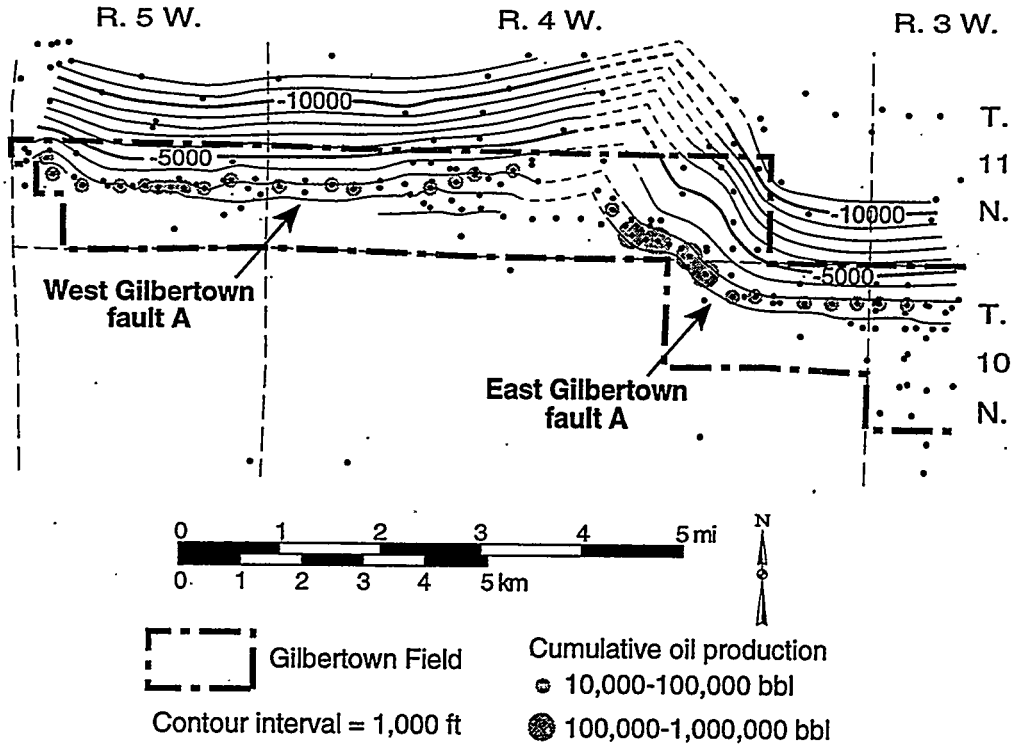

Figure 67.–Structural contour map of West Gilbertown fault A and East Gilbertown Fault A showing distribution of wells with cumulative oil production from the Selma Group exceeding 10,000 barrels.

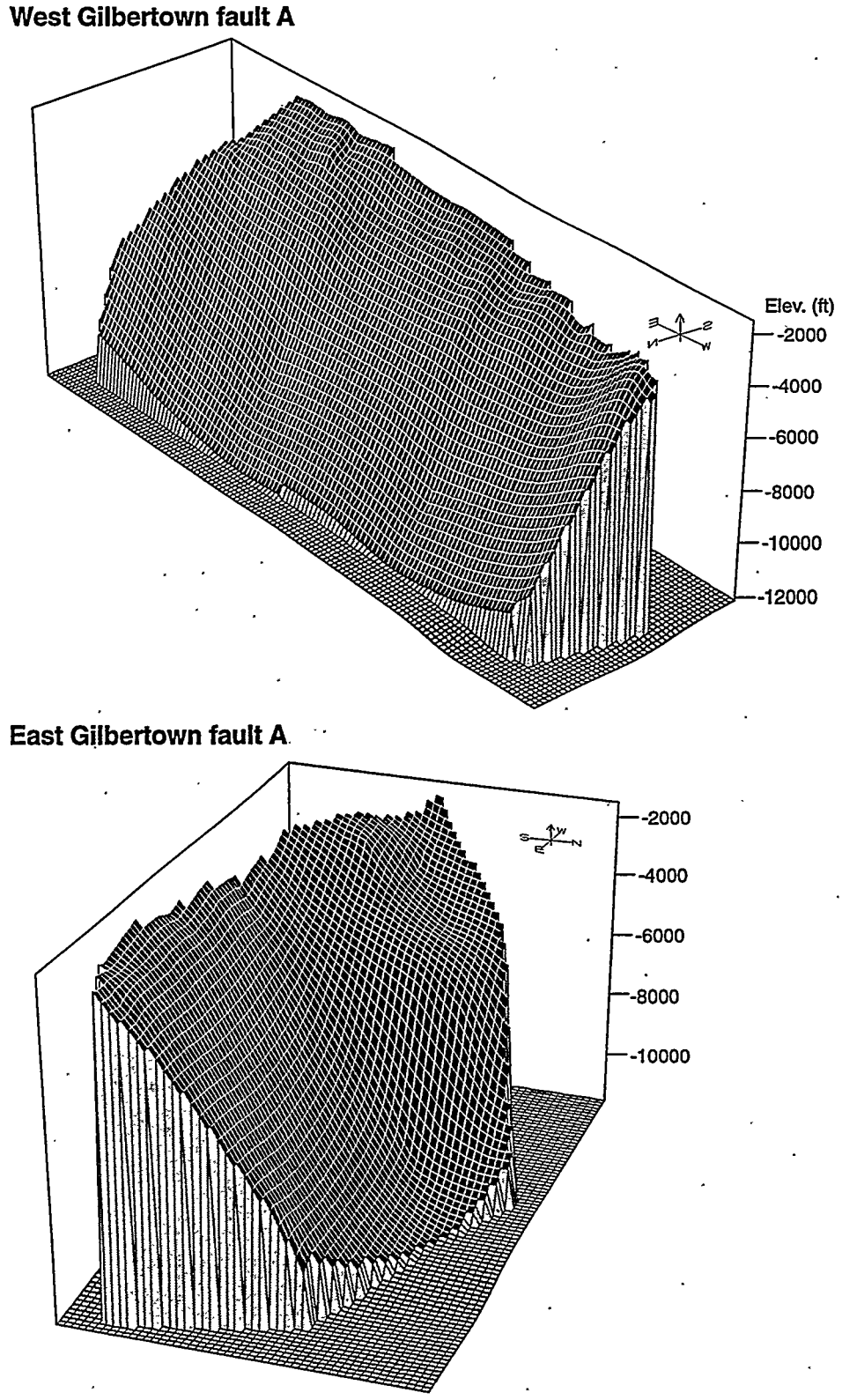

Figure 68.--Three-dimensional grid plots of faults where oil has been produced from the Selma Group in Gilbertown Field. Plots generated using Geographix Isomap.

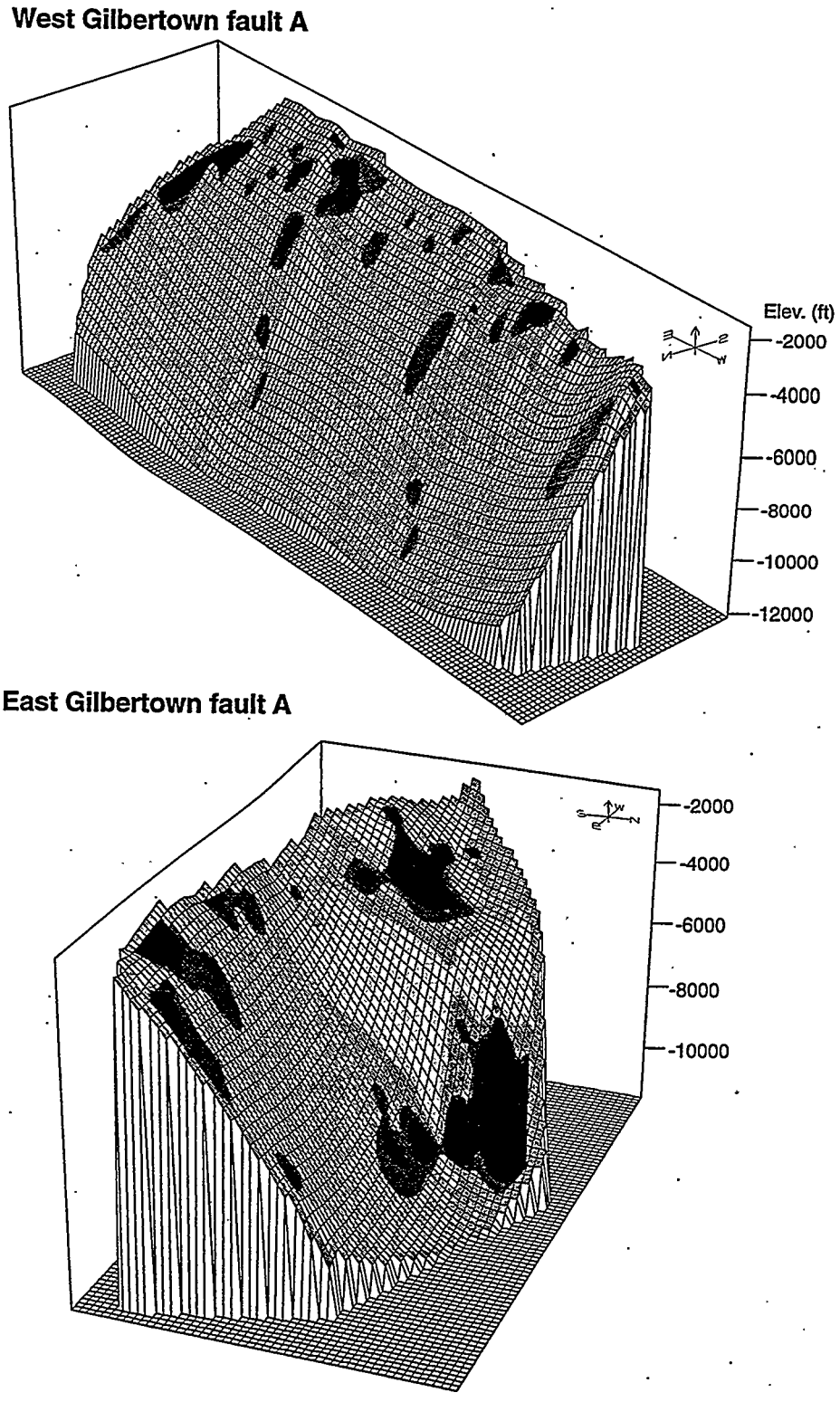

Figure 69.--Total curvature of faults where oil has been produced from the Selma Group in Gilbertown Field. Plots generated using Geographix Isomap.

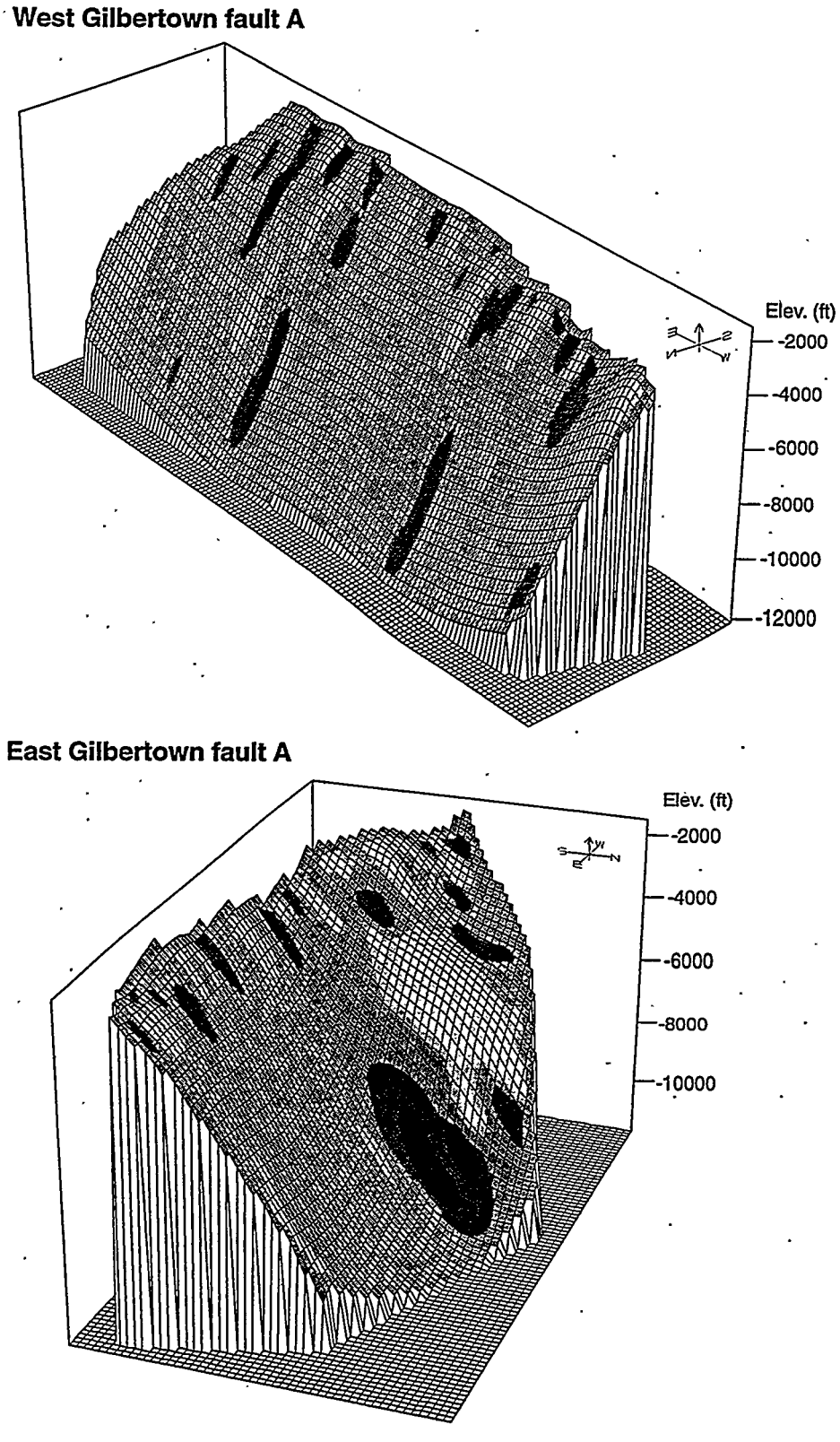

Figure 70.--Strike (X) curvature of faults where oil has been produced from the Selma Group in Gilbertown Field. Plots generated using Geographix Isomap.

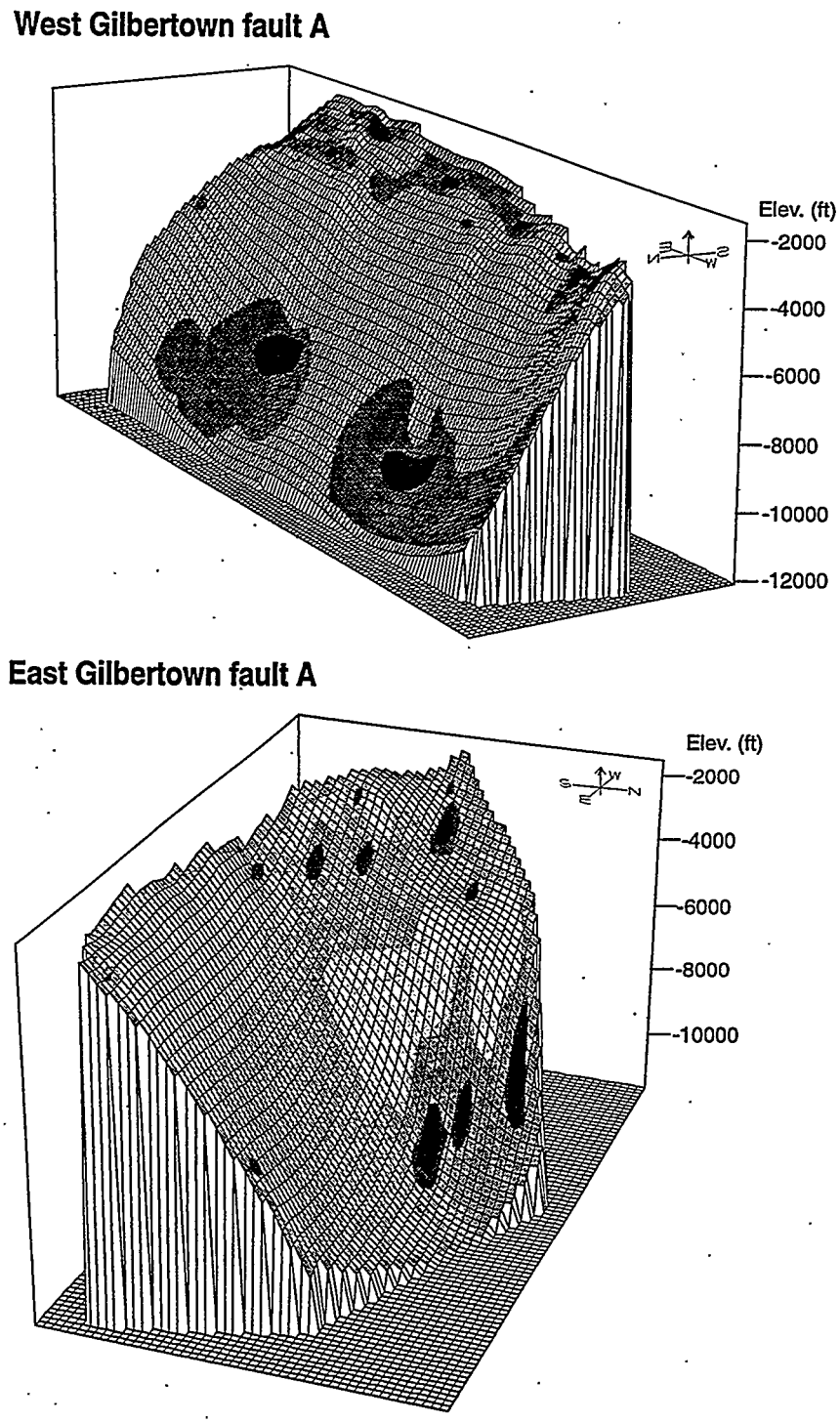

Figure 71.--Dip (Y) curvature of faults where oil has been produced from the Selma Group in Gilbertown Field. Plots generated using Geographix Isomap.

remains planar downward to the Smackover Formation. In the relay zone, however, alternating zones of positive and negative curvature define zones where the fault steepens then flattens.

The impact of fault curvature on fracturing is ideally a function of the slip direction on the fault. For example, where movement is strictly dip-slip, only horizontal fault bends (dip curvature) should cause fracturing. Conversely, where movement is strictly strike-slip, only the curvature of fault grooves and ridges (strike curvature) should be effective. And in areas of oblique slip, total curvature should be effective.

Structural relationships suggest that tectonic transport of the hanging-wall block of the Gilbertown fault system was due north. Therefore, dip slip should prevail in the central part of West Gilbertown fault A and along East Gilbertown fault A east of the relay zone (fig. 67). A minor component of oblique slip is apparent at the extremities of West Gilbertown fault A, where the fault plane locally curves by more than 10°. The greatest component of oblique slip in the field is in the relay zone where East Gilbertown fault A locally strikes more than 45° to the regional transport direction.

Seal Analysis

Regardless of the distribution of strain and curvature, production would not be possible from the Eutaw Formation or the Selma Group without effective reservoir seals to trap the hydrocarbons. Although faults can be discrete discontinuities cutting across large volumes of rock, hydrologic conditions along fault planes vary considerably depending on the thickness and permeability of the fault gouge and the strata juxtaposed on opposite sides of the fault plane (Bouvier and others, 1989; Knipe, 1997). Juxtaposition diagrams, which are fault-plane projections showing the contacting formations, are thus of great utility for evaluating reservoir seals in faulted regions because they can be used to identify permeability barriers, zones of leakage, and reservoir spillpoints (Allan, 1989).

Juxtaposition Diagrams

Juxtaposition diagrams were made of West Gilbertown fault A, East Gilbertown fault A, and the West Bend fault, which are the principal faults affecting oil production and hydrocarbon trapping in Gilbertown Field (fig. 72). The deepest known oil production in the Eutaw Formation and the Selma Group is included on the juxtaposition diagrams. For display purposes, marker beds bounding the seven stratigraphic intervals of the Eutaw Formation (intervals E1 through E7) are shown only for the footwalls.

Juxtaposition relationships are relatively simple along West Gilbertown fault A. Only along the westernmost part of the fault are Eutaw strata in the hanging wall and footwall juxtaposed (fig. 72). Elsewhere, productive Eutaw shale and sandstone in the footwall are juxtaposed with Selma chalk. Note that the oil–water contact is at the highest elevation where Eutaw strata are in contact on both sides of the fault. Approximately 1,000 feet of Selma strata are in contact along the fault plane, and the deepest oil production comes from the middle of this interval. The area where the Porters Creek Formation is juxtaposed with the Selma Group has a lenslike shape, thickening from less than 50 feet near the ends of the fault to more than 250 feet in the central part. Conversely, the area where the Porters Creek is in contact on both sides of the fault is thickest at the extremities. Above this, Porters Creek and younger strata, which are dominantly interbedded shale and sandstone, are in contact.

Along the West Bend fault, juxtaposition relationships reflect increasing vertical separation toward the east (fig. 72). Juxtapositions were difficult to plot at the conjugation of the West Bend and East Gilbertown fault system because of limited well control and are thus not shown. As along West Gilbertown fault A, productive Eutaw strata in the footwall are juxtaposed with chalk everywhere except near the western tip of the fault. However, deepest known oil is at the top of where Eutaw strata are in contact on both sides of the fault. The zone where Selma strata are juxtaposed across the fault thins eastward from more than 750 feet to less than 500 feet. At the western end of the diagram, nearly the full thickness of the Porters Creek Formation is in contact on both sides of the fault. Farther east, however, the full thickness of the Porters Creek Formation is juxtaposed with the Selma Group, and so is much of the interbedded shale and sandstone of the Naheola Formation.

The most complex fault juxtapositions in Gilbertown Field are along East Gilbertown fault A (fig. 72). One of the main complicating factors is the juncture of East Gilbertown faults A and B in the east-central part of the cross section, which is also apparent in some of the structural contour maps (figs. 21, 22). This juncture almost certainly extends laterally along less of the fault plane than is shown in the juxtaposition diagram (compare Figure 72 with Figure 21), but the available well control necessitates using data from the hanging wall of East Gilbertown fault B.

Eutaw strata in the footwall of East Gilbertown fault A are nearly everywhere juxtaposed with Selma chalk (fig. 72). The Eutaw markers define a broad arch that marks the intersection of the fault with the footwall uplift where most oil is produced. Note that all known oil is entirely above the base of the chalk in the hanging-wall block. More than 1,000 feet of Selma strata are juxtaposed across the fault at the west end of the diagram, but where East Gilbertown faults A and B

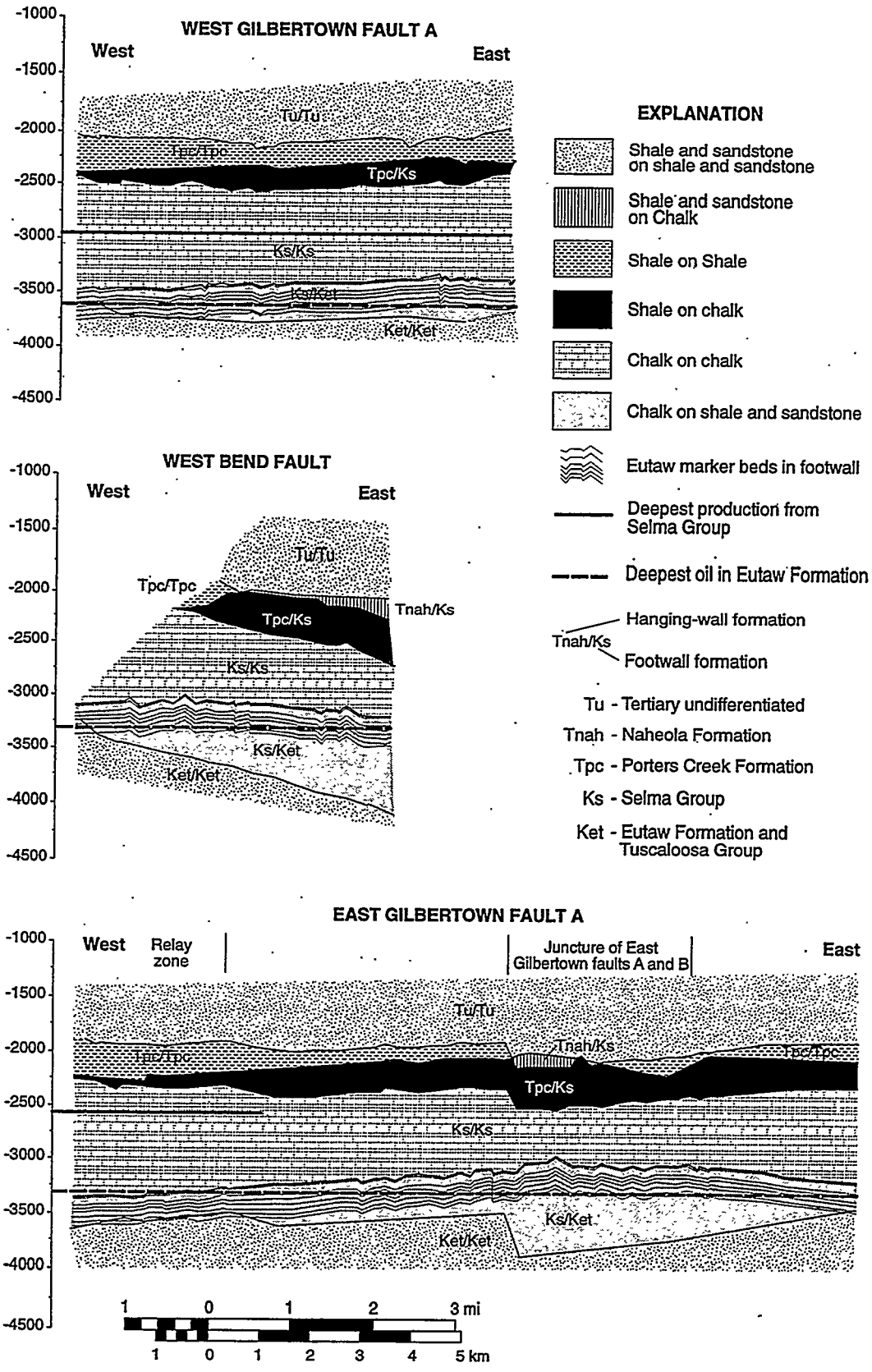

Figure 72.--Juxtaposition diagrams showing formations in contact along the Gilbertown and West Bend fault systems. Data projected to vertical planes striking east.

join, less than 500 feet of the Selma Group is in contact. An opposite relationship exists where less than 50 feet of Porters Creek clay shale is juxtaposed with chalk at the west end of the diagram. Where the faults join, the full thickness of the Porters Creek Formation and part of the Naheola Formation are juxtaposed with the Selma Group. Moreover, at least part of the Porters Creek Formation is juxtaposed on both sides of the fault everywhere but the juncture between East Gilbertown faults A and B.

Seal Diagrams

Knipe (1997) emphasized the importance of understanding the permeability characteristics of juxtaposed strata, as well as the mechanical properties of those strata when subjected to shear strain, when evaluating fault seals. For example, sand-on-sand juxtapositions can promote leakage of fluid across faults or can form cataclastic fault seals where intensely sheared. Argillaceous units tend to smear along fault planes and may thus form effective fault seals, and mineralization of fault gouge is yet another sealing mechanism. The limited amount of core in Gilbertown Field makes direct evaluation of fault-related shear fabrics and cementation impossible, but production experience provides critical information that can be used to identify and classify the seals. Using this information, the juxtaposition diagrams can be modified into seal diagrams (figs. 72, 73).

No oil has been produced from the interbedded sandstone and shale of the Tuscaloosa Group or similar strata in the Tertiary section in Gilbertown Field, so these strata are considered to be effectively non-sealing (fig. 73). However, smearing of clay along the faults and localized shale–sandstone juxtapositions may form subtle traps that have thus far been overlooked during regional development.

All Eutaw oil production in Gilbertown Field comes from footwall uplifts where shale and sandstone are juxtaposed with chalk (figs. 73, 74). Selma chalk clearly forms the topseal for the Eutaw reservoirs, but the characteristics of the associated fault seal are imprecisely known. Considering that oil is produced from faulted and fractured chalk in the hanging walls, it is doubtful that chalk forms the seal for the footwall reservoirs of the Eutaw Formation. Alternatively, smeared Eutaw sandstone and shale are interpreted to form the seal within the footwall, and the high glauconite content of Eutaw sandstone should contribute to the clay-smear potential of the formation. Mineralization of the fault gouge also cannot be ruled out. Coincidence of the deepest Eutaw oil with the highest non-sealing strata along West Gilbertown fault A suggests that the elevation of the oil is controlled by a spillpoint. Spillpoint control along the West Bend fault is not apparent, because non-sealing strata are above the deepest oil at the western fault tip. Indeed, the distribution of oil in the Eutaw Formation is extremely variable (figs. 38–40), and internal heterogeneity within the sandstone units and potential leakage along the fault may have a strong influence on this distribution.

Every well that has produced oil from the Selma Group penetrates chalk in the hanging walls of the faults, whereas only dry holes have been drilled where wells penetrate chalk only in the footwalls (fig. 74). This relationship is a direct reflection of the predominance of hanging-wall deformation indicated by the dipmeter and FIL data (figs. 61, 62). Thus, the chalk is reservoir in the hanging walls and forms a seal in the footwalls. The clay shale of the Porters Creek Formation has long been considered the topseal for fractured Selma chalk reservoirs (Braunstein, 1953) and forms an extremely thick, argillaceous seal that extends the length of Gilbertown Field (figs. 72–74). In cross section, the fractured chalk reservoirs can be characterized as wedge-shaped bodies sealed by poorly fractured chalk in the footwall and Porters Creek clay shale in the hanging wall (fig. 74).

Less clear, however, are the strike-parallel lateral sealing mechanisms within the Selma Group. No lateral seal is apparent along West Gilbertown fault A, where production comes from as deep as the middle of the Selma Group (figs. 72, 73). Along East Gilbertown A, Selma production comes from the structurally highest region near the western tip of the fault, but the deepest production comes from below the apparent spillpoint defined by the argillaceous seal. These relationships suggest that the controls on the distribution of oil in the Selma Group are complex and are perhaps the product of heterogeneous deformation and mineralization. For example, decreasing vertical separation near the tips of the productive faults at the top of the Selma Group may be associated with limited fracturing and may thus contribute to the development of lateral seals.

PRODUCTION ANALYSIS

In a field with a production history as long as Gilbertown, hindsight is a valuable tool that can be used to identify ways that the field can be revitalized. The first part of this section discusses the decline characteristics of Eutaw and Selma wells and the relationship of long-term production patterns to field development. The remaining parts center on geographic patterns of cumulative oil production in each reservoir and the methodologies and technologies that may help revitalize the field.

Well Histories

Production data have been collected for all wells in Gilbertown Field and are being analyzed. Although individual wells in Gilbertown field have reported as

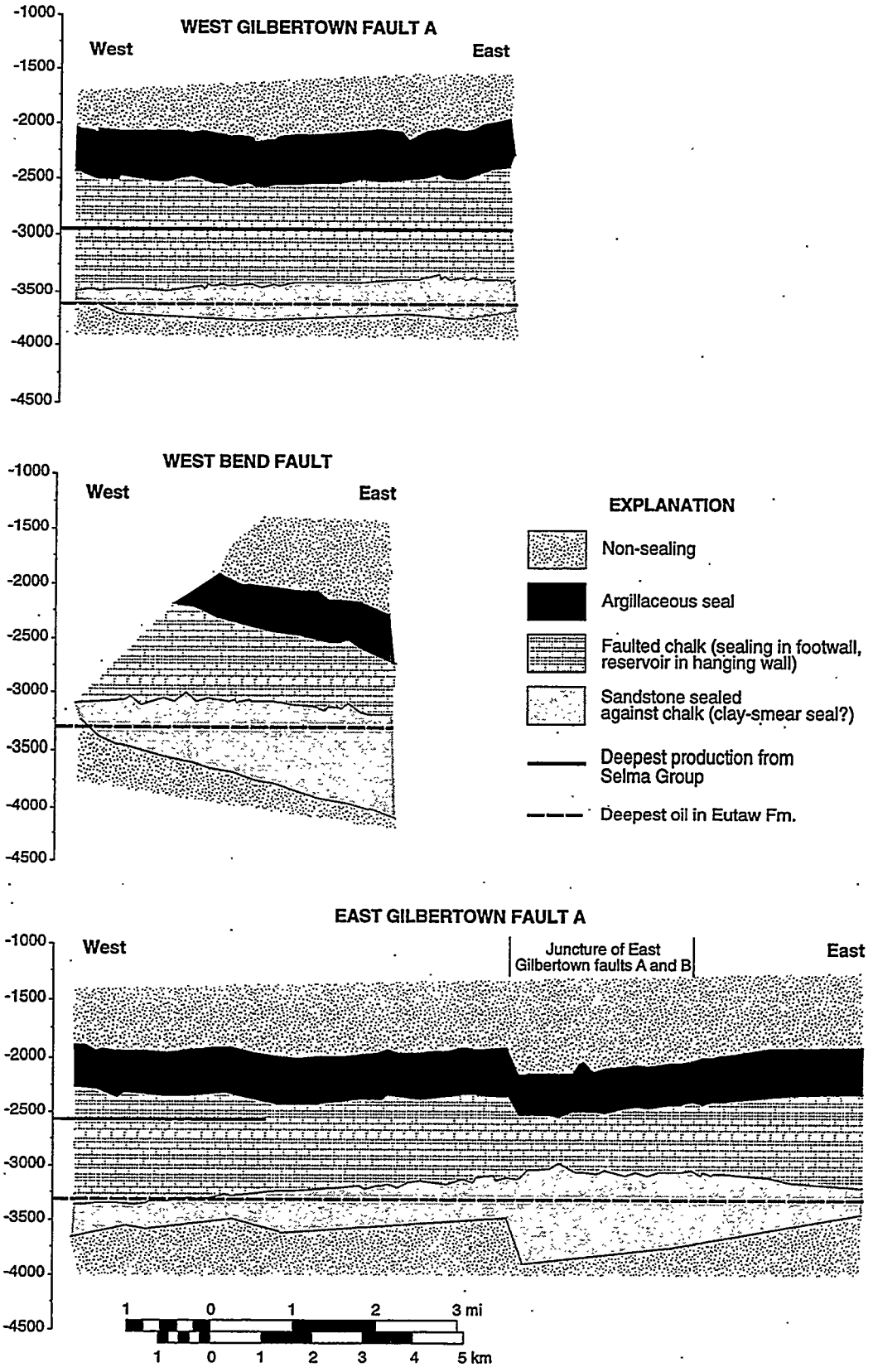

Figure 73.--Seal diagrams based on interpretation of the characteristics of juxtaposed strata along the Gilbertown and West Bend fault systems. Data projected to vertical planes striking east.

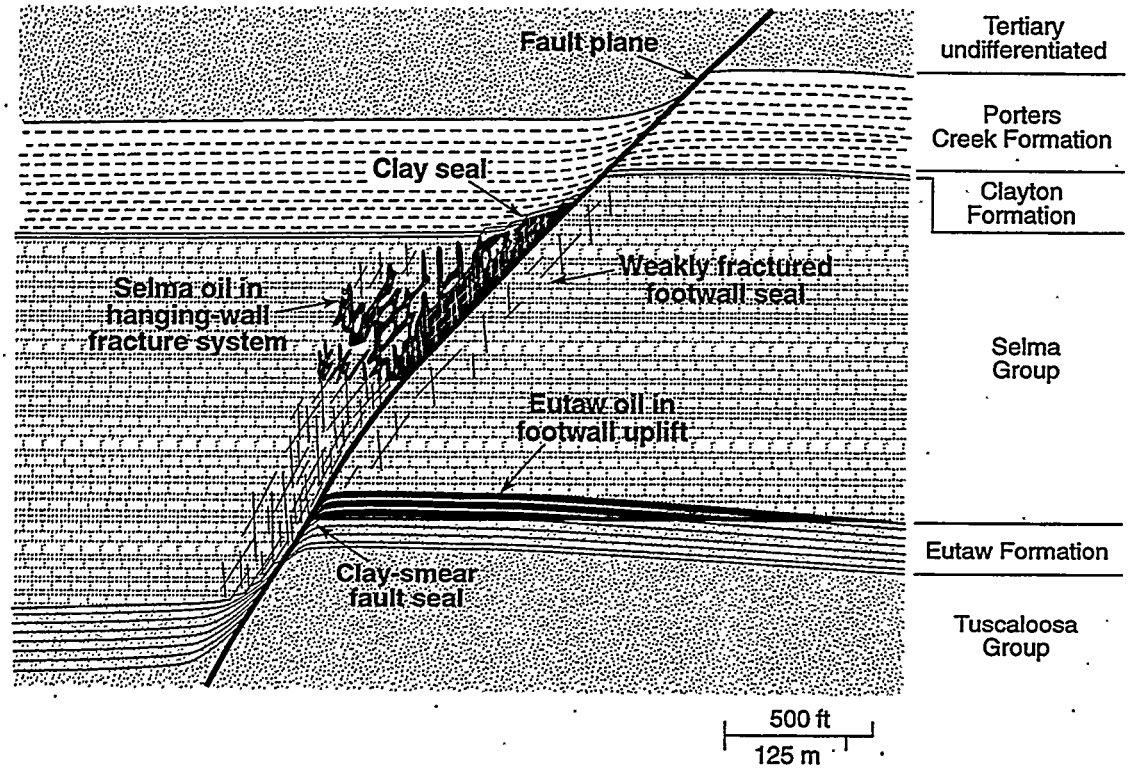

Figure 74.--Model of trapping mechanisms and critical seals for oil in Gilbertown Field.

much as 46 years of production, production records are not uniform. Oil production data are available for most wells, but water and gas production data are largely lacking. Although monthly oil production records are available for many wells, only annual data are available for most wells completed before 1970. In addition, production from some wells was commingled with that from other wells. Even so, annual oil production data provide sufficient information to characterize the production histories of most wells and to distinguish key differences between wells completed in Selma chalk and Eutaw sandstone.

Differences in the decline characteristics of Eutaw and Selma wells reflect production from conventional and fractured reservoirs, respectively (fig. 75). Eutaw wells have an average lifespan of more than 22 years, whereas Selma wells have a shorter average lifespan of 13 years. Peak production from both units is typically reached within 2 years; Eutaw wells peak at an average of 17,100 barrels per year, and Selma wells peak at an average of 13,100 barrels per year. The difference between Eutaw and Selma wells is readily apparent when examining cumulative production. Average cumulative production of Selma wells is 52,000 barrels, whereas the average for Eutaw wells is more than three times as great at 158,000 barrels. This is a conservative estimate, because many Eutaw wells are still producing.

Decline curves of the five most productive Eutaw wells parallel the development history of Gilbertown Field (fig. 75). All five wells were drilled and put on line between 1945 and 1949 as Alabama's oil industry began to burgeon. The wells peaked by 1952 and declined exponentially until the late 1960s. The simplicity of this decline reflects production with limited well maintenance during the first production phase in the field. Production slacked from the late 1960s into the mid 1970s, which is a time when abandonment of the field appeared eminent. Increasing production between 1975 and 1984 signifies rejuvenation of the field by Belden and Blake, Incorporated. Following this period, however, production began declining erratically as wells required continual tinkering to maintain economic production.

Four of the five most productive Selma wells were drilled in 1944 and 1945 (fig. 75). Like the Eutaw wells, the Selma wells peaked early and declined exponentially, although the decline of Selma production is more erratic. All five wells were abandoned between 1960 and 1974. Well 239 is typical of many Selma wells that were shut in for 5 years or longer and were then put back on line. Although many Selma wells were abandoned prior to 1974, the history of Selma production parallels that from the Eutaw Formation. For example, Belden and Blake drilled and completed many new Selma wells while rejuvenating the field during the late 1970s and early 1980s. However, production of oil from the Selma Group declined sharply during the late 1980s, and production ceased during 1995. Even so, significant opportunities remain to revitalize Eutaw and Selma production in Gilbertown Field.

Eutaw Production Patterns

Oil is produced from the Eutaw Formation in the footwall block of West Gilbertown fault A and in the faulted anticline and horst defined by East Gilbertown fault A and the West Bend fault (figs. 76–83). Productive wells in the western part of the field are concentrated in a small footwall uplift immediately south of West Gilbertown fault A, and wells that have produced more than 100,000 barrels of oil are in the most elevated part of the footwall uplift (fig. 76). In the eastern part of the field, wells that have produced more than 100,000 barrels are distributed throughout the horst and faulted anticline.

Comparison of production patterns with net sandstone isolith maps indicates little relationship between sandstone thickness and production (figs. 41–47). Structural position, however appears to be a critical control on production. Production in intervals E1 through E5, for example, is restricted to the structurally highest part of the horst (figs. 41–45). In interval E6, by comparison, production is restricted to the flanks of the faulted anticline (fig. 46). In the eastern part of the field, E7 production is restricted to the west flank of the faulted anticline (fig. 47). In the western part of the field, E7 is the only productive interval of the Eutaw, and production is distributed sporadically through the footwall uplift associated with West Gilbertown fault A.

Core analysis and completion data establish that the distribution of oil in the Eutaw Formation is extremely heterogeneous and that no single oil–water contact exists (figs. 84, 85). Localized leakage along the fault may be responsible for this distribution, and cementation of the sandstone is apparently another major source of heterogeneity. For example, sandstone in interval E6 contains more carbonate cement in the structurally highest part of the horst than in the flanks of the structure. Pinchout of E7 sandstone in the immediate footwall of East Gilbertown fault A (fig. 47) is another limiting factor.

Because of high water saturation, waterflooding has not been successful in the Eutaw Formation. Indeed, dilution of oil by breakthrough of injected fluids can have an extremely adverse effect on the economics of Eutaw reservoirs. Therefore, it appears that the best opportunities to revitalize Eutaw production are through infill drilling and recompletion of existing wells. During the final phase of this project, we will attempt to identify sites that appear favorable for infilling and to identify zones in existing wells where oil may remain untapped.

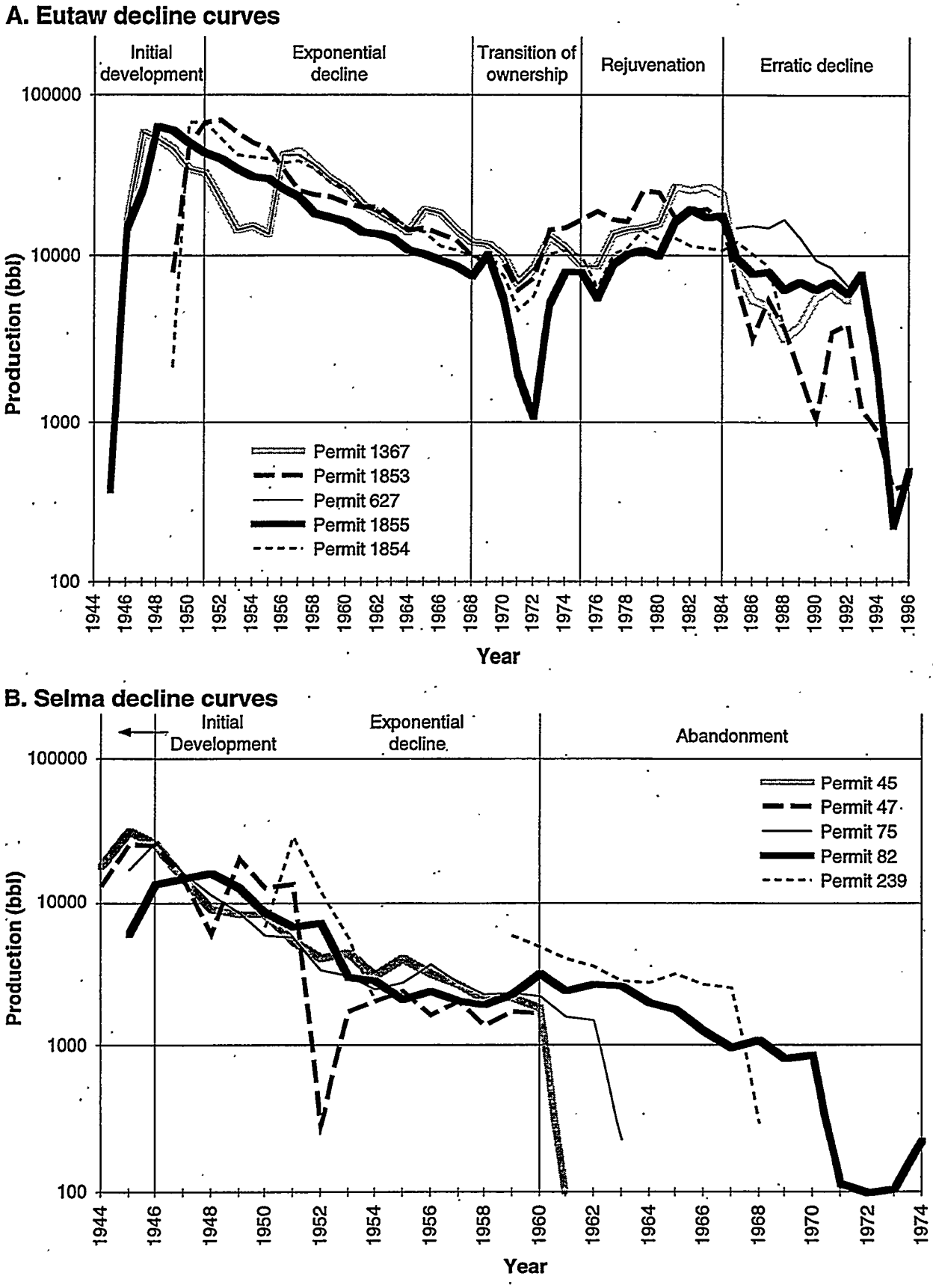

Figure 75.--Production history curves of the most productive Eutaw and Selma wells in Gilbertown Field.

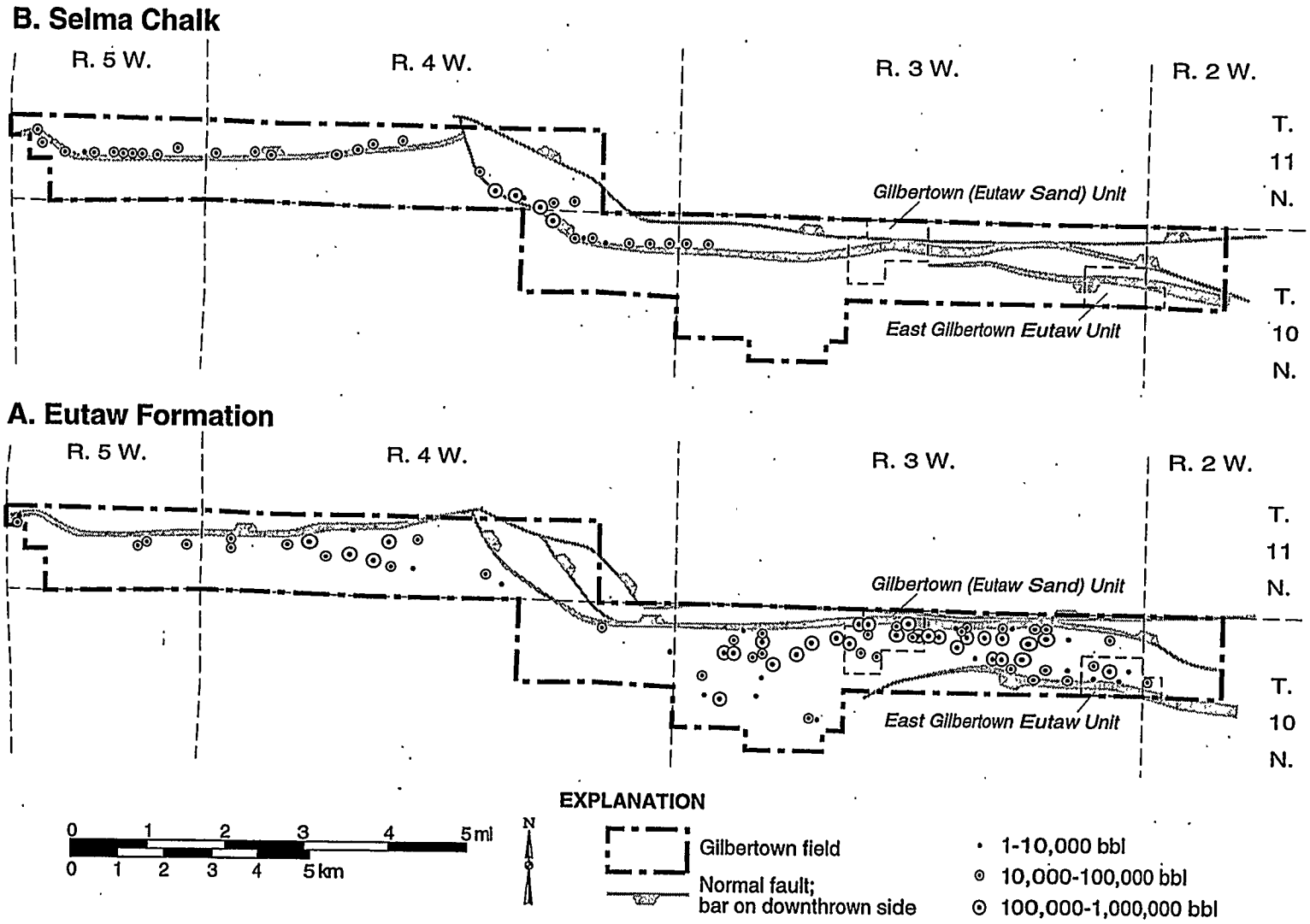

Figure 76.--Relationship of oil production to fault patterns in the Eutaw Formation and Selma Group, Gilbertown Field.

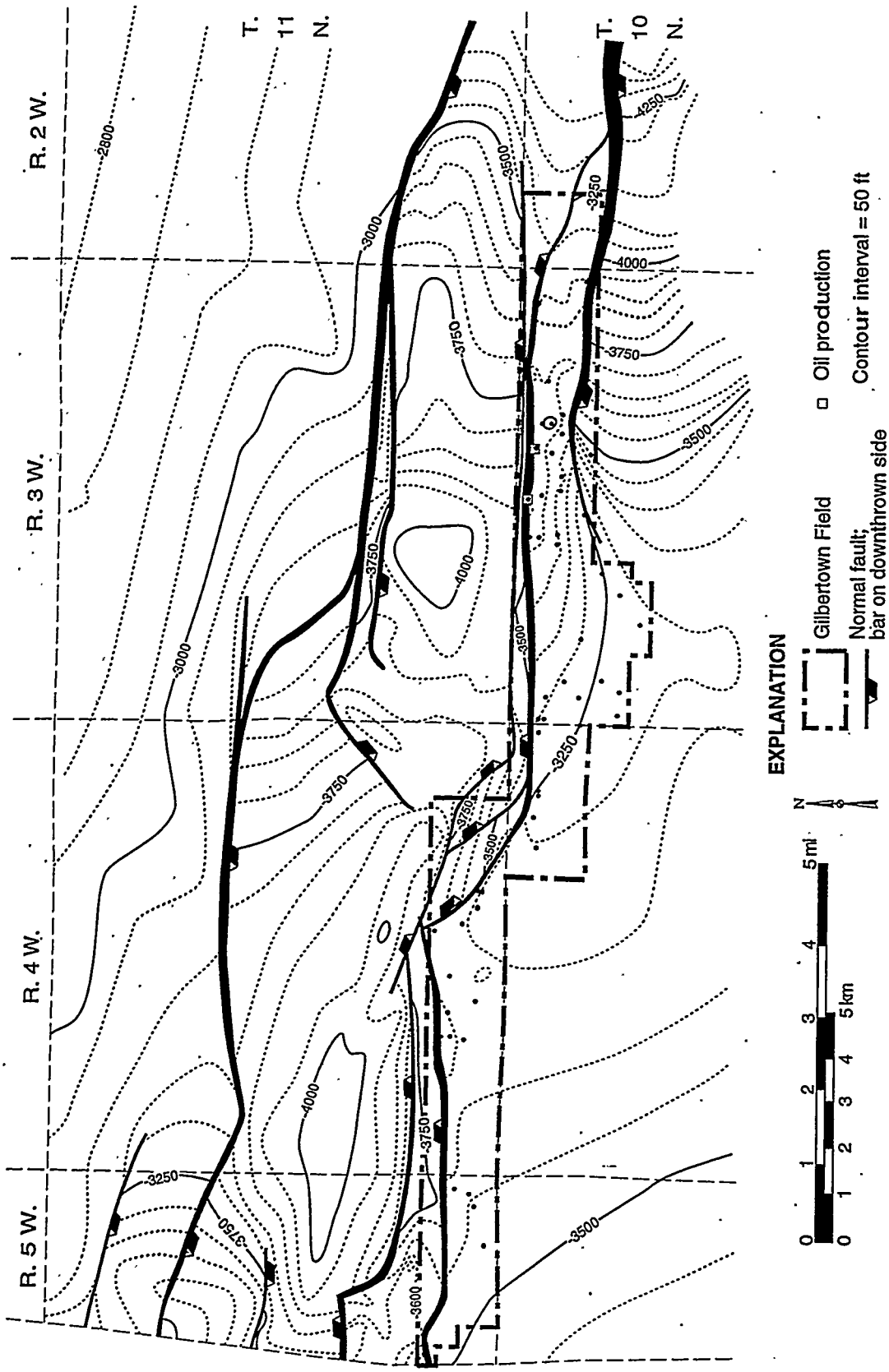

Figure 77.--Relationship of oil production to structure in interval E1 of the Eutaw Formation in Gilbertown Field.

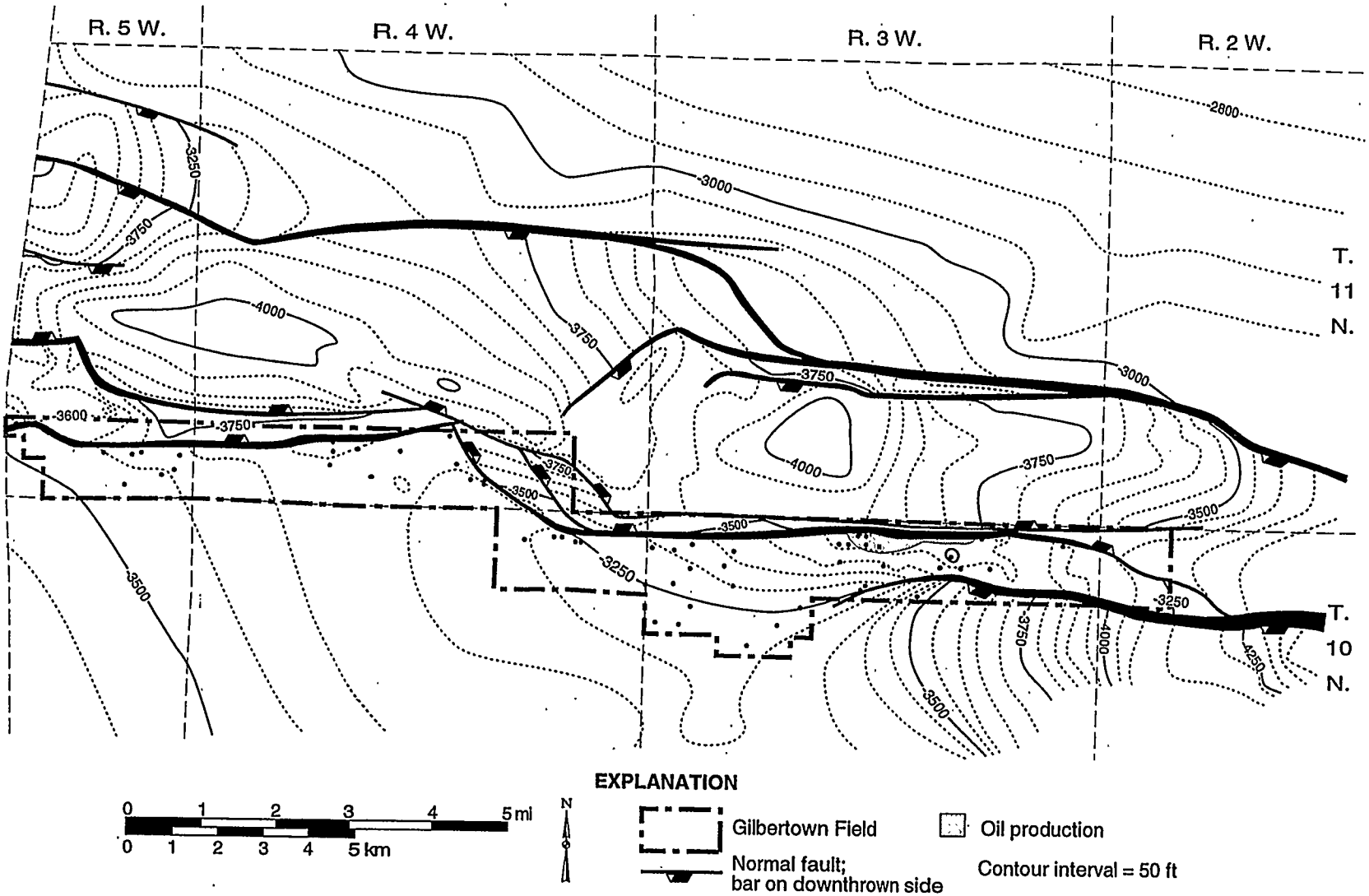

Figure 78.--Relationship of oil production to structure in interval E2 of the Eutaw Formation in Gilbertown Field.

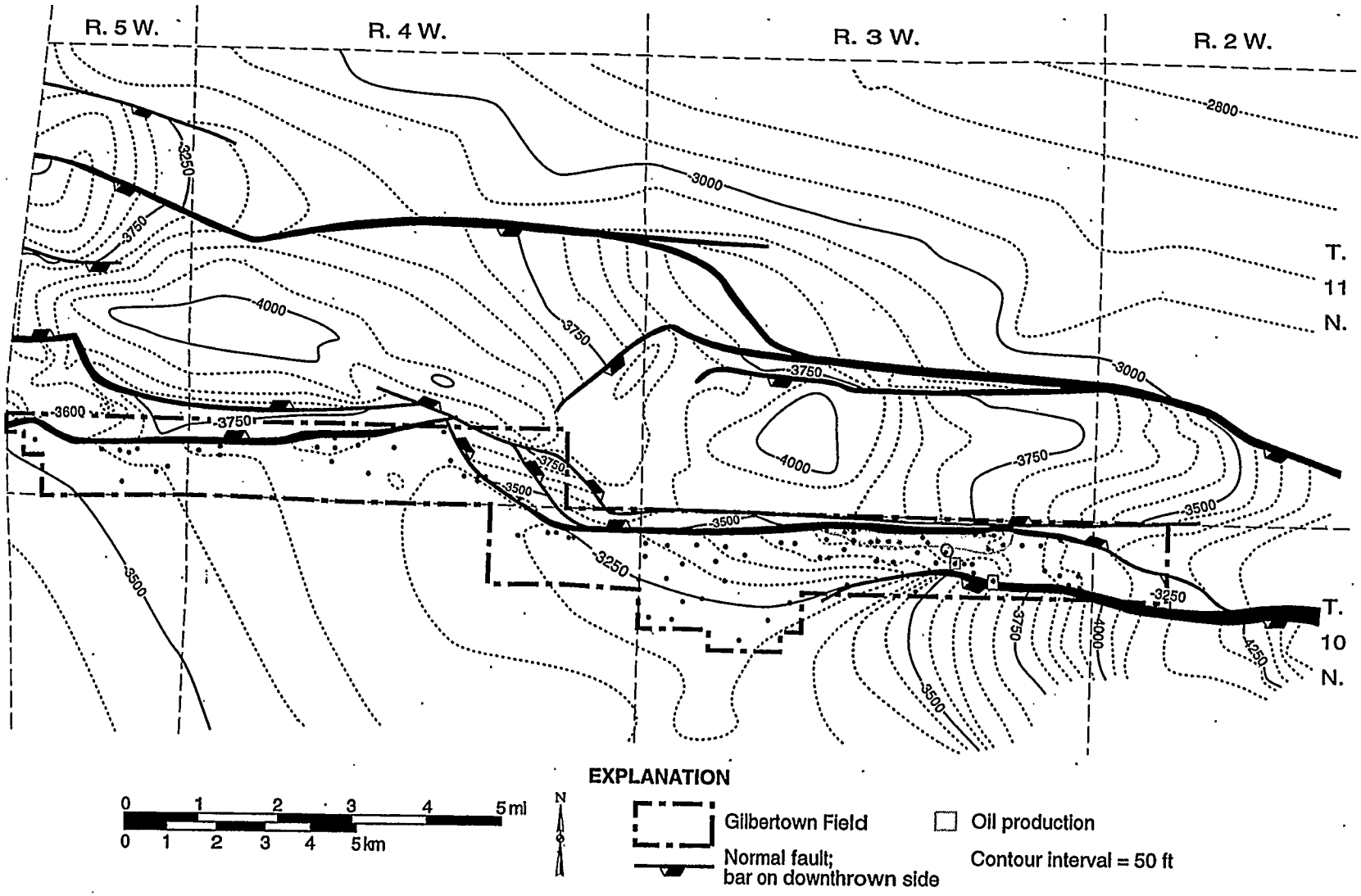

Figure 79.--Relationship of oil production to structure in interval E3 of the Eutaw Formation in Gilbertown Field.

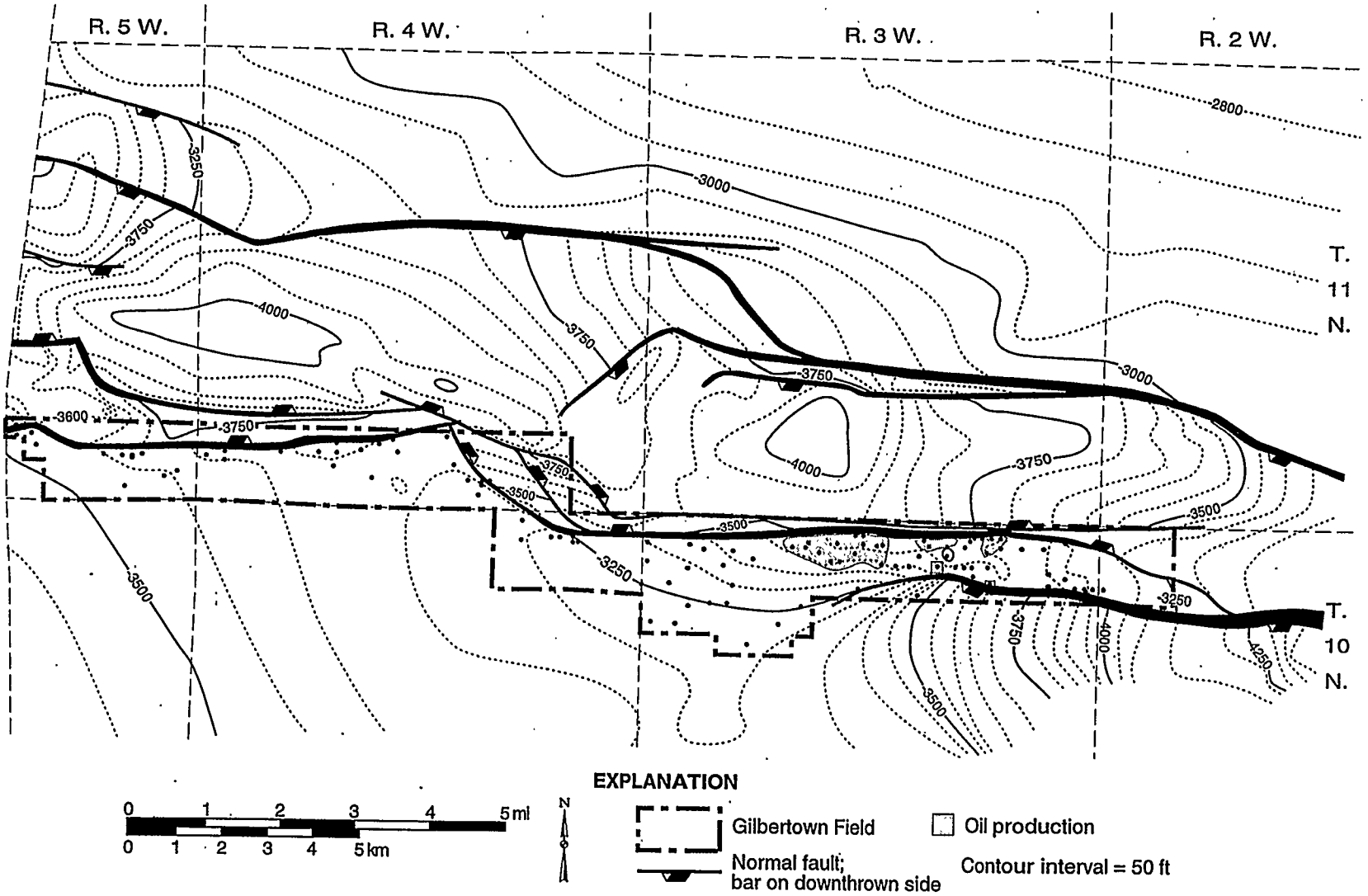

Figure 80.--Relationship of oil production to structure in interval E4 of the Eutaw Formation in Gilbertown Field.

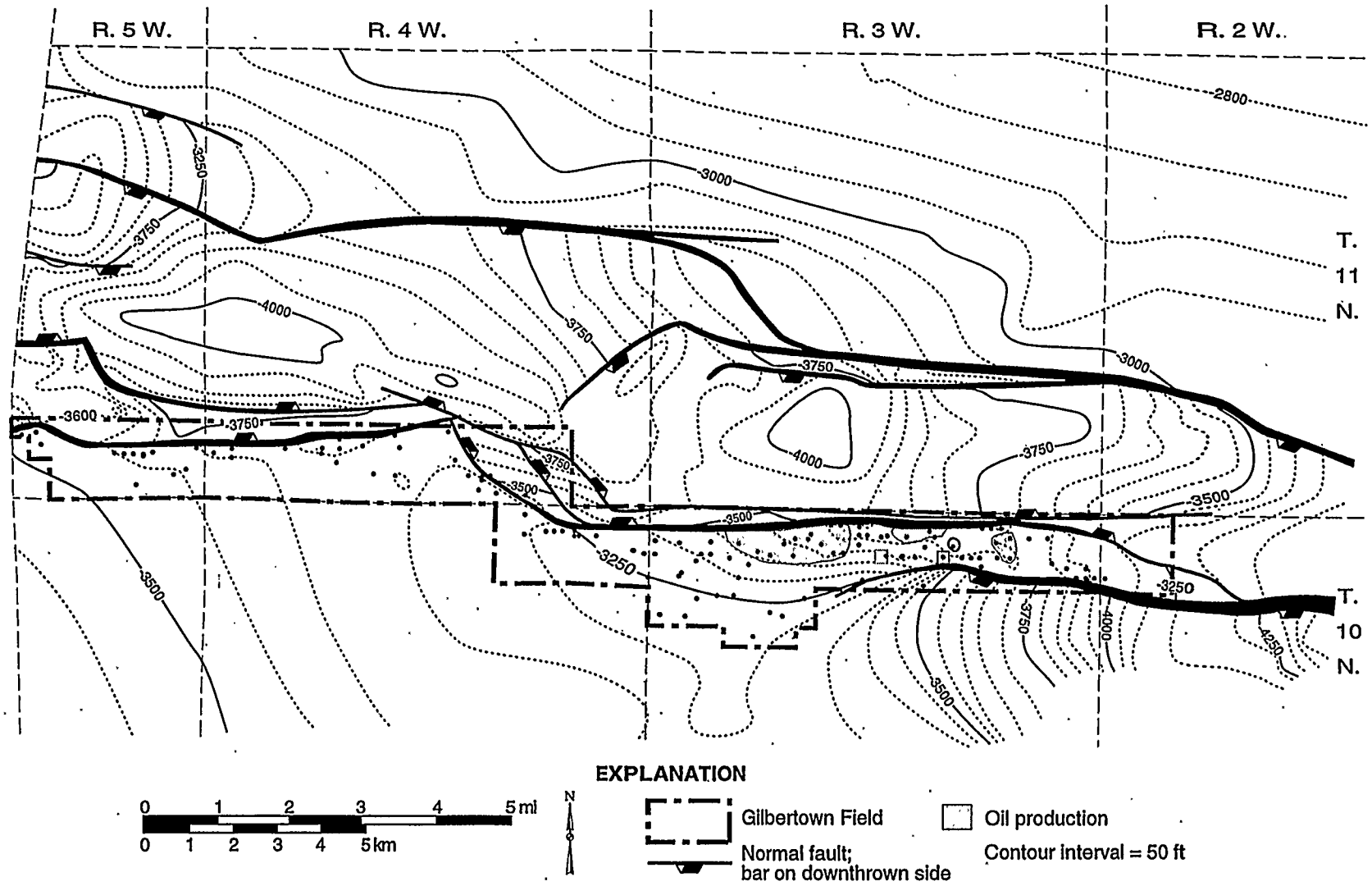

Figure 81.--Relationship of oil production to structure in interval E5 of the Eutaw Formation in Gilbertown Field.

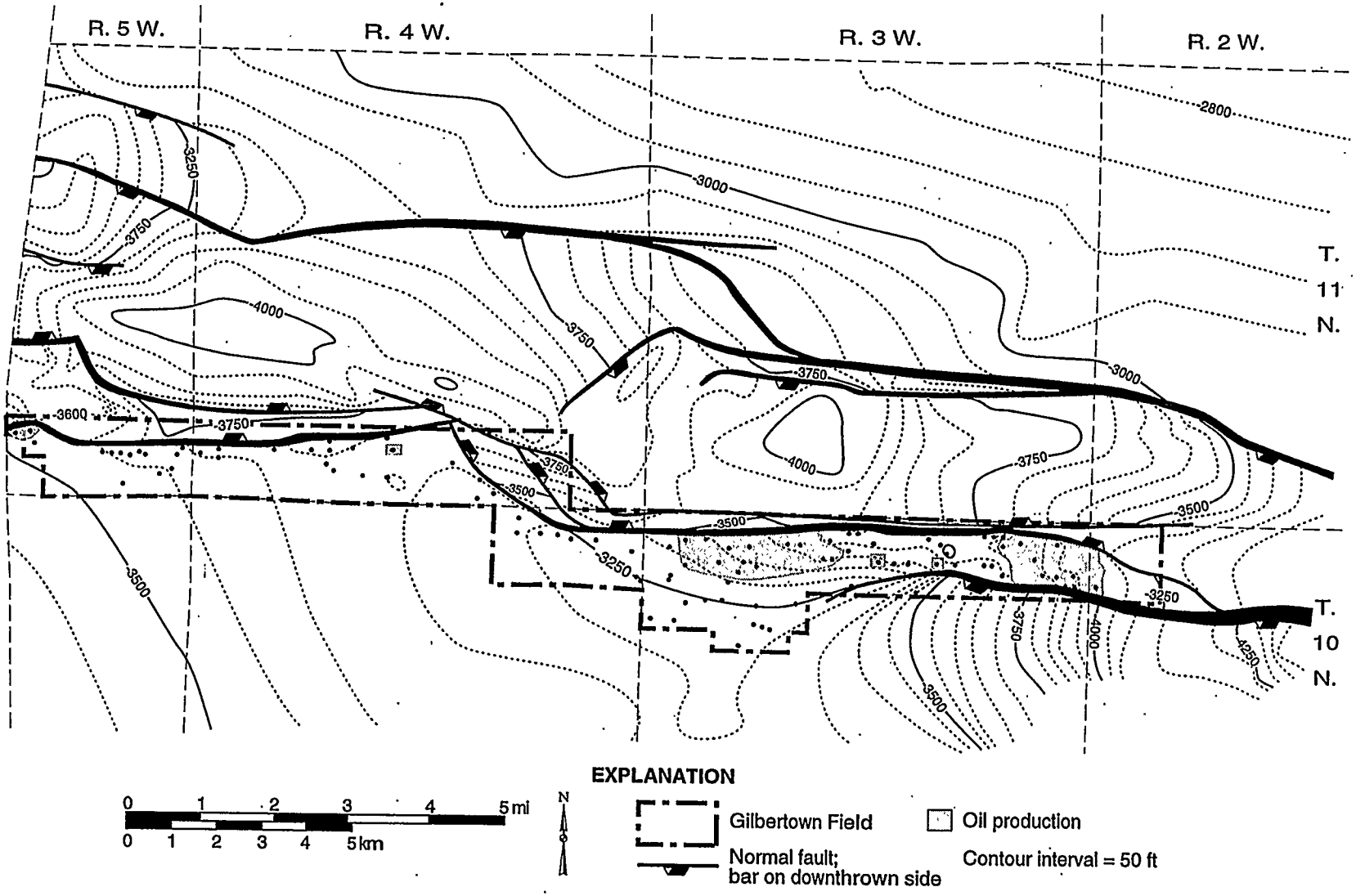

Figure 82.--Relationship of oil production to structure in interval E6 of the Eutaw Formation in Gilbertown Field.

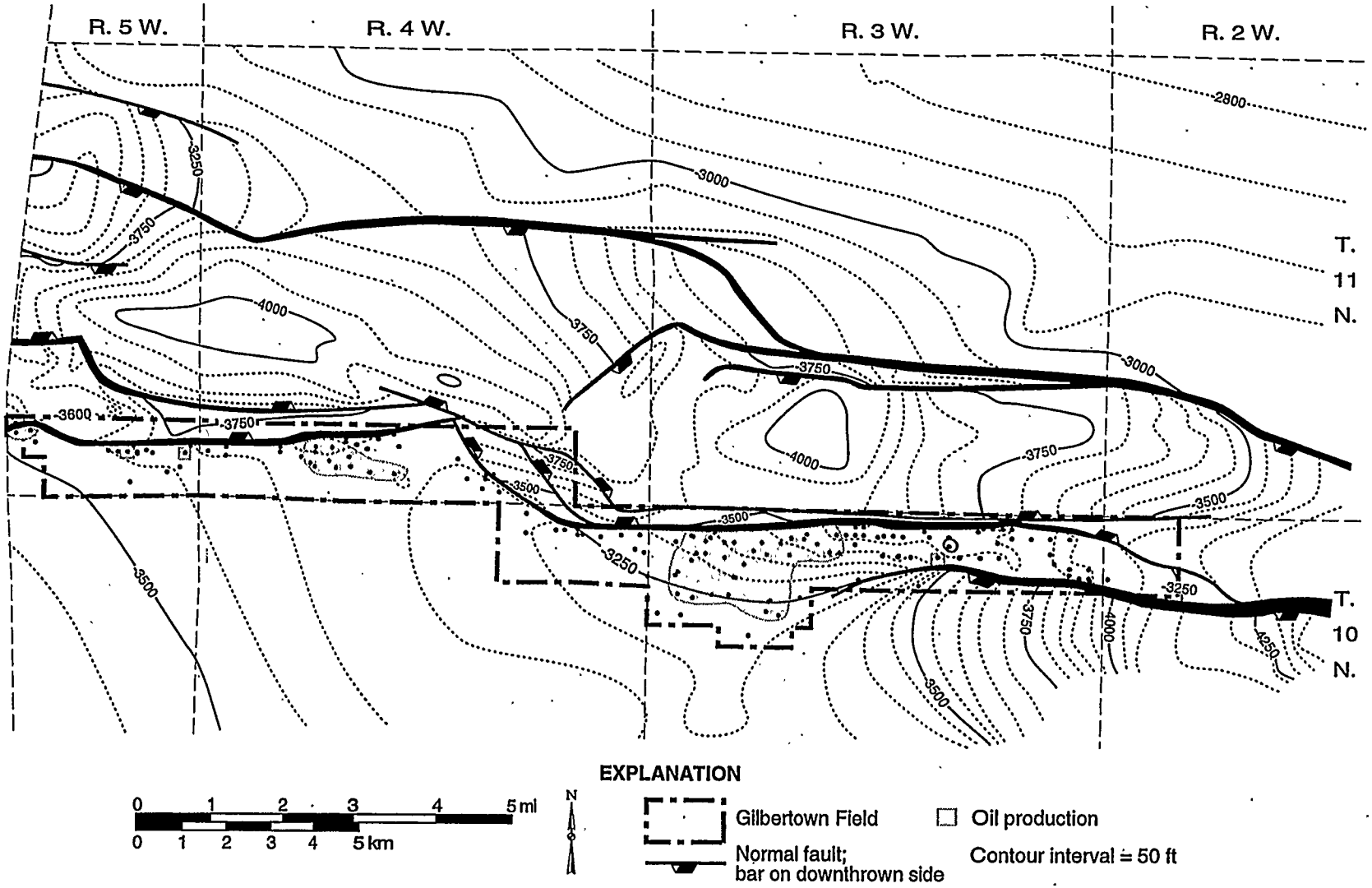

Figure 83.--Relationship of oil production to structure in interval E7 of the Eutaw Formation in Gilbertown Field..

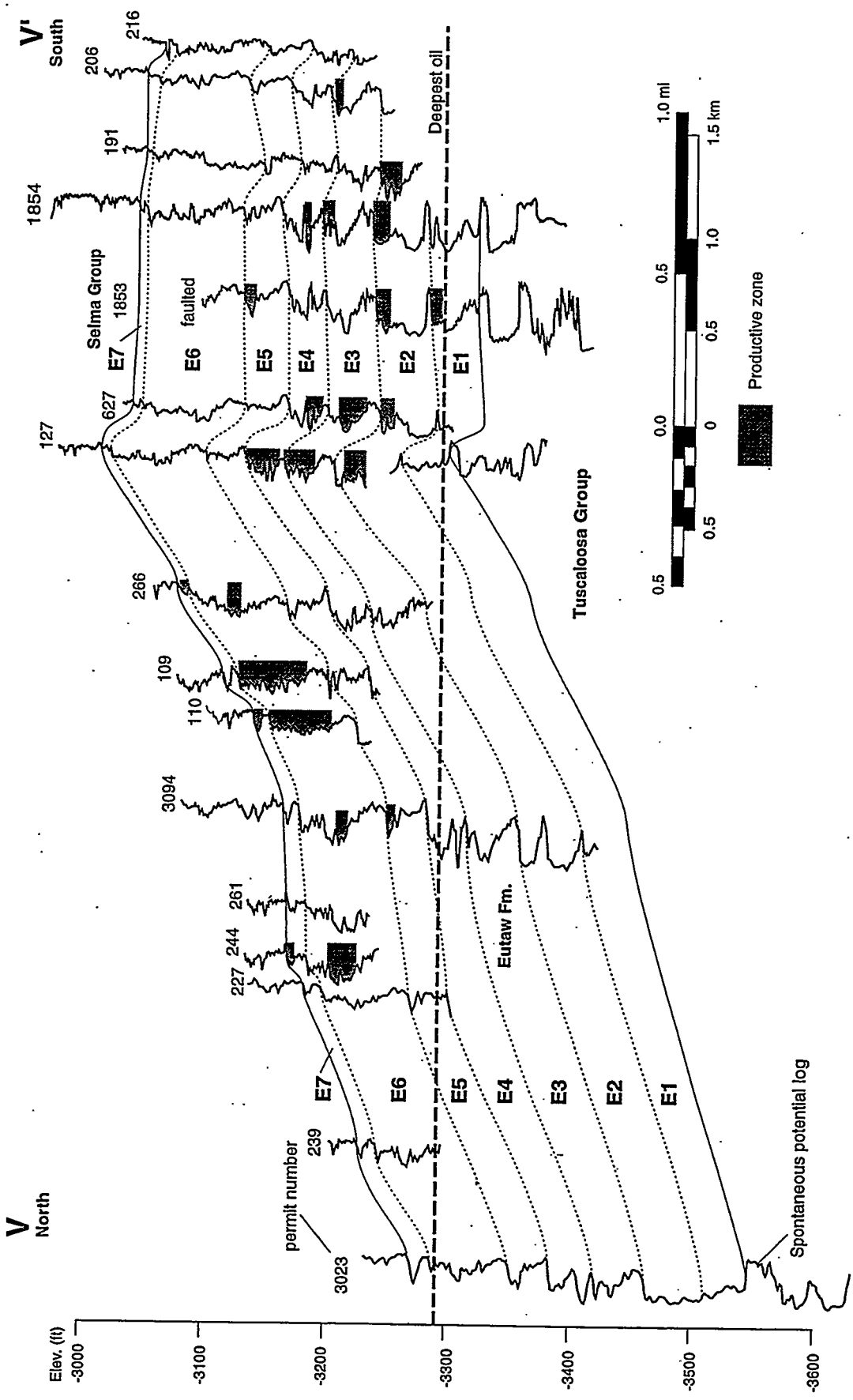

Figure 84.--Structural cross section V-V' showing the distribution of oil production in eastern Gilbertown Field. See Figure 37 for location.

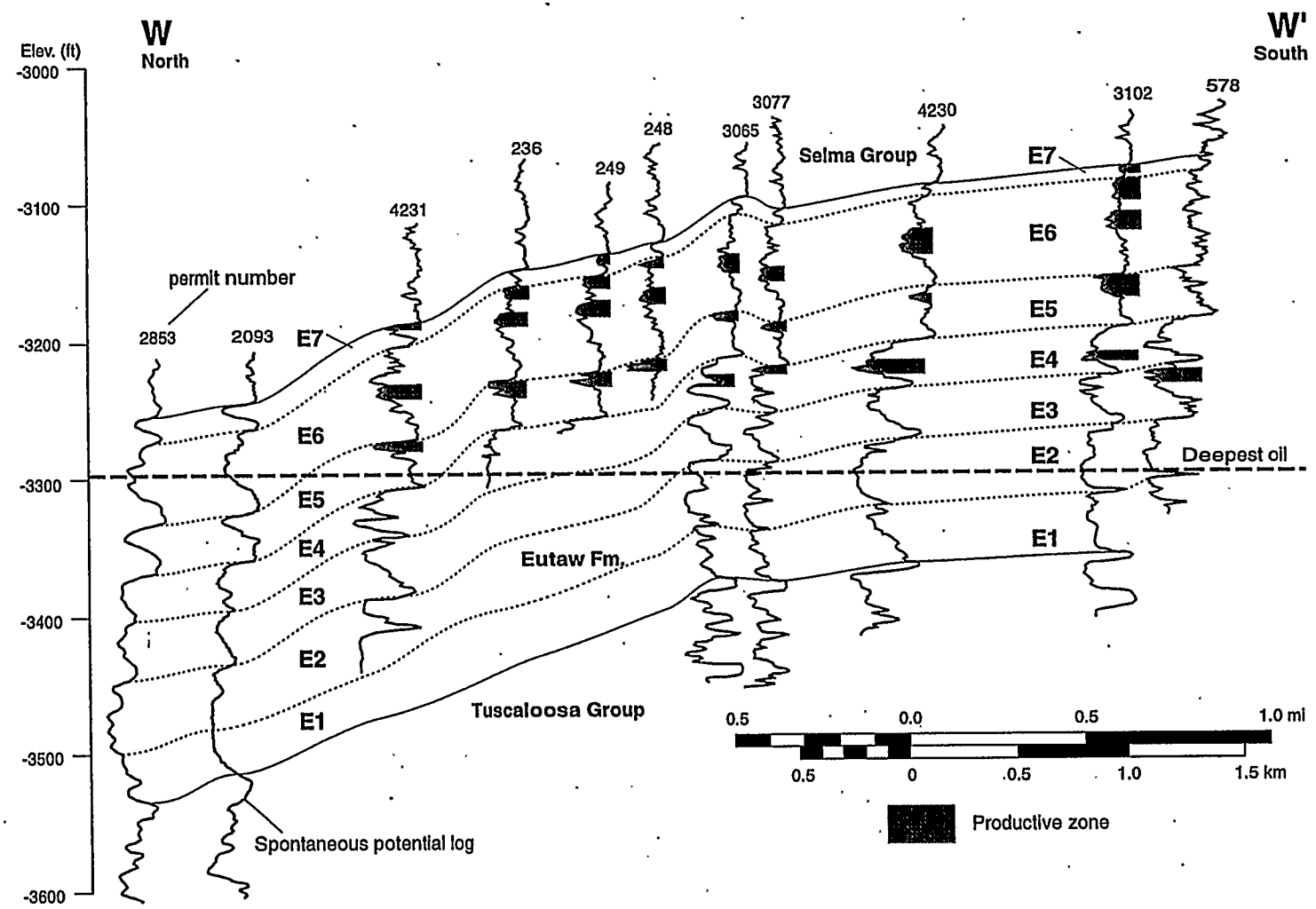

Figure 85.--Structural cross section W-W' showing the distribution of oil production in eastern Gilbertown Field. See Figure 37 for location.

Selma Production Patterns

The Selma Group has produced oil only in the western part of Gilbertown field from West Gilbertown fault A and East Gilbertown fault A (fig. 76). Oil has been produced along nearly the full length of West Gilbertown fault A, whereas Selma production is restricted to the western part of East Gilbertown fault A. Cumulative oil production along West Gilbertown fault A is relatively consistent, typically on the order of 10,000 barrels per well. Cumulative production is more variable along East Gilbertown fault A, especially in the relay zone where four wells have produced more than 100,000 barrels.

Production patterns provide the best evidence that fault curvature affected fracturing in the Selma Group (figs. 67–71). Along West Gilbertown A, most successful chalk wells are located near the extremities of the fault where total curvature is greatest. In the central part of the fault, where strike and dip curvature are least, only 3 of 11 wells penetrating the proximal hanging wall produced oil from the Selma Group (fig. 67). The four most productive chalk wells are in a secondary fault bend within the relay zone, which is a major zone of oblique slip. However, drilling success in this area is only slightly over 50 percent, suggesting heterogeneous reservoir conditions. The success rate is higher along the eastern fault segment, where strata have been transported through a uniform dip curvature.

Examining perforated intervals suggests possibilities for infill drilling (fig. 86). In the western part of West Gilbertown fault A, where 9 out of 13 wells produced oil from the Selma Group, perforated zones are in the hanging-wall block immediately below the Porters Creek topseal. This clearly is a good strategy for development with vertical wells (fig. 87). Note, however, that a deeper fault remains undeveloped (fig. 86). One suggestion, therefore, is to drill farther south where the deeper fault intersects the topseal. Farther east, the highest perforation zones in many wells are 150 to 400 feet below the topseal. Thus, a tall oil column potentially remains untapped, particularly in the central part of West Gilbertown fault A. Low success rate along this part of the fault indicates significant risk, some of which may be offset by horizontal drilling (fig. 87). Perhaps the best opportunity for renewed development in the Selma Group is to drill horizontal wells just below the hanging-wall topseal at a low angle to strike of the fault plane, thereby maximizing the amount of fractured chalk that can be contacted.

SUMMARY OF ACCOMPLISHMENTS

Gilbertown Field, established in 1944, is the oldest oil field in Alabama and produces oil from fractured chalk of the Cretaceous Selma Group and sandstone of the Eutaw Formation. Nearly all of Gilbertown field is still in primary recovery, although waterflooding has been attempted locally. The objective of this project is to analyze the geologic structure and burial history of Mesozoic and Tertiary strata in Gilbertown Field and adjacent areas in order to suggest ways in which oil recovery can be improved. Indeed, the decline of oil production to marginally economic levels in recent years has made this type of analysis timely and practical. Key technical advancements being sought include understanding the relationship of requisite strain to production in Gilbertown reservoirs, incorporation of synsedimentary growth factors into models of area balance, quantification of the relationship between requisite strain and bed curvature, determination of the timing of hydrocarbon generation, and identification of the avenues and mechanisms of fluid transport.

Structural maps and cross sections establish that the Gilbertown fault system is part of a horst-and-graben system that is interpreted to be detached at the base of the Louann Salt. Sequential restoration of cross sections suggests that the fault system began forming as a half graben during the Jurassic. The Early Cretaceous was the major episode of structural growth and subsidence of the half graben. By the end of the Early Cretaceous, however, the growth rate of antithetic faults in the eastern part of the field became effectively equal to that of synthetic faults. Thus, the half graben began collapsing, and the overall structural geometry of Cretaceous and younger strata is that of a full graben. Cross sections demonstrate significant growth of the graben during Cretaceous time but show limited growth in the Tertiary section.

Geologic mapping of formations and fracture systems has added significantly to knowledge of the geology of the Gilbertown area. Faults offset strata as young as Miocene, whereas Quaternary alluvial deposits cut across structures in the area. An excellent exposure of one fault shows that deformation is restricted mainly to the hanging wall and that shear fractures and drag folds are significant structural components. Fracture studies reveal two distinct orthogonal joint systems in the study area. One joint system is interpreted to have formed as part of the tectonic stress field responsible for regional extension, whereas the other system apparently is forming today in response to regional uplift and unroofing.

Analysis of burial history indicates that the subsidence history of Jurassic and Tertiary strata in the Gilbertown area is typical of extensional basins. Factoring out the tectonic component of subsidence suggests that more than half of the total effective

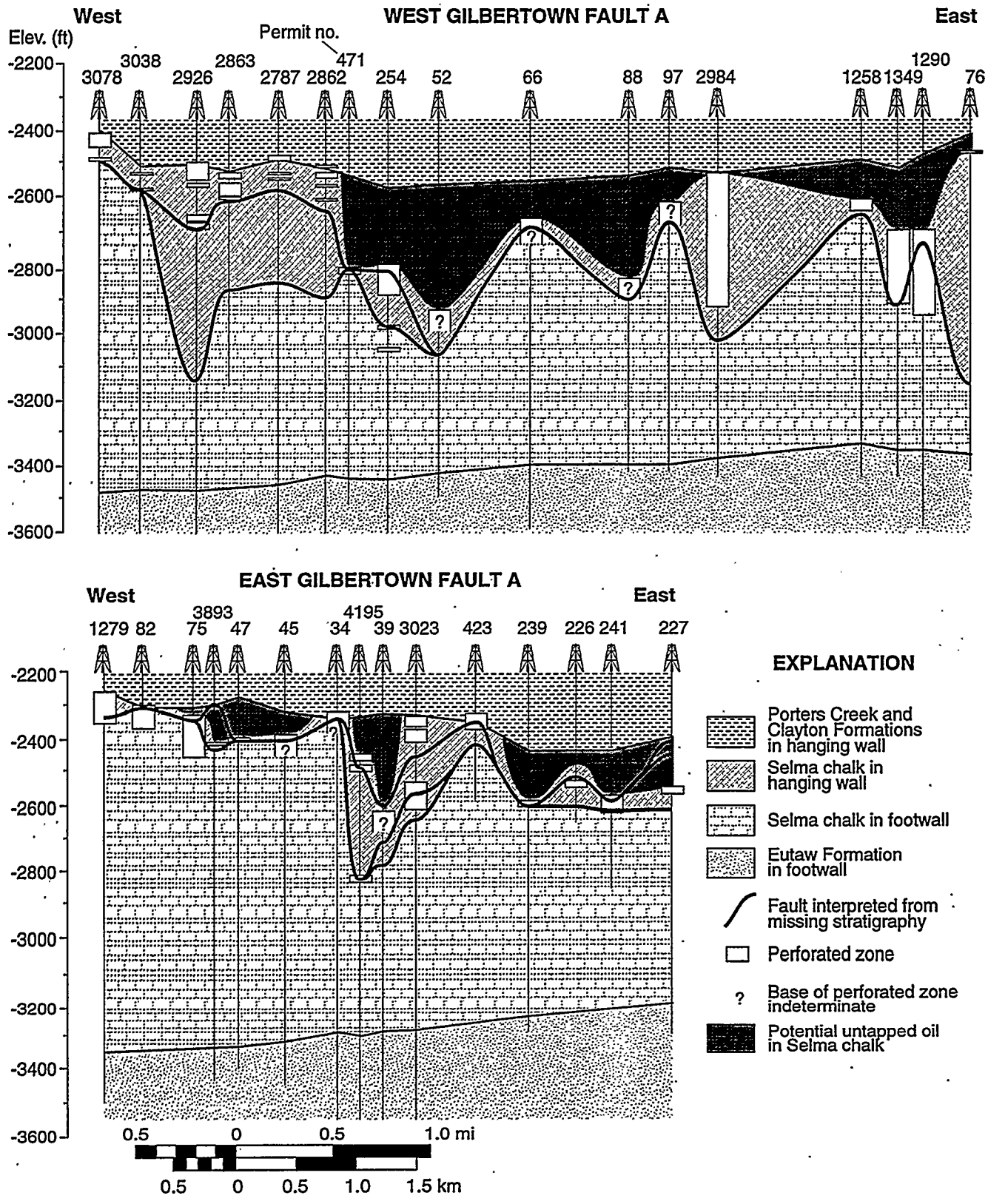

Figure 86.--Strike cross sections showing distribution of complete zones in the Selma Group and possible untapped oil column below reservoir seal.

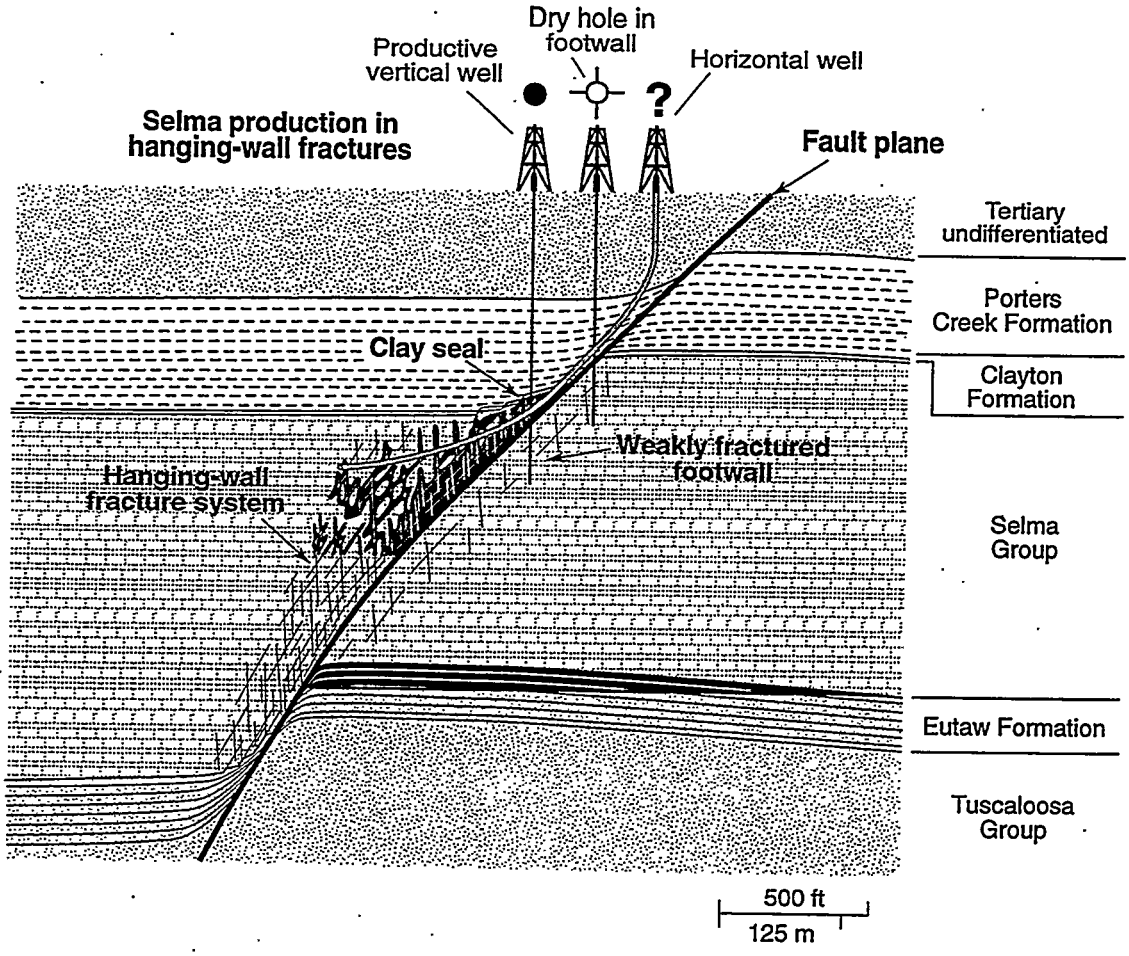

Figure 87.--Model of trapping mechanisms, sealing, and oil production from the Selma Group in Gilbertown Field. Horizontal drilling has potential to revitalize Selma oil production.

subsidence in the Gilbertown area can be accounted for by sediment loading and compaction. Thermal modeling demonstrates that source rocks in the Upper Cretaceous section are undermature. The most likely scenario is that oil was generated in the Smackover Formation and migrated along faults and fractures into what is now Gilbertown Field.

The Eutaw Formation was divided into seven flooding-surface-bound parasequences that could be mapped throughout the Gilbertown area. These parasequences are interpreted to have been deposited during regional transgression as part of a barrier shoreline system. Glauconite and carbonate cement are key sources of reservoir heterogeneity in the Eutaw Formation. High glauconite content makes the Eutaw a low-resistivity, low-contrast formation, and the limited log suite prevents characterization of the sandstone using shaly sand methodology. However, commercial core analyses enable quantification of basic reservoir properties.

The Selma Group was deposited on a muddy carbonate shelf, and eight stratigraphic intervals were traced throughout Gilbertown Field. Isotopic analysis indicates that mineralization of fractures occurred during burial and that slickensides continued forming near maximum burial. Evidence from resistivity, dipmeter, and fracture identification logs indicates that reservoir-scale deformation is mainly in the hanging walls of the faults. This deformation apparently includes minor faults, fractures, and drag folds.

Structural modeling included area balancing, curvature analysis, and seal analysis. New area balancing techniques were developed to characterize growth strata. Requisite strain calculations indicate that Jurassic strata deep in the Gilbertown graben contain a large component of small-scale deformation and that deformation in Upper Cretaceous strata is restricted to the fault zones, especially hanging-wall drag folds. Curvature analysis indicates that the faults where oil is produced from the Selma Group contain numerous fault bends. Transport of strata through these bends appears to have had a strong control on fracturing. Eutaw oil is produced strictly from footwall uplifts, whereas Selma oil is produced from fault-related fractures. Fault-seal analysis suggests that clay smear and mineralization may be significant trapping mechanisms in the Eutaw Formation. The critical seal for Selma reservoirs, by contrast, is where Porters Creek clay shale in the hanging wall is juxtaposed with Selma chalk in the footwall, reflecting the predominance of hanging-wall deformation.

The decline characteristics of Eutaw and Selma wells differ markedly, reflecting development in conventional and fractured reservoirs, respectively. Decline curves of the most productive wells, moreover, are affected significantly by the field's development history, which included an episodes of near abandonment in the late 1960s followed by one of rejuvenation during the 1970s. Plotting production and completion patterns on maps and cross sections identifies opportunities for revitalization through infill drilling. In the Selma Group, for example, a tall oil column may remain untapped, and horizontal drilling may be the most viable technology to revive Selma production.

TECHNOLOGY TRANSFER

The Geological Survey of Alabama is maintaining an aggressive technology transfer program that includes contacts with industry, technical presentations, and workshops. Contact with industry has been maintained throughout the project and is promoting revitalization of Gilbertown Field. A web site is also being prepared that will be devoted to disseminating the results of the Gilbertown project.

Drs. Jack C. Pashin and Richard H. Groshong, Jr. attended the Annual Meeting of the American Association of Petroleum Geologists in April and met with operators and others working in the region to discuss progress on the project and how results of this project can be used to guide redevelopment of Gilbertown Field. Operators were receptive and have offered additional geophysical and engineering information that will help ensure successful completion of the research. A group of private investors is now raising money to drill three new wells in the Eutaw Formation, and we have been approached for information by entrepreneurs who are considering implementation of a horizontal drilling program in Selma chalk.

Drs. Pashin and Groshong presented papers on area balance and strain in extensional structures at an American Association of Petroleum Geologists Hedberg Conference entitled, *Reservoir Scale Deformation—Characterization and Prediction*, which was held from June 22–28 in Bryce, Utah. Dr. Groshong presented a paper called *Predicting Fractures from Area Balanced Cross Sections*, which emphasized the theoretical aspects of the Gilbertown project. Immediately following Dr. Groshong's paper, Dr. Pashin presented a paper called *Area Balance, Strain, and Fracturing in Coalbed and Chalk Reservoirs: Case Studies of Extensional Structures in the Black Warrior and Gulf Coast Basins,* which showed the application of area balance to coalbed methane reservoirs and emphasized theoretical modifications required to model growth structures of the Gilbertown area. Dr. Pashin also presented a similar paper called *Area Balance in Extensional Structures: Comparison Between the Black Warrior*

and Gulf Coast Basins in a session on Department of Energy reservoir management and characterization programs at the American Association of Petroleum Geologists Eastern Section Meeting, which was held in Lexington, Kentucky, from September 27–30.

Drs. Pashin and Groshong will present two poster sessions at the American Association of Petroleum Geologists Annual Meeting in Salt Lake City, Utah in May 1998. Dr. Pashin's presentation will be in a session entitled, *Revitalization of Marginal Oil Fields: Global Case Studies*; his poster is called *Revitalizing Fractured Chalk and Glauconitic Sandstone Reservoirs in Gilbertown Field, Gulf Coast Basin, USA*. Dr. Groshong's poster is in a session entitled, *3-D Imaging of Structural Forms* and is called *Well-based 3-D Visualization of Mature Oil Reservoirs Associated with the Gilbertown Graben, Southwest Alabama.*

Papers have also been accepted for publication and presentation at the upcoming meeting of the Gulf Coast Association of Geological Societies, which will be held in Corpus Christi, Texas in October. At this meeting, Dr. Pashin will present a paper called *Area-Balanced Structural Model of a Fractured Chalk Reservoir: Toward Revitalizing Gilbertown Field, Choctaw County, Alabama.* Dr. Groshong will be presenting a paper on the deep structure of the Gilbertown fault system called *Structure and Evolution of North Choctaw Ridge Field, Alabama, a Salt-Related Footwall Uplift Along the Peripheral Fault System, Gulf Coast Basin.*

An annual report summarizing progress on this project was published in the U.S. Department of Energy's Fossil Energy series in May 1997. We have received 50 copies of the report that are being distributed to operators and other appropriate parties. During October, Rick Groshong and Jack Pashin conducted an informal one-day workshop for industry personnel on faulting in Cretaceous Chalk. Participants had the opportunity to examine faulted chalk in outcrop. Regional tectonics, diagenesis, and the implications for hydrocarbon production in the Gilbertown area were discussed. A workshop summarizing results of the Gilbertown project is being planned for this coming fall and will be conducted with the cooperation of the Eastern Gulf Regional Resource Center of the Petroleum Technology Transfer Council.

SUGGESTIONS FOR FUTURE WORK

Significant progress has been made toward understanding the structural geology of Gilbertown Field, and we have drawn some insight into the technologies that are best suited to revitalize the field. However, three major tasks remain to complete the project, which will be finished at the end of September 1998. These tasks include parts of Task 4 (Structural Modeling), Task 5 (Burial and Thermal Modeling), and Task 6 (Production Analysis), and a detailed description of the remaining work is given below.

Our current working hypothesis is that the deformation responsible for the open fractures is localized to the drag zone in the hanging wall of the master fault zones. Future plans call for developing and testing this hypothesis. An obstacle to be overcome is the general lack of detailed information close to the fault, specifically in the drag zone. The resources available include dipmeters, FILs, structural modeling capabilities, and an outcrop analog at Coffeeville Landing. Using these resources, we will conduct a multifaceted investigation.

We will perform a SCAT analysis (Statistical Curvature Analysis Technique) of the dipmeter logs (Bengtson, 1981; Groshong, 1998) for the purpose of identifying the structure in the drag zone and will construct a composite cross section based on the result. We will create fracture abundance profiles from the FILs and correlate the fracture abundance to distance from the fault and curvature to test the relationship between drag folding and fracturing. Next, structural models of strain in drag folds will be generated. Factors to be considered include identifying the best structural model, the relationship between the dip of bedding and strain, the asymmetry of drag across the fault, and the possible role of compaction in the growth structure. We will further examine the faults and drag fold at Coffeeville Landing to compare our subsurface inferences and model predictions to the observations.

Data are being compiled to generate burial history curves of additional wells in the Gilbertown area, and a vitrinite reflectance map of the Eutaw Formation is being compiled. A key focus of ongoing work is obtaining hard vitrinite reflectance data from Jurassic strata, because the TAI data used in this report appear to correlate with unreasonably low reflectance. Reflectance data will be used to refine the Lopatin models (Waples, 1980) and to develop kinetic models of hydrocarbon generation (Burnham and Sweeney, 1989; Sweeney and Burnham, 1990). To provide more paleogeothermal information, additional carbonate samples will be sent for isotopic analysis.

Productivity analysis is nearly complete, but additional work remains to assess the productivity of wells and to identify areas where oil may remain untapped. Future work on the Eutaw Formation will focus on identifying zones for infill drilling and recompletion. Work on the Selma will include using the results of structural modeling to determine the potential for success of new vertical wells, as well as the viability of horizontal wells.

As this project draws toward completion, technology transfer efforts will continue to accelerate. Manuscripts

are being prepared for publication in refereed journals, conference proceedings, and government documents. Oral and poster presentations are already scheduled for technical meetings, and a major workshop is in preparation. Moreover, a web page is being composed that is devoted to disseminating the results of the Gilbertown project.

ACKNOWLEDGMENTS

We would like to thank the many producers of oil and gas in south Alabama. This project would not be possible without their interest. Special acknowledgment goes to Professor Charles D. Haynes of the University of Alabama, who donated a wealth of reservoir data that are vital to this project. The Eastern Gulf Region of the Petroleum Technology Transfer Center and the Computer Visualization Laboratory of the University of Alabama are thanked for providing access to advanced computational facilities.

REFERENCES CITED

Ahr, W. M., 1973, The carbonate ramp: An alternative to the shelf model: Gulf Coast Association of Geological Societies Transactions, v. 23, p. 221–225.

Allan, U. S., 1989, Model for hydrocarbon migration and entrapment within faulted structures: American Association of Petroleum Geologists Bulletin, v. 78, p. 355–377.

Asquith, G. B., and Gibson, C. R., 1982, Basic well log analysis for geologists: Tulsa, Oklahoma, American Association of Petroleum Geologists Methods in Exploration Series, 216 p.

Bailey, R. J., and Atherton, M. P., 1969, The petrology of a glauconitic sandy chalk: Journal of Sedimentary Petrology, v. 39, p. 1420–1431.

Bengtson, C. A., 1981, Statistical curvature analysis techniques for structural interpretation of dipmeter data: American Association of Petroleum Geologists Bulletin, v. 65, p. 312–332.

Benson, D. J., 1988, Depositional history of the Smackover Formation of southwest Alabama: Gulf Coast Association of Geological Societies Transactions, v. 38, p. 197–205.

Berg, R. R., and Avery, A. H., 1995, Sealing properties of Tertiary growth faults, Texas Gulf Coast: American Association of Petroleum Geologists Bulletin, v. 79, p. 375–393.

Berner, R. A., 1981, A new geochemical classification of sedimentary environments: Journal of Sedimentary Petrology, v. 51, p. 359–365.

Bolin, D. E., Mann, S. E., Burroughs, Delores, Moore, H. E., Jr., and Powers, T. J., 1989, Petroleum atlas of southwestern Alabama: Alabama Geological Survey Atlas 23, 218 p.

Bouvier, J. D., Kaars–Sijpesteijn, C. H., Kluesner, D. F., Onyejekwe, C. C., and van der Pal, R. C., 1989, Three-dimensional seismic interpretation and fault sealing investigations, Nun River field, Nigeria: American Association of Petroleum Geologists Bulletin, v. 73, p. 1397–1414.

Braunstein, Jules, 1953, Fracture-controlled production in Gilbertown Field, Alabama: American Association of Petroleum Geologists Bulletin, v. 37, p. 245–249.

Brown, D. A., 1987, The flow of water and displacement of hydrocarbons in fractured chalk reservoirs: Geological Society of London Special Publication 34, p. 201–218.

Burnham, A. K., and Sweeney, J. J., 1989, A chemical kinetic model of vitrinite maturation and reflectance: Geochimica et Cosmochimica Acta, v. 53, p. 2649–2657.

Cardott, B. J. and Lambert, M. W., 1985, Thermal maturation by vitrinite reflectance of Woodford Shale, Anadarko Basin, Oklahoma: American Association of Petroleum Geologists Bulletin, v. 69, p. 1982–1998.

Chamberlin, R. T., 1910, The Appalachian folds of central Pennsylvania: Journal of Geology, v. 18, p. 228–251.

Chaudhuri, A. K., Chanda, S. K., and Dasgupta, Somnath, 1994, Proterozoic glauconitic peloids from south India: Their origin and significance: Journal of Sedimentary Research,

Christie–Blick, N., and Biddle, K. T., 1985, Deformation and basin formation along strike-slip faults: Society of Economic Paleontologists and Mineralogists Special Publication 37, p. 1–34.

Claypool, G. E., and Mancini, E. A., 1989, Geochemical relationships of petroleum in Mesozoic reservoirs to carbonate source rocks of Jurassic Smackover Formation, southwestern Alabama: American Association of Petroleum Geologists Bulletin, v. 73, p. 904–924.

Cloud, P. E., Jr., 1955, Physical limits of glauconite formation: American Association of Petroleum Geologists Bulletin 39, p. 484–492.

Coleman, M. L., 1985, Geochemistry of diagenetic non-silicate minerals: Kinetic considerations: Philosophical Transactions of the Royal Society of London, v. A–315, p. 39–56.

Cook, M. R., 1993, The Eutaw aquifer in Alabama: Alabama Geological Survey Bulletin 156, 105 p.

Cook, P. L., Jr., Schneeflock, R. D., Bush, J. D., and Marble, J. C., 1990, Trimble field, Miss.: 100 bcf of bypassed, low resistivity Cretaceous Eutaw pay at 7,000 ft: Oil & Gas Journal, Oct. 22, 1990, p. 96–102.

Copeland, C. W., Newton, J. G., and Self, D. M., eds., 1976, Cretaceous and Tertiary faults in southwestern Alabama: Alabama Geological Society, Fourteenth Annual Field Trip Guidebook, 114 p.

Current, A. M., 1948, Gilbertown Field, Choctaw County, Alabama: Tulsa, Oklahoma, American Association of Petroleum Geologists, Structure of Typical American Oil Fields, v. 3, p. 1–4.

Curtis, C. D., and Coleman, M. L., 1986, Controls of the precipitation of early diagenetic calcite, dolomite, and siderite concretions in complex depositional sequences, *in* Gautier, D. L., ed., Roles of organic matter in sediment diagenesis: Society of Economic Paleontologists and Mineralogists Special Publication 38, p. 23–33.

Dahlstrom, C. D. A., 1969, Balanced cross sections: Canadian Journal of Earth Sciences, v. 6, p. 743–757.

Dasgupta, Somnath, Chaudhuri, A. K., and Fukuoka, Masato, 1990, Compositional characteristics of glauconitic alterations of K-feldspar from India and their implications: Journal of Sedimentary Petrology, v. 60, p. 277–287.

Davison, I., 1986, Listric normal fault profiles: Calculation using bed-length balance and fault displacement: Journal of Structural Geology, v. 8, p. 209–210.

de Charpal, O., Guennoc, P., Montadert, L., and Roberts, D. G., 1978, Rifting, crustal attenuation, and subsidence in the Bay of Biscay: Nature, v. 275, p. 706–711.

Dickson, J. A. D., Smalley, P. C., Raheim, A., and Stijfhoorn, D. E., 1990, Intracrystalline carbon and oxygen isotope variations in calcite revealed by laser microsampling: Geology, v. 18, p. 809–811.

Eaves, Everett, 1976, Citronelle oil field, Mobile County, Alabama: American Association of Petroleum Geologists Memoir 24, p. 259–275.

Engelder, J. T., 1985, Loading paths to joint propagation during a tectonic cycle: An example from the Appalachian Plateau, USA: Journal of Structural Geology, v. 7, p. 45–76.

Engelder, J. T., and Lacazette, A., 1990, Natural hydraulic fracturing, *in* Barton, N., and Stephansson, O., eds., Rock joints: Rotterdam, A. A. Balkema, p. 35–44.

Epard, J.–L., and Groshong, R. H., 1993, Excess area and depth to detachment: American Association of Petroleum Geologists Bulletin, v. 77, p. 1291–1302.

Falvey, D. A., and Middleton, M. F., 1981. Passive continental margins: Evidence for a pre-breakup deep crustal metamorphic subsidence mechanism: 26th International Geological Congress, Colloquia C3.3, Geology of Continental Margins, Oceanological Acta, supplement to v. 4, p. 103–114.

Frazier, W. J., and Taylor, R. S., 1980, Facies changes and paleogeographic interpretations of the Eutaw Formation (Upper Cretaceous) from western Georgia to central Alabama, *in* Tull, J. F., ed., Field Trips for the Southeastern Section of the Geological Society of America, Birmingham, Alabama, p. 1–27.

Galliher, E. W., 1935, Glauconite genesis: Geological Society of America Bulletin 46, p. 1351–1366.

Galloway, W. E., 1986, Growth faults and fault-related structures of prograding terrigenous clastic continental margins: Gulf Coast Association of Geological Society Transactions, v. 36, p. 121–128.

Gibson, T. G., Mancini, E. A., and Bybell, L. M., 1982, Paleocene to middle Eocene stratigraphy of Alabama: Gulf Coast Association of Geological Society Transactions, v. 32, p. 449–458.

Griggs, D. T., and Handin, J. H., 1960, Observations on fracture and a hypothesis of earthquakes: Geological Society of America Memoir 79, p. 347–364.

Groshong, R. H., Jr., 1990, Unique determination of normal fault shape from hanging-wall bed geometry in detached half grabens: Eclogae Geologicae Helvetiae, v. 83, p. 455–471.

___1994, Area balance, depth to detachment and strain in extension: Tectonics, v. 13, p. 1488–1497.

___ 1998, 3-D Structural Geology: Heidelberg, Springer–Verlag, in press.

Groshong, R. H., Jr., and Epard, J.–L., 1994, The role of strain in area-constant detachment folding: Journal of Structural Geology, v. 15, p. 613–618.

___ 1996, Computerized cross section balance and restoration, *in* D. G. DePaor, ed., Structural geology and personal computers: Amsterdam, Elsevier Science Ltd., Pergamon Imprint, p. 477–498.

Guthrie, G. M., and Raymond, D. E., 1992, Pre-Middle Jurassic rocks beneath the Alabama Gulf Coastal Plain: Alabama Geological Survey Bulletin 150, 155 p.

Hansen, W. R., 1965, Effects of the earthquake of March 27, 1964, at Anchorage, Alaska: U.S. Geological Survey Professional Paper 542–A, 16 p.

Harris, J. F., Taylor, G. L., and Walper, J. L., 1960, Relation of deformational structures in sedimentary rocks to regional and local structure: American Association of Petroleum Geologists Bulletin, v. 44, p. 1853–1873.

Harris, P. M., and Dodman, C. A., 1982, Jurassic evaporites of the U.S: Gulf Coast: the Smackover–Buckner contact, *in* Hanford, C. R., Loucks, R. G., and Davies, G. R., eds., Depositional and diagenetic spectra of evaporites—a core workshop: Society of Economic Paleontologists and Mineralogists Core Workshop 3, p. 174–192.

Hermansson, L., 1990, Influence of production on chalk failure in Valhall field: Society of Petroleum Engineers Paper 20952, 9 p.
Hilchie, D. W., 1978, Old (pre 1958) electrical log interpretation: Golden, Colorado, Douglas W. Hilchie, Incorporated, 163 p.
Hopkins, O. B., 1917, Oil and gas possibilities of the Hatchetigbee anticline, Alabama: U.S. Geological Survey Bulletin 661–H, p. 281–313.
Horsfield, W. T., 1980, Contemporaneous movement along crossing conjugate normal faults: Journal of Structural Geology, v. 2, p. 305–310.
Horton, J. W., Zietz, Isidore, and Neathery, T. L., 1984, Truncation of the Appalachian Piedmont beneath the Coastal Plain of Alabama: Geology, v. 12, p. 51–55.
Hudson, J. D., 1977, Stable isotopes and limestone lithifications: Journal of the Geological Society of London, v. 133, p. 637–660.
Hughes, D. J., 1968, Salt tectonics as related to several Smackover fields along the northeast rim of the Gulf of Mexico basin: Gulf Coast Association of Geological Societies Transactions, v. 18, p. 320–330.
Jenyon, M. K., 1986, Salt tectonics: New York, Elsevier, 238 p.
Joiner, T. J., and Moore, D. B., 1966, Structural features in south Alabama, *in* Copeland, C. W., ed., Facies changes in the Alabama Tertiary: Alabama Geological Society, Fourth Annual Field Trip Guidebook, p. 11–19.
Keller, P., 1990, Rift structures: Geometric and kinematic model of bed length balanced graben structures: Eclogae Geologicae Helvetiae, v. 83, p. 473–492.
Knipe, R. J., 1992, Faulting processes and fault seal, in Larsen, R. M., Brekke, H., Larsen, B. T., and Talleras, E., eds., Structural and tectonic modelling and its application to petroleum geology: Amsterdam, Elsevier, p. 325–342.
Knipe, R. J., 1997, Juxtaposition and seal diagrams to help analyze fault seals in hydrocarbon reservoirs: American Association of Petroleum Geologists Bulletin, v. 81, p. 187–195.
Kopaska–Merkel, D. C., and Schmoker, J. W., 1994, Regional porosity evolution in the Smackover Formation of Alabama: Carbonates and Evaporites, v. 9, p. 58–75.
Krause, R. G. F., and Geijer, T. A. M., 1987, An improved method for calculating the standard deviation and variance of paleocurrent data: Journal of Sedimentary Petrology, v. 57, p. 779–780.
Kugler, R. L., Pashin, J. C., Carroll, R. E., Irvin, G. D., and Moore, H. E., 1994, Reservoir heterogeneity in Carboniferous sandstone of the Black Warrior basin: Bartlesville, Oklahoma, U.S. Department of Energy Fossil Energy Report DOE/BC/14448–11, 179 p.
Lachenbruch, A. H., 1962, Mechanics of thermal contraction cracks in ice-wedge polygons in permafrost: Geological Society of America Special Paper 70, 69 p.
La Pointe, P. R., and Hudson, J. A., 1985, Characterization and interpretation of rock mass joint patterns: Geological Society of America Special Paper 199, 37 p.
Light, M. A., 1952, Evidence of authigenic and detrital glauconite: Science, v. 115, no. 2977, p. 73–75.
Lisle, R. J., 1994, Detection of zones of abnormal strains in structures using Gaussian curvature analysis: American Association of Petroleum Geologists Bulletin, v. 78, p., 1811–1819.
Lowe, J. T., and Carington, D. B., 1990, Occurrence of oil in the Austin Chalk at Van field, Van Zandt County, Texas—a unique geologic setting: Gulf Coast Association of Geological Societies Transactions, v. 40, p. 485–493.
MacNeil, F. S., 1946, Geologic map of the Tertiary formations of Alabama: U.S. Geological Survey Preliminary Map 45, scale 1:500,000.
Mancini, E. A., and Benson, D. J., 1980, Regional stratigraphy of Upper Jurassic Smackover carbonates of southwest Alabama: Gulf Coast Association of Geological Societies Transactions, v. 30, p. 151–165.
Mancini, E. A., Mink, R. M., Bearden, B. L., and Wilkerson, R. P., 1985, Norphlet Formation (Upper Jurassic) of southwestern and offshore Alabama: Environments of deposition and petroleum geology: American Association of Petroleum Geologists Bulletin, v. 69, p. 881–898.
Mancini, E. A., Mink, R. M., Payton, J. W., and Bearden, B. L., 1987, Environments of deposition and petroleum geology of Tuscaloosa Group (Upper Cretaceous), South Carlton and Pollard fields, southwestern Alabama: American Association of Petroleum Geologists Bulletin, v. 71, p. 1128–1142.
Mancini, E. A., Mink, R. M., Tew, B. H., Kopaska–Merkel, D. C., and Mann, S. D., 1991, Upper Jurassic Smackover plays in Alabama, Mississippi, and the Florida panhandle: Gulf Coast Association of Geological Societies Transactions, v. 41, p. 475–480.
Mancini, E. A., and Payton, J. W., 1981, Petroleum geology of South Carlton field, lower Tuscaloosa "Pilot Sand," Clarke and Baldwin Counties, Alabama: Gulf Coast Association of Geological Societies Transactions, v. 31, p. 139–147.
Mancini, E. A., and Tew, B. H., 1993, Eustasy versus subsidence: Lower Paleocene depositional sequences from southern Alabama, eastern Gulf Coastal Plain: Geological Society of America Bulletin, v. 105, p. 3–17.
___1997, Recognition of maximum flooding events in mixed siliciclastic–carbonate systems: Key to global chronostratigraphic correlation: Geology, v. 25, p. 351–354.
Mann, S. D., 1988, Subaqueous evaporites of the Buckner Member, Haynesville Formation,

northeastern Mobile County, Alabama: Gulf Coast Association of Geological Societies Transactions, v. 38, p. 187–196.

Martin, R. G., 1978, Northern and eastern Gulf of Mexico continental margin stratigraphic and structural framework, *in* Bouma, A. H., Moore, G. T., and Coleman, J. M., eds., Framework, facies, and oil-trapping characteristics of the upper continental margin: American Association of Petroleum Geologists Studies in Geology, v. 7, p. 21–42.

McBride, E. F., 1963, A classification of common sandstones: Journal of Sedimentary Petrology, v. 33, p. 664–669.

McClay, K. R., and Scott, A. D., 1991, Experimental models of hanging wall deformation in ramp–flat listric extensional fault systems: Tectonophysics, v. 188, p. 85–96.

McDonald, W. J., 1993, Horizontal oil well applications and oil recovery assessment: Bartlesville, Oklahoma, U.S. Department of Energy Fossil Energy Report DOE/BC/14861–1, 5 p.

McKenzie, D., 1978, Some remarks on the development of sedimentary basins: Earth and Planetary Science Letters, v. 40, p. 25–32.

McQuillan, H., 1973, Small-scale fracture density in Asmari Formation of southwest Iran and its relation to bed thickness and structural setting: American Association of Petroleum Geologists Bulletin, v. 57, p. 2367–2385.

Meling, M., 1993, Description and interpretation of North Sea fractured chalk formations: Society of Petroleum Engineers Paper 25640, 11 p.

Mink, R. M., Bearden, B. L., and Mancini, E. A., 1985, Regional Jurassic geologic framework of Alabama coastal waters area and adjacent Federal waters area: State Oil and Gas Board of Alabama Oil and Gas Report 12, 58 p.

Moore, D. B., 1971, Subsurface geologic map of southwest Alabama: Alabama Geological Survey Special Map 99.

Mozley, P. S., and Wersin, P., 1992, Isotopic composition of siderite as an indicator of depositional environment: Geology, v. 20, p. 817–820.

Murray, G. E., Jr., 1961, Geology of the Atlantic and Gulf Coastal Province of North America: New York, Harper and Brothers, 692 p.

Narr, W., 1991, Fracture density in the deep subsurface: Techniques with applications to Point Arguello oil field: American Association of Petroleum Geologists Bulletin, v. 75, p. 1300–1323.

Nickelsen, R. P., and Hough, V. D., 1967, Jointing in the Appalachian Plateau of Pennsylvania: Geological Society of America Bulletin, v. 78, p. 609–630.

Nicol, A., Walsh, J. J., Watterson, J., and Bretan, P., 1995, Three dimensional geometry and growth of conjugate normal faults: Journal of Structural Geology, v. 17, p. 847–862.

Odin, G. S., and Matter, A., 1981, De glauconiarum origine: Sedimentology, v. 20, p. 611–641.

Odom, E., 1984, Glauconite and Celadonite minerals, *in* Baile, S. W., ed., Reviews in Mineralogy, v. 13, p. 545–572.

Oxley, M. L., and Minihan, E. D., 1969, Alabama exploration underway: Oil and Gas Journal, v. 67, p. 207–212.

Pashin, J. C., Groshong, R. H., Jr., and Wang, Saiwei, 1995, Thin-skinned structures affect gas production in Alabama coalbed methane fields: Tuscaloosa, Alabama, University of Alabama, Intergas '95 Proceedings, p. 1–14.

Pashin, J. C., Osborne, W. E., and Rindsberg, A. K., 1991, Outcrop characterization of sandstone heterogeneity in Carboniferous reservoirs, Black Warrior basin, Alabama: Bartlesville, Oklahoma, U.S. Department of Energy Fossil Energy Report DOE/BC/14448–6, 126 p.

Pashin, J. C., Raymond, D. E., Rindsberg, A. K., Alabi, G. G., and Groshong, R. H., 1997, Area balance and strain in an extensional fault system: Strategies for improved oil recovery in fractured chalk, Gilbertown field, southwestern Alabama: U.S. Department of Energy Fossil Energy Report DOE/PC/91008–2, 67 p.

Petersen, K., Foged, N., Olsen, A., and Rasmussen, F. O., 1992, Natural stress field in a chalk reservoir predicted by spatial finite element analysis: Danmarks Geologiske Undersoegelse Report NEI–DK–1133, 12 p.

Pollard, D. D., and Aydin, A, 1988, Progress in understanding jointing over the last century: Geological Society of America Bulletin, v. 100, p. 1181–1204.

Puckett, T. M., 1992, Distribution of ostracodes in the Upper Cretaceous (late Santonian through middle Maastrichtian) of Alabama and Mississippi: Gulf Coast Association of Geological Societies Transactions, v. 42, p. 613–632.

Rosendahl, B. R., 1987, Architecture of continental rifts with special reference to East Africa: Annual Review of Earth and Planetary Science, v. 15, p. 445–503.

Rosenkrans, R. R., and Marr, J. D., 1967, Modern seismic exploration of the Gulf Coast Smackover trend: Geophysics, v. 32, p. 184–206.

Russell, E. E., Keady, D. M., Mancini, E. A., and Smith, C. C., 1983, Upper Cretaceous lithostratigraphy and biostratigraphy in northeast Mississippi, southwest Tennessee and northwest Alabama, shelf chalks and coastal clastics: Tuscaloosa, Alabama, Alabama Geological Survey, Southeastern Section Society of Paleontologists and Mineralogists Guidebook, 72 p.

Salvador, Amos, 1987, Late Triassic–Jurassic paleogeography and origin of the Gulf of Mexico

basin: American Association of Petroleum Geologists Bulletin, v. 71, p. 419–451.

Sassen, R. and Moore, C. H., 1988, Framework of hydrocarbon generation and destruction in eastern Smackover trend: American Association of Petroleum Geologists Bulletin, v. 72, p. 649–663.

Schlumberger, 1989, Log Interpretation Principles/Applications: Houston, Texas, Schlumberger Educational Services, variously paginated.

Schmidt, Volkmar, and McDonald, D. A., 1979, The role of secondary porosity in the course of sandstone diagenesis: Society of Economic Paleontologists and Mineralogists Special Publication, no. 26, p. 175–207.

Scholle, P. A., 1977, Chalk diagenesis and its relationship to petroleum exploration: oil from chalk a modern miracle?: American Association of Petroleum Geologists Bulletin, v. 61, p. 982–1009.

Sclater, J. G., and Christie, P. A. F., 1980, Continental stretching: An explanation of the post-mid-Cretaceous subsidence of the central North Sea basin: Journal of Geophysical Research, v. 85, p. 3711–3739.

Scott, D. L., and Rosendahl, B. R., 1989, North Viking graben: An east African perspective: American Association of Petroleum Geologists Bulletin, v. 73, p. 155–165.

Selvig, A., 1991, North Sea chalk reservoirs: An appealing target for horizontal wells?: Society of Petroleum Engineers Paper 22930, 14 p.

Sharma, Bijon, Honarpour, M. M., Szpakiewicz, M. J., and Schatzinger, R. A., 1990a, Critical heterogeneities in a barrier island deposit and their influence on various recovery processes: Society of Petroleum Engineers Formation Evaluation, March 1990, p. 103–112.

Sharma, Bijon, Honarpour, M. M, Jackson, S. R., Schatzinger, R. A., and Tomutsa, Livlu, 1990b, Determining the productivity of a barrier island sandstone deposit from integrated facies analysis: Society of Petroleum Engineers Formation Evaluation, December 1990, p. 413–420.

Simon, D. E., Coulter, G. R., King, George, and Holman, George, 1982, North Sea chalk completions—a laboratory study: Journal of Petroleum Technology, v. 34, p. 2531–2536.

Skuce, A. G., 1996, Forward modelling of compaction above normal faults: An example from the Sirte basin, Libya: Geological Society of London Special Publication 99, p. 135–146.

Stearns, D. W., and Friedman, Melvin, 1972, Reservoirs in fractured rock: American Association of Petroleum Geologists Memoir 16, p. 82–106.

Suppe, J., 1983, Geometry and kinematics of fault-bend folding: American Journal of Science, v. 284, p. 684–721.

Sweeney, J. J., and Burnham, A. K., 1990, Evaluation of a simple model of vitrinite reflectance based on chemical kinetics: American Association of Petroleum Geologists Bulletin, v. 74, p. 1559–1570.

Szabo, M. W., Osborne, W. E., and Copeland, C. W., 1988, Geologic map of Alabama: Alabama Geological Survey Special Map 220, scale 1:250,000.

Takahashi, J., 1939, Synopsis of glauconization, in Trask, P. D., ed., Recent marine sediments: American Association of Petroleum Geologists, Tulsa, Oklahoma, p. 503–513.

Teufel, L. W., 1991, Failure of chalk during waterflooding of the Ekofisk field: Society of Petroleum Engineers Paper 24911, 10 p.

___1992, Geomechanical evidence for shear failure of chalk during production of the Ekofisk field: Society of Petroleum Engineers Paper 22755, 8 p.

Teufel, L. W., and Farrell, H. E., 1990, In situ stress and natural fracture distribution in the Ekofisk field, North Sea: Sandia National Laboratories Report SAND–90–1058C, 33 p.

Teufel, L. W., and Warpinski, N. R., 1990, Laboratory determination of effective stress laws for deformation and permeability of chalk: Sandia National Laboratories Report SAND–90–1113C, 16 p.

Tew, B. H., 1992, Sequence stratigraphy, lithofacies relationships, and paleogeography of Oligocene strata in southeastern Mississippi and southwestern Alabama: Alabama Geological Survey Bulletin 146, 73 p.

Tolson, J. S., Copeland, C. W., and Bearden, B. L., 1983, Stratigraphic profiles of Jurassic strata in the western part of the Alabama coastal plain: Alabama Geological Survey Bulletin 122, 425 p.

Toulmin, L. D., LaMoreaux, P. E., and Lanphere, C. R., 1951, Geology and ground-water resources of Choctaw County, Alabama: Alabama Geological Survey Special Report 21, 197 p.

Veizer, J., 1983, Trace elements and isotopes in sedimentary carbonates, in Reeder, R. J., ed., Carbonates: Mineralogy and chemistry: Washington, D. C., Mineralogical Society of America Reviews in Mineralogy, p. 265–300.

Veizer, J., and Hoefs, J., 1976, The nature of O18/O16 and C13/C12 secular trends in sedimentary carbonate rocks: Geochimica et Cosmochimica Acta, v. 40, p. 1387–1395.

Velde, B., 1985, On the origin of glauconite and chamosite granules: Geo–Marine Letters, v. 5, p. 47–49.

Wang, Saiwei, Groshong, R. H., Jr., and Pashin, J. C., 1993, Thin-skinned normal faults in Deerlick Creek coalbed-methane field, Black Warrior basin, Alabama, *in* Pashin, J. C., ed., New Perspectives on the Mississippian System of Alabama: Alabama

Geological Society 30th Annual Field Trip Guidebook, p. 69–78.

Waples, D. W., 1980, Time and temperature in petroleum formation: American Association of Petroleum Geologists Bulletin, v. 64, p. 916–926.

Watts, N. L., 1983, Microfractures in chalks of the Albuskjell field, Norwegian sector, North Sea: possible origin and distribution: American Association of Petroleum Geologists Bulletin, v. 67, p. 201–234.

Wilhelm, O., and Ewing, M., 1972, Geology and history of the Gulf of Mexico: Geological Society of America Bulletin, v. 83, p. 585–600.

Wilson, G. V., Kidd, J. T., and Shannon, S. W., 1976, Relationships of surface and subsurface faults in Choctaw and Clarke Counties, Alabama, *in* Copeland, C. W., Newton, J. G., and Self, D. M., eds., Cretaceous and Tertiary faults in southwestern Alabama: Alabama Geological Society, Fourteenth Annual Field Trip Guidebook, 114 p.

Wilson, G. V., and Tew, B. H., 1985, Geothermal data for southwest Alabama: Correlations to geology and potential uses: Alabama State Oil and Gas Board Oil and Gas Report 10, 125 p.

Withjack, M. O., Islam, Q. T., and La Point, P. R., 1995, Normal faults and their hanging-wall deformation: American Association of Petroleum Geologists Bulletin, v. 79, p. 1–18.

Woodring, W. P., Stewart, R., and Richards, R. W., 1940, Geology of the Kettleman Hills oil field, California: U.S. Geological Survey Professional Paper 195, 170 p.

Worrall, D. M., and Snelson, S., 1989, Evolution of the northern Gulf of Mexico, with emphasis on Cenozoic growth faulting and the role of salt, *in* Bally, A. W., and Palmer, A. R., eds., The geology of North America; an overview: Boulder, Colorado, Geological Society of America, The Geology of North America, Volume A, p. 97–138.

Xiao, H. B., and Suppe, J., 1980, Origin of rollover: American Association of Petroleum Geologists Bulletin, v. 76, p. 509–529.